ADVANCED CERAMICS

Edited by
E C SUBBARAO

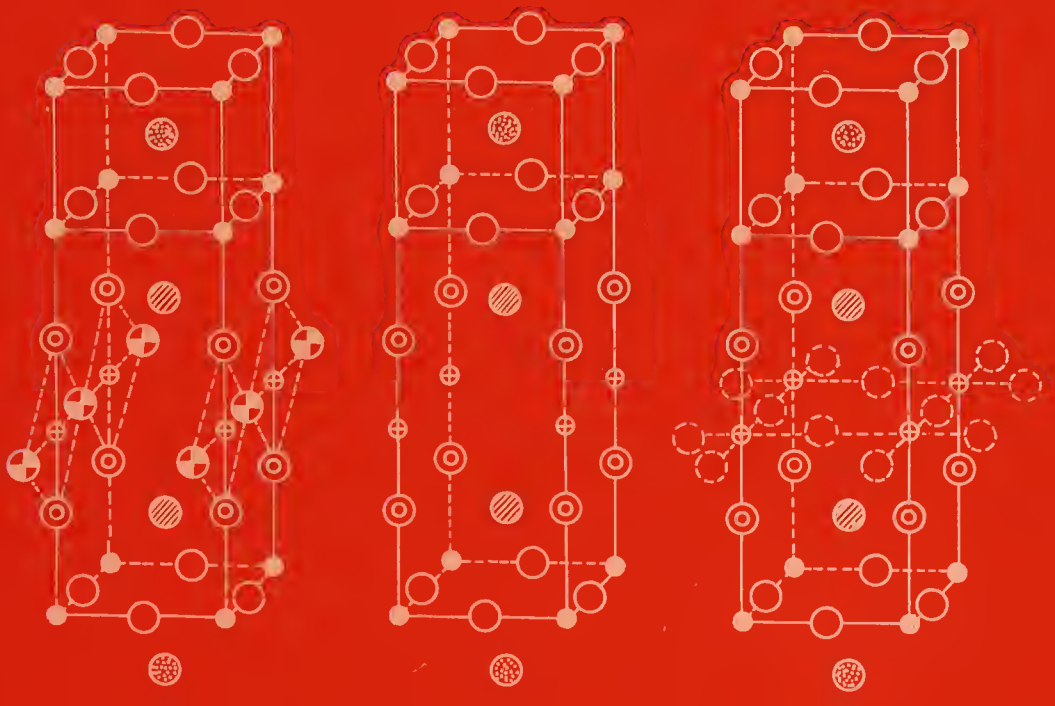

INDIAN ACADEMY OF SCIENCES
BANGALORE 560 080

ADVANCED CERAMICS

Edited by
E C SUBBARAO
Tata Research Development
and Design Centre, Pune

1988
INDIAN ACADEMY OF SCIENCES
BANGALORE 560 080

The cover shows the structure of different phases of $YBa_2Cu_3O_{7-\delta}$ from the paper by C N R Rao

Reprinted from *Sādhanā* – Academy Proceedings in Engineering sciences
Volume 13, pp. 1–156, 1988

Edited by E C Subbarao, phototypeset by Book-Makers (I) Pvt. Ltd., Bangalore 560 003 and printed for the Indian Academy of Sciences by Phoenix Printing Company Pvt. Ltd, Attibele Industrial Area, Bangalore 562 107

CONTENTS

Foreword

Stages in the progress of human civilization have often been characterized by the materials used, such as the Stone Age, Iron Age etc. Ceramics represent one of the oldest materials used by the human race, both as objects of utility and of beauty. Traditional ceramics have responded to basic human needs by providing building materials for shelter and pots for cooking and storage, besides refractories for high temperature furnaces, optical glass for spectacles, microscopes and telescopes, electrical and thermal insulation etc. Ceramics are made from inexpensive materials which occur abundantly in nature and hence are widely used.

As we approach the twenty-first century, three technologies – bio-technology, electronics and advanced materials – are becoming dominant. Among advanced materials, ceramics are moving to the centre of the stage. This is due to the steady progress in our scientific understanding of the structure–processing–property correlations in ceramics, often in quantitative terms. This special volume on advanced ceramics attempts to capture the breathtaking strides being made in this field.

The sharp distinction between traditional and advanced ceramics–in terms of starting materials, processing, properties and applications–is emphasized in an overview of the field in the first paper.

Many novel techniques have been developed for the synthesis of powders and the fabrication of ceramics. These techniques aim at atomic level mixing, fine particle size and high reactivity, enabling low temperature sintering in order to overcome the major disadvantages of traditional ceramic processing, namely compositional inhomogeneity and high temperature sintering. In his paper, Chakravorty examines organometallic routes for synthesis of ceramics.

The discovery in late 1986 of superconductivity in ceramics at unimaginably high temperatures (near 100 K) has been the most important achievement in decades in science as a whole and certainly in centuries in ceramics. Room-temperature superconducting ceramics appear to be around the corner. The fantastic range of applications, from loss-free power transmission, powerful magnets for medical use and nuclear fusion technology, to levitated trains, computers etc. has already electrified the science and technology community the world over like nothing else in recent history and is sure to change the way of human life. C N R Rao provides a crisp review of this fast changing field.

At the moment, the most important use of advanced ceramics in volume and value is in electronics. While alumina is by far the largest item for use as substrates, insulators etc., specialized ceramics–ferro-electric, piezoelectric, semiconducting and magnetic–play a critical role as projected by V C S Prasad in his paper.

Ceramics are best known as excellent electric insulators, but it is now possible to confer high electrical conductivity where the charge carriers can by choice be electrons or ions. "Super" ionic conductivity in ceramics is due to specific ions, for

example, oxygen in zirconia and sodium in beta-alumina. Maiti & Paria discuss the high temperature fuel cell which is based on oxygen ion conduction of doped zirconia.

In spite of their chemical inertness, high temperature stability and abundance, ceramics have always been disqualified for structural applications due to their poor tensile strength and the brittle fracture they are subject to. These handicaps are rapidly being overcome by several approaches. Ceramics composed of the first few elements in the periodic table–B, C, Al, N, O, Si–are proving to be excellent structural materials in auto and aerospace applications. The synthesis and fabrication of these unique light element ceramics require unconventional methods, which are reviewed by K J Rao and his associates.

Zirconia undergoes a martensitic phase transformation. A range of zirconia-based ceramics are now available which, through a process of transformation toughening, exhibit such high fracture toughness that these have been christened as 'ceramic steel'. The science underlying these engineering ceramics is covered by Bhaduri in his paper.

An excellent example of increased productivity in manufacturing is illustrated by Komanduri in the use of ceramic tool materials, which increase the machining speeds markedly even though more stable machines are called for.

The best characteristics of metals and ceramics are exploited by coating metallic components by ceramics. The coated components have extended life under the severe environments encountered in a variety of industries. The materials, techniques and properties of such ceramic coatings are discussed by Karthikeyan & Mayuram.

Limitations of space prevented us from covering, in this volume, other equally exciting topics in advanced ceramics. It is however hoped that the present papers demonstrate that the subject of ceramics is undergoing a great renaissance and that we are on the threshold of an exciting Ceramic Age. Excellence in ceramic science leading to advanced engineering ceramics is a prerequisite for industrial progress and for the social well-being of nations in decades to come.

I am indebted to the authors for their excellent contributions to this volume and to the reviewers of *Sādhanā* for fearless criticism.

July 1988

E C SUBBARAO
Guest Editor

Advanced ceramics – an overview

E C SUBBARAO

Tata Research Development and Design Centre, 1, Mangaldas Road, Pune 411 001, India

Abstract. In sharp contrast to conventional ceramics, advanced ceramics use extensively processed starting materials of controlled purity and particle size, and novel fabrication techniques such as tape casting, chemical vapour deposition, *in situ* oxidation, injection moulding, followed by fast, often low temperature, sintering. Advanced ceramics exhibit unusual behaviour at times and quantum jumps in properties. Improved fracture toughness of structural ceramics makes them suitable candidates for stringent engineering applications. Composites involving special ceramics display some outstanding properties, e.g. piezoelectrics. Examples of dielectrics, super conductors, optical fibres and ionic conductors are cited.

Keywords. Materials preparation; processing; superconductors; optical fibres; toughened ceramics; composites.

1. Introduction

From the beginning of civilisation, ceramics provided objects of utility and beauty. Shelter for mankind is based on adobe, brick, tile, cement and window glass. Cooking and storing of food has always been done in ceramicware ranging from clay pots to modern glass-ceramics. The abundant and widespread availability of basic ceramic raw materials – clay, sand and other minerals – in nature enabled ceramics to meet basic human needs over the millennia. The growth in world population guaranteed the expansion of the traditional ceramic industry.

Superimposed on this steady, but slow, growth of ceramics, has been an important qualitative change in recent decades, based on a deeper scientific understanding of the composition-structure-processing-property correlations of ceramics. This arose in response to the stringent requirements of sophisticated applications in electronics, space, nucleonics and energy, among others. Ceramics to meet these newer, engineering applications are termed advanced ceramics (Subbarao 1987). Together with biotechnology and electronics, advanced ceramics has moved to the centre-stage of the second industrial revolution to propel mankind into the twenty-first century. The characteristics of these new-born industries are manifold increases in properties and performance, as well as typical annual growth rates of 50–100% (Kenney & Bowen 1983).

In this exciting area, a few pockets of excellence exist in India, which have made respectable contributions to the worldwide progress in advanced ceramics.

In this paper, the distinction between advanced and conventional ceramics is outlined, followed by an overview of the new material preparation techniques, their unusual processing methods, and the quantum jumps observed in their properties for meeting the stringent requirements of emerging engineering applications.

2. Characteristics

The important differences between conventional and advanced ceramics are summarised in table 1.

Modern applications call for enhanced, reliable properties, which can be met only when the starting materials have reproducible characteristics. This is not possible with naturally occurring minerals and ores, even after beneficiation. The higher cost of processed materials has to be justified by enhanced performance. Empiricism and experience which guided conventional ceramics are totally inadequate, and often inappropriate, for advanced ceramics, which can progress only through knowledge gained by multidisciplinary research and development.

3. Material preparation

The materials for advanced ceramics must possess:

(i) high purity – may be as high as 99·99%;
(ii) small and uniform particle size, which gives rise to large surface area and high reactivity;
(iii) reproducibility – homogeneous distribution of intentionally added impurities, called dopants, which may be present at ppm level.

Novel preparation techniques, such as sol-gel (Roy & Roy 1984; Lannutti & Clark 1985; Sen & Chakravorty 1986), precursors (Rao 1986; Mazdiyasni 1982), alkoxides (Mazdiyasni 1982), and topochemistry (Gopalakrishnan 1986), for this purpose arose from developments in solid state chemistry. These methods have made it possible to

Table 1. Distinctions between conventional and advanced ceramics.

Characteristic	Conventional	Advanced
Raw materials	Natural minerals with little or no processing e.g. clay, sand	Processed materials c.g. Al_2O_3, ZrO_2, Si_3N_4, SiC, SiAlON
Processing	Pressing, extrusion, slip casting, drying, firing	Tape casting, hot isostatic pressing, injection moulding, CVD, *in situ* oxidation
Properties	Refractoriness, thermal & electrical insulation	Fracture toughness, electrical conductivity, electro-optics, dielectrics, piezoelectrics, magnetics, superconductivity
Applications	Refractories, sanitary-ware, sheet glass, building materials	Diesel engine, optical fibre, substrate, ferrites, capacitors, transducers

produce some materials which could not be produced otherwise. For example, utilising solid solution precursors of $Ca_{1-x}Mn_xCO_3$, a variety of oxides in the Ca-Mn-O system have been synthesised (Vidyasagar *et al* 1985). Some of the mixed carbonates which occur in nature could be made in the laboratory only by the precursor method. Similarly, dehydration as well as insertion and removal of protons, lithium ions etc. into compounds in a reversible way can be accomplished through topochemical reactions. Hydrolysis of zirconium tetrabutoxide in alcohol solution can be used to produce monodispersed ZrO_2 powders (Ogihara *et al* 1987).

Chemically prepared zirconia can be sintered to high density at 1400°C, several hundred degrees less than the usual temperatures (Gupta *et al* 1977). The incorporation of small quantities of La in $BaTiO_3$ to decrease its electrical resistivity by a factor of 10^{10} is best accomplished by a solution-decomposition route. These new methods enable mixing at an atomic scale, compared to the gross particle mixing by mechanical means, employed in conventional ceramic processing. The atomic level mixing means shorter diffusion distances for material transport (about 10 Å compared to about 10,000 Å in mixing of ceramic powders), leading to decreased temperatures and duration for sintering, besides greater compositional homogeneity. The disordered atomic arrangement in a gel is a better starting point for making glasses, which are amorphous in nature, compared to the use of well-crystallised oxides and other salts (Chakravorty 1988).

Alumina is by far the most important base material for advanced ceramics and accounts for over 80% of the raw materials employed in engineering ceramics. The other materials of importance are $BaTiO_3$, TiO_2, lead zirconate titanate (PZT), lead lanthanum zirconate titanate (PLZT), ZrO_2, SiC, Si_3N_4 and SiAlON.

4. Processing

While all the conventional ceramic processes such as pressing, slip casting, extrusion, drying, firing etc., are available for advanced ceramics, some newer fabrication technologies are developed to meet specific requirements. These include:

(i) Isostatic and hot isostatic pressing to achieve higher end point density and freedom from defects such as laminations, density gradients etc.

(ii) Tape casting to produce thin sheets of large area from a slurry of alumina, titanates etc., spread by a blade on a moving plastic sheet (Williams 1976; Prasad 1988). The surface of such substrates has a high degree of evenness (typically a few microns per linear meter). These sheets are often stacked in the green condition, with metal electrode paste applied over the entire area or as thin lines, and then the stack is fired to produce multilayer capacitors. Alumina sheets with a network of resistor and conductor paste, in the form of thin lines, are stacked (upto 150 layers) and fired to produce multilayer ceramic chips for modern computers. The manufacture of multilayer ceramics including metallic interconnections is often completed in a single firing operation (Dougherty & Greer 1983).

(iii) Injection moulding for small intricate shapes with projections and perforations.

(iv) Chemical vapour deposition of preforms from which optical fibres are drawn (MacChesney 1981, pp. 537–561).

(v) *In situ* oxidation. A component is cast from molten aluminium alloy and oxidation is allowed to take place at the moving liquid/solid interface to result in an

alumina component of the desired shape. The multitude of steps normally employed in the fabrication of alumina components is replaced by a single casting-oxidation step, which is completed at a much lower temperature and shorter time than those employed for sintering of alumina ceramics.

(vi) Electrophoretic deposition of beta-alumina electrode tubes for Na-S battery (Krishnarao *et al* 1986).

(vii) Sintering at a lower temperature and in shorter time. Ceramic dielectrics are now fired at temperatures below 1000°C compared to the usual 1300–1350°C employed for sintering titanate dielectrics. The entire sintering operation is completed in 1–2 h, much shorter than the traditional 20–24 h. The resulting energy saving is substantial. These improvements in sintering are due to:

(a) increased sinterability of the highly reactive, small particle size initial powders;
(b) sintering aids which provide transient liquid phase (Ramesh Choudhary & Subbarao 1981; Prasad 1988); and
(c) lower melting compositions such as niobates in place of titanates (Prasad 1988).

Since advanced ceramics are often used in engineering applications, often as components in a larger assembly, their dimensional tolerance, integrity and reproducibility are considerably more critical than those of conventional ceramics. Finishing operations, such as grinding, polishing etc., are expensive and may introduce defects and therefore should be employed sparingly. Hence, processing methods preferred for advanced ceramics are those which give the final net shape within required dimensional tolerance, with little or no subsequent finishing operations.

The high cost of starting materials, stringent specifications on properties and dimensions, and the need for reproducibility usually dictate the automation of the fabrication steps. The controls inherent in automation require a deeper knowledge of composition-structure-processing-property interdependence. The recent advances in ceramic science are making this possible.

5. Properties

The properties of advanced ceramics are both quantitively and, more importantly, qualitatively different from those of conventional ceramics. Following the successive replacement of vacuum tubes by transistors, integrated circuits and large scale integrated circuits (LSI), miniaturisation of other circuit elements such as ceramic capacitors has become necessary. This is achieved by gradual increase in the dielectric constant of capacitor materials by almost an order of magnitude every decade (figure 1). While TiO_2 and $BaTiO_3$ are new classes of dielectric materials, improvements in the last 30 years are due to modification of the basic titanate material. These innovations include fine grain size to inhibit domain reorientations (Buessem *et al* 1966), stacking of thin layers in a multilayer capacitor (Prasad 1988) or development of an insulating layer surrounding semiconducting titanate grain (Goodman 1981; Wernicke 1981).

While barium titanate is valued for its high electrical resistivity ($> 10^{10}$ ohm cm) when it is used as a capacitor, it can be made semiconducting (resistivity $\simeq 10^2$ ohm cm) by doping it with a small amount of La or many other ions (analogous to semi-

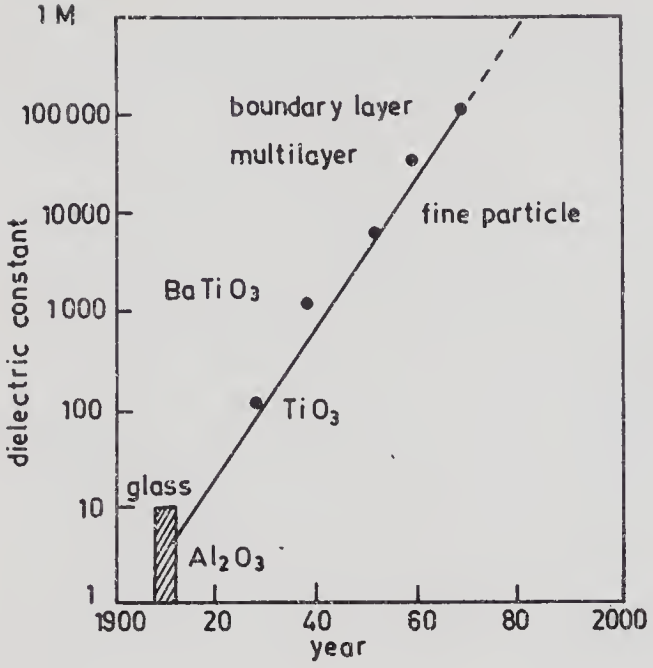

Figure 1. Chronology of enhancement of dielectric constants of ceramic dielectrics.

conductor technology). The electrical resistivity of such a semiconducting barium titanate increases sharply (by about 10^4) in the vicinity of its ferroelectric Curie temperature (Kulwicki 1981). This positive temperature coefficient of resistivity (PTCR) is made use of for motor protection, self-regulating heaters, etc.

Zirconia, doped with CaO, MgO, Y_2O_3 etc., exhibits a cubic, fluorite type structure. It has been established that the dopant cations (Ca^{2+}, Mg^{2+}, Y^{3+} etc.) replace the Zr^{4+} ions and the charge balance is restored by the creation of an appropriate number of oxygen ion vacancies (Subbarao 1980). The existence of the oxygen ion vacancies, whose concentration is fixed by the amount of dopant and remains independent of temperature and oxygen partial pressure, leads to oxygen ion diffusion at rates a million-fold higher than that of cations (Subbarao 1981). Accompanying the mass transport of oxygen ions through the cubic zirconia lattice, there is a charge transport according to the Nernst–Einstein relationship

$$E = (RT/4F) \ln [P_{O_2}/P_{O_2(\text{ref})}] \tag{1}$$

where E is the EMF set up when a zirconia membrane separates gases with oxygen partial pressures of P_{O_2} and P_{O_2} (reference, say air), R is the gas constant, T is absolute temperature and F is the Faraday constant. Zirconia oxygen probes, using (1), measure oxygen contents in flue gases, heat treatment furnaces, molten steel etc. Application of a potential, dictated by (1), to a zirconia membrane can pump oxygen into or out of a gas stream to attain a desired oxygen content (down to a few parts per billion) (Subbarao & Maiti 1987). When the oxygen required for combustion in a fuel cell is transported across a zirconia membrance, the EMF developed becomes available to perform useful work. Such a zirconia-based high temperature fuel cell is an efficient power source without any moving parts (Maiti & Paria 1988).

In a beta-alumina lattice, Na^+ ions occupy some of the interstices between the spinel alumina blocks. The fact that only a few of the available sites are occupied by the Na^+ ions and the inter-ionic distances are larger than the size of the Na^+ ion enables easy sodium ion diffusion, making beta-alumina a suitable solid electrolyte separating two molten electrodes – sodium and sulphur – in a high energy density

battery, called the sodium-sulphur battery (Subbarao 1980). Since these batteries have a much higher energy density per unit weight or volume, compared to the conventional lead-acid battery, they are good candidates for load levelling and, possibly, automotive applications.

Since superconductivity was discovered in 1911 in solid mercury by Kammerlingh Onnes, only a few metals have exhibited this unique property. The transition from the normal to the super conducting state (which is signalled by a near total loss of electrical resistivity) arises a few degrees above absolute zero (less than 10 K) in these metals (table 2). After a gap of nearly 40 years during which the superconducting transition temperature nearly stagnated, a number of intermetallics in which the superconducting transition temperature was in the range of 10–20° K were found. Nb_3Ge exhibiting a record T_c of 23 K (table 2) was discovered in 1973. After a gap of 13 years, Bednorz & Müller (1986) found that a rare earth–Ba–Cu oxide exhibits superconductivity at 36 K. This outstanding discovery started an intense scientific effort all over the world and a T_c of 100 K, above the liquid nitrogen temperature (77 K), was achieved in a matter of weeks for a number of oxides. Originally thought of as $La_{2-x}M_xCuO_4$ where M = Ba, Sr, the superconducting oxide was reported as $Y_{1\cdot2}Ba_{0\cdot8}CuO_4$ (Wu *et al* 1987) with K_2NiF_4 structure type. Ganguly *et al* (1987a) reported a T_c of 100–120 K for oxides in the system Y-Ba-Cu-O. The compound $YBa_2Cu_3O_{7\pm\delta}$ was found to have a perovskite-type (and not K_2NiF_4 type) structure (Ganguly *et al* 1987b). Other reports in this field, all in a space of three months, are by Uchida *et al* (1987). Chu *et al* (1987), Cava *et al* (1987) and Rao & Ganguly (1987). It may be noted from table 2 and figure 2 that metals exhibit superconducting transition temperatures (T_c) under 10 K, intermetallic compounds have T_c upto 23 K and oxides, discovered in 1986–87, have T_c between 36 and 120 K. There are claims of oxides with T_c of 240 K, not much below the temperature of an ordinary refrigerator, if not of a room. The critical current density of these superconducting oxides is steadily increasing, so that deviee research has already begun. Superconductors are often used in the form of wires, made into coils, for producing intense magnetic fields. The production of flexible, long shapes from the conven-

Table 2. Superconducting materials and critical temperatures.

Metals	T_c (K)	Intermetallics	T_c (K)	Oxides	T_c(K)
Ti	0·53	Pb_2Au	7·0	$La_{2-x}M_xCuO_4$	$\geqslant 36$
Zr	0·7	SnSb	3·9	M = Ba, Sr	
Hf	0·35	Tl_3Bi_5	6·4	$Y_{1\cdot2}Ba_{0\cdot8}CuO_4$	
Th	1·32	WC	2·5–4·2	$YBa_2Cu_3O_{7\pm\delta}$	~100
V	5·1	MoC	7·6–8·3	Bi-Sr-Ca-Cu-O	~105
Nb	9·22	MoN	12·0	Tl-Ba-Ca-Cu-O	85–130
Ta	4·38	NbN	14·7		
Zn	0·79	Nb_3Sn	18·07		
Cd	0·54	Nb_3Al	18		
Hg	4·12	V_3Si	16·8–17·1		
Al	1·14	V_3Ga	16·8		
Ga	1·07	Nb-25% Zr	10·8		
In	3·37	Nb-60% Ti	8·7		
Tl	2·38	Nb-Al-Ge	20		
Sn	3·69	Nb_3Ge	23·2		
Pb	7·26				

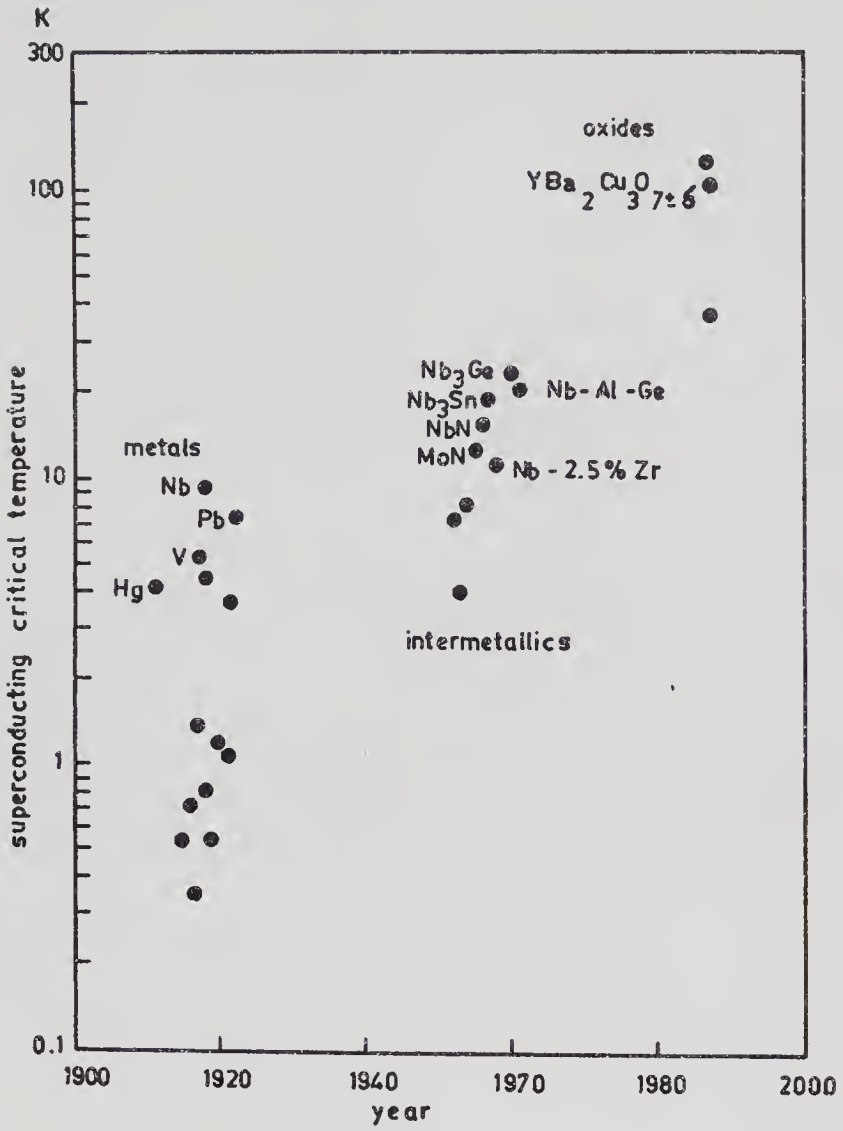

Figure 2. Remarkable trend of critical temperatures of superconducting metals, intermetallics and oxides.

tionally brittle ceramics is a challenging task. Novel fabrication techniques are being conceived, besides the established thin film methods.

This discovery of superconducting ceramics, when it is translated into commercial technology, is likely to have a major impact on electrical engineering practice including power transmission, energy storage, computer size, levitated transport (train and ship), nuclear fusion, medical diagnostics etc. (Rao 1988a).

Glass fibres have been used for decades for reinforcing plastics, as well as for thermal and sound insulation. The current interest in silica glass fibre stems from the discovery of its ability to transmit electrical signals over long distances with little attentuation (MacChesney 1981, pp. 537–561). Transmission losses are attributed to the presence of transition metal ions in starting materials which can be reduced through purification. For example, a single glass fibre can send 2×10^{10} bits of information per second over a distance of 68 km length of fibre. This is equivalent to sending the data in 200 encyclopaedia volumes per second. The distance between repeaters in presently installed fibres is 30 km, which is expected to increase to

300 km. The repeaters, located between the light source and detectors in an optical fibre system, control the shape, time and strength of the weakening optical signals. The additional advantages of optical glass fibre over the conventional copper wire for transmission of information are its light weight, the abundance of raw materials, its lower cost, environmental stability, and insensitivity to electromagnetic interference. The material preparation and fibre production technologies, as well as the clean environment of the production facilities, are more akin to the semiconductor industry than to a ceramic factory. More recently, fluoride glasses (ZrF_4-ThF_4-BeF_2) have shown lower transmission losses (0·01 to 0·001 dB/km) compared to about 0·2 dB/km for silica optical fibres. The decreasing trend of losses of transmission fibres is shown in figure 3 (Tummala & Shaw 1987). It shows that they have decreased from 10–200 dB/km for multicomponent glasses 20 years ago to 2–4 dB/km for present commercial silica fibres, and to 0·1 dB/km for laboratory fibres.

While ceramics are quite strong under compression, they are generally weak in tension and are rarely free from flaws which lead to brittle fracture, often catastrophically. This deficiency has been overcome in the case of glass by placing the surface under compression, either through a heat treatment operation, called tempering, or through ion exchange from molten salts. In crystalline ceramics, the presence of cracks and other flaws cannot be completely avoided. Therefore, recourse is taken to methods for inhibiting crack growth. One way to do so is by the incorporation of fibres. Another way is to utilise a phase transformation to absorb

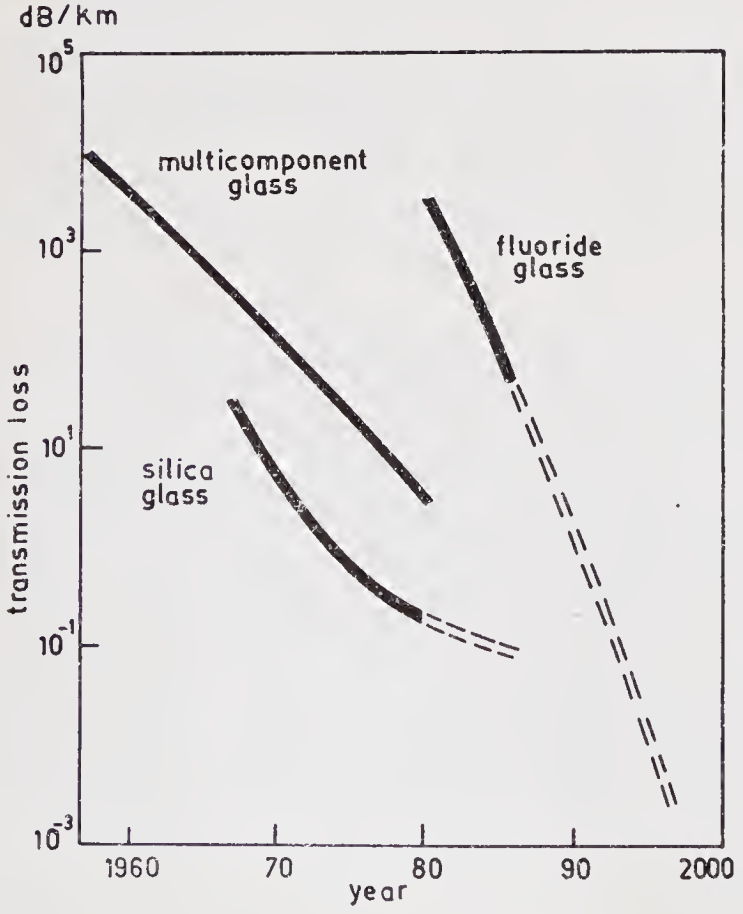

Figure 3. Trend of transmission losses of optical fibres.

the energy associated with a stress concentration. In fact, both can be combined as was done by Claussen (1986) in the case of fibre-reinforced transformation-toughened zirconia. While fibre-reinforcement as a strengthening mechanism has been practised for quite sometime, strengthening and toughening of ceramics via a phase transformation was first demonstrated in zirconia by Garvie *et al* (1975). Here the volume change accompanying the martensitic phase transition of zirconia (tetragonal to monoclinic) is exploited. The underlying mechanisms are reviewed by Bhaduri (1988). The transformation-toughened zirconia ceramics are used as dies for hot extrusion of ferrous and non-ferrous metals, engine and pump components, textile thread guides etc.

Silicon carbide, silicon nitride (Si_3N_4) and its derivative SiAlON are excellent structural ceramics, as discussed by Rao (1988b), and are good machining tool bits (Komanduri 1988).

Only a third of the fuel energy is utilised in the shaft power of an internal combustion or a diesel engine, with one-third wasted in the coolant and another third escaping with the exhaust (Horton & Compton 1984). Since metal components limit the temperature of operation of the engine, necessitating efficient cooling, advanced ceramic components are under examination for various parts of the engine. Significant improvement in engine efficiency is achieved because of the higher temperature at which the engine with ceramic components (as coatings, liners, or as such) can be operated, with consequent higher Carnot efficiency, and requiring less cooling. The higher operating temperatures also have a favourable effect on engine emissions. The ceramic coating technology is reviewed by Karthikeyan & Mayuram (1988).

One more point needs to be emphasized regarding structural ceramics. In order to achieve optimal benefit from structural ceramics, one should, instead of making a simple replacement of a metal part by a ceramic item, redesign the part taking into account the unique properties, including brittle fracture, of ceramics.

Only the unique, new or enhanced properties of advanced ceramics are discussed here. It must however be emphasized that all the other properties which have made conventional ceramics such useful materials are also exhibited by advanced ceramics. These include extreme inertness to environment and temperature, lightness, abundance of raw materials, a range of thermal expansion and thermal conductivity etc. If conventional ceramics responded to the basic needs of man, advanced ceramics answer the challenges posed by sophisticated industries.

6. Composites

A single-phase material with many excellent properties may still suffer from some deficiencies. This can be overcome by combining the desirable properties of two materials in the form of a composite. Fibre-reinforced materials, such as bamboo in adobe, steel rods in concrete, glass fibres in plastics, are well-established structural materials. Porous insulating materials are composites of solid and gas phases. Most ceramic products are composed of crystalline and glassy phases. Bone is a unique composite of a crystalline phosphate and a pore phase, with three dimensional connectivity for both phases. This has formed the basis for the development of

biocompatible ceramics, glasses and glass-ceramics for biomedical applications and as implants.

The chronological improvements in properties and the role of composites may be illustrated by the development of piezoelectric materials. In early 1940's the ferroelectric behaviour of barium titanate was discovered. Since a ferroelectric is, by definition, a piezoelectric, barium titanate became an important piezoelectric material. In the late 1940's, when it was demonstrated that ceramic barium titanate can be poled to confer non-isotropic domain orientation, ceramic barium titanate became the first piezoelectric, which is not a single crystal (unlike quartz, Rochelle's salt, potassium dihydrogen phosphate etc.), and has all the unique properties of a ceramic – stability, ease of fabrication etc. Further, the piezoelectric properties of barium titanate were much higher than those of the single crystal piezoelectrics e.g. quartz. Soon after the discovery of ferroelectricity in $BaTiO_3$, a varicty of ionic substitutions (for Ba and Ti) were attempted which resulted in a number of new ferroelectrics, such as $PbTiO_3$, which is isostructural (perovskite-type) with $BaTiO_3$. In 1950, $PbZrO_3$ was found to be isostructural with $BaTiO_3$ and also to possess spontaneous polarization. However, each crystallographic plane in it has its spontaneous polarization aligned in one direction but neighbouring planes have their polarization in opposite directions. Spontaneously polarized materials with antiparallel orientation of polarization in adjacent planes, leading to net zero polarization, are termed antiferroelectrics, in analogy with antiferromagnets. $PbZrO_3$, thus, became the first antiferroelectric. A study of the perovskite compositions in the binary system $PbTiO_3$-$PbZrO_3$ revealed a morphotropic phase boundary near the equimolar composition, which exhibits greatly enhanced piezoelectric modulus (Jona & Shirane 1962). Efforts over the next quarter century have not produced any piezoelectric material better than lead zirconate titanate (PZT). Newnham *et al* (1980) have produced PZT-polymer composites which have piezoelectric properties one to two orders of magnitude better than PZT itself. These composites contain only 10% of PZT mixed with 90% of inexpensive polymer. The size and distribution of the two phases are important parameters, but equally crucial is the connectivity of each phase. By assigning values of 0 (for unconnected), 1 (for rods), 2 (for sheets) and 3 (for three-dimensional continuity), one can make two-phase composites with connectivities ranging from 1–0 to 3–3. A variety of ingenious fabrication processes (some of which mimic natural products) are devised to make these composites. Some of these composites can be extruded as flexible cables.

7. Conclusions

Novel methods of preparing starting materials and new techniques of fabricating ceramic products have enhanced the properties of advanced ceramics in some cases and conferred unusual properties in others. As a result, ceramics have become very versatile. Thus, the electrical behaviour of ceramics ranges from being excellent insulators to electronic and ionic conductors and more recently to high temperature superconductors. While most ceramics are still mechanically weak and brittle, special ceramics are amongst the toughest, strongest and hardest materials available today. It looks as though civilisation has made a full circle, starting with clay-based ceramics at the beginning and having come to advanced ceramics at the present.

References

Bednorz T G, Müller K A 1986 *Z. Phys.* B64: 189–193

Bhaduri S B 1988 *Sādhanā* 13: 97–117

Buessem W R, Cross L E, Goswami A 1966 *J. Am. Ceram. Soc.* 49: 33

Cava R J, Van Dover R B, Batlogg B, Rietman E A 1987 *Phys. Rev. Lett.* 58: 408–410

Chakravorty D 1988 *Sādhanā* 13: 13–18

Chu C W, Hor P H, Meng R L, Gao L, Huang Z J, Wang Y Q 1987 *Phys. Rev. Lett.* 58: 405–407

Claussen N 1988 in *Advances in ceramics. 24. Science and technology of zirconia III* (Westerville: Am. Ceram. Soc.) (in press)

Dougherty W E, Greer S E 1983 *IEEE Trans. Components, Hybrids, Manuf. Tech.* CMHT-6: 150–153

Ganguly P, Raychoudhuri A K, Sreedhar K, Rao C N R 1987a *Pramana – J. Phys.* 28: L229–L231

Ganguly P, Mohan Ram R A, Sreedhar K, Rao C N R 1987b *Pramana – J. Phys.* 28: L321–L323

Garvie R C, Hannink R H J, Pascoe R T 1975 *Nature (London)* 258: 703–704

Goodman G 1981 in *Grain boundary phenomena in electronic ceramics* (ed.) L M Levinson *Advances in ceramics* (Columbus: Am. Ceram. Soc.) 1: 215–231

Gopalakrishnan J 1986 *Proc. Indian Natl. Sci. Acad.* 52: 48–66

Gupta T K, Bechtold J H, Kuznickie R C, Cadoff L H, Rossing B R 1977 *J. Mater. Sci.* 12: 2421–2426

Horton E J, Compton W D 1984 *Science* 225: 587–593

Jona F, Shirane G 1962 *Ferroelectric crystals* (London: Pergamon)

Karthikeyan J, Mayuram M M 1988 *Sādhanā* 13: 139–156

Kenney G R, Bowen H K 1983 *Am. Ceram. Soc. Bull.* 62: 590–597

Komanduri R 1988 *Sādhanā* 13: 119–137

Krishnarao D U, Malage A B, Baral D, Subbarao E C 1986 *Bull. Mater. Sci.* 8: 1–11

Kulwicki B M 1981 in *Grain boundary phenomena in electronic ceramics* (ed.) L M Levinson *Advances in ceramics* (Columbus: Am. Ceram. Soc.) 1: 138–151

Lannutti J J, Clark D E 1985 *Ceram. Int.* 11: 91–96

MacChesney J B 1981 in *Preparation and characterization of materials* (eds) J M Honig, C N R Rao (New York: Academic Press)

Maiti H S, Paria M K 1988 *Sādhanā* 13: 59–71

Mazdiyasni K S 1982 *Ceram. Int.* 8: 42–56

Newnham R E, Bowen L J, Klicker K A, Cross L E 1980 *Mater. Eng.* 2: 93–106

Ogihara T, Mizutani N, Kate M 1987 *Ceram. Int.* 13: 35–40

Prasad V C S 1988 *Sādhanā* 13: 37–58

Ramesh Choudhary K, Subbarao E C 1981 *Ferroelectrics* 37: 689–692

Rao C N R 1986 *Proc. Indian Natl. Sci. Acad.* 52: 1–24

Rao C N R 1988a *Sādhanā* 13: 19–35

Rao C N R, Ganguly P 1987 *Curr. Sci.* 56: 47–50

Rao K J 1988b *Sādhanā* 13: 73–95

Roy R A, Roy R 1984 *Mater. Res. Bull.* 19: 169

Sen A, Chakravorty D 1986 *Proc. Indian Natl. Sci. Acad.* 52: 159–175

Subbarao E C (ed.) 1980 *Solid electrolytes and their applications* (New York: Plenum)

Subbarao E C 1981 *Advances in ceramics* 3: 1–24

Subbarao E C 1988 *Trans. Indian Ceram. Soc.* 46: 65–76

Subbarao E C, Maiti H S 1988 *Advances in ceramics 24. Science and technology of zirconia III* (Westerville: Am. Ceram. Soc.) (in press)

Tummala R R, Shaw R B 1987 *Ceram. Int.* 13: 1–11

Uchida S, Takagi H, Kitazawa K, Tanaka S 1987 *Jpn. J. Appl. Phys.* 26: L1

Vidyasagar K, Gopalakrishnan J, Rao C N R 1985 *J. Solid State Chem.* 58: 29

Wernicke R 1981 in *Grain boundary phenomena in electronic ceramics* (ed.) L M Levinson *Advances in ceramics* (Columbus: Am. Ceram. Soc.) 1: 261–271

Williams J C 1976 in *Treatise on materials science and technology* (ed.) W F Wang (New York: Academic Press) 9: 176–198

Wu M K, Ashburn J R, Torng C J, Hor P H, Meng R L, Gao L, Huang Z J, Wang Y Q, Chu C W 1987 *Phys. Rev. Lett.* 58: 908–910

Organometallic route to nanocomposite synthesis

D CHAKRAVORTY

Advanced Centre for Materials Science, Indian Institute of Technology, Kanpur 208 016, India

Present Address: Indian Association for the Cultivation of Science, Jadavpur, Calcutta 700 032, India

Abstract. The nature and scope of different varieties of nanocomposite materials are described. The practical and basic aspects of the physical properties of nanocomposites are discussed. The principles underlying the preparation of diphasic materials involving either ceramic-metal or glass-metal combinations are delineated. The sol-gel technique involving suitable organometallic compounds has been shown to be a versatile method for making these materials. A brief survey is given about the different materials made to date following the organometallic route.

Keywords. Nanocomposite; organometallic compound; sol-gel; ceramic-metal composites; glass-metal composites; diphasic xerogel.

1. Introduction

Nanocomposites are materials containing one or more phases having dimensions of the order of a few nanometers dispersed in a suitable matrix (Roy & Roy 1984). Strictly speaking, the above definition should include solids containing defect clusters, e.g., the Willis (1964) clusters in UO_{2+x} and the Koch–Cohen (1969) clusters in $Fe_{1-\delta}O$ consisting of particular arrangements of vacancies and interstitials spread over several unit cells of the lattices concerned but coherently meshed in the host matrix. Solids exhibiting ordered or disordered intergrowth of two phases of similar structure but different compositions (Rao 1986, p. 10) could also fall under the same category. However, in the present discussion we restrict ourselves to systems which are diphasic (or multiphasic) in the phase rule sense.

There are a wide variety of nanocomposites which have been commercially exploited. Cermets consisting of fine metal grains dispersed in an oxide have been used as resistors in electronic circuits (Abeles *et al* 1975). Photosensitive, photochromic (Armistead & Stookey 1965), thermally darkenable photochromic (Seward 1975) and polychromatric glasses (Stookey *et al* 1978) depend for their respective properties on a microstructure consisting of nano-scale distribution of metal or halide particles within a glass matrix. The use of cobalt alumina cermets in solar photothermal conversion has been reported (Andersson *et al* 1980). Nano-size metal grains dispersed on a suitable substrate comprise an important group of catalysts for the chemical industry (Sinfelt 1977).

Glass-metal nanocomposites exhibit semiconduction due to electrons tunnelling from one metal grain to the next (Chakravorty *et al* 1977). In certain situations such composites have shown memory switching (Chakravorty & Murthy 1975). In some of the composites subjeeted to an ion-exchange treatment an enhanced ionic conductivity has been observed (Mozhi & Chakravorty 1982; Shrivastava & Chakravorty 1987). The latter phenomenon appears to have a correlation with the morphology of the glasses concerned at the nanolevel.

The physics of ultrafine particles has emerged as a rapidly growing field of research in recent years (Marlow 1982, p. 2). Most of the studies to date have been related to small metallic particles. Quantum-size effects have been investigated by measuring the specific heats of indium (Novotny & Meincke 1973) and palladium (Comsa *et al* 1977) nanoparticles. Analyses of electrical resistivity data for small particles of aluminium and silver show phonon softening (Ohshima *et al* 1977) as compared to that of the bulk material. Gorkov & Eliashberg (1965) theoretically predicted an anomalous enhancement of the static polarizability of fine metallic particles. Attempts at experimental verification of this phenomenon have, however, not proved successful so far (Meier & Wyder 1972; Duprec & Smithard 1972; Strassler & Rice 1972). Superconducting order as a function of particle size has been investigated theoretically (Schmidt 1967) and results predict a smooth temperature variation near the transition point. Such "rounded" phase transition in the so-called zero-dimensional superconductors has been studied by a variety of experimental techniques. Some of these are measurements of magnetic susceptibility on small aluminium particles (Buhrman & Halperin 1973), specific heat of granular aluminium films (Worthington *et al* 1978), ultrasonic attenuation in aluminium films (Tachiki *et al* 1975; Robinson *et al* 1974), nuclear magnetic resonance on fine aluminium and on tin particles (Kobayashi *et al* 1974). Thin films comprising small superconducting metallic grains have been reported to show a higher transition temperature as compared to bulk samples (Novotny & Meincke 1973). This phenomenon has been explained on the basis of surface phonon softening due to a high surface-to-volume ratio in these materials.

Apart from the effects of small size on the conventional properties of materials as explored by some of the investigations delineated above, studies on the electronic structure of ultra-fine metallic particles are expected to throw light on the understanding of the metallic and nonmetallic states of matter (Edwards 1986, p. 265). An interesting problem of fundamental importance in this regard is a possible metal-insulator transition at a critical diameter of the metallic particle (Wood & Ashcroft 1982).

It should be apparent from the above discussion that in order to investigate the effect of small size on the various physical properties of different materials one has to essentially prepare a nanocomposite comprising a distribution of small particles of the species in an inert matrix. Some of the conventional methods of preparing such composites have been discussed earlier (Chakravorty 1982). The sol-gel method has recently emerged as a versatile technique for preparing a wide variety of materials (Sen & Chakravorty 1986, p. 159). One of the most attractive features is that the processing can be carried out at fairly low temperatures. Glass-metal nanocomposites have recently been made by exploiting this method. The purpose of the present paper is to briefly review the present status of this technique.

2. Diphasic xerogels

Principles involved in the synthesis of di- or polyphasic xerogels with special reference to ceramic-metal composite systems have been discussed by Roy & Roy (1984). Two preparation routes have been proposed. In the first, a suitable solution containing all the components to be present in the ultimate product is prepared thereby forming a sol. The latter is then gelled, the process comprising the usual hydrolysis and polycondensation reactions (Yoldas 1982). After the desiccation step a xerogel is formed. Depending on the heat treatment given to the xerogel the product may lead to either a single-phase or a poly-phase material. In the second scheme the starting point is the preparation of a mixture of a sol comprising the oxide component and a solution containing the metallic salt, the latter acting as the metal phase precursor. After gelling this mixture it is dried to obtain the xerogel. This consists, in most of the cases studied by these workers, of two noncrystalline oxide phases, viz. the single component oxide and the heavy metal oxide phase, respectively. The two-phase solid prepared by either of the two processes deseribed as above is then subjected to reduction treatment in a nitrogen and hydrogen gas mixture (95% N_2, 5% H_2) at temperatures ranging from 200° to 700°C. Some of the starting materials used in the preparation of the different ceramic-metal composites are aluminium-isopropoxide, zirconyl chloride and silicon-tetraethoxide for the matrix phases and metallic salts like copper nitrate, stannous chloride and nickel nitrate for the metal phase. The presence of metallic islands of different types having diameters ranging from 5 to 50 nm has been verified by detailed electron microscopic investigation. In table 1 some of the preparational features have been summarised.

3. Glass-metal composites

Gels prepared from metal alkoxide solutions are porous and have large surface areas (Brinker & Scherer 1985). They should therefore be ideal materials for use as catalyst carriers. In fact, it was observed by Karatani & Minakuchi (1983) that glucose oxidase on silica gel made by the hydrolysis-polycondensation reaction of tetraethyl ethoxysilane exhibited a much higher enzymatic activity than that immobilized on conventional porous glasses. This high activity has been ascribed to the high density of silanol groups on the alkoxy-derived gel. This principle has been extended to the preparation of the catalyst-carrier composite, viz., small metal particles in a silica glass. Ueno *et al* (1983) prepared a catalyst system of Ni/SiO_2 by hydrolysing a mixed solution of $Si(OC_2H_5)_4$ and ethylene glycol solution of nickel hydroxide followed by drying, calcining and reduction treatment at 450°C. The metal particles were found to be highly dispersed, their sizes varying from 3 to 12 nm.

A variety of glass-metal nanocomposites have been investigated in the author's laboratory (Chakravorty 1984). Organometallic compounds have been used to prepare some composites of this type. Two approaches have been followed. In the first, a fairly low melting glass (essentially based on B_2O_3 in our case) has been prepared with a suitable organometallic compound forming one consituent of the raw materials used during the melting operation. The product after quenching has a structure consisting of fine metal granules with diameters ranging from 5–50 nm

Table 1. Summary of nanocomposites prepared by organometallic routes.

System	Method	Microstructural features	Properties measured	Reference
1. *Ceramic-metal composites* Al_2O_3: copper Platinum, Nickel Zirconia: Copper Nickel Silica: copper, Tin	Sol + solution ↓ Gel ↓ Xerogel ↓ Reduction treatment Ceramic metal composite	Noncrystalline (or microcrystalline) ceramic matrix with small metallic islands of size varying between 5–50 nm	Photosensitivity	Roy & Roy (1984) Hoffman *et al* (1984)
2. *Glass-metal composites* (a) Ni/SiO_2	Hydrolysis of a mixed solution of $Si(OC_2H_5)_4$ and ethylene glycol solution of nickel hydroxide ↓ Gel ↓ Reduction Glass-metal composite	Nickel particles of size between 3 and 12 nm	Catalytic activity	Ueno *et al* (1983)
(b) Ni/50 BaO. $50B_2O_3$ (wt%) Nickel content: varying between 0·1 and 0·3 wt%	Melting of mixture of oxide components and $Ni(C_9H_6ON)_2.2H_2O$	Nickel particles of size between 5 and 8 nm	Optical absorption Magnetic behaviour	Datta & Chakravorty (1983) Datta *et al* (1984)
(c) Ni/SiO_2 Nickel content: 0·8 wt%	Sol of $Si(OC_2H_5)_4$ and $Ni(C_9H_6ON)_2$ $2H_2O$ ↓ Gel ↓ Xerogel	Particle size between 5 and 30 nm	Magnetic behaviour	Datta *et al* (1986)
(d) Co/50BaO $50B_2O_3$ (wt%) Cobalt content 0·4 wt% (approximately)	Melting of oxide components with $[Co(C_5H_5N)_4](SCN)_2$	Particle size between 5 and 35 nm	—	S S Mitra & D Chakravorty (1986, unpublished)
e) Pd/50BaO $50B_2O_3$ (wt%) Palladium content: Varying between 0·1 and 0·3 wt% (approximately)	Melting of oxide components with $[Pd(C_5H_5N)_4](SCN)_2$	Particle size between 3 and 9 nm	—	S S Mitra & D Chakravorty (1986, unpublished)

dispersed in the glass matrix. The choice of the organometallic species obviates the need for the reduction step as followed by previous workers. It is believed that

favourable oxygen fugacities are attainecl locally within the melt as a result of the breaking up of the compound which releases carbon, hydrogen and nitrogen atoms. The composites prepared so far consist of nickel, cobalt and palladium respectively in a barium borate glass. Nickel has been introduced in the form of oxinate $Ni(C_9H_6ON)_2.2H_2O$ (Datta & Chakravorty 1983), cobalt and palladium as complexes formed between pyridine and the corrcsponding thiocyanates $[Co(C_5H_5N)_4](SCN)_2$ and $[Pd(C_5H_5N)_4](SCN)_2$, respectively. The amounts of metal content in the glasses range between 0·1 and 0·4 wt%.

In the second teehnique, a sol is first prepared containing both the glass and the metal precursors, viz. silicon tetraethoxide and nickel oxinate, in ethyl alcohol. The sol is then allowed to gel and subsequently dried, cooled and then heat-treated to a temperature of around 750°C for 2 h (Datta *et al* 1986). The resultant product has a microstructure consisting of fine metallic nickel granules having diameters in the range 5 to 30 nm dispersed in the silica glass matrix. Table 1 gives a summary of the salient features of the preparational and characterization aspects of the above materials.

So far the physical properties investigated comprise only the optical obsorption (Datta & Chakravorty 1983), magnetic susceptibility and EPR (Datta *et al* 1984, 1986). The optical absorption has been explained satisfactorily on the basis of the usual effective medium thcories (Granqvist & Hunderi 1977). Low temperature magnetic susceptibility of nickel nanogranules in borate glass shows a broad range of transition temperatures between 77 K and 300 K. A similar trend has also becn shown by the EPR data. The results indicate a superparamagnetic behaviour. It is expected, however, that with narrow distribution of particle sizes of the metallic species effected by controlling the process parameters, it will be possible to undertake investigations on some of the fundamental aspects of fine particle physics.

4. Concluding remarks

Organometallic compounds have been used to make nanocomposite materials of the ceramic-metal and glass-metal varieties respectively. The processing parameters have been investigated by several workers. It now seems possible to combine a wide variety of metallic species with different oxide systems in a composite structure by suitable choice of starting materials. A more recent innovation has bcen to exploit the compositional heterogeneity on a "nano" scale to make densified products in several oxidc systems (Komarneni *et al* 1986). It is expected that the sol-gel technique of materials processing of the type discussed in this article will lead to preparation of materials exhibiting novel physical properties.

References

Abeles B, Sheng P, Coutts M D, Arie Y 1975 *Adv. Phys.* 24: 407–461
Andersson A, Hunderi O, Granqvist C G 1980 *J. Appl. Phys.* 51: 754–764
Armistead W H, Stookey S D 1965 US Pat. no. 3108860
Brinker C J, Scherer G W 1985 *J. Non-Cryst. Solids* 70: 301–322
Buhrman R A, Halperin W P 1973 *Phys. Rev. Lett.* 30: 692–695

Chakravorty D 1982 *Curr. Sci.* 51: 671–676
Chakravorty D 1984 *Bull. Mater. Sci.* 6: 193–200
Chakravorty D, Bandyopadhyay A K, Nagesh V K 1977 *J. Phys. D: Appl. Phys.* 10: 2077–2087
Chakravorty D, Murthy C S 1975 *J. Phys. D: Appl. Phys.* 8: L162–L165
Comsa G H, Heitkamp D, Rade H S 1977 *Solid State Commun.* 24: 547–550
Datta S, Bahadur D, Chakravorty D 1984 *J. Phys. D: Appl. Phys.* 17: 163–169
Datta S, Chakravorty D 1983 *J. Mater. Sci. Lett.* 2: 329–331
Datta S, Mitra S S, Chakravorty D, Ram S, Bahadur D 1986 *J. Mater. Sci. Lett.* 5: 89–90
Dupree R, Smithard M A 1972 *J. Phys. C: Solid State Phys.* 5: 408–414
Edwards P P 1986 in *Advances in solid state chemistry* (ed.) C N R Rao (New Delhi: Indian National Science Academy)
Gorkov L P, Eliashberg G M 1965 *Zh. Eksp. Teor. Fiz.* 48:1407 [Engl. Transl.: *Sov. Phys. JETP* 1965 21: 940–947]
Granqvist C G, Hunderi O 1977 *Phys. Rev.* B16: 3513–3534
Hoffman D, Komarneni S, Roy R 1984 *J. Mater. Sci. Lett.* 3: 439–442
Karatani H, Minakuchi H 1983 *J. Chem. Soc. Jpn.* (11): 1577 (in Japanese)
Kobayashi S, Takahashi T, Sasaki W 1974 *J. Phys. Soc. Jpn.* 36: 714–719
Koch F B, Cohen J B 1969 *Acta Cryst.* B25: 275–287
Komarneni S, Suwa Y, Roy R 1986 *J. Am. Ceram. Soc.* 69[7]: C155–C156
Marlow W H (ed.) 1982 *Aerosol microphysics II* (Berlin, Heidelberg, New York: Springer Verlag)
Meier F, Wyder P 1972 *Phys. Lett.* A39: 51–52
Mozhi T A, Chakravorty D 1982 *J. Mater. Sci. Lett.* 1: 426–428
Novotny V, Meincke P P M 1973 *Phys. Rev.* B8: 4168–4199
Ohshima K, Fujita T, Kuroishi T 1977 *J. Phys. (Paris)* C2–38: 163–165
Rao C N R (ed.) 1986 *Advances in solid state chemistry* (New Delhi: Indian National Science Academy)
Robinson D A, Maki K, Levy M 1974 *Phys. Rev. Lett.* 32: 709–712
Roy R A, Roy R 1984 Mater. Res. Bull. 19: 169–177
Schmidt V V 1967 in *Proc. 11th Int. Conf. on Low Temperature Physics* (ed.) M P Malkow (Moscow: Moscow Publishing House)
Sen A, Chakravorty D 1986 in *Advances in solid state chemistry* (ed.) C N R Rao (New Delhi: Indian National Science Academy)
Seward T P III 1975 *J. Appl. Phys.* 46: 689–694
Shrivastava A, Chakravorty D 1987 *J. Phys. D: Appl. Phys.* 20: 380–385
Sinfelt J H 1977 *Science* 195: 641–646
Stookey S D, Beall G H, Pierson J E 1978 *J. Appl. Phys.* 49: 5114–5123
Strassler S, Rice M J 1972 *Phys. Rev.* B6: 2575–2577
Tachiki M, Salvo H, Robinson D A, Levy M 1975 *Solid State Commun.* 17: 653–656
Ueno A, Suzuki H, Kotera Y 1983 *J. Chem. Soc., Faraday Trans.* 79: 127–136
Willis B T M 1964 *Proc. Br. Ceram. Soc.* 1: 9
Wood D M, Ashcroft N W 1982 *Phys. Rev.* B25: 6255–6276
Worthington T, Lindenfeld P, Deutscher G 1978 *Phys. Rev. Lett.* 41: 316–319
Yoldas B E 1982 *J. Non-Cryst. Solids* 51: 105–121

High-temperature ceramic oxide superconductors[+]

C N R RAO

Solid State and Structural Chemistry Unit, Indian Institute of Science, Bangalore 560 012, India

Abstract. High-temperature superconductivity in oxides of the type $La_{2-x}Ba_x(Sr_x)CuO_4$, $YBa_2Cu_3O_{7-\delta}$, $La_{3-x}Ba_{3+x}Cu_6O_{14}$ and Bi(Tl)-Ca-Sr(Ba)-Cu-O systems is discussed, with special emphasis on the experimental findings from the author's laboratory. The importance of holes on oxygen and of the Cu^{1+} (d^{10}) state is examined. A transition is shown to occur from chain- to sheet-superconductivity in $YBa_2Cu_3O_{7-\delta}$ accompanying a change in oxygen stoichiometry. Some of the important material parameters and technological applications are briefly presented. There is every hope that materials with T_c close to room temperature will be discovered in the near future. All the high T_c oxides found hitherto have perovskite-related structures with two-dimensional Cu-O sheets.

Keywords. High-temperature superconductivity; ceramic oxide superconductors; bismuth cuprates; thallium cuprates; $LnBa_2Cu_3O_7$; rare earth cuprates.

1. Introduction

The phenomenon of superconductivity has been an area of vital interest for the past several decades, ever since Kammerlingh Onnes discovered in 1911 that mercury becomes superconducting at 4·2 K. Many materials, mostly metals and alloys, and more recently, molecular systems including organic charge-transfer compounds, have been investigated for superconductivity, but the superconducting transition temperature did not cross 23 K till 1986. The average rate of increase in T_c was about 3 degrees per decade and it appeared as though 23 K was the upper limit for the T_c. The highest T_c's (in the 20 K region) were exhibited by the A15 compounds such as Nb_3Sn and Nb_3Ge. Some of the metal oxides also showed superconductivity, the highest T_c amongst them being exhibited by $BaPb_{1-x}Bi_xO_3$ and $LiTi_2O_4$, both around 13 K.

Bednorz & Mueller (1986) showed the possibility of high-temperature superconductivity in oxides of the La-Ba-Cu-O system. It was established in January 1987 that these oxides had the general formula $La_{2-x}Sr_x(Ba_x)CuO_4$ and possessed the K_2NiF_4 structure; T_c values in these oxides were in the 20–40 K region, the compositions corresponding to the maximum T_c in the Sr and Ba systems being $x = 0{\cdot}2$ and 0·15, respectively (Cava *et al* 1987; Chu *et al* 1987; Ganguly *et al* 1987a;

[+]Contribution No. 485 from the Solid State and Structural Chemistry Unit.

Uchida *et al* 1987). Following on the heels of this discovery, superconductivity above liquid nitrogen temperature was reported in March 1987 in the Y-Ba-Cu-O system (Wu *et al* 1987). It was soon found that the oxide responsible for superconductivity in this system did not possess the K_2NiF_4 structure, but instead had the defect perovskite structure with the composition $YBa_2Cu_3O_{7-\delta}$ (Ganguly *et al* 1987b; Rao *et al* 1987b; Siegrist *et al* 1987). In the last few weeks, the big news has been the discovery of superconductivity in Bi and Tl cuprates containing alkaline earth metals; these oxides show T_c's in the 100–120 K range (Chu *et al* 1988; Ganguli *et al* 1988; Rao *et al* 1988; Subramanian *et al* 1988; Sheng & Hermann 1988).

The discovery of superconductivity above the liquid nitrogen temperature in oxide materials has raised much hope because of its important technological implications. Equally importantly, this has given a big boost to research in ceramic oxides. In what follows, some of the highlights of research on high T_c oxide superconductors will be presented, with particular reference to the results obtained in the author's laboratory (Rao 1988). In addition, some of the special features of these ceramic oxides will be indicated along with their possible technological applications. It may be remarked here that research efforts in this laboratory related to the high-temperature superconducting oxides were initiated in the early part of January 1987, soon after information about the $La_{2-x}Ba_x(Sr_x)CuO_4$ system became available through the American participants in the International Conference on Valence Fluctuation held in Bangalore.

2. $La_{2-x}Ba_x(Sr_x)CuO_4$

Oxides of the general formula A_2BO_4 possess the quasi two-dimensional K_2NiF_4 structure (figure 1) wherein the B ions interact only in the *ab* plane. The structure and properties of the oxides of the K_2NiF_4 system have been examined in some detail recently by Ganguly & Rao (1984). It has been known for sometime that orthorhombic La_2CuO_4 is a relatively low-resistivity material ($\sim$1 ohm cm at 300 K, see figure 2) and becomes antiferromagnetic at low temperatures. Substitution of La by Ba or Sr in $La_{2-x}Ba_x(Sr_x)CuO_4$ ($x > 0{\cdot}05$) makes the structure tetragonal (at room temperature) and superconductivity manifests itself at low temperatures (Rao & Ganguly 1987a). Superconductivity is also found in the 15–40 K region in oxides of the type $(La_{1-y}Ln_y)_{2-x}Ba_x(Sr_x)CuO_4$ where Ln = Pr, Nd, Gd etc. (Ganguly *et al* 1987a; Mohan Ram *et al* 1987a). These oxides, containing planar CuO_2 units, show maximum T_c around a specific value of x (Sreedhar *et al* 1987). Electrical resistivity values of these oxides in the normal state above T_c are in the $10^{-2}-10^{-3}$ ohm.cm range (figure 2) which correspond closely to Mott's minimum metallic conductivity (Rao & Ganguly 1985).

There have been several investigations of La_2CuO_4 and $La_{2-x}Ba_x(Sr_x)CuO_4$ in the last few months. Antiferromagnetism in La_2CuO_4 has been established by neutron scattering and diffraction studies, the T_N being close to 290 K with a low-temperature Cu-moment of 0·43 μ_B (Mitsuda *et al* 1987). Besides establishing the magnetic structure, these studies have shown the occurrence of the orthorhombic-tetragonal distortion at 505 K. Muon spin rotation has also been employed to examine antiferromagnetism in La_2CuO_4 (Uemura *et al* 1987). The work of Shirane *et al* (1987) has shown that La_2CuO_4 is in a 2-dimensional *afm* quantum fluid state wherein spins are ordered instantaneously over long distances, but there is no

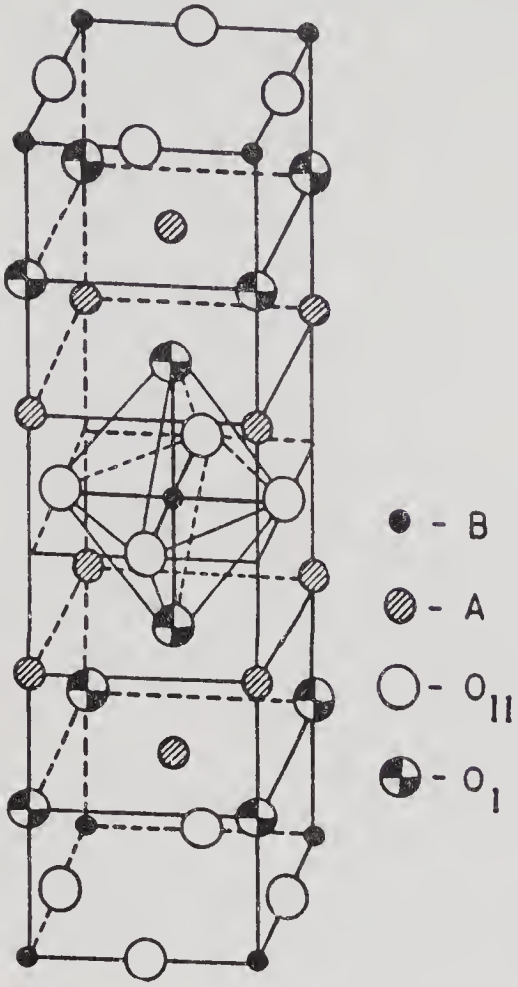

Figure 1. The K_2NiF_4 structure of oxides of the formula A_2BO_4.

measurable time-averaged moment. More interestingly, studies of oxygen-excess La_2CuO_4 has shown it to be superconducting with a T_c of 40 K (Beille *et al* 1987); La-deficient samples also exhibit superconductivity in this temperature region.

Superconducting $La_{2-x}Ba_x(Sr_x)CuO_4$ undergoes a tetragonal-orthorhombic distortion around 180 K (Day *et al* 1987; Paul *et al* 1987). ESR studies have thrown light on microscopic magnetic interactions in these oxides (Thomann *et al* 1987). Static and dynamic aspects of the tetragonal-orthorhombic distortion in $La_{2-x}Sr_xCuO_4$ have been studied by neutron scattering and related studies and a classical soft phonon behaviour involving CuO_6 octahedra has been observed (Birgeneau *et al* 1987).

3. $YBa_2Cu_3O_{7-\delta}$ and related oxides

Wu *et al* (1987) reported superconductivity above liquid N_2 temperature in $Y_{1.2}Ba_{0.8}CuO_4$. This composition was actually biphasic, consisting of green Y_2BaCuO_5 and a black oxide. We had initiated studies (Ganguly *et al* 1987b) on the Y-Ba-Cu-O system with compositions of the type $Y_{3-x}Ba_{3+x}Cu_6O_{14-\delta}$ by analogy with $La_{3-x}Ba_{3+x}Cu_6O_{14-\delta}$ (Er-Rakho *et al* 1981). This was because Y_2CuO_4 (unlike La_2CuO_4) does not crystallize in the K_2NiF_4 structure. By comparing the X-ray diffraction patterns of $Y_{3-x}Ba_{3+x}Cu_6O_{14-\delta}$ and Y_2BaCuO_5, it was possible to identify the phase responsible for the high T_c (90–95 K) superconductivity as

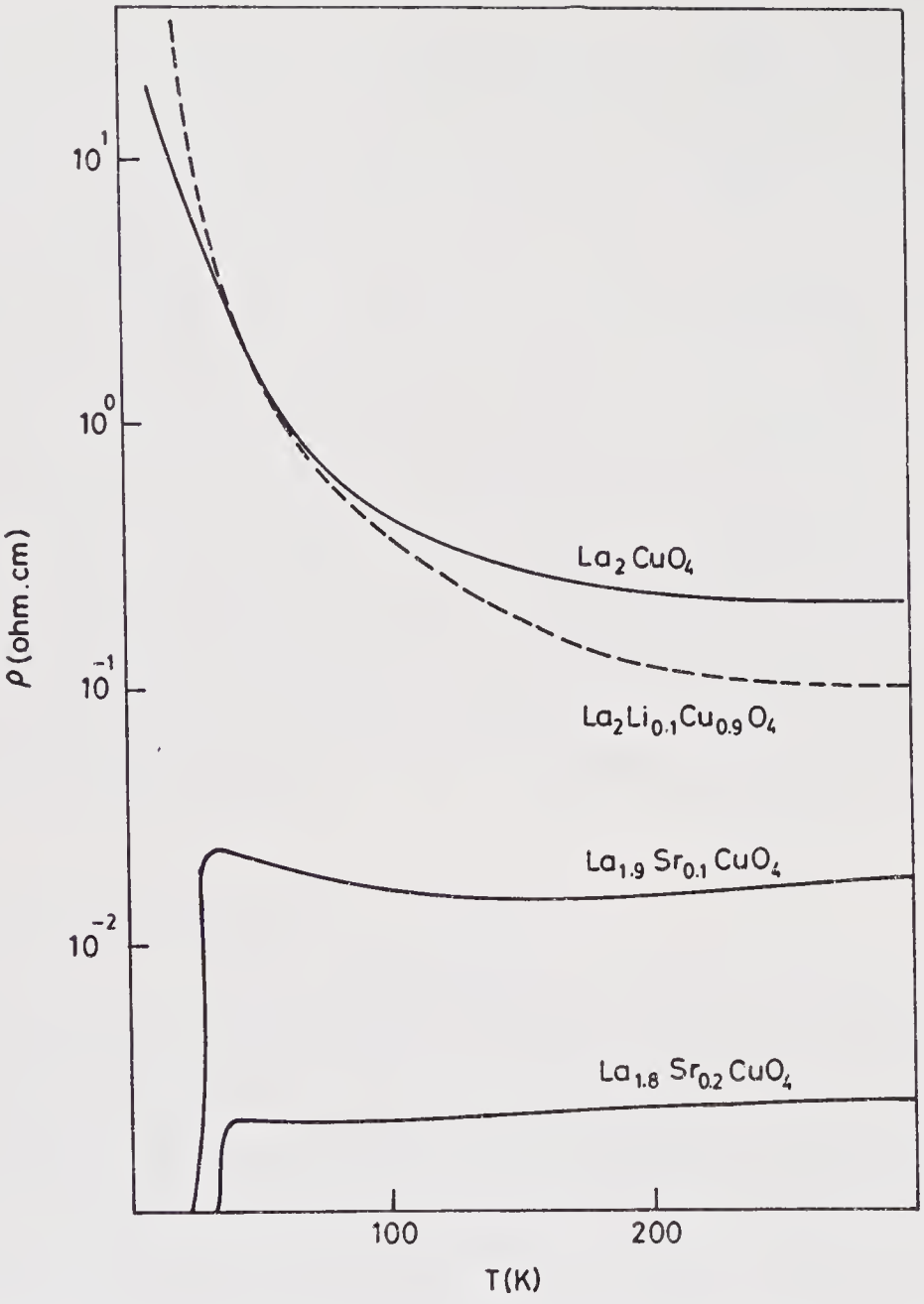

Figure 2. Electrical resistivity behaviour of $La_{2-x}Sr_xCuO_4$ and La_2CuO_4 (from Ganguly *et al* 1987a).

orthorhombic $YBa_2Cu_3O_{7-\delta}$ (Rao *et al* 1987b). AC susceptibility (Meissner effect) measurements showed the superconductivity to be a bulk property. Soon, many other related oxides such as $Y_{1-x}Ln_xBa_2Cu_3O_{7-\delta}$ (Ln = La, Lu etc) as well as $LnBa_2Cu_3O_{7-\delta}$ (Ln = Er, Dy, Gd etc.) were found to be high T_c superconductors, all with $T_c \approx 90$ K (Mohan Ram *et al* 1987b; Raychaudhuri *et al* 1987; Tarascon *et al* 1987; Xiao *et al* 1987). Obviously Y and Ln ions play no role in the superconductivity; they only help to keep the structure together.

Superconductivity in $YBa_2Cu_3O_{7-\delta}$ is extremely sensitive to oxygen stoichiometry (Rao *et al* 1987a, 1988a; Rao & Ganguly 1987b). Thus, the $\delta \geqslant 0{\cdot}6$ sample is non-superconducting and tetragonal. Oxygen is readily intercalated into the $\delta \geqslant 0{\cdot}5$

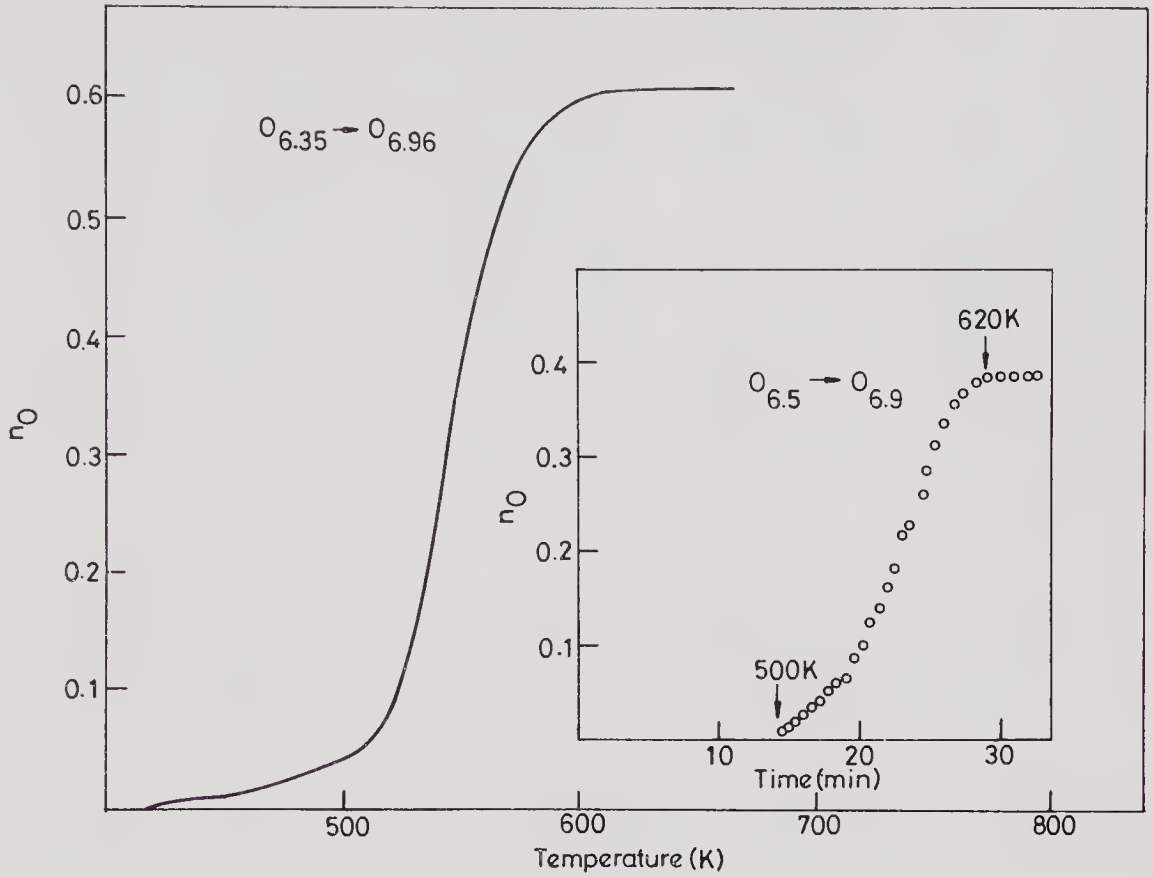

Figure 3. TGA curves showing the oxidation of $YBa_2Cu_3O_{6\cdot5}$ to $YBa_2Cu_3O_7$. Inset shows the rate of oxygen intercalation in a $O_{6\cdot5}$ sample (from Rao *et al* 1988a).

samples and the stoichiometry reaches close to $YBa_2Cu_3O_7$ on intercalation (figure 3). Structures of the orthorhombic ($\delta = 0\cdot0$) and the tetragonal ($\delta = 1\cdot0$) phases differ in an interesting manner. Besides the CuO_2 sheets, the stoichiometric ($\delta = 0\cdot0$) phase contains Cu-O-Cu chains (or corner-linked CuO_4) units which are absent in the non-superconducting ($\delta = 1\cdot0$) sample (David *et al* 1987; Bordet *et al* 1987). In figure 4 we compare the orthorhombic and tetragonal structures of the $\delta = 0\cdot0$ and the $\delta = 1\cdot0$ samples. In the $\delta = 0\cdot6 - 1\cdot0$ range, it seems that the tetragonal phase has disordered oxygens giving rise to distorted CuO_6 octahedra as indicated in figure 4c (Jorgensen *et al* 1987). In general, oxygen non-stoichiometry in the $YBa_2Cu_3O_{7-\delta}$ system has to be understood in terms of both disorder and structural distortion.

The variation of the superconducting transition temperature of orthorhombic $YBa_2Cu_3O_{7-\delta}$ with δ (in the δ-range 0·0–0·5) is most interesting. In figure 5, the resistivity data of a few members with different δ values is shown while in figure 6, the T_c values from the resistivity data are plotted against δ (Rao *et al* 1988a). In figure 6, we also show results from the magnetic measurements of Johnston *et al* (1987). Although the actual T_c values vary in the different sets of data (figure 6), we see that the T_c is nearly constant around 90 K at low δ (0·0–0·2) and drops to a lower value ($\sim$60 K) above $\delta = 0\cdot2$ showing a plateau-like behaviour. The T_c in the plateau region is similar to that of $La_{2-x}Ba_x(Sr_x)CuO_4$ (of the K_2NiF_4 structure). Since in this composition range, the Cu-O-Cu chains of $YBa_2Cu_3O_7$ will be depleted, we believe that the $\sim$60 K plateau is characteristic of superconductivity due to CuO_2

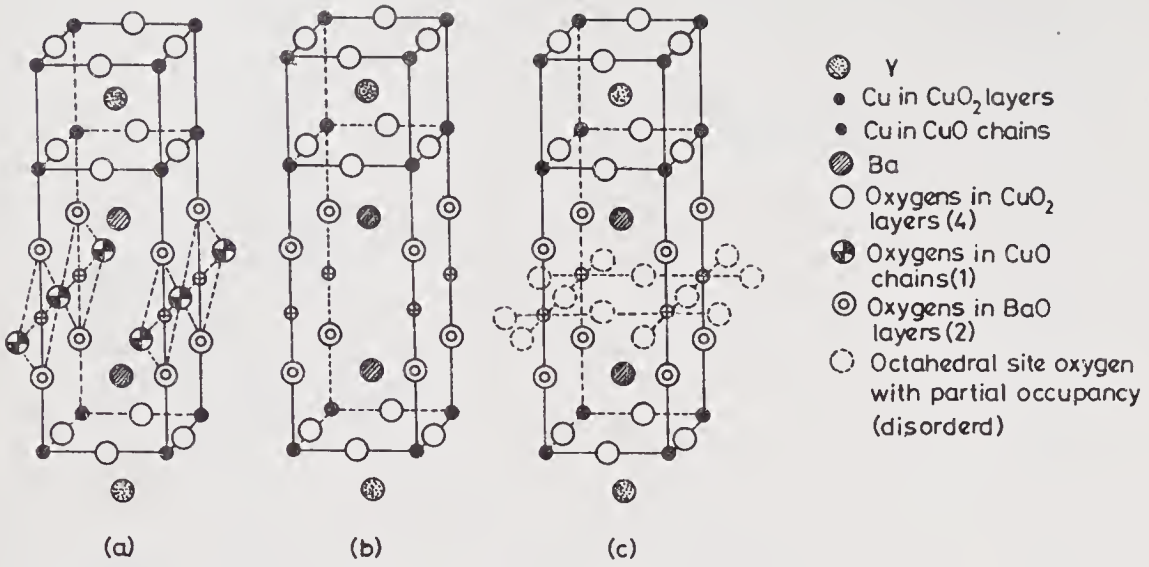

Figure 4. Structures of $YBa_2Cu_3O_{7-\delta}$: (a) Orthorhombic structure of the superconducting phase with $\delta = 0{\cdot}0$; (b) tetragonal structure of the non-superconducting phase with $\delta = 1{\cdot}0$; (c) disordered structure of the tetragonal phase with CuO_6 octahedra (where the site occupancy is small).

sheets while the 90 K T_c is characteristic of the sheets in the presence of Cu-O-Cu chains. Figure 6 may therefore be taken to represent a transition from chain-type to sheet-type superconductivity brought about by the change in oxygen stoichiometry.

Several workers have in recent months synthesised derivatives of $YBa_2Cu_3O_{7-\delta}$ where Cu is substituted by Zn, Ni, Co, Fe and such ions or Ba is substituted by La and other ions. Such substitution in general lowers T_c or destroys the superconductivity, the oxide generally being tetragonal and oxygen-deficient. It should be noted that non-superconducting $YBa_2Cu_3O_{7-\delta}$ compositions also possess the tetragonal structure. Weakly orthorhombic or nearly tetragonal samples prepared by low-temperature methods are non-superconducting as well. Bulk superconductivity has, however, been recently reported in tetragonal $YBa_2(Cu_{0{\cdot}96}Co_{0{\cdot}4})_3O_{7-\delta}$ (Langen *et al* 1988).

4. Other La-Ba-Cu-O and related systems

The $La_{3-x}Ba_{3+x}Cu_6O_{14+\delta}$ family of oxides were considered to be high T_c superconductors (Mitzi *et al* 1988) even though they did not possess Cu-O chains (Er-Rakho *et al* 1981). It is now known that these oxides are related to the 123 oxides (Segre *et al* 1987), the relative occupation of the 01/05 sites determining the orthorhombicity. Truly high T_c is found in this system only in the orthorhombic structure when $x = 1$, $\delta \approx 0{\cdot}0$ (Ganapathi *et al* 1988). All other compositions ($x \neq 1$, $\delta \neq 0{\cdot}0$) are generally tetragonal. In figure 7, the various rare-earth-containing families of oxides investigated by us for superconductivity are shown.

5. Bismuth and thallium cuprates

Two new families of superconducting cuprates with structures related to the

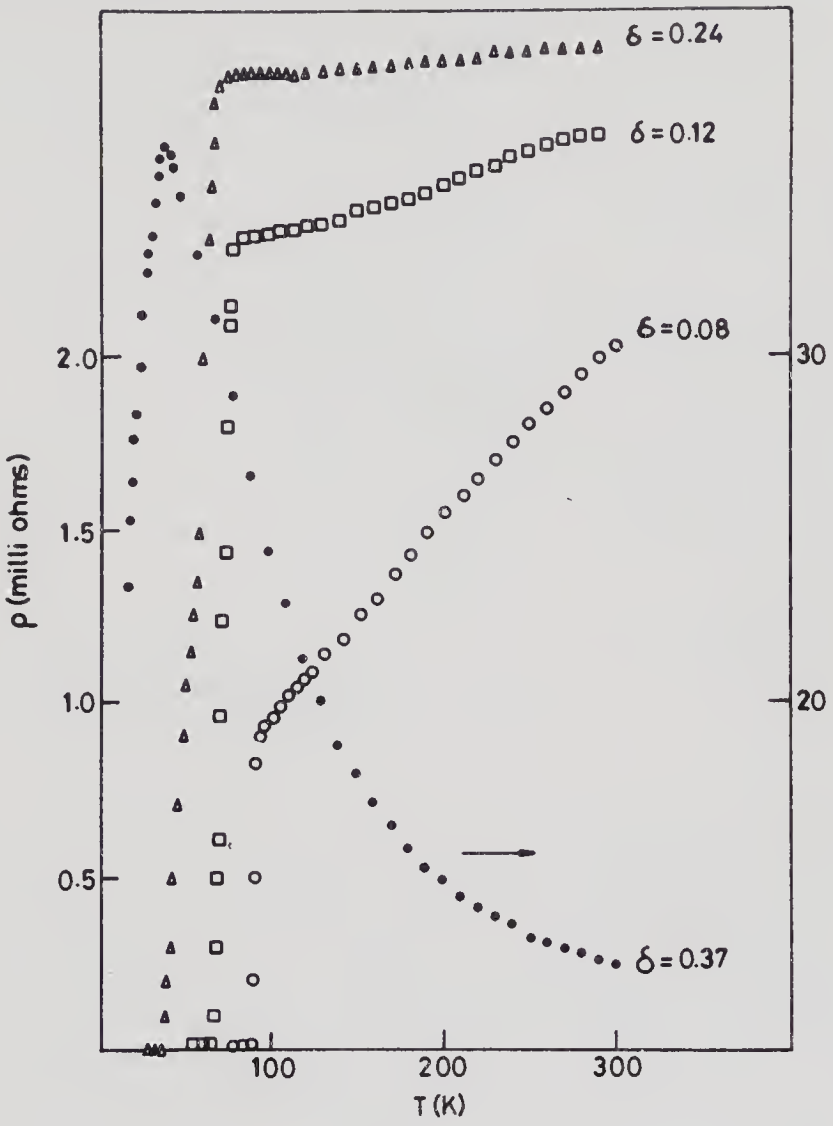

Figure 5. Electrical resistivity behaviour of $YBa_2Cu_3O_{7-\delta}$ for different values of δ (unpublished results from this laboratory).

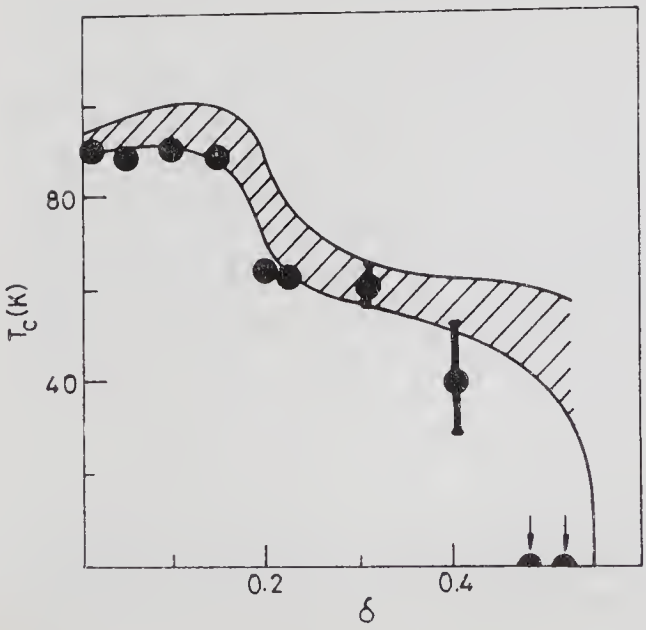

Figure 6. Variation of T_c of $YBa_2Cu_3O_{7-\delta}$ with δ. Magnetic measurements of Johnston *et al* (1987) are indicated by the cross-hatched region. Our resistivity data are shown by full dark circles (from Rao *et al* 1988a).

(21) $La_{2-x}Ba_x(Sr_x)CuO_4$ (SC)

(212) $La_2SrCu_2O_6$

(415) $La_4BaCu_5O_{13}$

(336) $La_{3-x}Ba_{3+x}Cu_6O_{14-\delta}$ (SC)

(123) $LnBa_2Cu_3O_{7-\delta}$ (SC)
(Ln = La, Y, Eu, Gd, Ho, Er etc)
$(Ln,Ba)_{n+1}Cu_nO_{3n+1}$

(212) $Ln_2BaCu_2O_x$
$LnBa_2Cu_2O_x$

(223) $Ln_2Ba_2Cu_3O_x$

Figure 7. Various families of oxides investigated for superconductivity. SC stands for superconducting. Numbers in parenthesis on the left of each system are the popular designations.

Aurivillius family of oxides with T_c's in the 100 K region have been discovered. The initial discovery of superconducting bismuth cuprates was by Michel *et al* (1987) who found T_c in the 7–22 K range in oxides of the type $Bi_2Sr_2Cu_2O_{7+\delta}$. Maeda *et al* (1988) then found high T_c (~ 100 K) in a Bi-Ca-Sr-Cu-O system. High T_c superconductivity (≈ 110 K) is exhibited by bismuth cuprates of the type $Bi_2(Ca,Sr)_3Cu_2O_{8+\delta}$ (Chu *et al* 1988; Hazen *et al* 1988; Rao *et al* 1988; Subramanian *et al* 1988; Tarascon *et al* 1988). In figure 8, we compare the structures of $Bi_4Ti_3O_{12}$ with that of $Bi_2CaSr_7Cu_2O_9$. In figure 9, we show the variation of resistivity and AC susceptibility of a sample to indicate the high T_c behaviour. The bismuth cuprates have less oxygen lability and seem to be more stable. The exact composition of the 110 K material is more complex than that indicated by the formula $Bi_2(Ca,Sr)_3Cu_2O_{8+\delta}$.

Thallium cuprates of the Tl-Ba-Cu-O and Tl-Ca-Ba-Cu-O systems show high T_c superconductivity with onset in the 100–120 K range (Hazen *et al* 1988; Ganguli *et al* 1988; Sheng & Hermann 1988). In figures 10 and 11, we show the resistivity and susceptibility behaviour of typical members of the Tl-Ca-Ba-Cu-O system. The structure of the 2122 oxide is identical to that of the corresponding bismuth compound, $Bi_2CaSr_2Cu_2O_{8+\delta}$. All these oxides of Bi and Tl contain Cu-O sheets.

Electron microscopic studies of the Bi and Tl cuprates show the extensive presence of defects and dislocations just as in the Aurivillius family of oxides. Intergrowths are also present in these systems and they may be responsible for the high T_c's (200–300 K) found in some of the samples in this laboratory.

6. Role of oxygen

Having established the crucial role of oxygen in the superconductivity of these ceramic oxides, we have further explored the mechanism of superconductivity by means of X-ray photoemission and related studies. Variable-temperature XPS studies

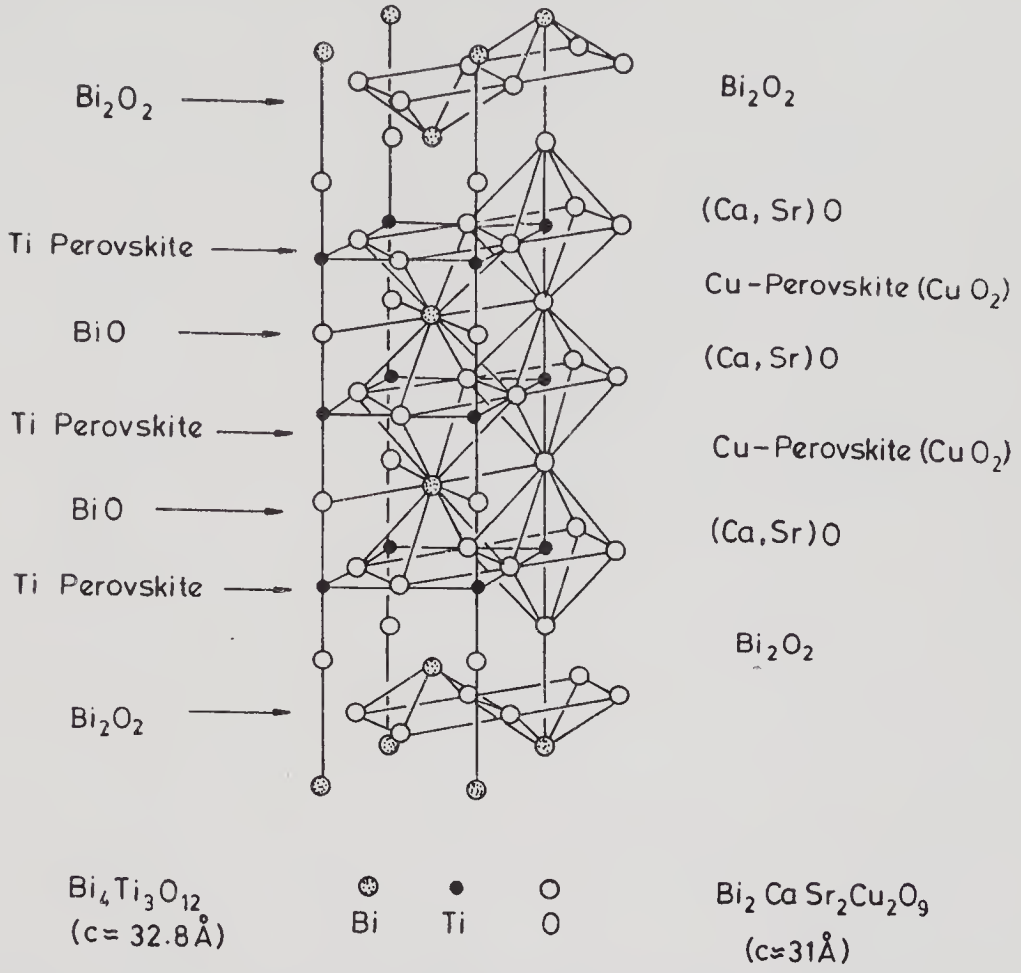

Figure 8. Structure of the orthorhombic Aurivillius phase $Bi_4Ti_3O_{12}$ and a likely structure of orthorhombic $Bi_2CaSr_2Cu_2O_9$. The recently reported X-ray structure (Subramanian *et al* 1988) of the latter is identical to this.

on $La_{1.8}Sr_{0.2}CuO_4$ and $YBa_2Cu_3O_7$ in the O(1s) and Cu(2*p*) regions (Sarma & Rao 1987; Sarma *et al* 1987) show the presence of molecular oxygen species (probably in the peroxide form) with a high O(1s) binding energy of ~533 eV, the proportion of which increases with the lowering of temperature (figure 12). The Cu(2*p*) spectrum shows the presence of a well-screened d^{10} state (Cu^{1+}) at 933 eV along with a poorly screened d^9 state (Cu^{2+}) at 942 eV. The proportion of the d^{10} state increases with the lowering of temperature. There is no evidence for Cu^{3+} in the Cu(2*p*) or Auger spectra. Auger spectra however clearly show the presence of Cu^{1+} (figure 13). Based on these findings, it is proposed that holes are present on oxygen rather than on copper in $YBa_2Cu_3O_7$ and $La_{2-x}Ba_x(Sr_x)CuO_4$ (note that both are hole conductors). The oxygen holes (O^-) could then dimerize to give peroxide-type species (O_2^{2-}). Such oxygen holes are found in the Tl and Bi cuprates as well. Holes in the O(2*p*) valence bands are favoured by the Cu^{1+} (d^{10}) state, just as holes in the S(3*p*) or Se(4*p*) valence bands are generally favoured in Cu^{1+} chalcogenides.

7. Some unusual features of the ceramic oxide superconductors

The most unusual feature of the new sensational high-T_c oxides is that they are

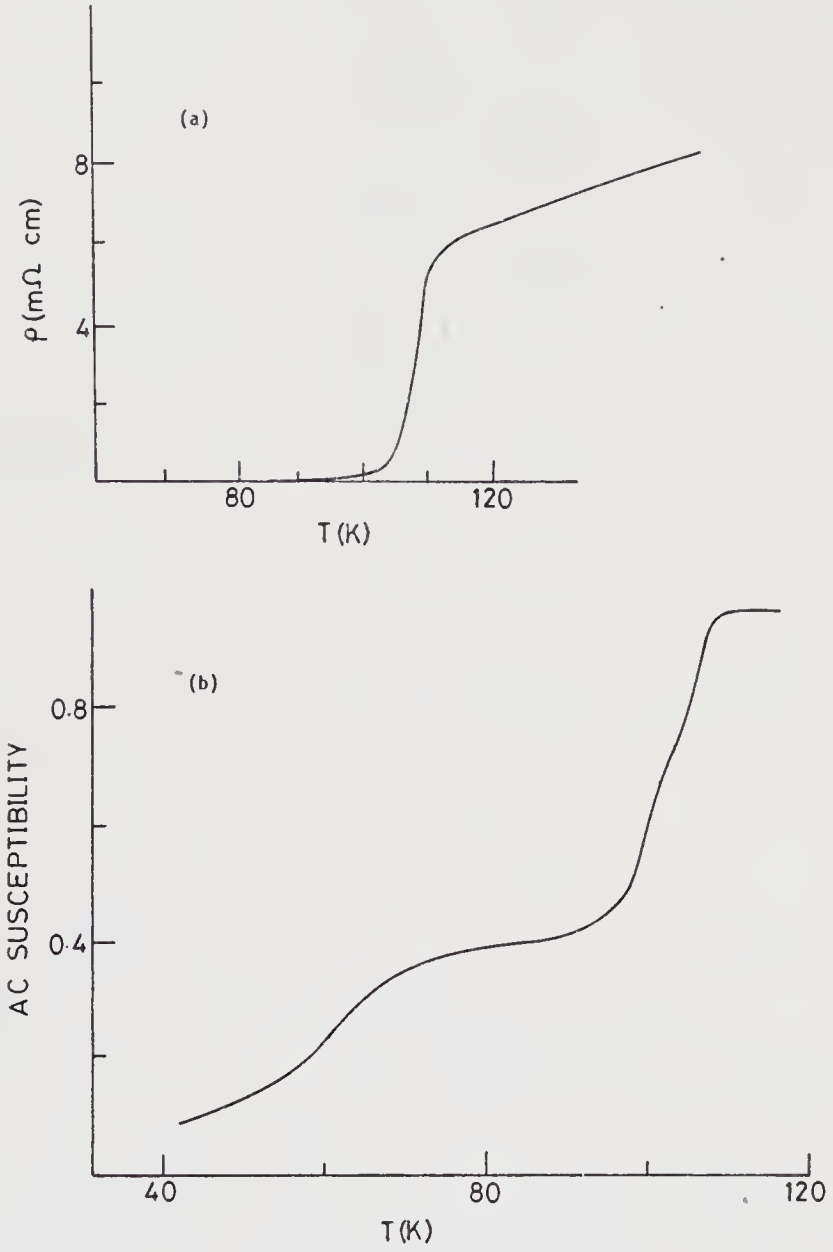

Figure 9. Resistivity and AC susceptibility data of a sample of $Bi_2(Ca,Sr)_3Cu_2O_{8+\delta}$. (From Tarascon *et al* 1988.)

ceramic materials (and not metals). As mentioned earlier, in the normal state, they are poor conductors. While $La_{2-x}Sr_xCuO_4$ seems to exhibit measurable ^{18}O isotope effect, there appears to be essentially no isotope effect in the $YBa_2Cu_3O_{7-\delta}$ system (Batlogg *et al* 1987). This means that the traditional BCS* theory is not valid in these oxide superconductors. While electron-phonon interaction could still play an indirect role, the actual nature of the role is not clear at present. The optical gap in $YBa_2Cu_3O_7$ seems to be $\sim 200\ cm^{-1}$ (Cardona *et al* 1987; Genzel *et al* 1987). A high-energy excitonic band (0·5 eV) whose intensity varies with T_c seems to be present in $La_{2-x}Sr_xCuO_4$ and this may be of significance. Such bands need to be further explored. While a large number of papers on theoretical models have appeared in the

*BCS – Bardeen, Cooper, Schreiffer

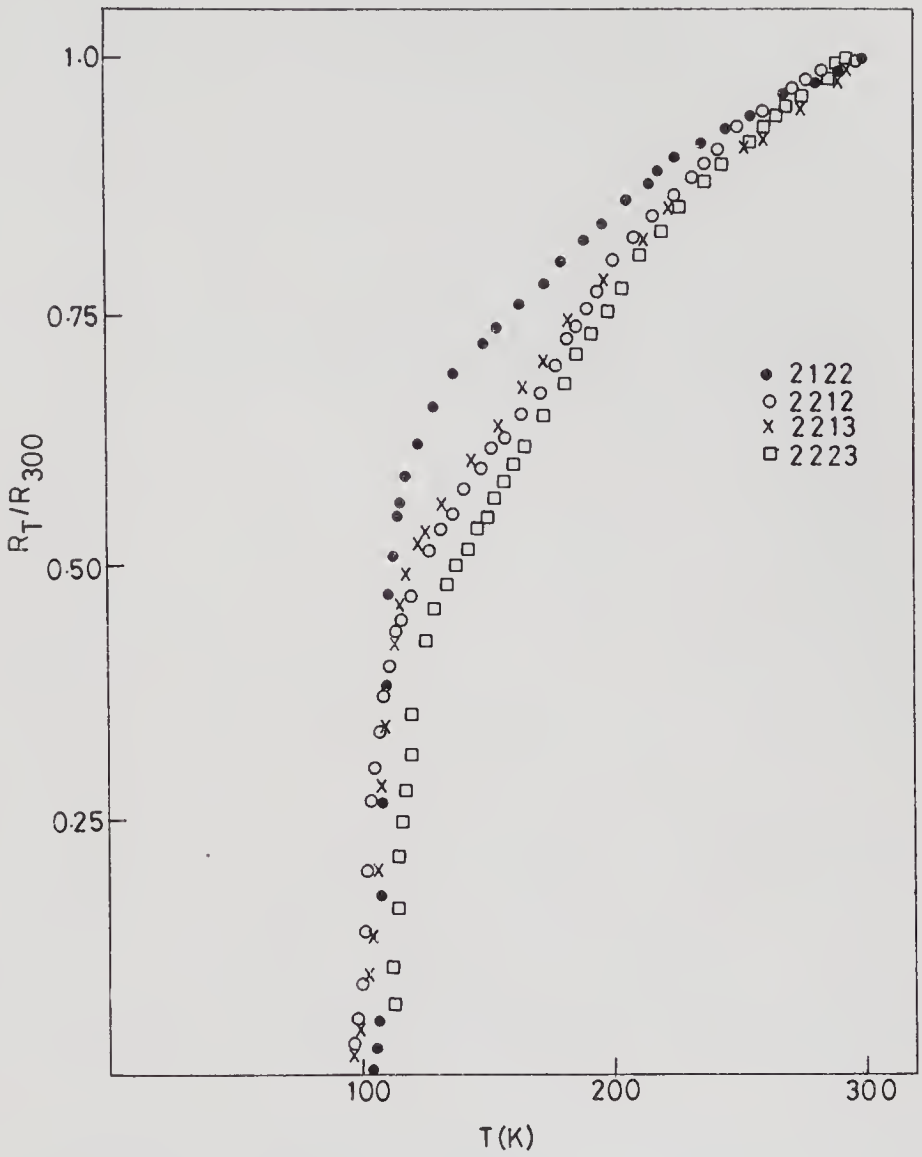

Figure 10. Resistivity behaviour of 2122, 2212, 2213 and 2223 members of the Tl-Ca-Ba-Cu-O system (from the author's laboratory). Better samples of 2223 show a T_c of 125 K.

literature in the last few months, there is yet no simple model or theory to explain high T_c in the oxide superconductors. It seems best to get good experimental data and look for models later. One of the noteworthy features is that T_c seems to increase with the number of Cu-O layers in the unit cell. The oxygen hole concentration also seems to increase in the same direction as T_c.

Electron microscopic studies of $YBa_2Cu_3O_7$ show the presence of certain domains (see figure 14) and twin boundaries in addition to other defects (see for example, Rao *et al* 1987c, 1988a; Subbanna *et al* 1987). The nature of the domains is causing curiosity. Noting that the coherence length is only a few angstroms, people are wondering about the origin and implications of such domains. Are they due to the co-occurrence of metallic and insulating phases (with different stoichiometry)? If so, what does the observed structure mean? The broad bands or domains (figure 14) found by us sometime ago (Rao *et al* 1987c), seem to be due to different orientations

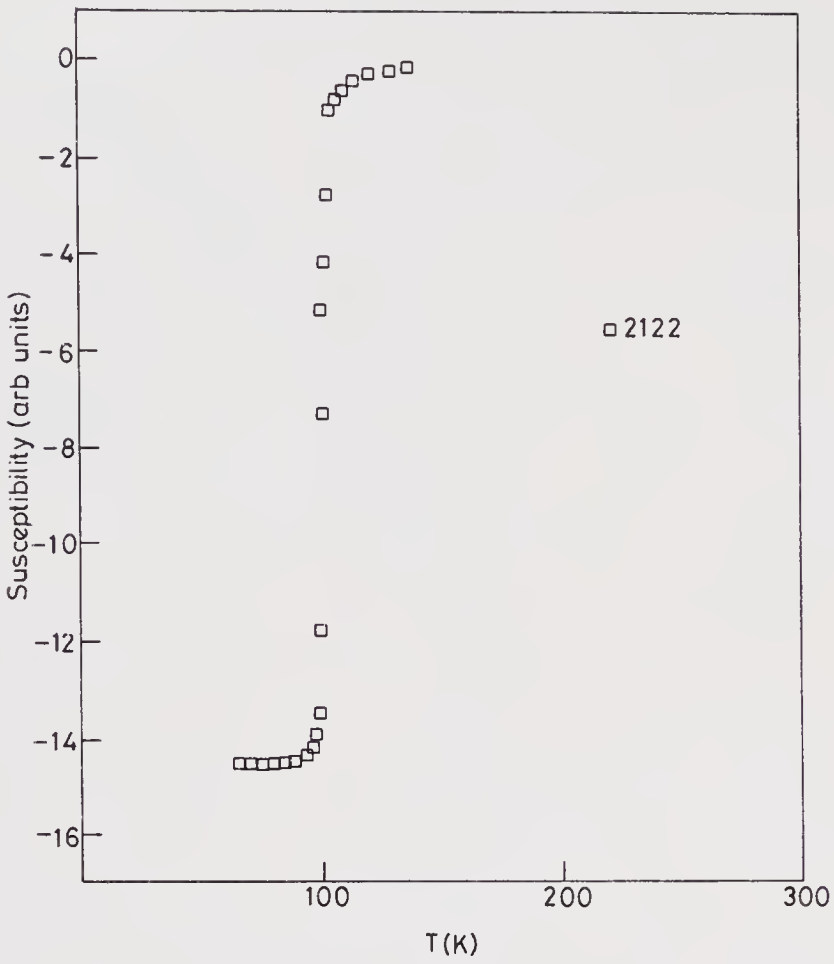

Figure 11. AC susceptibility data of the 2122 member of the Tl-Ca-Ba-Cu-O system (from the author's laboratory).

of the $(CuO_2)_\infty$ units (Rao *et al* 1988a). Such macroscopic features may be responsible for the unstable very high T_c ($\sim$300 K) behaviour of some oxides.

An interesting property of $YBa_2Cu_3O_7$ in the superconducting state is that it absorbs electromagnetic radiation over a wide range of frequencies from a few MHz to a few GHz (Bhat *et al* 1987). The absorption is extremely sensitive to temperature, particle size and the magnetic field and crucially depends on the presence of ambient oxygen. It is suggested that Josephson junctions formed by oxygen and the superconducting grains may be responsible for this effect.

8. Material parameters and applications

Since these new oxide superconductors are ceramic materials, there are inherent problems in obtaining them in the desired shape and form. However, there has already been considerable success in making wires, tapes and films. During the processing of these materials, there is a tendency to lose the labile oxygen which renders them non-superconducting; this can be solved by reheating the processed material in oxygen or by proper insulation in the initial stage itself. Another difficulty with these oxide ceramics is their chemical instability. Success in technological

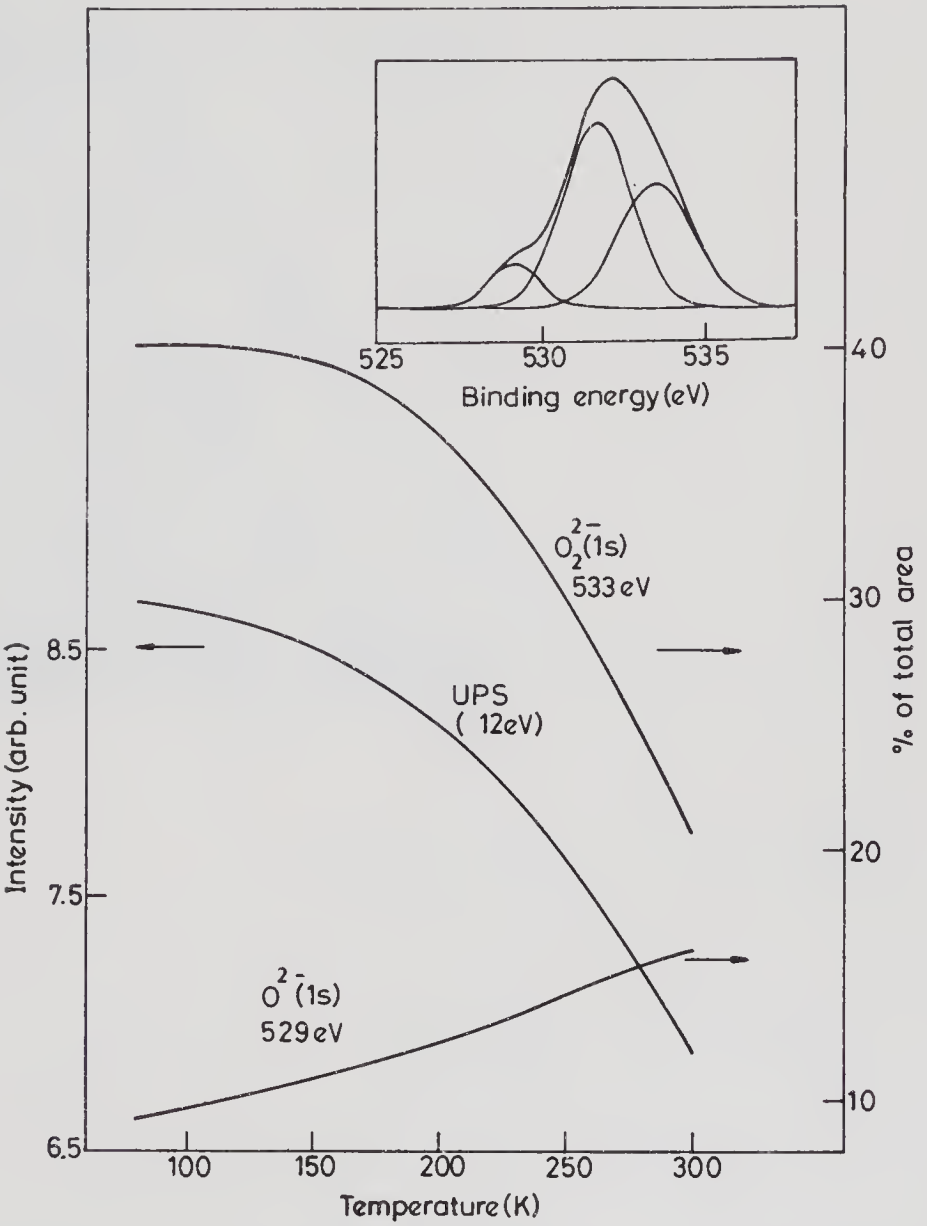

Figure 12. Temperature-variation of O(ls) peak intensity due to O^{2-} and O_2^{2-} species (at 529 and 533 eV respectively) in $YBa_2Cu_3O_7$. Temperature-variation of the intensity of He II spectrum at 12 eV is also shown. Inset shows the O(ls) signal at 80 K as consisting of three Gaussians peaking at 529, 531 and 533 eV, the one at 531 eV being due to O^- or impurity species (from Rao *et al* 1987a).

applications will depend on several factors (material parameters, cost etc.) as shown below.

Since $YBa_2Cu_3O_7$ is superconducting well above the liquid nitrogen temperature, it holds much promise. We shall briefly examine the material parameters of this ceramic oxide. Electronic properties of this oxide are anistropic (just as the structure). Some of its important properties are as follows (Malozemoff *et al* 1987):

1. It is a Type II superconductor.
2. Hall carrier density: 4×10^{21} cm^{-3} (for a material of resistivity ~ 400 $\mu\Omega$ cm just above the T_c).

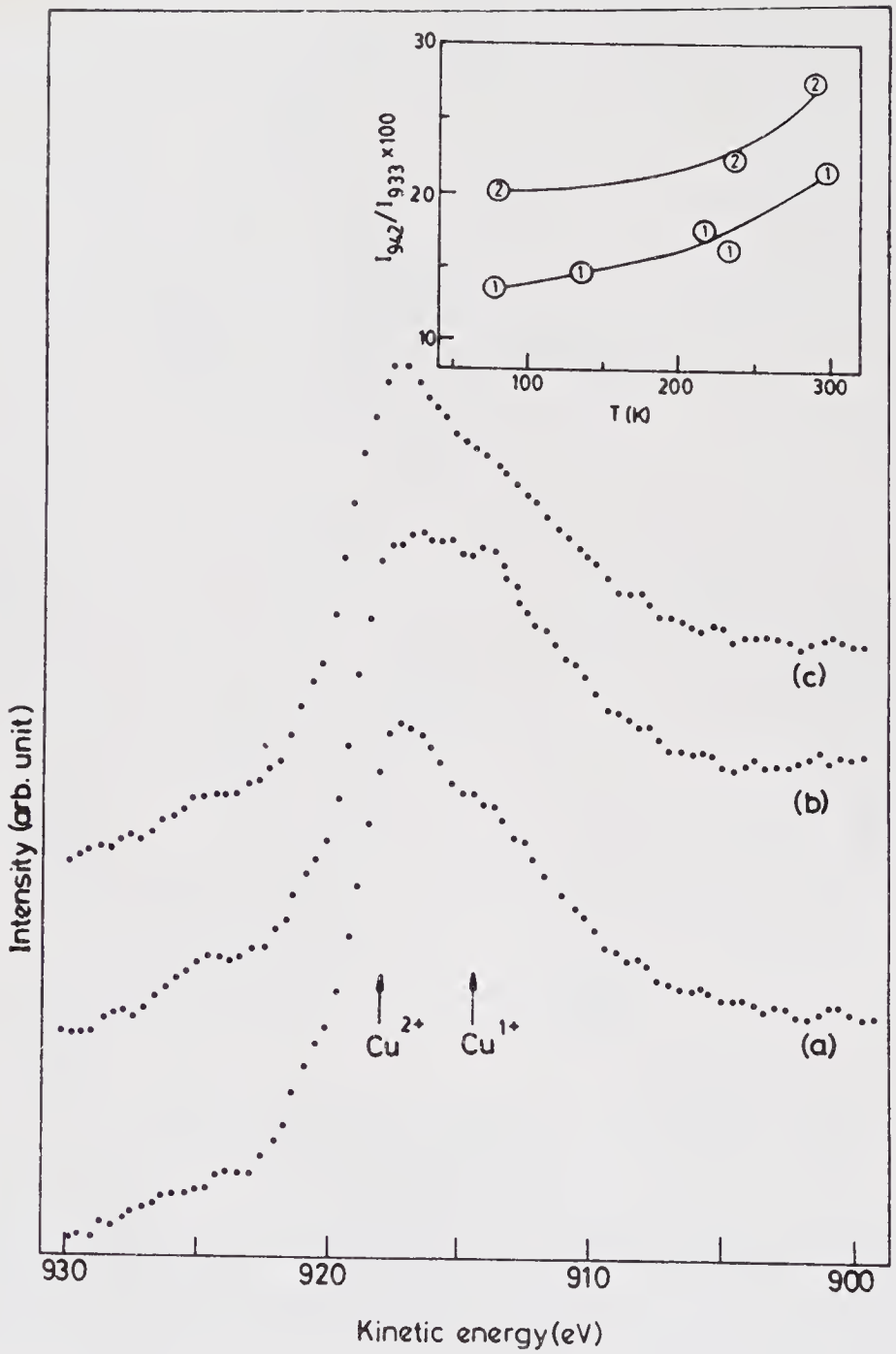

Figure 13. Cu(L_3VV) Auger spectrum of $YBa_2Cu_3O_7$ at different temperatures. In the inset, the temperature variation of the intensity of the 942 eV feature relative to that of the 933 eV feature in the Cu($2p_{3/2}$) spectrum is shown. 1 and 2 refer to independent sets of measurements (from Sarma & Rao 1987).

3. $dH_{c2}/dT = 2T/K$,
   BCS coherence length $\approx 1{\cdot}4$ nm,
   London penetration depth ≈ 200 nm,
   Mean free path $\approx 1{\cdot}2$ nm.
4. $H_c(O) \approx 1\ T$.
5. $H_{c2}(O) \approx 120\ T$.

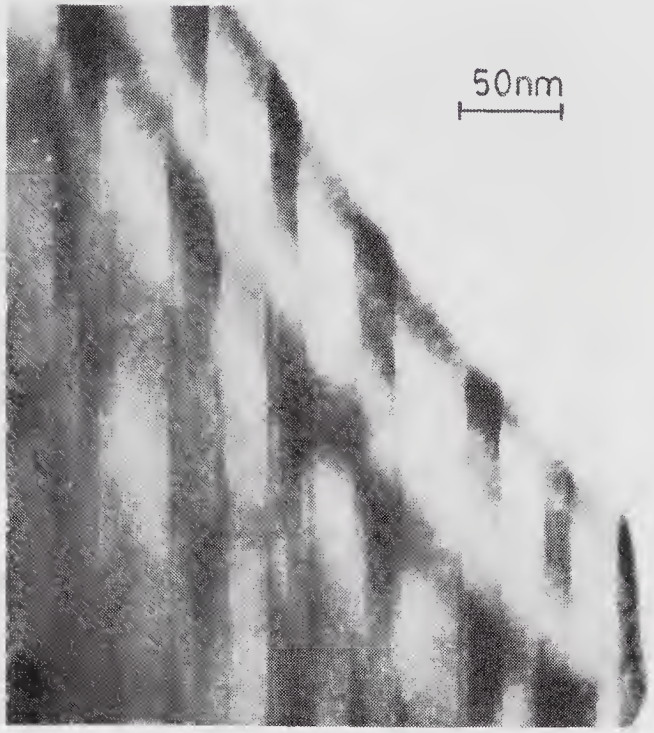

Figure 14. Bands (domains) in electron micrographs of $YBa_2Cu_3O_7$ (From Rao *et al* 1987c).

6. Critical current density: in ceramic samples $\sim 10^3$ A/cm^2 at 77 K,
in films (on $SrTiO_3$) $\sim 10^5$ A/cm^2 at 77 K,
in crystals and films $\sim 10^6$ A/cm^2 at 4·2 K.
Depairing current density: $10^7 - 10^8$ A/cm^2 (estimated).

The big market for superconducting materials is in magnetic resonance imaging for medical applications. The other magnetic applications with commercial implications are in high energy physics, high field magnets for scientific investigations and magnetic separation. Magnetic confinement of plasma (fusion), levitating transportation vehicles and magnetohydrodynamics are some of the applications where commercialization will not be in the near future. In all these applications the factors that will determine the use of the new ceramics are cost advantages and material performance characteristics. The most crucial material parameter is the critical current density; it is necessary to obtain high values in large scale production of the ceramic material. Even if this becomes possible, the material cost per ampere metre will be crucial. The biggest factor is the refrigeration cost. At present, the cost of $YBa_2Cu_3O_7$ (for use at 77 K) seems to be much higher than traditional superconductors. It is however hopeful that the usable current density of $YBa_2Cu_3O_7$ will soon be higher than Nb_3Sn for high-field applications. In the mean time, problems of fabrication and chemical stability have to be sorted out.

Use of these superconducting oxides for power transmission lines is a possibility. While the cost factor (of the material and for refrigeration) has to be carefully examined, there is every hope that $YBa_2Cu_3O_7$ at 77 K can be used profitably in the long run at least for underground lines.

The most immediate application that seems realistic is the use of $YBa_2Cu_3O_7$ as interconnects in computers. Other electronic applications are in mm-wave detection, high-speed digital and analog signal processing and digital Josephson technology. Electronic instruments utilizing superconductivity such as sensitive SQUID magneto-

meters, high speed samplers and voltage standards based on Josephson effects as well as non-Josephson devices such as superconducting bolometers and SIS mixers are areas where success is likely. Transistor-like devices compatible with oxide superconductors need to be explored vigorously.

The new bismuth cuprates are promising since they are more stable chemically and with respect to oxygen stoichiometry; good films have already been made. Thallium cuprates may not be used as they are poisonous.

9. Concluding remarks

The tremendous possibilities for wide application of $YBa_2Cu_3O_7$ and other high T_c ceramic oxides make this area of research most exciting. Clearly, the high-temperature ceramic oxide superconductors constitute the most sensational discovery since the transistor; it has given a great boost to research in solid state science and engineering. There is no doubt that within a short time frame, some commercial applications will become a reality even with existing materials. The future offers unlimited vistas and opportunities in electromagnetic technology as well as in oxide ceramics research. Synthesis of materials with T_c's close to room temperature or higher is no longer a remote possibility.

The author thanks the Department of Science and Technology, Government of India, and the University Grants Commission for support of this research. He also expresses his deep sense of gratitude to his collaborators for their enthusiastic participation in the research activities related to oxide superconductors.

References

Batlogg B, Cava R J, Jayaraman A, van Dover R B, Kouroukis G A, Sunshine S, Murphy D W, Rupp L W, Chen H S, White A, Short K T, Mujsce A M, Rietman E A 1987 *Phys. Rev. Lett.* 58: 2333–2336

Bednorz J G, Mueller K A 1986 *Z. Phys.* B64: 189–193

Beille J, Cabanel R, Chaillout C, Chevalier B, Demazeau G, Deslandes F, Etourneau J, Le Jay P, Michel C, Provost J, Raveau B, Sulpice A, Tholence J, Tournier R 1987 *C.R. Acad. Sci. Paris* 18: 304–308

Bhat S V, Ganguly P, Ramakrishnan T V, Rao C N R 1987 *J. Phys. C, Solid State* 20: L559–563

Birgeneau R J, Chen C Y, Gabbe D R, Jenssen H P, Kastner M A, Peters C J, Picone P J, Thio T, Thurston T R, Tuller H L 1987 (to be published)

Bordet P, Chaillot C, Capponi J J, Chenavas J, Marezio M 1987 *Nature (London)* 327: 687–689

Cardona M, Genzel L, Liu R, Wittlin A, Mattausch H, Garcia-Alvarado F, Garcia-Gonzalez E 1987 *Solid State Commun.* 64: 727–732

Cava R S, van Dover R B, Batlogg B, Reitman E A 1987 *Phys. Rev. Lett.* 58: 408–410

Chu C W, Bechtold J, Gao L, Hor P H, Huang Z J, Meng R L, Sun Y Y, Wang Y Q, Xue Y Y 1988 *Phys. Rev. Lett.* 60: 941–943

Chu C W, Hor P H, Meng R L, Gao L, Huang Z J, Wang Y Q 1987 *Phys. Rev. Lett.* 58: 405–407

David W I F, Harrison W T A, Gunn J M F, Moze O, Soper A K, Day P, Jorgensen J D, Beno M A, Capone D W, Hinks D G, Schuller I K, Soderholm L, Segre C U, Zhang K, Grace J D 1987 *Nature (London)* 327: 310–312

Day P, Resseinsky M, Prassides K, David W I F, Moze O, Siper A 1987 *J. Phys. C, Solid State.* 20: L429–434

Er-Rakho L, Michel C, Provost J, Raveau B 1981 *J. Solid State Chem.* 37: 151–156

Ganapathi L, Ganguli A K, Mohan Ram R A, Rao C N R 1988 *J. Solid State Chem.* 73: (in print)

Ganguli A K, Subbanna G N, Umarji A M, Bhat S V, Rao C N R 1988 *Pramana-J. Phys.* 30: L483–L490

Ganguly P, Rao C N R 1984 *J. Solid State Chem.* 53: 193–216

Ganguly P, Mohan Ram R A, Sreedhar K, Rao C N R 1987a *Solid State Commun.* 62: 807–809

Ganguly P, Raychaudhuri A K, Sreedhar K, Rao C N R 1987b *Pramana-J. Phys.* 28: L229–L231
Genzel L, Wittlin A, Kuhl J, Mattausch H, Bauhofer W, Simon A 1987 *Solid State Commun.* 63: 843–846
Hazen R M *et al* 1988 *Phys. Rev. Lett.* 60: 1657–1660
Johnston D C, Jacobson A J, Newsam J M, Lewandowski J T, Goshorn D P, Xie D, Yelon W B 1987 *ACS Symposium Series* 351, chap. 14
Jorgensen J D, Beno M A, Hinks D G, Soderholm L, Volin K J, Hitterman R L, Grace J D, Schuller I K, Segre C U, Zhang K, Kleefisch M S 1987 *Phys. Rev.* (in print)
Langen J, Veit M, Galffy M, Jostarndt H D, Erle A, Blumenröder S, Schmidt H, Zirngiebl E 1988 *Solid State Commun.* 65: 973–976
Maeda H, Tanaka Y, Fukutomi M, Asano T 1988 *Jpn. J. Appl. Phys.* (to be published)
Malozemoff A P, Gallagher W J, Schwall R E 1987 *ACS Symposium Series* 351, chap. 27
Mohan Ram R A, Ganguly P, Rao C N R 1987a *Phase Transitions* 10: 107–121
Mohan Ram R A, Vasantacharya N Y, Rao C N R 1987b *J. Solid State Chem.* 69: 186–188
Michel C, Hervieu M, Borel M M, Grandin A, Deslandes F, Provost J, Raveau B 1987 *Z. Phys.* B68: 421
Mitzi D B, Marshall A F, Sun J Z, Webb D J, Beasley M R, Geballe T H, Kapitulnik A 1988 *Phys. Rev.* (in print)
Mitsuda S, Shirane G, Sinha S K, Johnston D C, Alvarez M S, Vaknin D, Moncton D E 1987 *Phys. Rev.* B36: 822–825
Paul D M, Balakrishnan G, Bernhoeft N R, David W I F, Harrison W T A 1987 *Phys. Rev. Lett.* 58: 1976–1978
Rao C N R 1987 *Progress in high-temperature superconductivity. Proc. Adriatico Conference, Trieste* (Singapore: World Scientific Co.)
Rao C N R 1988a *J. Solid State Chem.* 73: (April issue)
Rao C N R (ed.) 1988b *Chemistry of oxide superconductors* (Oxford: Blackwell Scientific Publishers)
Rao C N R, Ganapathi L, Mohan Ram R A 1988a *Mater. Res. Bull.* 23: 123–127
Rao C N R, Ganguly P 1985 in *The metallic and non-metallic states of matter* (eds) P P Edwards, C N R Rao (London: Taylor and Francis)
Rao C N R, Ganguly P 1987a *Curr. Sci.* 56: 47–49
Rao C N R, Ganguly P 1987b *Jpn. J. Appl. Phys.* 26: L882–L885
Rao C N R, Ganguly P, Gopalakrishnan J, Sarma D D 1987a *Mater. Res. Bull.* 22: 1159–1163
Rao C N R, Ganguly P, Raychaudhuri A K, Mohan Ram R A, Sreedhar K 1987b *Nature* (*London*) 326: 856–857
Rao C N R, Ganguly P, Sreedhar K, Mohan Ram R A, Sarode P R 1987c *Mater. Res. Bull.* 22: 849–854
Rao C N R, Umarji A M, Mohan Ram R A, Vijayaraghavan R, Nanjundaswamy K S, Somasundaram P, Ganapathi L 1988b *Pramana-J. Phys.* 30: L359–L365
Raychaudhuri A K, Sreedhar K, Rajeev K P, Mohan Ram R A, Ganguly P, Rao C N R 1987 *Philos. Mag. Lett.* 56: 29–34
Sarma D D, Rao C N R 1987 *J. Phys. C, Solid State* 20: L659–L661
Sarma D D, Sreedhar K, Ganguly P, Rao C N R 1987 *Phys. Rev.* B36: 2371–2373
Segre C U, Dabrowski B, Hinks D G, Jorgensen J D, Beno M A, Schuller I K 1987 *Nature* (*London*) 329: 227–229
Sheng Z Z, Hermann A M 1988 *Nature* (*London*) 332: 55–58, 138–139
Shirane G, Endoh Y, Birgeneau R J, Kastner M A, Hidaka-Y, Oda M, Suzuki M, Murakami T 1987 *Phys. Rev. Lett.* 59: 1613–1616
Siegrist T, Sunshine S, Murphy D W, Cava R J, Zahurak S M 1987 *Phys. Rev.* B35: 7137–7138
Sreedhar K, Ramakrishnan T V, Rao C N R 1987 *Solid State Commun.* 63: 835–837
Subbanna G N, Ganguly P, Rao C N R 1987 *Mod. Phys. Lett.* B1: 155–165
Subramanian M A, Torardi C C, Calabrese J C, Gopalakrishnan J, Morrissey K J, Askew T R, Flippen R B, Chowdhry U, Sleight A W 1988 *Science* 239: 1015–1018
Tarascon J M, McKinnon W R, Greene L H, Hull G W, Vogel E M 1987a *Phys. Rev.* B35: 3238–3242
Tarascon J M *et al* 1987b *Proc. MRS Meeting*, Anaheim
Tarascon J M *et al* 1988 (to be published)
Thomann H, Johnston D C, Tindall P J, Goshorn D P, Klemm R A 1987 *Phys. Rev. Lett.* 59: 509–512
Uchida S, Takagi H, Kitazawa K, Tanaka S 1987 *Jpn. J. App. Phys.* 26: L1–14
Uemura Y J, Kossler W J, Yu X H, Kempton J R, Schone H E, Opie D, Stronach C E, Johnston D C, Alvarez M S, Goshorn D P 1987 (to be published)
Wu M K, Ashburn J R, Toring C J, Hor P H, Meng R L, Gao L, Huang Z J, Wang Y Q, Chu C W 1987 *Phys. Rev. Lett.* 58: 908–909
Xiao G, Streitz F H, Gavrin A, Chien C L 1987 *Solid State Commun.* 63: 817–820

Electronic ceramics

V C S PRASAD

Materials Development Department, Bharat Electronics Ltd, Bangalore 560 013, India

Abstract. Electronic ceramics represent an important segment of advanced ceramics and will probably constitute a major share of the advanced ceramic markets at least till 2000 AD. Yet, other than ferrites, this area has not been sufficiently examined in this country. Therefore, this review covers briefly the science and technology status, the markets and the possible future projections of these ceramics the world over *vis a vis* the Indian situation and indicates the scope for indigenous effort in this vital area of electronic components.

Keywords. Multilayer ceramics; grain boundary devices; PZT ceramics; dielectric resonators; barium titanate; tape casting.

1. Introduction

Since electronic ceramics are expected to constitute a major share of the advanced ceramic markets at least till 2000 AD (Rah 1986), it is important to examine this topic in the Indian context *vis a vis* the world situation. Included in this review are multilayer ceramics, the newer ceramics and very briefly the sensors and the microwave dielectrics. Typical useful features of these devices and their availability status in India are given in table 1. The literature review is by no means exhaustive but serves to highlight the important aspects. Dielectric and optical materials were recently reviewed by Subbarao *et al* (1981, pp. 217–245) and ferrites by Das (1981, pp. 75–100), Alam & Nair (1981) and Jain & Sarnot (1982).

2. Multilayer ceramics

Multilayer ceramics are evolved mainly to increase the volumetric efficiency of the components thereby achieving circuit miniaturization. In the case of multilayer capacitors, high capacitance density can be achieved (Goodman 1981) by connecting a number of dielectric layers in parallel using internal metal electrodes. In the case of multilayer packages used for packaging of integrated circuits, the third dimension is used to increase the number of metal conductors for increasing the I/O counts. In the case of more complex packages called modules, the third dimension is used to accomodate a number of functions (Schwartz 1984) including that of substrate, interconnections, cooling, environmental protection etc. In the case of multilayer

Table 1. Different electronic ceramics and their useful features.

Item	Useful features	Availability from indigenous sources
Multilayer capacitors	High volumetric efficiency and wide capacitance range, possibility of replacing the Ta capacitors reducing the dependence on the scarce Ta metal. Suitability for surface mount assembly	NA*
Multilayer packages and substrates	Packaging of high reliability IC, scope for manufacture of high component density custom made substrates for miniaturisation and cost reduction. Indispensable as a hybrid substrate	NA
IBL capacitors	High volumetric efficiency, better temperature and loss characteristics compared to the conventional barrier layer capacitors	NA
PTC resistors	Semiconductivity at room temperature and insulating characteristics above the Curie point. Useful for a number of devices based on current limiting, and temperature sensing characteristics. Typical applications are in industrial and consumer electronics, telecommunications and power engineering	Scantily available but likely to be available soon in larger quantities
Varistors	High nonlinear current voltage characteristics with much greater current and energy handling capacity than the Zener diodes. Useful for transient surge suppression. Typical applications are in industrial and consumer electronics, telecommunications and power engineering	NA
PZT ceramics		
a) Homogenous	Large electromechanical coupling coefficient resulting in a number of devices in the sonic and ultrasonic frequency range and also for use as resonators and filters with better volumetric efficiency, temperature characteristics and large band width when compared to their conventional counterparts	Scantily available but likely to be available soon in larger quantities
b) Composites	Flexibility, low density and very high voltage coefficients specially suited for hydrophone applications, considerable scope for tailoring properties to specific requirements	NA
Dielectric resonators	Improved volumetric efficiency and better temperature stability and ease of manufacture when compared with their conventional counterparts	NA

*NA – not available

Development to suit the surface mount assembly is being done wherever possible

multicomponent substrates (MMC), the third dimension is used to increase the number of components embedded in a single monolithic substrate (Utsumi *et al* 1985).

2.1 *Multilayer capacitors*

Because of the scope for circuit miniaturization and the possibility of using the components (as chips) in surface mount assembly applications, the usage of multilayer capacitors (MLC) is growing rapidly the world over. For example, in the

US, in the last decade, the annual growth rate (Blum *et al* 1985) averaged between 25% to 35% and the growth has followed closely that of the integrated circuits. There are many excellent articles (e.g., Capozzi 1975) on the seience and technology of the manufacture of MLC capacitors. The main R & D thrust areas are the following:

a) Improving the capacitance density as much as possible by the development of ultrathin high density tapes (Tormey *et al* 1984, pp. 140–149) and also higher dielectric constant compositions.
b) Developing suitable dielectric compositions which can cofire with less noble metal electrodes to reduce the costs and also to reduce the dependence on the precious and scarce noble metals (e.g. Burn & Secaur 1986, unpublished).
c) Developing suitable dielectric compositions to have improved dielectric saturation characteristics to extend the range for higher voltage applications (e.g., Subbarao *et al* 1981, pp. 217–245).
d) Improving the lot to lot variations through the complete characterization of the initial raw materials and instituting process controls (e.g. Stynes 1981, unpublished).
e) Working for process innovations to minimize some of the inherent problems associated with the MLC capacitor manufacture such as the delamination problems etc, e.g. the Corning ACE process or the fugitive electrode process (Newnham & Hiremath 1985).

The typical dielectric materials of promise are still the $BaTiO_3$ based compositions (such as the Z5U and X7R. Figure 1 shows the improvements in the latter over the years, Cantagrel 1986). However, lead based perovskite relaxor materials (such as lead magnesium niobate, PMN) which sinter at temperatures as low as 900°C for use with near hundred percent silver electrodes ($\geqslant$85% Ag) are some of the latest compositions being tried by the industry (Takamizawa *et al* 1981; Yonezewa 1983). The processing and powder purity strongly influence the dielectric behaviour of these materials (Swartz *et al* 1984 and Chen *et al* 1986).

Achieving high yield and reliability are some of the technological problems receiving considerable attention in the MLC capacitor manufacture. The reasons for the poor yield and reliability are gross defects and processing accidents which are often

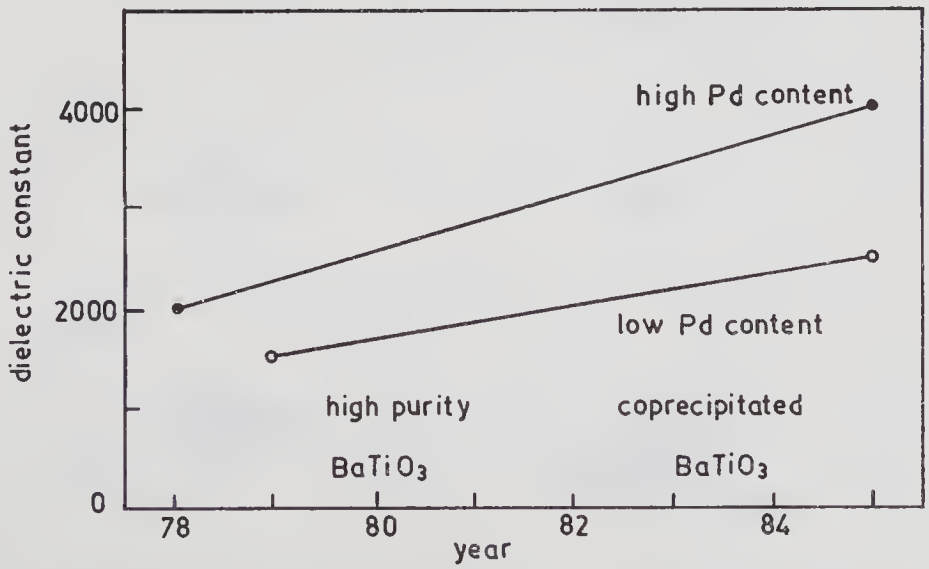

Figure 1. X7R dielectric formulation improvements (Cantagral 1986).

aggravated by complex interactions between ceramic dielectric, flux and electrode materials (R E Newnham 1984, unpublished). In addition, other interactions arise from the organic binders and vehicles used in tape casting, from the solder and other materials used in terminations, encapsulation and from the environment etc.,

2.2 *IC packages*

The standard ceramic IC packages are three-layered structures (Reiss & Glicksmann 1981) the top layer containing the seal ring, the middle one the bonding pads, and the bottom one the die pad (figure 2). Appropriate conductor patterns (with refractory metal conductors such as Mo or W) are printed on green alumina ceramics, laminated and cofired to give rise to monolithic ceramic packages. The chip carriers are the space saving, cheaper versions of the standard dual in-line packages (DIP). For housing complicated ICs with high I/O count, (say > 8, 4 and sometimes even 64) the pin grid array (Ohr 1983) was introduced by IBM. IBM makes some highly complex custom-made ceramic packages for housing ICs used in high speed computers. For example, some of the IBM arrays have 23 layers and 261 pins housing multiple IC chips (Schwartz 1984). However, for most of the applications, the DIP and the chip carriers are used and the latter is going to replace the DIP particularly in the 40–84 pin count range where the DIP's size and the cost are too high to be competitive.

The main R&D areas of interest for packaging (Schwartz 1984) are the

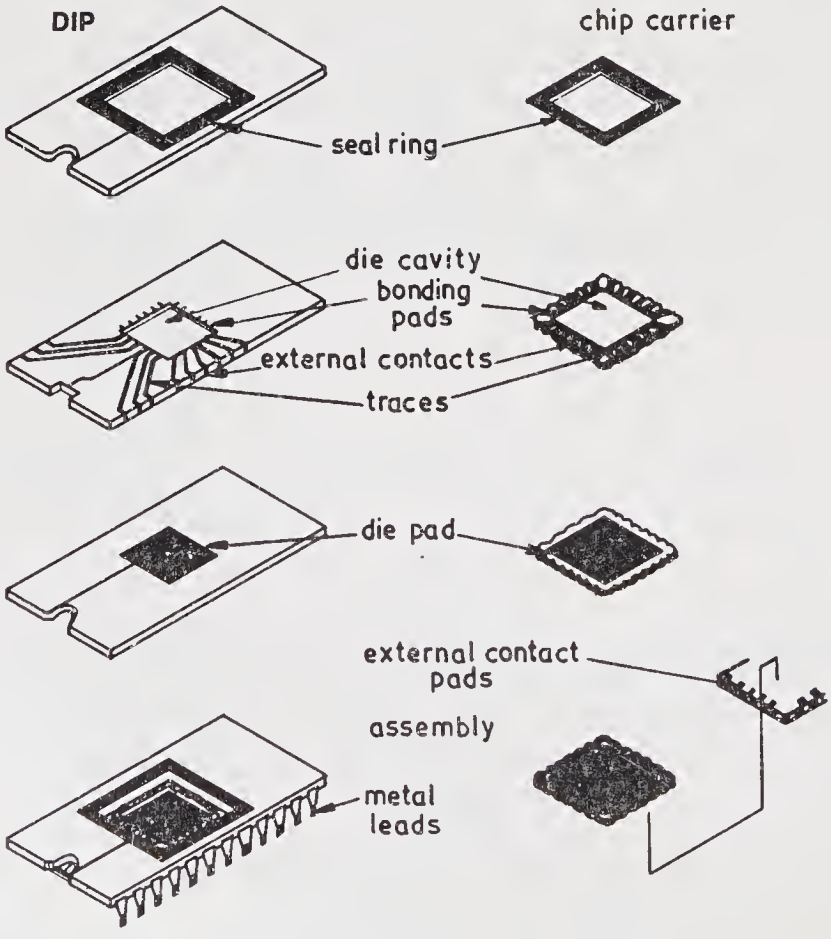

Figure 2. Exploded view of a DIP and a chip carrier (Reiss & Glicksman 1981).

Table 2. Ceramic materials currently used in substrates and packages.

Material	Dielectric constant	Thermal expansion (10^{-6}/°C)	Thermal conductivity (W/mK)	Strength (MPa)
Alumina 96%	10	7·1	21	280
Alumina 92%	9·5	6·9	17	320
Alumina 90%	8·5	7·0	17	280
Alumina 55% + glass 45%	7·5	4·2	4·2	300
SiC	40	3·4	33	280
BeO	7·0	8·0	25	170

Reference: Schwartz (1986)

development of low dielectric constant ceramics of matching thermal expansion to that of silicon and processes capable of finer resolutions for printing the conductor patterns. New methods of synthesizing the starting powders, improved precursor materials, clean room operations, and optical processing will be the additional future R & D thrust areas in ceramic packaging. Schwartz (1986) gives the list of ceramic packaging materials that are currently used (table 2) and those under consideration for the future (table 3).

2.3 *Multilayer multicomponent substrates*

The demand for greater circuit miniaturization and consequent cost reduction resulted in innovative packaging techniques using the multilayer ceramic technology in which the passive components such as capacitors, resistors and wiring conductors are integrated into the package (Utsumi *et al* 1985). Such a package is called the monolithic multicomponent ceramic package (MMC). In this package, in addition to the insulator layers printed with conductors and resistors, dielectric layers prepared with materials of suitable dielectric properties are cofired. An exploded vertical section of the MMC substrate for a voltage controlled crystal oscillator is shown in figure 3. The total substrate size is 17 mm × 10 mm × 1 mm, involving 8 capacitor elements and 10 resistor elements as shown within the dotted lines of the circuit. The typical flow sheet for the fabrication of such a package is shown in figure 4. This process is more or less a combination of the multilayer capacitors and multilayer packaging processes. It is different from the more commonly used multilayer hybrid technology in that the insulation layers are made of ceramic tape instead of being printed with insulating glass paste. The use of conventional capacitors instead of printed capacitors in the package would result in an extremely complex type of

Table 3. Ceramics for future use in substrates and packages.

Ceramic	Dielectric constant	Thermal expansion ($\times 10^{-6}$/°C)	Thermal conductivity (W/mK)	Strength (MPa)
Aluminum nitride	8·8	4·6	84–250	360
Silicon nitride	6·0	3·2	33	590
Glass-ceramics	4·5–6·5	2·5–6·5	0·84–2·1	241
Mullite	6·1	4·5	2·1	210

Reference: Schwartz (1986)

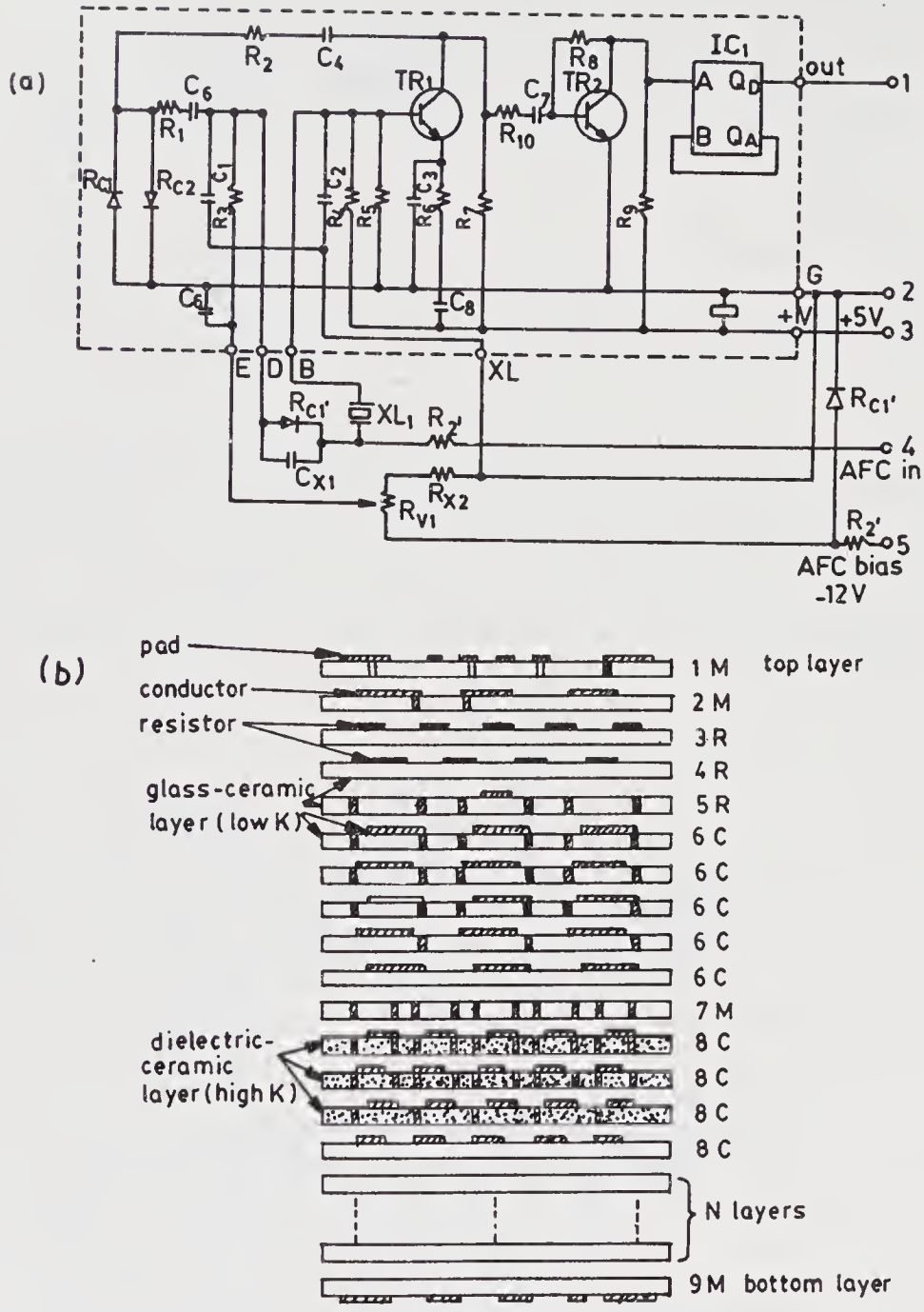

Figure 3. MMC substrate, (a) circuit diagram and (b) exploded vertical section (Utsumi *et al* 1985).

wiring network resulting in high values of lead inductances consuming the real estate space. The integration of capacitor elements into the package minimizes this problem.

The necessity of cofiring the insulators, dielectrics, conductors, and resistors imposes considerable restriction on the choice of materials to be used in this type of package. For example, the Japanese (Utsumi *et al* 1985) have used a mixture of alumina and lead borosilicate (55% and 45% respectively) for the insulator layers, low firing lead based compositions such as $Pb(Fe_{2/3}\cdot W_{1/3})O_3$-$Pb(Fe_{1/2}\cdot Nb_{1/2})O_3$ binary systems for the dielectric layers, Ag-Pd, Pd and Au for internal conductors,

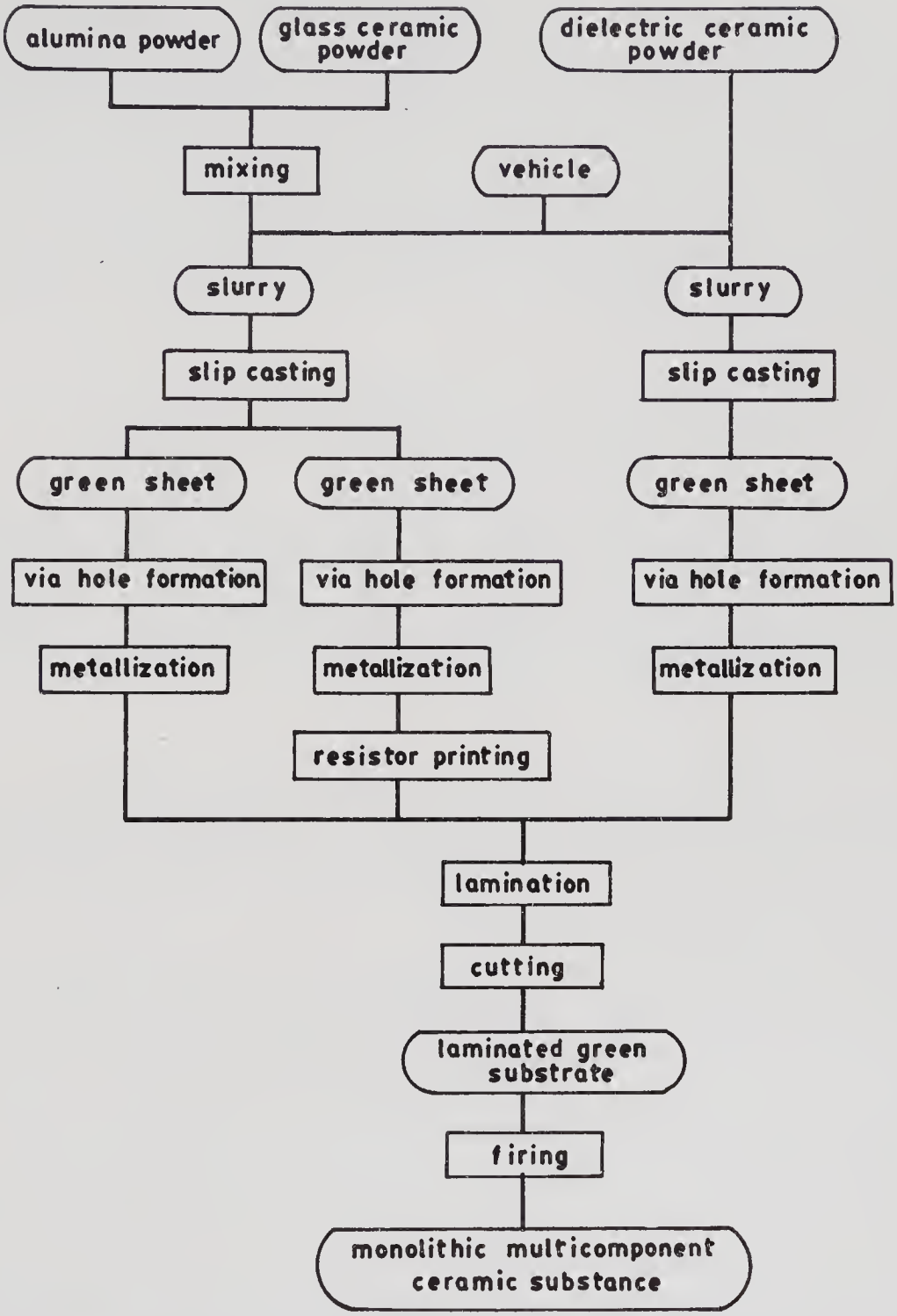

Figure 4. Flow sheet for multilayer multicomponent package (Utsumi *et al* 1985).

Au and Au-Pt for external terminations and RuO_2 based pastes for the resistor materials. The composite substrate can be fired at 900°C. These composite substrates were used in the development of voltage controlled crystal oscillator circuits (VCXO) and RC active filters. The VCXO are used in digital communication equipment as clock generators and as timing signal generators. A size reduction to 1/10th and a weight reduction to 1/3rd is claimed to have been achieved by integrating the different passive components in the substrate.

In addition to the above devices using the multilayer technology, a number of electronic ceramic devices are being contemplated in multilayer configurations such as multilayer barrier layer capacitors, multilayer PTC thermistors, multilayer piezoelectric transducers and resonators, multilayer fuel cells, composite multilayer devices etc. particularly using the fugitive electrode process (Newnham & Hiremath 1985). Many advantages in addition to volumetric efficiency are foreseen in most of these devices. For example, a multilayer sonar transducer can be driven with much lower voltages involving the use of smaller size transformers than when using thick solid transducers, a multilayer PTC device can have a much lower room temperature resistance than a solid PTC etc.

3. Devices based on grain boundary phenomenon

The properties of polycrystalline electrical ceramics are greatly influenced by the electrical and mechanical boundary conditions existing at grain and phase boundaries. Properties may be engineered into polycrystalline systems which never could be obtained in single crystals alone. Notable examples are internal boundary layer (IBL) capacitors, positive temperature coefficient of resistance (PTCR) devices and varistors exhibiting highly nonlinear current-voltage characteristics.

3.1 *IBL capacitors*

In the IBL capacitors, anomalously high dielectric constants are obtained in materials with semiconducting grains surrounded by insulating boundaries (Waku 1969). The value is directly proportional to the diameter of the grains and inversely proportional to the thickness of the boundary. Goodman (1981, pp. 215–231) has presented an excellent review on this topic.

Although ferroelectric $BaTiO_3$ ceramics were originally used for this application, $SrTiO_3$ ceramics have become more popular because of their better temperature characteristics (these have almost flat temperature capacitance curves, figure 5a), higher stability with respect to capacitance change under *d.c.*, biasing field and lower loss over a wide frequency range. Typical dielectric properties of a material developed with regard to high dielectric constant are given in figure 5b.

Usually the insulating second phase layers around the semiconducting grains are formed by painting on the ceramic a paste consisting of low melting glasses such as $PbO\text{-}Bi_2O_3\text{-}B_2O_3$. When this coated ceramic is refired, the low melting glass penetrates the grain boundaries and dissolves in the excess TiO_2 phase of the ceramic giving rise to insulating boundary layers (Wernicke 1981, pp. 261–271). The structure (schematic) and equivalent circuit of a grain boundary are shown in figure 6 (Wernicke 1981, pp. 272–281). Work on single fire processes to achieve the insulating boundaries through solute segregation is also being attempted (Yan & Rhodes 1983).

The capacitance density of an $SrTiO_3$ boundary layer dielectric is generally higher than that of the electrode barrier layer (table 4) although for the packaged capacitor, this difference is less and even insignificant for some types. These capacitors are increasingly used in the field of TV, VCR, radio etc. They are also being tried as replacements of organic film capacitors because of their markedly increased capacitance range.

Composition	: $Sr_{100}(Ti_{100}Nb_{1\cdot5})O_{300+\delta}$	k_{eff}	= 9400 at 25°C
Additions	: 0·1 wt% Al_2O_3 0·2 wt%SiO_2	$\tan\delta$	= 0·6%
Sintering	: 1450°C in H_2/N_2	$\Delta C/C_{25}$	< ±1% (−55 to 125°C)
Second firing	: 1100°C	ρ_{eff}	> $10^{11}\,\Omega$ cm at 1 kV/cm

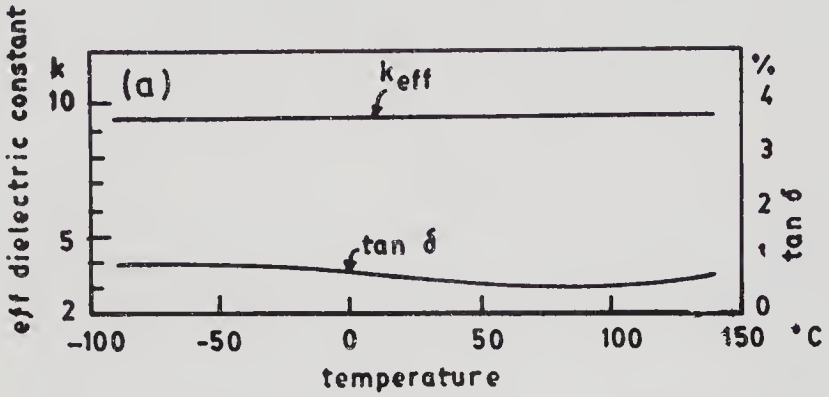

Composition	: $Sr_{100}(Ti_{100}Nb_{1\cdot0})O_{300+\delta}$	k_{eff}	= 65,000 at 25°C
Addition	: 0·05 wt% SiO_2	C/A	= 110 nF/cm²
Sintering	: 1470°C in H_2/N_2	$\tan\delta$	= 0·7%
Second firing	: 1150°C	$\Delta C/C_{25}$	< ±22% (−55 to 125°C)
		ρ_{eff}	> $10^{10}\,\Omega$ cm at 1 kV/cm

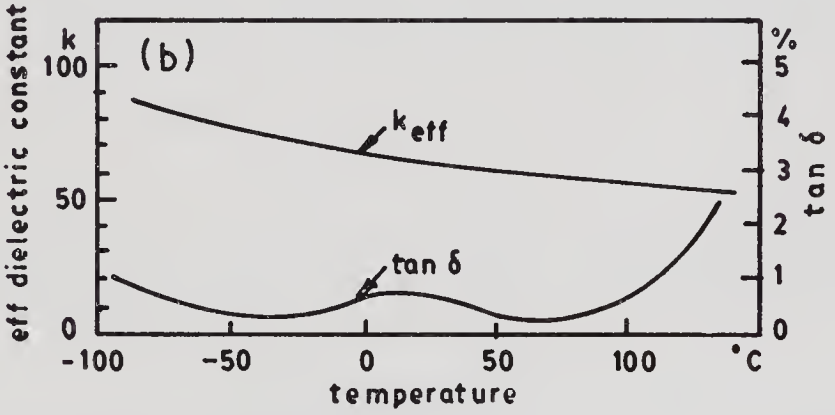

Figure 5. Dielectric properties of a boundary layer capacitor material developed with regard to (a) a low temperature coefficient (b) a high dielectric constant (Wernicke 1981, pp. 272–281).

3.2 *PTC resistors*

These devices also have a semiconductive grain structure interleaved with a very narrow barrier layer system at the boundary just as in the case of the IBL capacitors. However, the barrier layer here is the intrinsic boundary layer due to the barium vacancy diffusion (Daniels *et al* 1979) whose thickness can be controlled by the cooling rates.

In $BaTiO_3$, which is a component of all PTC resistors, the resistivity change occurs near the Curie temperature at around 130°C and may encompass 8 orders (Daniels & Wernicke 1976). The PTC mechanism was first explained by Heywang (1961) by means of a grain boundary barrier model (figure 7) according to which the Schottky-type grain boundary barriers originate from two-dimensional layers of negative

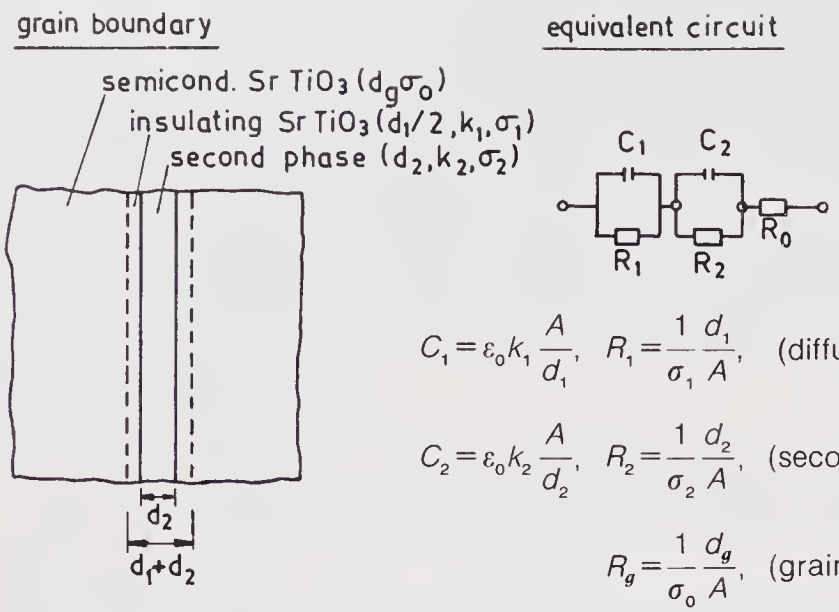

$$C_1 = \varepsilon_0 k_1 \frac{A}{d_1}, \quad R_1 = \frac{1}{\sigma_1}\frac{d_1}{A}, \quad \text{(diffusion layers)}$$

$$C_2 = \varepsilon_0 k_2 \frac{A}{d_2}, \quad R_2 = \frac{1}{\sigma_2}\frac{d_2}{A}, \quad \text{(second phase layers)}$$

$$R_g = \frac{1}{\sigma_0}\frac{d_g}{A}, \quad \text{(grain resistance)}$$

$$\frac{1}{k_{eff}} = \frac{1}{dg}\left(\frac{d_1}{k_1} + \frac{d_2}{k_2}\right), \qquad \frac{1}{\sigma_{eff}} = \frac{1}{dg}\left(\frac{d_1}{\sigma_1} + \frac{d_2}{\sigma_2}\right) + \frac{1}{\sigma_0},$$

where k represents the dielectric constant, d the thickness, σ the conductivity, A the area of cross-section, R the resistance, C the capacitance, ε_0 the permittivity of vacuum.

Figure 6. Structure and equivalent circuit of a grain boundary (Wernicke 1981, pp. 272–281).

charge caused by acceptor states at the boundary. The acceptor character could arise due to the oxygen adsorption. These surface states take up conduction electrons from the immediate vicinity, thus giving rise to a negatively charged boundary layer

Table 4. Capacitance density of commercial capacitors*.

Type	Packaged capacitor	Dielectric only (mfd/cm³)
Electrode barrier layer		
Disk, 0·1 mfd, Y5U, 75V	0·1	0·76
Disk, 0·1 mfd, Y5U	0·14	
$BaTiO_3$ GBBL		
Tube 0·1 mfd, Y5 (?) 63V	0·65	3·22
Disk 0·022 mfd, Y5T		0·085
$SrTiO_3$ GBBL		
Tube, 0·01 mfd, Y5U	0·27	2·27
Disk, 0·1 mfd, Y5U	0·13	
Disk, 0·1 mfd, Y5R, 25V	0·25	2·53
Monolithic, conventional		
0·1 mfd, Z5U	4·03	13·5
0·1 mfd, Z5U	2·69	7·93

*50 V rated, unless otherwise indicated
Reference: Goodman (1981)

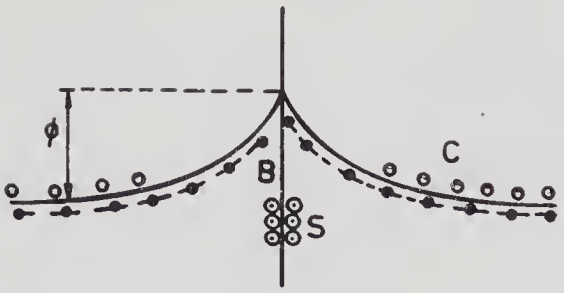

Figure 7. A potential barrier caused by surface states S at a grain boundary B of donor-doped $BaTiO_3$ (schematic), ϕ is the height of the potential barrier, C conduction band (Daniels *et al* 1979).

with, on both sides, a positive space charge that forms a symmetrical potential barrier for the remaining conduction electrons. The resistivity is proportional to $\exp(e\phi/KT)$ where ϕ is the height of the potential barrier. According to the theory $\phi \alpha N_s^2/\varepsilon n$ where N_s is the density of surface states, ε the dielectric constant and n the concentration of the conduction electrons. Since ϕ is inversely proportional to the dielectric constant, the height of the potential barrier rapidly increases at a temperature above the Curie point where the dielectric constant sharply decreases (figure 8). This would explain the steep rise in the electrical resistivity above the Curie point. Below the Curie point, the surface states are wholly or partly compensated by the proper alignment of the spontaneous polarization (figure 9) that is associated with the ferroelectric state. Therefore, the resistivity is low.

Ihrig (1983) attempted a modification of this model by assuming a constant density dispersion of the grain surface acceptor energies and studied the PTC effect as a function of different technological parameters. Daniels *et al* (1979) have improved the

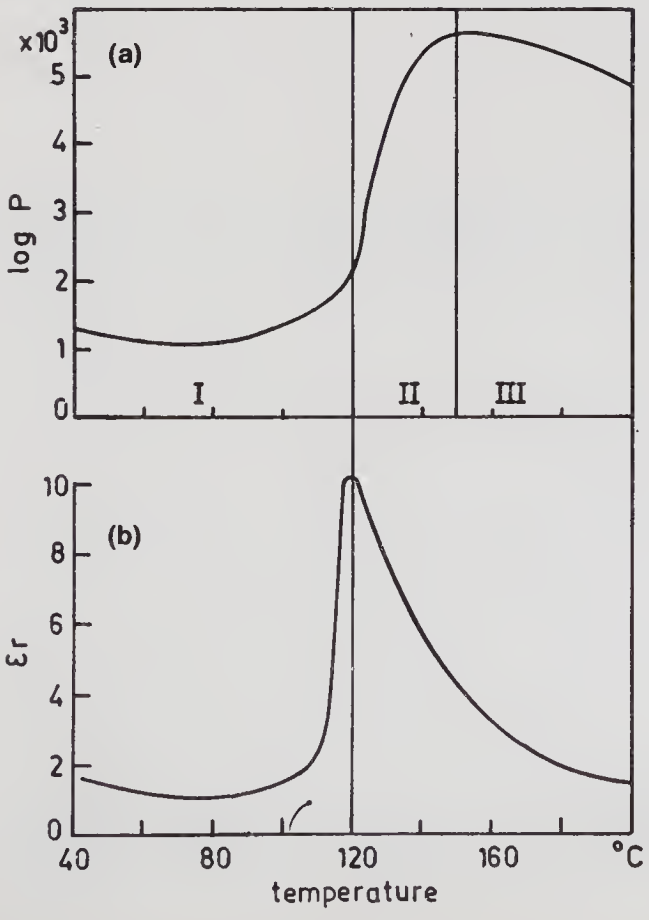

Figure 8. (a) Variation of resistivity with temperature of a $BaTiO_3$ PTC thermistor. (b) Variation of the permittivity with temperature of ceramic $BaTiO_3$ (Jonker 1981).

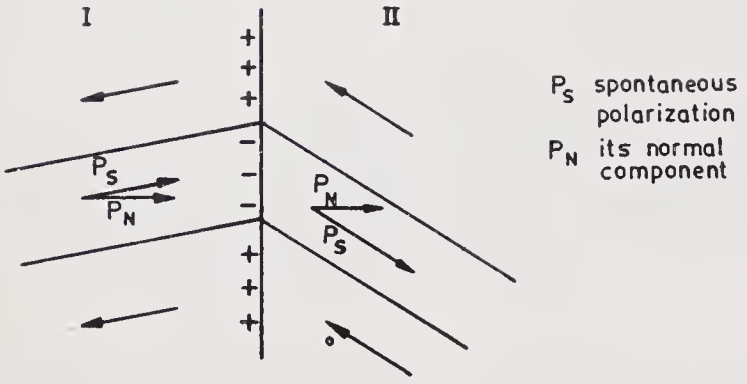

Figure 9. Ferroelectric domains at a boundary between two crystallites of different orientations, with compensating surface charges (Jonker 1981).

understanding of the PTC mechanism by using the defect chemistry of doped $BaTiO_3$. An exhaustive review on PTC materials technology was made by Kulwicki (1981). Ryan & Subbarao (1962) showed that the charge carriers in semiconducting $BaTiO_3$ are of the *n*-type using the Hall effect measurement.

Considerable effort in PTC materials technology has been made to lower the cold resistivity without losing the PTC jump. The cold resistivity is not only influenced by the charge carrier density and the intrinsic mobility of the material but also by the presence of the residual grain boundary barriers or charge. A homogenous grain structure is expected to minimise the grain boundary barrier (Ihrig 1983) through the formation of a homogenous domain structure. Therefore, a homogenous microstructure is required to get a high performance PTC device.

The PTC phenomenon has been utilized to produce a number of commercial devices such as degausser elements for colour TV, motor starters and crankcase heaters for refrigeration and air conditioning compressors, time delay relays, air heaters for hair dryers, hair curlers, food warmers and a wide range of thermistors and current limiters for electronic applications.

3.3 *Varistors*

Varistors based on ZnO are novel ceramic semiconductor devices with highly nonlinear current-voltage characteristics (figure 10) similar to back-to-back Zener diodes but with much greater current and energy handling capabilities. The varistors are

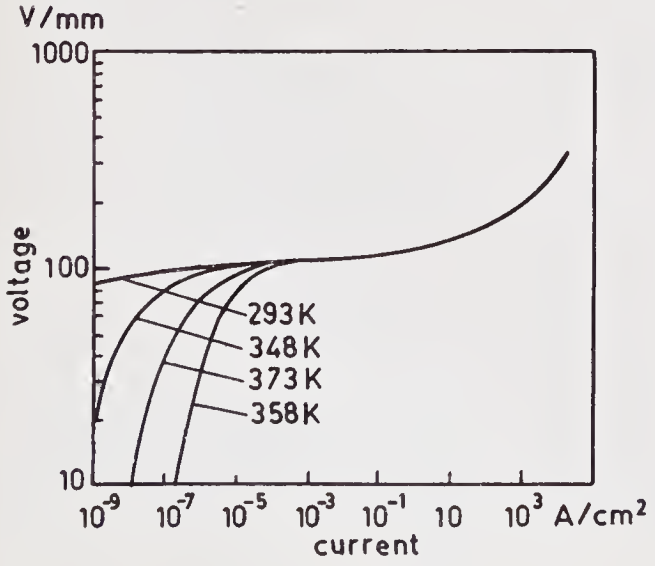

Figure 10. Current-voltage characteristics of a varistor (Matsuoka 1981).

produced by a ceramic sintering process that gives rise to a structure composed of conductive ZnO grains surrounded by electrically insulating barriers. These barriers are derived from trap states at the grain boundaries induced by additive elements such as Si, Co, Pr, Mn etc., A typical composition given by Matsuoka (1971) contains 97 mol% ZnO, 1 mol% Sb_2O_3 and ½ mol% each of Bi_2O_3, CaO, MnO and Cr_2O_3. Excellent reviews (Matsuoka 1981; Levinson & Philipp 1986) on this topic exist in the literature. Varistors based on semiconducting silicon carbide were the earlier versions but they have a lower surge current capacity than the ZnO varistors.

The nonlinear current properties of the ZnO varistors were explained (Mahan 1982, p. 333) in terms of the formation of a Schottky barrier adjacent to the interface of each ZnO grain. The nonlinear electrical behaviour is caused by electrons trying to get past this barrier. Electron transport through the interface is believed to be a two-step process, whereby first the electron goes from a ZnO grain to the interface and secondly on to the next ZnO grain.

The application of ZnO varistors is predominantly in the field of circuit overvoltage protection, although it is used sometimes as a circuit element. These components have come into prominence with the advent of the solid state circuitry because the solid state components cannot in general withstand the amount of overvoltage imposed upon the circuitry by typical power system transients. On the application of an external field, the device is insulating upto a certain level, the breakdown field, above which it becomes highly conducting (figure 10).

4. Piezoelectrics

A number of piezoelectric compositions, most of them proprietary, are developed in the lead zirconate titanate system more commonly known commercially as PZT-4, PZT-5A and 5H, PZT-6A and 6B, PZT-7A etc. These still form the basis for most ceramic piezoelectric transducers (Jaffe *et al* 1971). A great amount of effort has been concentrated, particularly in Japan, upon modifications to the PZT compositions to trim properties and facilitate fabrication for specific device structures and a wide range of options are now available, from very low coercivity (ultra-soft) high sensitivity compositions to heavily self-biased high coercivity hard compositions (Takahashi & Takahashi 1972). Some are based on ternary and quaternary systems such as $Pb(Zn_{1/3}\,Nb_{2/3})O_3$-$Pb(Sn_{1/3}\,Nb_{2/3})O_3$-$PbTiO_3$-$PbZrO_3$ suitable for high power applications (Nishida *et al* 1980). Development work on relaxor compositions with larger strain, lower hysteresis and ageing effects than for normal varieties of PZT is an interesting area of activity (Uchino *et al* 1980) with application in precise position control etc. These compositions are generally in the family $Pb(Mg_{1/3}\,Nb_{2/3})\,O_3$-$PbTiO_3$ (0·9 PMN-0·1 PT). Typical electromechanical and thermo-mechanical data for these ceramics are given in figure 11. These ceramics reveal huge strains upto 0·1% (i.e. a 1 cm sample can elongate by 10 μm) without hysteresis, eminently suitable as electrostrictive actuators (Uchino 1986).

A very important new direction of work in the PZT ceramics is the synthesis of composite PZT consisting of ceramic powders and polymers with controlled connectivity (Skinner *et al* 1978) of the phases to expand the range of properties substantially when compared with the conventional PZT ceramics. For example, in one such 3-3 composite of PZT and rubber, the longitudinal voltage coefficient g_{33} is

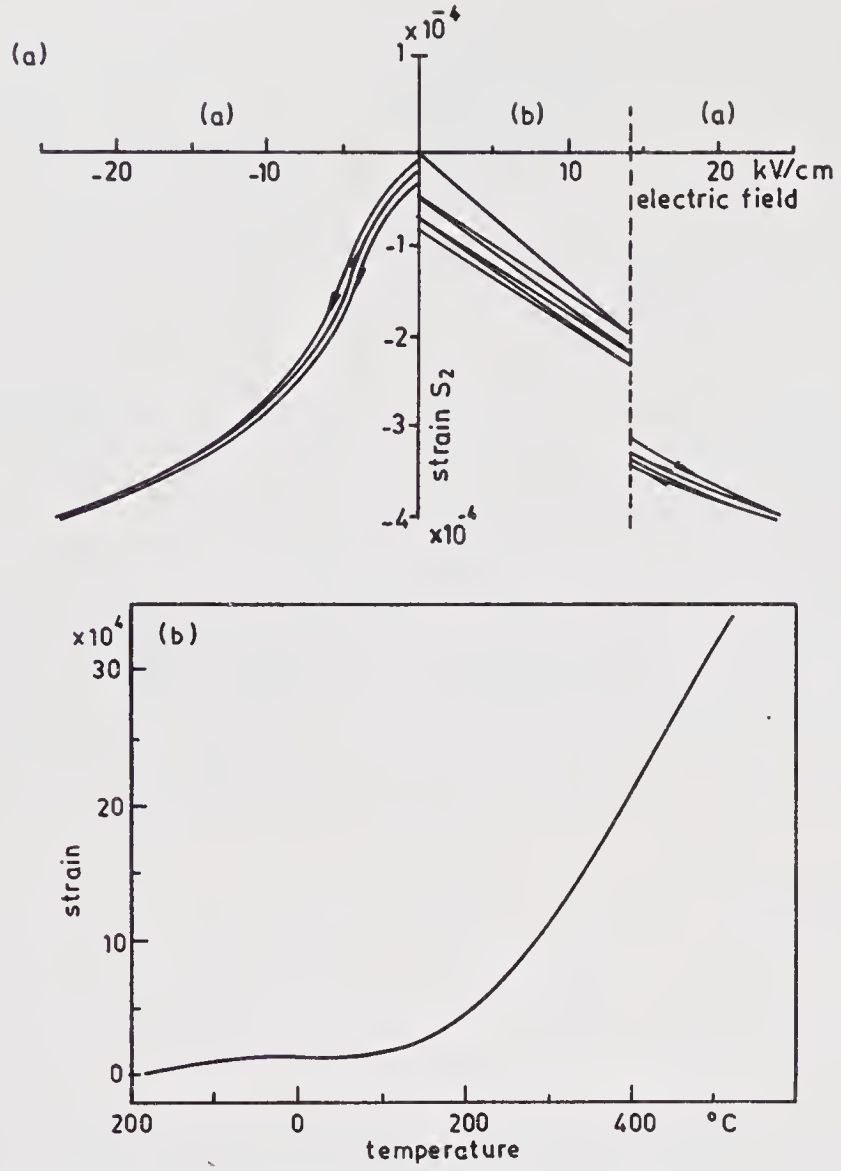

Figure 11. (**a**) Transverse strain of a ceramic specimen of 0·9 PMN:0:0·1 PT in a typical hard PZT 8 piezoelectric ceramic under slowly varying electric fields. Strain levels are comparable in the two materials but the relaxor is more reproducible because of the field induced deaging in the PZT. (**b**) Thermal strain in ceramic 0·9 PM N:0·1 PT. Linear expansion is about 10^{-5}/°C at 400°C and less than 10^{-6}/°C at room temperature (Cross 1984).

improved 15 times as compared to normal PZT as shown in table 5 which gives a comparison of several transducer materials. A flexible, low density, compliant piezoelectric transducer with high g_{33} has considerable advantage in hydrophone applications (Skinner *et al* 1978) when compared with normal PZT ceramics.

Piezoelectric ceramics are not only used as transducers but also as resonators and filters (Schuessler 1974; Onoe 1979). Ceramic filters are piezoelectric ceramic substrates with electrodes (interdigital patterns) designed to convert electric signals to mechanical vibrations to obtain filter characteristics by utilizing the mechanical resonance of the substrates. Suitable vibration modes are selected depending upon the filter frequencies needed. Ceramic filters are characterized by small size, high selectivity and high stability as compared to the conventional LC filters and do not

Table 5. Comparison of several transducer materials.

Property	PVF_2	Homogenous PZT-501A	Flexible 3–3 composite
Density			
$\times 10^3$ kg/m^3	1·8	7·9	3·3
Compliance	High	Low	High
$d_{33} \times 10^{-12}$ c/N	14	400	100
ε_R	10	2000	40
$g_{33} \times 10^3$ Vm/N	140	20	300

Reference: Skinner *et al* 1978

require adjustment (e.g. Cross 1984). They play an important role in radio circuits, determining their selective performance and in video circuit separating audio from video signals. The FM single chip IC radio uses PZT ceramics as discriminators. Typical transmission characteristics of a monolithic filter element are shown in figure 12.

The PZT ceramics in their shear mode are also used in delay lines for colour TV sets and also in high frequency military communication and detection. These ceramics are also one of the candidate materials for use as substrate for surface acoustic wave (SAW) devices. High frequency filters can be easily fabricated by merely varying the interdigital transducer (IDT) pitch. This can be accomplished by utilizing IC manufacturing techniques. However, $LiNbO_3$ single crystal substrates are more popular for this application in spite of their somewhat higher cost.

5. Sensors

The various special properties of ceramics such as the grain boundary phenomenon (e.g. positive temperature coefficient of resistivity, voltage dependent resistivity etc.), the piezoelectric effects, oxygen ion conductivity, or controlled pore structure (water vapour condensation) etc. are going to be utilized increasingly for the next generation of sensors for various applications (e.g. Fisher 1986; Murata & Itoh 1985). Ceramic sensors can be optimized and tailored to specific applications. Given the extremely diverse and specialised nature of the market, interest by the process

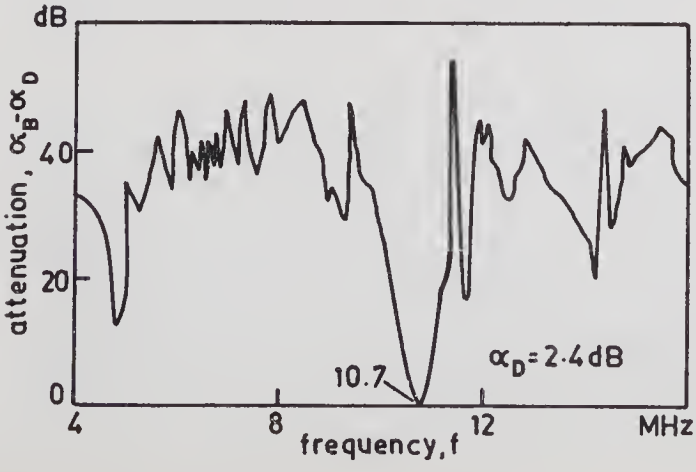

Figure 12. Transmission characteristic of monolithic filter element (coupling coefficient 1·65%, matching resistors 125 Ω, transmission loss $a_D = 2{\cdot}4$ dB (Schuessler 1974)

industry could have a strong guiding effect on ceramic sensor development (Wachtman J B Jr, unpublished).

An interesting and very important line of development is the integration of sensing elements on to the same silicon chip as microcircuitry (Allen 1984). Force, proximity, heat, motion and chemical analysis sensors are being developed very actively.

6. Dielectric resonators

These ceramics work on the principle that dielectric samples exhibit electromagnetic resonance as soon as the wavelength gets shorter than the sample size. If the resonant frequency versus time, temperature etc., is stable, such devices are very useful for making microwave filters and oscillators allowing size reduction and easier manufacturing (Plourde 1981). The applications are in military communication equipment, TV satellite reception etc.

A number of materials have been studied for these applications which include the zirconate systems, barium nanotitanate ($Ba_2 Ti_9 O_{20}$), (Zr, Sn) TiO_4, $BaO\text{-}Nd_2O_3\text{-}TiO_2$, Ba(Zn, Ta) O_3, etc. An excellent review on high frequency dielectrics was recently presented by Wakino & Tamura (1986–unpublished). Two of the above compositions, the nanotitanate and the (Zr, Sn) TiO_4 seem to have been in commercial production. Since the damping constant, or the quality factor, depends on lattice imperfections and impurities, minimization of various defects in the grains is very essential for successful manufacture.

7. Processing and fabrication

A good deal of work is going on particularly in Japan and USA on the development of novel processing routes for the synthesis of high quality powders (high purity and controlled particle size) (e.g. Mazdiyasni 1984) for use as starting materials. However, the bulk of the commercial production still appears to be done using the powders prepared from the conventional solid state route because of the high cost of the former. Nevertheless, high quality powders will be increasingly used for the newer sophisticated applications (e.g. figure 1). Considerable control of the microstructure is being done through careful selection of the initial raw materials and careful processing for the majority of the items discussed and invariably for the devices based on grain boundary phenomenon.

A ceramic fabrication process that was exclusively developed for the fabrication of thin ceramics and multilayers is the tape casting process. In this process, ceramic powder in the form of a slurry (consisting also of binders, plasticizers, surfactants and solvents) is cast on to a moving carrier belt or tape, using a doctor blade to control the thickness. There are many excellent articles (Shanefield & Mistler 1971; Williams 1976) on the details of this process and a good deal of development effort is going on to minimise the extent of polymer and the total organic content in the ceramic slurries and also to remove the polymer phase through reactive chemical processing instead of burning (Tormey *et al* 1984). Cosintering of metals and ceramics in the multilayer ceramics is a careful operation necessitating close control.

In the case of PZT ceramics, fine powders prepared by the special processing routes are used in some applications such as substrates for SAW filters etc. Hot pressing techniques are being tried for the production of very high density material and also for translucent ceramics. Innovative processing techniques are being developed to fabricate composite PZT. One such is the lost wax technique to replicate skeletal structures described in detail by Skinner *et al* (1978). Semiconductor processing techniques such as photolithography and thin film technology are widely used for printing fine line conductor patterns on PZT ceramics used for filter applications. The other supporting technologies that are often used are screen printing, electroplating, brazing etc. In addition to materials processing technologies, special encapsulation and packaging techniques are to be evolved for some of the devices (e.g., ceramic filters for TV SIF stage) for successful production.

8. Status in India

A summary of R & D activities on different electronic ceramic materials in India is given in table 6. It is clear from the table that R & D work of fairly high quality has been done in most of the areas of electronic ceramics reviewed. However, total production technologies leading to a competitive position in the market place are yet to be significantly evolved by indigenous efforts. Bharat Electronics Ltd., Bangalore, and Central Electronics Ltd., Sahibabad, are engaged in such activity to some extent. In some areas such as PZT ceramics, although considerable amount of R & D work has been done by a number of institutions in the country, the extent of commercialization is not proportional. This is to some extent due to the small quantity demands for many of the items. On the other hand, in areas such as multilayer ceramics and related materials (including substrates) the effort is not significant, although these products are likely to command considerable markets including defence requirements in the future.

The availability status of the basic raw materials required for electronic ceramics is given in table 7. It can be seen that India has almost all the basic raw materials that are generally used in the production of electronic ceramics. However, the purity levels and the powder characteristics need to be further tailored to meet the exact requirements of many of the sophisticated applications.

9. Markets

In the field of advanced ceramics, electronic ceramics are expected to constitute a major share of the market at least till 2000 AD. The industry analysis division of the US Department of Commerce (Rah 1986) indicates markets worth $1825 million for advanced ceramics in the year 1985 out of which about $1700 million is for electronic ceramics. The predicted figure in 2000 AD is $3485 million for electronic ceramics out of a total of $5895 million for advanced ceramics. The markets in Japan are slightly higher, $1800 million in 1985 and $2200 million by 1990. These two countries together share more than 80% of the world market and this trend is expected to continue in the future also. The market figures indicated above are only approximate and are meant to convey general trends. The figures vary from source to source. A

Table 6. Summary of R&D activities on various electronic ceramic materials in India.

Nature of work	Centre/or centres where carried out*	Nearest application area
a) Mn-doped $BaTiO_3$ and study of the saturation characteristics of PLZT composition with different dopants	IIT, Kanpur (Desu & Subbarao 1981; Gururaja & Subbarao 1980)	Multilayer ceramic capacitors
b) Low temperature firable dielectric compositions	IIT, Kanpur (Ramesh Choudhary & Subbarao 1981) BEL, Bangalore (Mukherjee & Ravishankar 1978)	Multilayer ceramic capacitors
Low temperature firable glass ceramic compositions	BEL, Bangalore	Multilayer substrates
Tape casting process technology	BEL, Bangalore (Prasad & Kannan 1982)	Multilayer ceramics, alumina substrates and some PZT transducer devices
Effect of process variables, EPR studies for characterizing the internal boundary layers, microstructural studies etc.	IISc, Bangalore (Kutty *et al* 1984; Murugaraj & Kutty 1985). IIT, Kharagpur	IBL capacitors
a) Investigations on the PTC effect in $BaTiO_3$, effect of different dopants, process variables, study of the interfacial resistance and EPR studies.	IISc, Bangalore (Gajbhiye 1981) IIT, Kharagpur (Maiti *et al* 1986) IIT Madras	Devices based on PTC phenomenon
b) Process technology	BEL, Bangalore	Devices based on PTC phenomenon
Grain growth kinetics in ZnO varistors	NPL, Delhi (Kalsi & Das 1983)	ZnO varistors
Device development activity	BHEL, Hyderabad and W.S. Insulators Madras	ZnO varistors
a) Development of different PZT compositions, effect of process variables, different dopants etc.	NPL, Delhi, NCL, Poona (Deshpande & Roy Choudhary 1982) NCML, Bombay (Ramjilal & Ramakrishnan 1984) ARDE, Poona (Dhami *et al* 1986) BEL, Bangalore	Different PZT applications
b) Establishment of standards, biomedical applications etc.	NPL, Delhi (e.g. Bindal & Kumar 1985)	
c) Novel processing routes for powders	TIFR, Bombay (Palkar & Multani 1979) IISc, Bangalore (Kutty & Balachandran 1984) NCML, Bombay	Highly demanding PZT applications
d) Devices	BEL, Bangalore, CEL, Sahibabad, NPL, New Delhi, ARDE, Poona	

*Abbreviations used: ARDE – Armanents Research & Development Establishment; BEL – Bharat Electronics Ltd.; BHEL – Bharat Heavy Electricals Ltd.; CEL – Central Electronics Ltd.; IISc – Indian Institute of Science; IIT – Indian Institute of Technology; NCL – National Chemical Laboratory; NCML – Naval Chemical & Metallurgical Laboratory; NPL – National Physical Laboratory; TIFR – Tata Institute of Fundamental Research.

recent revised projection of the Japan Fine Ceramic Research Association (*Ceram. Ind. (Chicago)* 1986a) indicates a value of $ 18·8 billion for electronic and magnetic ceramics out of a total of $ 30·6 billion by the year 2000.

Table 7. Availability status in India of the major raw materials for electronic ceramics.

Raw materials	Purity of the powder available in India	Comments
Bauxite (oxide of aluminium)	Al_2O_3 – 99·5%	Suitability for technical and electronic ceramics yet to be established. India has one fifth of the total world resources of bauxite
Barytes (sulphate of barium)	$BaCO_3$ – 98·7%	Further improvements are required to make it suitable for many of the electronic ceramic applications
Galena (sulphide of Pb)	PbO – 99·5% (?)	Suitable for many of the PZT ceramic applications
Ilemenite (iron titanate)	TiO_2 – 98%	Although of pigment grade, fairly suitable for use in ceramic capacitor and PZT production particularly for commercial applications. Much purer powders are required for PTC applications
Rare earths (monazite beach sands)	La_2O_3, Pr_2O_3, Nd_2O_3 99·9%	Suitable for electronic ceramic applications
Zircon (silicate of zirconium)	ZrO_2, 96–97·5%	Suitable for use in dielectric and PZT production for commercial applications
Zinc blend (ZnS)	ZnO – 99·5%	Purer powders were tried for the laboratory investigations (Kalsi & Das 1983). But, considering the extremely competitive nature of the product, the cheapest raw materials which can give the required properties should be chosen

The current demand for electronic ceramics in India (author's own estimate) is about Rs. 240 million (approximately $ 20 million) which is expected to grow to about Rs. 1700 million (approximately $ 140 million) by the end of the century (a three-fold increase* during the 7th plan, and about 10% annual increase thereafter is assumed). Right now about 40 to 50% of the requirement seems to be met by indigenous production consisting mainly of ferrites and ceramic capacitors. However, most of this production is for commercial markets and not significantly for professional markets. Very few of the products that are under discussion in this review (table 1) are being manufactured in India right now. The approximate break up of the current demand position of different categories is given in table 8 which also includes the world sales for 1985 and the expected growth (%) during 1985–1990 for each of the categories. According to the table, ferrites constitute the major share of the markets in India (nearly 42%) whereas the world trend is different. In the latter case, packages and substrates constitute the major share (41%) followed by ceramic capacitors (24%). The same trend is likely to appear in India with the increasing use of integrated circuits and the general growth of the electronics industry. Japan dominates (Kenney & Bowen 1983) at least two areas of electronic ceramics, viz., the ceramic packages (at least 70–80% of the world market) and PZT ceramics (about

*A five-fold increase in electronic systems is predicted during the 7th plan.

Table 8. Estimated demand of different electronic ceramics in India as compared to world figures

Item	Estimated Indian market		World market sales in 1985+	
	Millions of rupees in 1986	Millions of dollars	Millions of dollars	Predicted growth till 1990 (%)
a) Substrates and packages	10	0·77	1,700	10
b) Other alumina ceramics for electron tubes, headers etc.	6	0·46		
Capacitors				
a) Discs	40	3·8	1,000	14
b) Multilayers	40	3·8		
Ferrites*	100	7·7	900	14
Piezoelectric ceramics (including telephones elements)	35	2·7	300	14
Thermistors and varistors	10	0·76	200	14
	241	≈ 20·00	4,100	

References: *Jain & Sarnot (1982); +*Ceram. Ind. (Chicago)* (1986b)

90% of the world market). The Indian market right now is about 0·5% of the world market.

10. Summary and concluding remarks

Circuit miniaturization and cost reduction are the two aspects at which most of the developments in electronic ceramics are aimed. This is particularly so for components like multilayer ceramics, the IBL capacitors, the dielectric resonators and many of the filters (table 1). Based on the unique grain boundary phenomenon in some of the electronic ceramics which is still to be adequately understood (particularly the structure and chemistry of the boundaries) a number of useful devices have been evolved such as the PTC thermistors, the IBL capacitors and the varistors etc. Efforts will continue to improve the characteristics of these devices for more demanding applications and some of them will find increasing use as sensors in different applications. The use of PZT ceramics is on the increase in the areas of communication and biomedical applications and newer composites are expected to diversify their scope still further. Many advantages are foreseen by the use of the majority of the electronic ceramic devices in multilayer configurations and therefore a good amount of work is expected in this direction. Development of newer innovative processing techniques to improve the device performance and reduce the costs are expected to continue.

Although there is a fair amount of R & D activity in many of the areas of electronic ceramics in the country, cost effective production techniques leading to a competitive position in the market place are yet to be significantly evolved. More emphasis therefore has to be placed on the technology development aspects in order to fill this gap. Perhaps the suggestion (*Am. Ceram. Soc. Bull.* 1986) by the Federation of the Materials Societies of US, viz., fostering the attitude that involvement in processing science and manufacturing technology is not a 'lower calling' than more traditional research and development, has to be followed vigorously in India. In

addition, the natural advantages of the raw materials have to be utilized better. The report (IPAG 1976) of the panel on interministerial coordination for indigenous development of electronic materials recommends electronic ceramics as one of the priority materials for indigenous development because it meets at least three of the five criteria laid down for selecting the projects for indigenization, viz., good development and production infrastructure, availability of raw materials and strategic importance. This recommendation holds good even today (nearly a decade after the recommendation), particularly in view of the important role electronic ceramics play in computers, communications, process control instrumentation and in a host of other commercial and military applications.

The author acknowledges the encouragement he received from the management of the Bharat Electronics Ltd. during the preparation of this review.

References

Alam M I, Nair N R 1981 *IPAG* 8: 420–422*
Allen R 1984 *High Technol.* 43–50
*IPAG** 1976 4: 80
Ceram. Ind. (*Chicago*) 1986a, 8: 14
Ceram. Ind. (*Chicago*) 1986b, 126 (3): 9
Am. Ceram. Soc. Bull. 1986 65: 1115–1117
Bindal V N, Ashok Kumar 1985 *J. Pure Appl. Ultrasonics* 7: 57–60
Blum S L, Kaslos S H, Wachtman J B Jr 1985 *Ceram. Ind.* (*Chicago*) 125 (1): 26–30
Cantagrel M 1986 *Am. Ceram. Soc. Bull.* 65: 1248–1249
Capozzi V F 1975 *Multilayer ceramic capacitor materials and manufacture* (New Jersey: Oxymetal Ind. Co.)
Chen J, Gorton A, Chan H M, Harmer M P 1986 *J. Am. Ceram. Soc.* C69: 303–305
Cross L E 1984 *Am. Ceram. Soc. Bull.* 63: 586–590
Daniels J, Hardtl K H, Wernicke R 1979 *Philips Tech. Rev.* 38: 73–82
Daniels J, Wernicke R 1976 *Philips Res. Rep.* 31: 544–559
Das B K 1981 in *Preparation and characterisation of materials* (eds) J M Honig, C N R Rao (New York: Academic Press)
Desu S B, Subbarao E C 1981 in *Grain boundary phenomenon in electronic ceramics* (eds) L M Levinson, D C Hill *Advances in ceramics* (Ohio: The American Ceramic Society) 1: 189–206
Deshpande S B, Roy Chowdhary P 1982 Proceedings of the IInd National Conference on Ferroelectrics and Dielectrics, pp. 121–123
Dhami G S, Pingle S V, Singh T G, Kulkarni S K 1986 Proceedings of the III National Symposium on Ultrasonics (to be published)
Fisher G 1986 *Am. Ceram. Soc. Bull.* 65: 622–628
Gajbhiye N S 1981 *Investigations on the positive temperature coefficient of resistance in polycrystalline barium titanate*, Ph D thesis, Indian Institute of Science, Bangalore
Goodman G 1981 in *Grain boundary phenomenon in electronic ceramics* (eds) L M Levinson, D C Hill *Advances in ceramics* (Ohio: The American Ceramic Society) 1: 215–231
Gururaja T R, Subbarao E C 1980 *Ferroelectrics* 23: 101
Heywang W 1961 *Solid-State Electron.* 3: 51
Ihrig H 1983 in *Additives and interfaces in electronic ceramics* (eds) M F Yan, A H Heuer *Advances in ceramics* (Ohio: The American Ceramic Society) 7: 117–127
Jaffe B, Cook W R, Jaffe H 1971 *Piezoelectric ceramics* (New York: Academic Press)
Jain A K, Sarnot S K 1982 *IPAG* 9: 175
Jonker G H 1981 in *Grain boundary phenomenon in electronic ceramics* (eds) L M Levinson, D C Hill *Advances in ceramics* (Ohio: The American Ceramic Society) 1: 135–166

*IPAG – Information planning and analysis group (a publication of the Electronics Commission of India).

Kalsi H S, Das B K 1983 *Bull. Mater. Sci.* 5: 33–38
Kenney G B, Bowen H K 1983 *Am. Ceram. Soc. Bull.* 62: 590
Kulwieki B M 1981 in *Grain boundary phenomenon in electronic ceramics* (eds) L M Levinson, D C Hill *Advances in ceramics* (Ohio: The Ameriean Ceramic Soeiety) 1: 138–154
Kutty T R N, Murugaraj P, Gajbhiye N S 1984 *Mater. Lett.* 2: 396
Kutty T R N, Balaehandran R 1984 *Mater. Res. Bull.* 19: 1479–1488
Levinson L M, Philip H R 1986 *Am. Ceram. Soc. Bull.* 65: 639–646
Mahan G D 1982 in *Grain boundaries in semiconductors* (eds) H J Leany, G E Pike, C H Seager (New York: North Holland)
Maiti H S, Chowdhary R N P, Basu R N 1986 Report on the development of PTC resistors for applieations in fluid flow and liquid level sensors, Materials Scienee Centre, Indian Inst. Teehnol. Kharagpur
Matsuoka M 1971 *Jpn. J. Appl. Phys.* 10: 736
Matsuoka M 1981 in *Grain boundary phenomenon in electronic ceramics* (eds) L M Levinson, D C Hill *Advances in ceramics* (Ohio: The Ameriean Ceramie Soeiety) 1: 290–308
Mazdiyasni K S 1984 *Am. Ceram. Soc. Bull.* 63: 591
Mukherjee J L, Ravishankar H S 1978 Proe. Symposium on Sintering and Sintered Produets, Dept. of Atomie Energy, India, pp. 281–290
Murata M, Itoh S 1985 *J. Electron. Eng.* 22 (2): 84–88
Murugaraj P, Kutty T R N 1985 *Mater. Res. Bull.* 20: 1473–1482
Newnham R E, Hiremath B V 1985 Materials Researeh Laboratory Report, Pennsylvania State University
Nishida M, Kawashima S, Ueda I, Ouehi H 1980 *J. Phys. Soc. Jpn.* 49 (Supplement 8): 200–202
Onoe M 1979 *Proc. IEEE* 67: 75–102
Ohr S 1983 *Electronic Design* 6: 135–146
Paikar V R, Multani M S 1979 *Mater. Res. Bull.* 14: 1353
Plourde J K 1981 *IEEE Trans. Microwave Theory Tech.* MTT-29: 754
Prasad V C S, Kannan P 1982 *Am. Ceram. Soc. Bull.* 61: 1234–1235
Rah H 1986 *Interceram* 4: 36
Ramjilal, Ramakrishnan P 1984 *Bull. Mater. Sci.* 6: 83–89
Ramesh Choudhary K, Subbarao E C 1981 *Ferroelectrics* 37: 689–692
Reiss E M, Glieksmann R 1981 *Solid State Technol.* 199–203
Ryan F M, Subbarao E C 1962 *Appl. Phys. Lett.* 1: 69–71
Sehwartz B 1984 *Am. Ceram. Soc. Bull.* 63: 577
Sehwartz B 1986 *Am. Ceram. Soc. Bull.* 65: 1032
Sehuessler H H 1974 *IEEE Trans. Sonics Ultrason.* SU–21:
Shanefield D J, Mistler R E 1971 *West. Electr. Eng.* 15(2)
Skinner D P, Newnham R E, Cross L E 1978 *Mater. Res. Bull.* 13: 599–607
Subbarao E C, Prasad V C S, Veerabhadra Rao K 1981 in *Preparation and characterization of materials* (eds) J M Honig, C N R Rao (New York: Aeademie Press)
Swartz S L, Shrout T R, Sehulze W A, Cross L E 1984 *J. Am. Ceram. Soc.* 67: 311–315
Takahashi S, Takahashi M 1972 *Jpn. J. Appl. Phys.* 11: 31–5
Takawizawa H, Utsumi K, Yonezawa M, Ohno T 1981 Proe. 31st Eleet. Comp. Conf., pp. 302–7
Tormey E S, Polar R L, Bowen H K 1984 in *Forming of ceramics* (eds) J A Mangels, G L Messing *Advances in ceramics* (Ohio: The Ameriean Ceramie Soe.) 9: 140–149
Uehino K 1986 *Am. Ceram. Soc. Bull.* 65: 647–652
Uchino K, Nomura S, Cross L E, Newnham R E 1980 *J. Phys. Soc. Jpn.* 49 (Supplement 8): 200–202
Utsumi K, Shimada Y, Ibeda T, Takamizawa K, Nagasako S, Fuji S, Nanematsu S 1985 *NEC Res. Dev.* 77(4): 1–12
Waku S 1969 Reports of Researehers and Applieations at Nippon Telephone and Telegraph Corp., Japan, pp. 18–22
Wernieke R 1981 in *Grain boundary phenomenon in electronic ceramics* (eds) L M Levinson, D C Hill *Advances in ceramics* (Ohio: The Ameriean Ceramie Soc.) 1: 261–281
Williams J C 1976 in *Treatise on materials science and technology* (ed.) F W Wang (New York: Academie Press) 9: 176–190
Yan M F, Rhodes W W 1983 in *Additives and interfaces in electronic ceramics* (eds) M F Yan, A H Heuer *Advances in ceramics* (Ohio: The Ameriean Ceramie Soeiety) 7: 226–238
Yonezewa M 1983 *Am. Ceram. Soc. Bull.* 62: 1375–1378

High temperature fuel cells

H S MAITI*[1] and M K PARIA[2]

[1]Electroceramics Section, Central Glass & Ceramic Research Institute, Calcutta 700 032, India
[2]Refractories Division, National Metallurgical Laboratory, Jamshedpur 831 007, India

Abstract. A high temperature fuel cell using a solid oxide electrolyte, and operated at temperatures above 700°C, is a highly efficient energy conversion device utilizing primarily gaseous fuels like H_2 and CO. It can also be operated in the reverse manner as a high temperature steam electrolyser to produce hydrogen. The operating principle and the construction details of different design concepts have been discussed. Nonavailability of suitable electrode and interconnection materials has hampered commercial exploitation. Recent trends in the development of these materials have been focussed upon, both in the national and the international context.

Keywords. Fuel cell; steam electrolysis; solid electrolyte; battery design; thin film.

1. Introduction

A fuel cell is an electrochemical device which directly converts the chemical energy of a fuel into electrical energy. In a fuel cell, the fuel and the oxidant, which is usually oxygen or air, are supplied continuously from an external source and power is also drawn continuously. In a conventional battery, on the other hand, the fuel and the oxidant are contained within and when these reactants are consumed the battery must be replaced or recharged.

Since a fuel cell produces power by electrochemical reactions, unlike thermal machines, its efficiency is not limited by the Carnot cycle. Thus it has the potential for highly efficient conversion of chemical to electrical energy. Furthermore, its efficiency is essentially independent of size; small power plants operate nearly as efficiently as the large ones. As the by-products are water, carbon dioxide and nitrogen, fuel cell power plants are clean and quiet. They have considerable flexibility and can be designed to use either liquid or gaseous fuels (e.g., hydrogen, hydrazine, hydrocarbon, methanol, coal gas etc.) and produce a wide range of DC or AC power outputs. Like batteries, they are modular in construction and can be configured in

*On leave from Indian Institute of Technology, Kharagpur

any capacity from milliwatts to megawatts. Above all their attraction lies in their flexibility and the many diverse applications they can be used in.

2. Classification of fuel cells

Fuel cells are classified into direct and indirect-fuelled systems based on the type of fuel used. In the direct-fuelled system, the fuel is readily oxidised electrochemically and is fed directly. In the other kind, the fuel is first converted in a fuel-processing subsystem to an easily oxidisable hydrogen-rich gas, which is then fed into the fuel cell. They can also be classified, based on the temperature of operation. The low temperature system operates below 260°C and the electrolytes are normally acids (H_2SO_4, H_3PO_4), solid polymer electrolytes or aqueous alkalies (KOH). The intermediate temperature systems (260–750°C) use molten carbonates (Li_2CO_3, Na_2CO_3) or molten alkalies (KOH). High temperature systems (>750°C) use solid oxide electrolytes (ZrO_2) which have sufficient thermal and structural stability above 750°C.

The low temperature fuel cells which consist of liquid electrolytes (acid or alkali) suffer from the problem of corrosion of container or carbonation of the electrolyte. Low temperature operation favours electrode polarisation and poisoning of the electrodes by impurities. Besides these problems, the difficulty of maintaining a stable 3-phase contact (liquid-solid-gas) creates design problems at the electrodes. The molten alkaline system is not attractive because of the complexity. The high temperature fuel cell (HTFC) based on solid oxide electrolyte has a favourable effect on the reaction kinetics and mass transfer at the electrodes due to high operating temperature (~1000°C). High current and power densities are obtained without much polarisation loss and without application of a noble metal catalyst.

The high temperature solid electrolyte fuel cell can also be used as a high temperature steam electrolyser (HTSE) by allowing the electrochemical reaction to take place in the reverse direction so that water vapour can be electrolysed at high temperature into hydrogen and oxygen by supplying electrical energy and heat to the same cell. The efficiency of HTSE is considerably higher than that of conventional low temperature water electrolysis (Spacil & Tedmon 1969). Overall plant efficiency of 40–50% has been predicted compared to below 30% for conventional electrolysis (Doenitz *et al* 1980).

3. Principles of HTFC and HTSE

Although the principle of HTFC was first conceived by Baur & Preis (1937) a laboratory model was developed only in the early sixties (Weissbart & Ruka 1962; Archer & Sverdup 1962; Carter *et al* 1963; Archer *et al* 1964). Extensive developmental programmes have been undertaken in the latter part of the seventies and the early eighties by three main research groups, namely, Westinghouse Electric Corporation, USA (Isenberg 1978, 1981; Feduska & Isenberg 1983), Brown Boveri, West Germany (Rohr 1968, 1978, pp. 431–462) and AERE, Harwell, UK (Markin 1972; Markin *et al* 1976, pp. 15–35). Presently, the principles of operations of HTFC and HTSE are well-understood and are shown schematically in figure 1 which

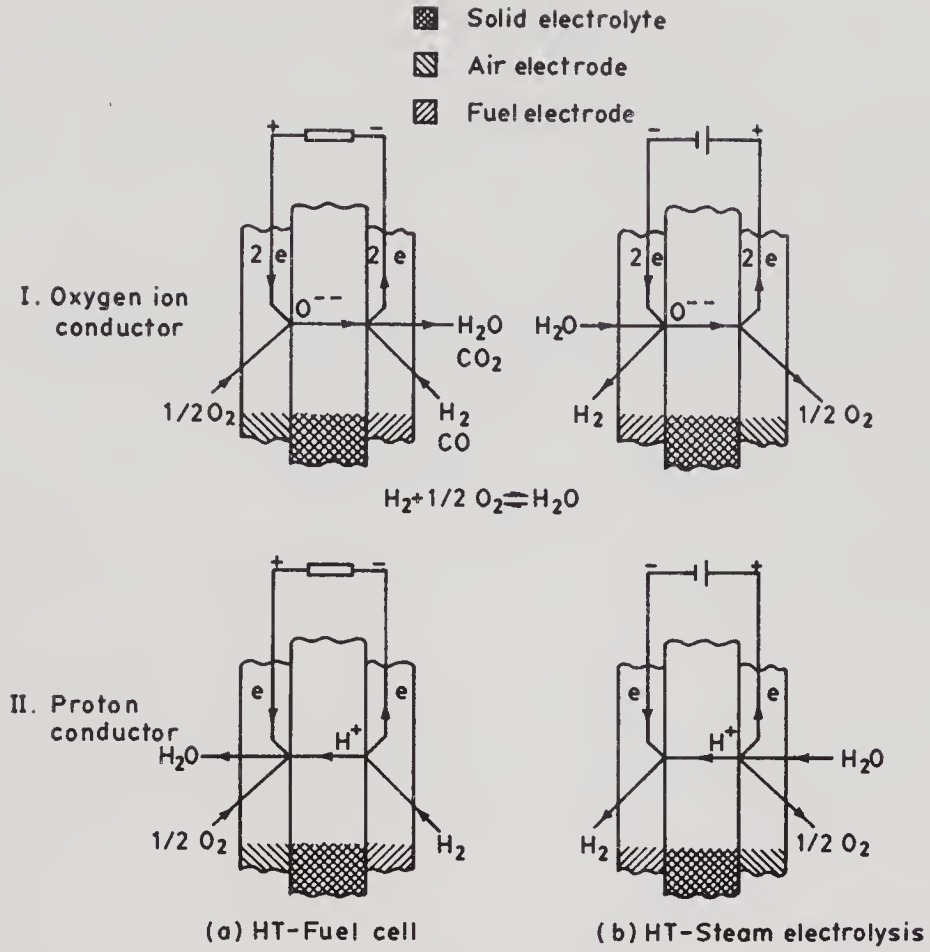

Figure 1. Principles of HTFC and HTSE.

includes the use of both oxide ion and proton ion conductors. The cell is usually made of thin-walled solid electrolyte tube. The inner and outer surfaces of the tube are coated with electronically conducting electrodes. A gaseous fuel like hydrogen or a mixture of H_2 and CO is led to the inner electrode, and oxygen or air is led to the outer electrode. Due to the difference in oxygen activity at the electrodes, an electrical potential is developed, the magnitude of which depends on the temperature and oxygen partial pressures at the electrodes. The theoretical EMF (E_0) of the cell is given by the equation

$$E_0 = (RT/4F) \ln [p_{O_2}(c)/p_{O_2}(a)], \tag{1}$$

where $p_{O_2}(c)$ and $p_{O_2}(a)$ are the oxygen partial pressures at the cathode and the anode, respectively.

During power generation, oxygen at the cathode picks up an electron forming an oxygen ion. This oxygen ion passes through the oxide solid electrolyte and reacts with H_2 or CO at the anode to form H_2O or CO_2. The electrons released at the anode by this electrochemical process flow back to the cathode through the external circuit. In this way, electrical energy is available in the external circuit. The theoretical EMF of the H_2/O_2 fuel cell (E_0^{FC}) is given by the equation

$$E_0^{FC} = (RT/2F) \ln [K p_{H_2} p_{O_2}^{\frac{1}{2}} / p_{H_2O}(a)], \tag{2}$$

where K = equilibrium constant of the reaction

$$H_2(g) + \tfrac{1}{2} O_2(g) \rightleftharpoons H_2O(g), \tag{3}$$

p_{H_2} and p_{H_2O} are the partial pressures of H_2 and H_2O respectively. Similarly for the proton ion conductor fuel cell, the EMF (E_H^{FC}) is given by the following equation.

$$E_H^{FC} = (RT/2F) \ln [K p_{H_2} p_{O_2}^{\frac{1}{2}} / p_{H_2O}(c)] \tag{4}$$

In case of the high temperature steam electrolysis, steam, electrical energy and heat are led to the same type of cell. All the reactions at the electrodes, the flow of ions within the electrolyte, and the flow of electrons in the external circuit, take the reverse direction. In case of an oxygen ion conductor, hydrogen is produced at the inner electrode and in case of a proton conductor, hydrogen is produced at the outer electrode and oxygen at the inner electrode (figure 1).

Hydrogen may be used as a fuel in the cell using either an oxide ion conductor or a proton conductor. But carbon monoxide can be used as a fuel only if an oxide ion conductor is used as the electrolyte and the cell reaction is

$$2CO + O_2 \rightleftharpoons 2CO_2. \tag{5}$$

When the fuel cell delivers a current I, the voltage E decreases below the theoretical value E_0, due to ohmic losses IR_i (R_i = internal resistance of the cell) and polarisation losses V_p at the electrodes. As an approximation

$$E = E_0 - IR_i - V_p. \tag{6}$$

The ratio

$$\eta_E = (E/E_0) = 1 - [(IR_i + V_p)/E_0], \tag{7}$$

is considered the voltage efficiency of the cell. The most important factor in the development of the fuel cell is the optimisation of efficiency in respect of ohmic loss and polarisation loss, taking into account other factors like life-time, material and manufacturing cost.

4. Materials for cell construction

4.1 *Solid electrolyte*

a) *Oxide ion conductor*: The oxide solid electrolyte to be used for construction of a fuel cell and a steam electrolyser should have the following characteristics at the operating temperature of about 1000°C: (1) high oxygen ion conductivity with negligible electronic conductivity, (2) phase stability, (3) mechanical strength, (4) gas tightness, (5) thermal shock resistance, (6) chemical resistance to the reacting gases, and (7) compatibility with the electrodes and interconnection materials. Most of these requirements are met satisfactorily by ceramic solid electrolyte of doped zirconia (Archer *et al* 1964). Attempts have been made to replace ZrO_2 by CeO_2 solid electrolyte. But CeO_2-based solid electrolytes suffer from the disadvantages that, due to the higher electronic conductivity in a reducing atmosphere, the cell voltage and efficiency are reduced (Kudo & Obayashi 1976; Ross & Benjamin 1977).

Doped ZrO_2 with lower valent metal oxides results in a higher oxygen ion

conduction and stabilisation of the cubic crystal structure over a very broad temperature range (Etsel & Flengas 1970). ZrO_2 is usually doped with 15 mol% calcium oxide or 10 mol% yttrium oxide (Archer *et al* 1964) or 4 mol% yttrium oxide and 4 mol% ytterbium oxide (Eysel & Rohr 1967). The specific electrical resistivities (ρ_E) at 800°C and 1000°C are given in table 1. The table also gives the allowed maximum wall thickness d_E of the solid electrolyte for power densities upto 0·25 W/cm^2, in the case that no other electrical losses would exist. Long term behaviour and life tests of cells with Y_2O_3/Yb_2O_3-doped ZrO_2 electrolyte at 1000°C showed that during a working period of more than three years, the required properties of the electrolyte were not affected (Rohr 1975; Brown Boveri 1975).

b) *Proton conductor*: The protonic solid electrolyte to be used for construction of HTFC/HTSE should have properties similar to oxide solid electrolytes. Proton conduction has been observed in a number of materials like β/β''-Al_2O_3 (Frase & Farrington 1984) doped $SrCeO_3$, stabilised ZrO_2, ThO_2, Cu_2O, CuO, NiO and SiO_2 etc. (Iwahara *et al* 1982, 1983). Among these materials only β/β''-Al_2O_3 and $SrCeO_3$ are potential materials so far as electrical conductivity is concerned. Even then their electrical conductivity has to be improved to reduce the operating temperature of the cell, $SrCeO_3$ doped with rare earths like Y_2O_3, Yb_2O_3 and Sc_2O_3 has been studied for fabrication of steam concentration cells and HTSE (Iwahara *et al* 1983a). The performance of the cell has been quite satisfactory as far as stability of the material is concerned. But no HTFC has so far been fabricated out of these materials even on a laboratory scale.

4.2 *Electrodes*

The performance of the HTFC depends not only on the quality of the solid electrolyte but also on the properties of the electrode material and the method of deposition. The electrical properties of the electrode materials are characterised by the ratio of resistivity (ρ_e) to thickness (d_e) and also by the polarisation voltage losses (V_p).

Due to the reducing atmosphere of the fuel electrode (anode) normal metals like cobalt and nickel may be used upto an operating temperature of 1000°C. Cermets of zirconia with nickel and cobalt are used for better thermal expansion matching (Markin *et al* 1976, pp. 15–35; Isenberg 1977). Polarisation losses of these electrodes are shown in table 2.

As an oxidising atmosphere prevails around the air electrode (cathode), only noble metals and oxides with appropriate thermal and chemical stability along with high electronic conductivity at the operating temperature, are suitable as cathode material. The use of a noble metal like platinum is ruled out because of its cost and insufficient

Table 1. Specific resistivity of zirconia solid electrolytes at 800°C and 1000°C (after Rohr 1978).

	800°C		1000°C	
Electrolyte	ρ_E(Ohm cm)	d_E(mm)	ρ_E(Ohm cm)	d_E(mm)
ZrO_2–15 mol% CaO	250	0·04	50	0·2
ZrO_2–10 mol% Y_2O_3	45	0·22	10	1·0
ZrO_2–4 mol% Y_2O_3 –4 mol% Yb_2O_3	20	0·50	5	2·0

Table 2. Polarisation losses of different electrode materials at 1000°C (after Rohr 1978).

Electrode	ρ_E/d_E(Ohm)	IR_i(mV) 0·5(A/cm^2)	V_p(mV) 0·5(A/cm^2)
Anode			
Nickel, PS*	<0·04	<20	<80
Ni- or Co-ZrO_2 (Cermet)	<0·2	<100	<70
Cathode			
$In_2O_3(SnO_2)$ CVD†	<0·3	<150	50–100
$LaNiO_3$(Bi) PS	<0·3	<150	50–100
$LaMnO_3$(Sr) PS	<0·2	<100	50–100

*PS – plasma deposited; †CVD – chemical vapour deposition.

long-term stability. A number of simple and mixed oxides like indium oxide-doped tin oxide (In_2O_3/SnO_2) (Sverdup *et al* 1969; Markin *et al* 1976, pp. 15–35) Sr-doped $LaMnO_3$ (Rohr 1975), perovskite type oxides like Bi-doped $LaNiO_3$ (Steiner *et al* 1972, p. 113) and Ca-doped $LaCoO_3$ (Ochno *et al* 1981; Nagata *et al* 1980, pp. 193–195) have been studied as cathode material. The electrode characteristics of some of the well-tested oxides are given in table 2. It may be noted that the ohmic loss (IR_i) at 0·5 A/cm^2 due to electrode resistance and polarisation losses (V_p) are more or less same.

4.3 *Interconnection material*

For making an HTFC battery, individual cells are connected in series by interconnection material (ICM) which joins the air electrode of one cell to the fuel electrode of the next cell. The interconnection material should have the following characteristics at the operating temperature of 1000°C: (1) high electronic conductivity and negligible ionic conductivity in both oxidising and reducing atmospheres; (2) good chemical and structural stability; (3) gas tightness and mechanical strength; and (4) good adherence and compatibility with ZrO_2 electrolyte and the electrodes. Several mixed oxides like $CoCr_2O_4$ with 2% Mn (Sun *et al* 1972), $LaCrO_3$ doped with Sr and Ni (Baukal *et al* 1976), $LaMnO_3$ doped with Nb_2O_5, Ta_2O_5 or WO_3 (Markin *et al* 1976) and $LaCrO_3$ doped with Mg and Al (Ruka 1978) have been studied but only $CoCr_2O_4$ and $LaCrO_3$ have shown satisfactory performance.

5. Cell characteristics and its stability

The voltage-current characteristics of an HTFC depend on the cell parameters and working condition, specially on the electrical properties and the dimensions of both electrolyte and electrodes as well as on the operating temperature and partial pressures of the reacting gases. For voltage-current and long term behaviour of the cells with conical or tubular shapes having diameters of $D_E \leqslant 25$ mm, heights of $h_E \leqslant 12$ mm and wall thicknesses of $d_E \geqslant 0{\cdot}4$ mm have been studied (Rohr 1978). The height of the cell is limited by the ratio ρ_e/d_e of the oxide cathode and the operating temperature ranges from 800°C to 1000°C. The reactants are either oxygen or air at the cathode and hydrogen or gas mixtures of hydrogen, carbon monoxide, water and carbon dioxide at the anode.

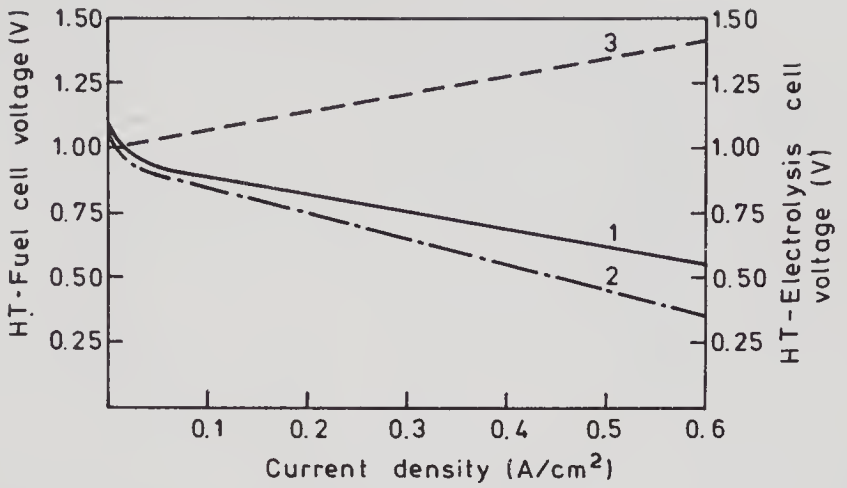

Figure 2. Observed current–voltage characteristics of an HTFC (curves 1 & 2) and HTSE (curve 3) at 1000°C (after Rohr 1978).

Typical voltage-current characteristics of an HTFC when operated with H_2 and O_2 or an H_2/CO mixture and air are shown in figure 2. At an operating temperature of 1000°C and thickness of the electrolyte, $d_E = 0{\cdot}5$ mm, maximum power densities of $0{\cdot}3$ W/cm^2 (H_2/O_2) or $0{\cdot}2$ W/cm^2 ($3H_2 + CO$/air) have been achieved. The experimental open circuit voltage varies from 0·9 to 1·1 V depending on the fuel gas and corresponds well with the theoretical value.

For making the HTFC economically viable, the life of the cell should be five to ten years. With an experimental unit cell at a operating temperature of 1000°C, the cell voltage and power density remained practically constant for more than three years (28,000 operation hours) (Rohr 1975). The test cell was of tubular solid electrolyte of 1·2 mm thickness, having plasma-sprayed electrodes of nickel (anode) and doped $LaNiO_3$ (cathode). With a constant load of 120 mA/cm^2 over a period of 28,000 h, practically constant values of open cell voltage (approximately 1 V) were obtained after some start-up effects during the first 1000 h of operation.

6. Design and fabrication of battery

For making a series connection of the cells in a battery, two basic concepts have been developed: (1) the self-sustaining module using ZrO_2 solid electrolyte tube segments with a minimum wall-thickness of 0·4 to 0·5 mm, sufficient to provide the necessary mechanical strength to the battery, and (2) the thin film design comprising a porous ceramic support coated with the electrolyte and electrode films of 30 to 100 μm thickness.

6.1 *Self-sustaining module concept*

The module is constructed in the form of a long tube from conical or cylindrical tubular segments, each forming a unit cell, by simply fitting one cell into the other. Only ZrO_2 electrolytes have so far been fabricated for this purpose. A number of techniques have been successfully employed to fabricate nonporous tubes. These techniques are conventional ceramic sintering followed by machining (Archer *et al*

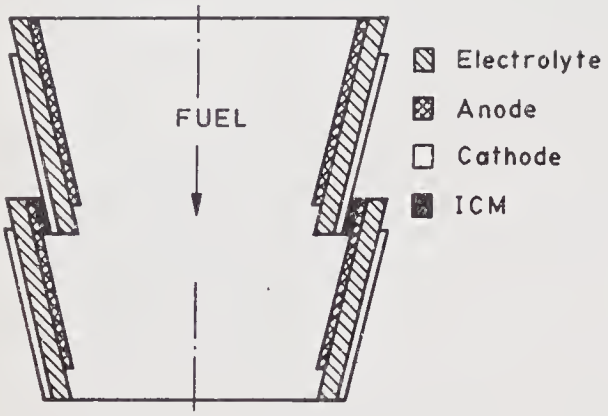

Figure 3. Schematic cross-section of a self-sustaining cell assembly.

1965, p. 51), isostatic pressing and sintering (Steiner 1972; Fischer *et al* 1971), electrophoresis (UK Patent 1972) and plasma spraying (Markin *et al* 1976, pp. 15–35). The application of cathode and anode materials have been tried by different techniques like plasma spraying, chemical vapour deposition, painting and screen printing followed by firing. Satisfactory porous electrode films have been obtained by painting or screen-printing techniques. The series connection of the electrode tubes is obtained by connecting the anode of one cell to the cathode of the next cell by a gas-tight and electron-conducting interconnection material (figure 3) which is usually applied by plasma spraying (Markin *et al* 1976, pp. 15–35). In this way 100 to 120 cells are connected in series; the performance of the battery is presented in figure 4. For a battery of 120 cells, total voltage 110–115 V and a maximum power output of 115 W corresponding to 0·22 W/cm^2 have been obtained at 1000°C with H_2/air as the reaction gases. The voltage losses in a 10-cell battery module under load at 1000°C, resulting from the ohmic resistances of the solid electrolyte (R_E), oxide cathode (R_c), nickel anode (R_A) and inter-connection material (R_{ICM}), as well as from the polarisation at the cathode and the anode ($V_C + V_A$) are

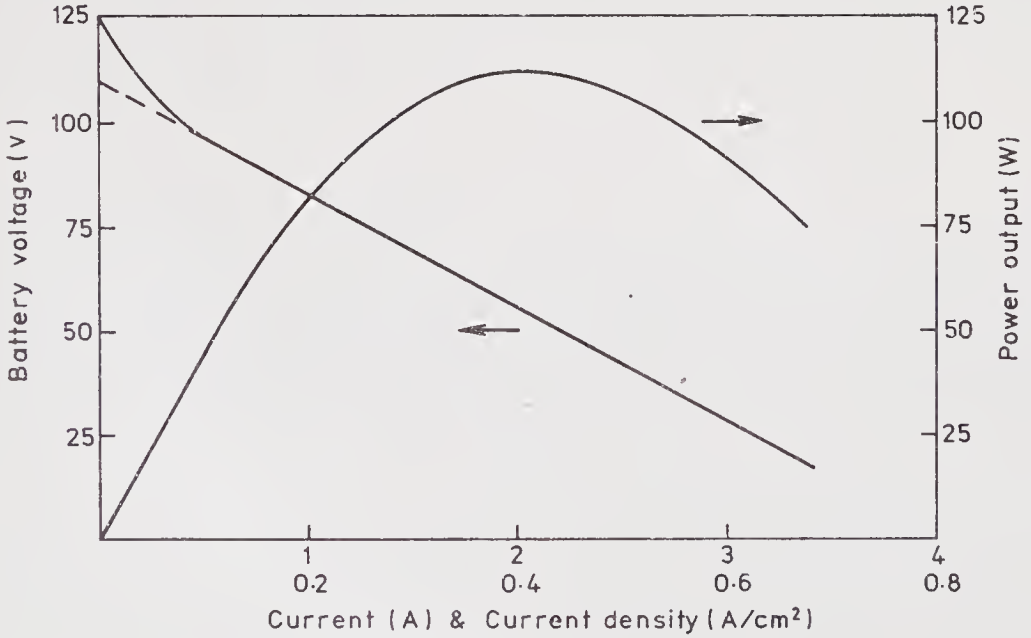

Figure 4. Current vs. voltage and power characteristics of a 120-cell assembly (after Rohr 1978).

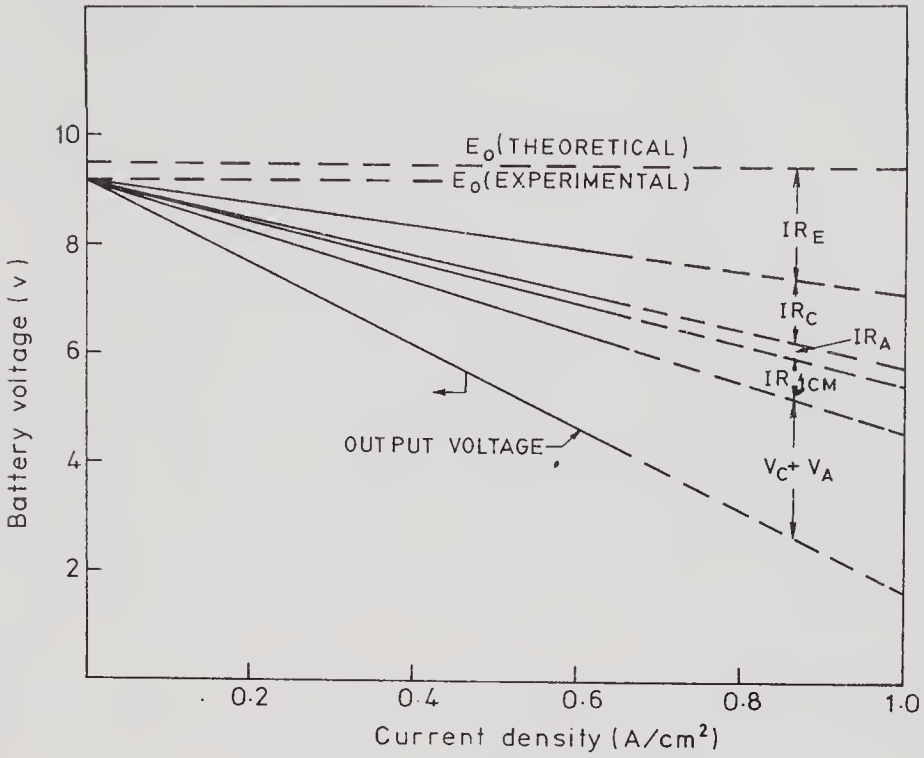

Figure 5. Relative magnitudes of various polarisation losses in a 10-cell battery module.

presented in figure 5. Improvement of battery performance has been obtained by reducing these polarisation losses in the thin film module concept.

6.2 *Thin film module concept*

Better design and reduction of battery manufacturing costs have been achieved in this module. The nonporous electrolyte, the interconnection film and the porous electrode films (both anode and cathode) are deposited on a porous support tube one after another as shown in figure 6. The technique employed for deposition of the films are either CVD, EVD (electrochemical vapour deposition), plasma spraying or combined spraying and sintering (Rohr 1978). The thicknesses of the different films are 30–100 μm. Using these techniques, multicell modules with tubular support (Isenberg

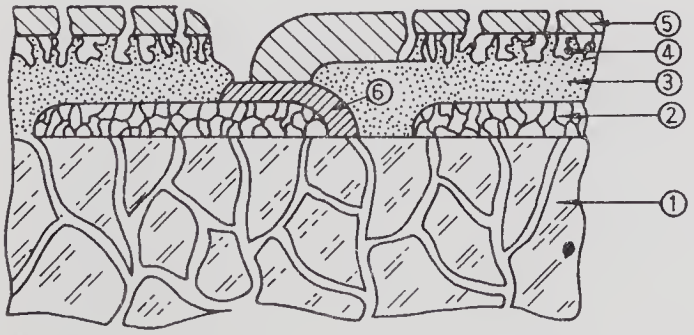

Figure 6. Schematic cross-section of a thin film module.

et al 1969) or plate-type support (Brown Boveri 1975) can be constructed. Consequently, besides the saving in materials and the simplification of the manufacturing process, the operating temperature may be brought down to 700–800°C as well, which reduces technological problems arising at high operating temperature.

7. HTFC integrated plant

For achieving maximum efficiency of the large scale HTFC power plant, some auxiliary equipment like heat exchangers, equipment for dressing of fuels and exhaust gases, combustion control etc. are necessary. A schematic flow diagram of one such integrated HTFC power plant of 220 MW capacity is shown in figure 7, which produces only DC power, and all the waste heat is utilised to generate process steam (Summers & Vidt 1981). This system was designed for an integrated aluminium production plant to study its economic and technical viability.

8. Technical status

The HTFC technology is still in the developmental stage. So far, neither an integrated power plant nor a prototype battery has been constructed for commercial power generation. However, extensive research and developmental programmes have been undertaken by a number of countries like USA, UK, West Germany and Japan. A few laboratory-scale battery modules have been fabricated both in USA and West Germany and they have been successfully operated for considerable lengths of time. The design of the battery module and the fabrication techniques have been found satisfactory on the laboratory scale, but further development is necessary before commercial exploitation becomes feasible. The cost of power generation has to be reduced mainly by increasing the life of the cell. It has been conceived that if the life of the cell is increased from 5 to 10 years the HTFC, with performance so far achieved, will be commercially viable (Rohr 1978). Test modules upto 5 KW output power have been fabricated by Westinghouse Electric Corporation, USA, and they are presently engaged in designing a 50 KW module.

In India, no attempt has so far been made to develop any HTFC module even on a laboratory scale. However, there have been some isolated activities on the material development, particularly on studies of the electrical and electrochemical properties of possible electrolyte and electrode materials. Subbarao at the Indian Institute of Technology (IIT), Kanpur, initiated the main activity in this direction within the country (Maiti 1975; Choudhary 1975). Later, the present authors continued and extended this activity at IIT, Kharagpur. They have designed, fabricated and tested a number of electrochemical cells (oxygen sensors and oxygen pumps which operate on the same principle as fuel cells) using imported electrolyte tubes (Paria 1982). A laboratory scale steam electrolyzer has also been fabricated and its performance studied (Maiti *et al* 1985). Moorthy and colleagues at BARC, Bombay studied the sintering characteristics of stabilized zirconia but have not made any serious attempt to prepare impervious electrolyte shapes required for fuel cell application. Karthikeyan and others of the Plasma Physics division of BARC have extensive experi-

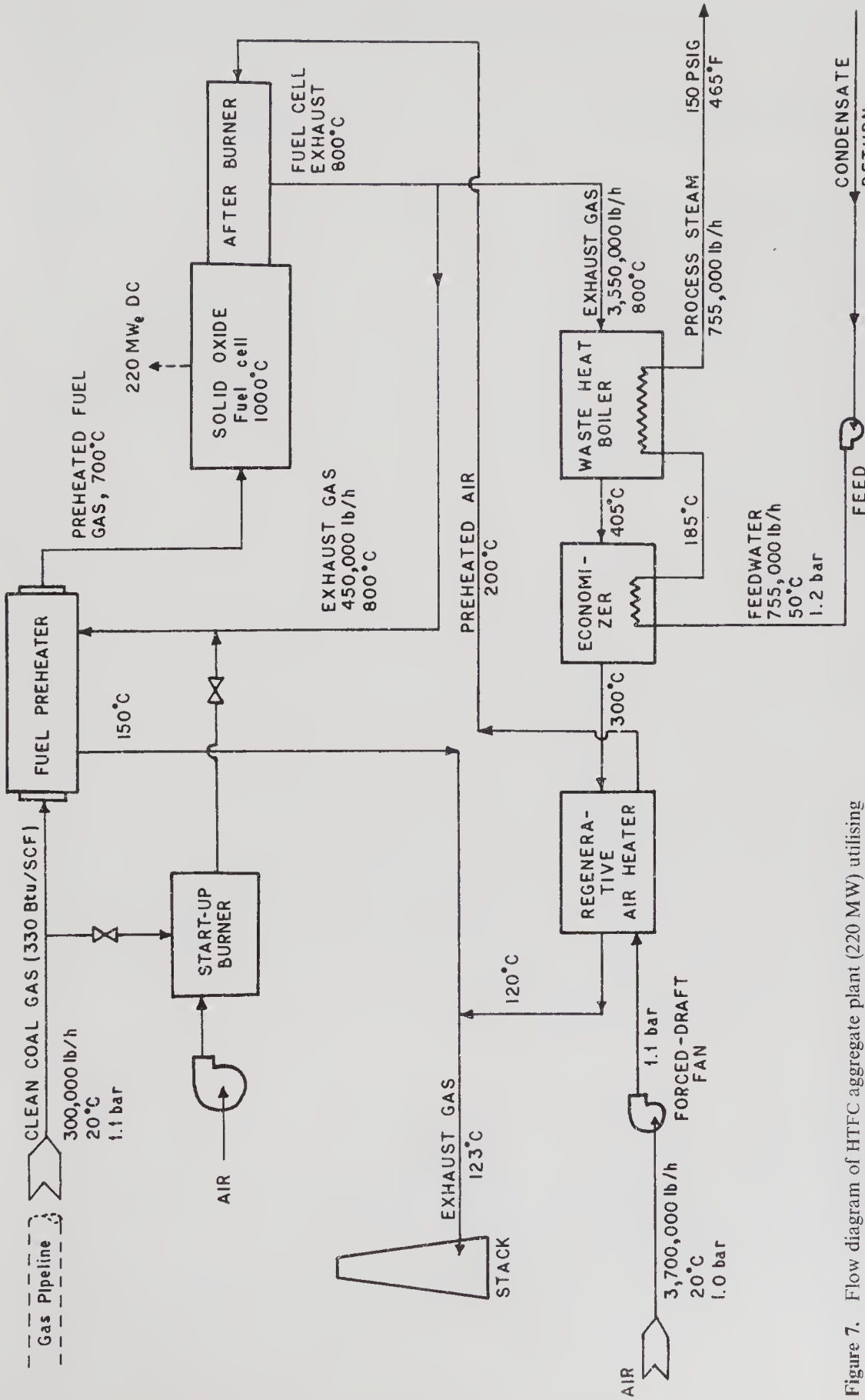

Figure 7. Flow diagram of HTFC aggregate plant (220 MW) utilising all waste heat as process steam (after Feduska & Isenberg 1983).

ence in plasma spraying of ceramic oxides in connection with their MHD project. It is possible to use this expertise to initiate any HTFC programme in this country.

9. Areas of application

The most important advantages of the HTFC power plants are
a) very high efficiency (overall plant efficiency is expected to be 45–55% for plant capacities of the order of megawatts);
b) very low level of pollution;
c) possibility of using the same plant either as a generator or for storage of electricity.

Hence, HTFC power plants are most suitable in remote areas like in space and under the sea where system weight and volume are the most important parameters. These can be used as captive power plants in small and medium scale industries in isolated places. HTFC is best suited for load levelling due to its dual mode of operation. It is very useful in congested areas particularly for avoiding environmental pollution.

10. Summary and conclusions

a) A high temperature fuel cell using a solid oxide electrolyte is one of the most efficient energy conversion devices without the limitations of the Carnot cycle. Expected plant efficiency is 45–55%.
b) It can be operated with fuels like pure hydrogen, gasified coal, natural gas etc.
c) It can be operated either in the fuel cell mode for power generation or in the reverse mode as a steam electrolyzer for generation of hydrogen.
d) Prototype batteries have been developed in some of the advanced countries and have been found satisfactory. Nevertheless some material problems still exist. Thin film design is likely to be more successful than the self-supported concept. Selection of electrode and inter-connection materials and their fabrication techniques appear to play a key role in the ultimate commercialization of the technology.
e) Great potentiality also exists in India for this technology as an alternative power source, particularly in remote and isolated areas.

References

Archer D H, Elikan L, Zahradnik R L 1965 *Hydrocarbon fuel technology* (ed.) B S Baker (New York: Academic Press)
Archer D H, Sverdup E F 1962 *Annu. Power Sources Conf.* 16: 34–39
Archer D H, Sverdup E F, Zahrardnik R L 1964 *Chem. Eng. Prog., Symp. Ser.* 60(6): 64–68
Baukal W, Kuhn W, Kleinschmager H, Rohr F J 1976 *J. Power Sources* 1: 203–207
Baur E, Preis H 1937 *Z. Elektrochem.* 43: 727–730
Brown Boveri 1975 Final Report on Project High Temperature Fuel Cell No: NT-332
Carter R E, Rocco W A, Spacil H S, Tragert W E 1963 *Chem. Eng. News* 41: 47–50
Choudhary C B 1975 *Electrical conduction in the cubic fluorite phase in the system* ZrO_2–$YO_{1.5}$–$TaO_{2.5}$, Ph.D. thesis, Indian Inst. Technol., Kanpur
Doenitz W, Schmidberger R, Steinheil E 1980 *Int. J. Hydrogen Energy* 5: 55–63
Etsel T H, Flengas S N 1970 *Chem. Rev.* 70: 339–376

Eysel H H, Rohr F J 1967 *BBC-Nachr.* 49: 532–540
Feduska W, Isenberg A O 1983 *J. Power Sources* 10: 89–102
Fischer W, Kleinschmager H, Rohr F J, Steiner R, Eysel H H 1971 *Chem.-Ing.-Tech.* 43: 1227–1232
Frase K G, Farrington G C 1984 *Annu. Rev. Mater. Sci.* 14: 279–295
Isenberg A O 1977 in *Proc. Symp. Electrode Materials and Process for Energy Conversion and Storage* (eds) J E D McIntyre, S Srinivasan, F G Will (Manchester: The Electrochem. Soc.) 77: 682–691
Isenberg A O 1978 High temperature Fuel Cell, Final Report DOE Contract No. EY-76-C-03-1197, Westinghouse Electric Corp., USA
Isenberg A O 1981 *Solid State Ionics* 3/4: 431–437
Isenberg A O, Pabst W A, Sverdup E F, Archer D H 1969 Proc. 6th Biennial Fuel Cell Symp., New York
Iwahara H, Uchida H, Maeda N 1982 *J. Power Sources* 7: 293–301
Iwahara H, Uchida H, Tanaka S 1983a *Solid State Ionics* 9/10: 1021–1026
Iwahara H, Uchida H, Maeda N 1983b *Solid State Ionics* 11: 109–115
Kudo T, Obayashi H 1976 *J. Electrochem. Soc.* 123: 415–419
Maiti H S 1975 *Electrical conduction and thermoelectric power in ThO_2–CaO electrolytes*, Ph.D. thesis, Indian Inst. Technol., Kanpur
Maiti H S, Datta A, Paria M K 1985 *Bull. Electrochem.* 1: 581–583
Markin T L 1972 *J. Power Sources* 4: 583–594
Markin T L, Bones R J, Dell R M 1976 in *Superionic conductors* (eds) G D Mahan, W L Roth (New York: Plenum)
Nagata S, Ochno Y, Sato H 1980 in *Applications of solid electrolytes* (eds) T Takahashi, A Kozawa (Tokyo: JEC Press)
Ochno Y, Nagata S, Sato H 1981 *Solid State Ionics* 3/4: 439–442
Paria M K 1982 *Tin dioxide ceramics*, Ph.D. thesis, Indian Inst. Technol., Kharagpur
Rohr F J 1968 *BBC-Nachr.* 48: 200–206
Rohr F J 1975 Proc. EUCHEM-Conf., Elman
Rohr F J 1978 in *Solid electrolytes* (eds) P Hagenmuller, W Van Gool (New York: Academic Press)
Ross Jr P N, Benjamin T G 1977 *J. Power Sources* 1: 311–321
Ruka R J 1978 *Proc. Symp. Industrial Water Electrolysis* (eds) S Srinivasan, F J Salzano, A R Landgrebe (Manchester: The Electrochem. Soc.) 75 (4): 56–59
Spacil H S, Tedmon J T 1969 *J. Electrochem. Soc.* 116: 1618–1633
Steiner R 1972 *Energy Convers.* 12: 31
Steiner R, Rohr F J, Fischer W 1972 *Proc. 4th Int. Symp. Fuel Cells, Antwerp*, p. 113
Summers W A, Vidt E J 1981 High temperature fuel cell, Report No. C1197-18, DOE Contract DE-4C-0379 EI 1
Sun C C, Hawk E W, Sverdup E F 1972 *J. Electrochem. Soc.* 119: 1432–1438
Sverdup E F, Archer D H, Glasser A D 1969 *Adv. Chem. Ser.* 90: 301–314
UK Patent 1972 UK Pat specification No. 1, 261, 317
Weissbart J, Ruka R 1962 *J. Electrochem. Soc.* 109: 723–726

Light element ceramics[+]

K J RAO*, K B R VARMA and A R RAJU

Materials Research Laboratory, Indian Institute of Science, Bangalore 560 012, India

Abstract. An overview of a few structurally important light element ceramics is presented. Included in the overview are silicon nitride, sialon, aluminium nitride, boron nitride, boron carbide and silicon carbide. Methods of preparation, characterization and industrial applications of these ceramics are summarized. Mechanical properties, industrial production techniques and principal uses of these ceramics are emphasized.

Keywords. Silicon nitride; sialon; aluminium nitride; boron nitride; boron carbide; silicon carbide.

1. Introduction

Some of the best known natural ceramics like silica, alumina, and carbon (in its various allotropic forms) are composed of only the light elements of the short periods in the periodic table. The best man-made ceramics such as borides, carbides, nitrides and oxides are also largely made up of light elements. The abundance of these light elements in nature and the extraordinary properties exhibited by a variety of ceramics resulting from their combination provides great attraction for research and development of light element ceramics.

Light element ceramics considered in this review are the stable binary, ternary and polynary ceramic phases obtained by chemical combination of the elements boron, carbon, nitrogen, oxygen, aluminium and silicon. Though alumina is a light element ceramic of great importance, it is not discussed here. Upon considering the volume of work reported in the literature and the proven importance of various light element ceramics, they are discussed in this report in the following order; silicon nitride, sialon, aluminium nitride, boron nitride, boron carbide and silicon carbide. Some of the ternaries and quarternaries related to these binaries are also discussed at appropriate places. Known methods of preparation of each material, particularly as relevant to large-scale manufacture, are first reviewed and then a brief presentation of their significant properties is given. Emphasis is placed on putting together well-documented data related to mechanical properties since light element ceramics are projected the world over as the advanced structural ceramics of the future.

[+]Contribution No. 76 from the Materials Research Laboratory

*For correspondence

2. Silicon nitride

2.1 *Methods of preparation*

There are several methods in vogue for the preparation of silicon nitride. They include (a) direct nitridation, (b) carbothermal reduction, (c) gas-phase reaction, (d) silicon-sulphur-nitrogen reaction and (e) liquid phase reaction.

2.1a *Direct nitridation*: A commercially-known nitridation process involves heating of pure Si powder (particle dia $< 10\ \mu m$) in the temperature range of 1200–1450° C in an atmosphere of NH_3/H_2 or N_2:

$$3\,Si + 2N_2 \longrightarrow Si_3N_4.$$

The above reaction is exothermic and the process yields Si_3N_4 lumps which are later crushed and milled to fine size particles. Hirao *et al* (1986) have adopted a method called self-propagating high temperature synthesis (SHS) to prepare fine Si_3N_4. In this process Si powder compacts are burnt in nitrogen at 10 MPa pressure. The method is suitable for obtaining homogeneous Si_3N_4 submicron particles with a uniform size distribution.

2.1b *Carbothermal reduction*: When a mixture of fine powders of carbon and silica is subjected to carbothermal reduction, followed by nitridation, Si_3N_4 lumps are obtained.

$$3SiO_2 + 6C + 2N_2 \xrightarrow{1200\text{–}1450^\circ C} Si_3N_4 + 6CO$$

The advantage of this method over direct nitridation is that both SiO_2 and C are more readily available than pure Si. It is always better to obtain the precursor in a finely divided form in order to prepare a final product with tailored properties. A sol-gel process has certain advantages in this context over conventional techniques using powder mixtures. In the sol-gel process, aqueous suspensions of oxides and hydrous oxides are mixed to give a composition corresponding to the required multicomponent ceramic. Szweda *et al* (1981) have examined the nitridation of gel powders in an N_2/H_2 atmosphere. A SiO_2 sol derived from a flame-hydrolyzed material was mixed with C powder ($C/SiO_2 = 2:1$) and nitrided between 1400 and 1600° C. The product was found to be either α-Si_3N_4 or β-Si_3N_4 depending on the drying process adopted. The final powder has been heated to 600–650° C in air to burn out excess carbon. The sol-gel preparative route uses organic compounds of silicon such as tetraethoxysilane $Si(OC_2H_5)_4$ which undergoes hydrolysis giving rise to SiO_2.

$$Si(OC_2H_5)_4 + 4H_2O \longrightarrow Si(OH)_4 + 4C_2H_5OH,$$
$$Si(OH)_4 \longrightarrow SiO_2 + 2H_2O.$$

Hydrolysis leads to substitution of alkoxy groups by hydroxyl groups which further condense into polymerized hydrous oxides. Silica gel thus derived from $Si(OC_2H_5)_4$ has been nitrided by Hoch and co-workers (Hoch *et al* 1977; Hoch & Nair 1979). Submicron α-Si_3N_4 was obtained by nitriding at 1350° C in NH_3 gas. Preparation of high purity Si_3N_4 from a disilane compound with the general formula $R_n X_{6-n} Si_2$ (R = H, alkyl, alkenyl, aryl; X = halogen atom, $n = 1-5$) by hydrolyzing it in the presence of C powder and nitriding the product at 1350–1550°C has been reported.

The product was a pale green powder containing approximately 93% α-Si_3N_4. Sharma *et al* (1984) and Hanna *et al* (1985) obtained Si_3N_4 by firing rice husk at 1200–1500°C for about 0·5–2 h in an ammonia atmosphere. The silicon nitride produced was in the form of α-Si_3N_4 with minor amounts of the β-form.

2.1c *Gas phase reaction*: Prochazka & Greskovitch (1978) have prepared Si_3N_4 powder with particle diameter in the range of 300–2000 Å by allowing SiH_4 to react with NH_3 at 500–900° C at atmospheric pressure. $SiCl_4$ and SiH_4 react with NH_3,

$$3SiCl_4(g) + 4\ NH_3(g) \longrightarrow Si_3N_4 + 12HCl(g),$$
$$3SiH_4(g) + 4\ NH_3(g) \longrightarrow Si_3N_4 + 12H_2(g).$$

The use of $SiCl_4$ leads to corrosive by-products while SiH_4 is even more hazardous due to its spontaneous flammability in air. Several workers (Cannon *et al* 1982; Danforth & Haggerty 1983) have employed a CO_2 laser (150 W power, 10·6 μm wavelength) as the heat source with both unfocussed and focussed geometries to prepare Si_3N_4 powder. Here SiH_4 is preferred over $SiCl_4$ since SiH_4 has an absorption band at 10·6 μm. When SiH_4 was heated with CO_2 laser in the presence of NH_3, it yielded monodisperse, pure, loosely agglomerated Si_3N_4 powders with a production rate of upto 10 g h^{-1}. Seiji *et al* (1986) have reported the preparation of Si_3N_4 layers at low pressures and temperatures of 800–1300° C using the (CVD) technique. Sugawara *et al* (1986) have employed the ion vapour deposition method (IVD) to prepare Si_3N_4 films. This method involves electron beam evaporation of Si and simultaneous nitrogen ion implantation which gives rise to Si_3N_4 films.

The plasma-activated vapour deposition method (Goodwin 1982) has been used for depositing Si_3N_4 films on substrates. This technique is particularly recommended for use in the electronic industry. Fletcher *et al* (1971, p. 145) achieved 7% conversion of Si powder into Si_3N_4 using 14% N_2 in Ar plasma. 15% conversion to a mixture of α and β-Si_3N_4 was reported by Canteloup & Mocellin (1975). Formation of ultrafine Si_3N_4 powder has been reported in an arc plasma (Segal 1986). Conditions favourable for deposition of Si_3N_4 on steel substrates by the CVD technique have been reported by Fumiyoshi & Hiroyuki (1986).

2.1d *Silicon-sulphur-nitrogen reaction*: Morgan (1984) has reported that ultrapure Si_3N_4 can be obtained from Cl-free reactants. Si powder was reacted at 900° C in a stream of 10% H_2S/Ar to form SiS_2. SiS_2 was then reacted with NH_3 at 1200–1450° C to give α-Si_3N_4. The synthesis of Si-S compounds, specifically silane thiols, silthians and mercaptosilanes has been described by Eaborn (1960, p. 333). Recently, the preparation of Si_3N_4 by the SiS_2 precursor route was reported by Morgan & Pugar (1985). The important role of nitrogen in the preparation of Si_3N_4 and related ceramics has been discussed by Morgan (1986).

2.1e *Liquid phase reaction*: Mazdiyasni *et al* (1978) have prepared α-Si_3N_4 in the form of fibre bundles (1·3 μm dia) by pyrolysis of hexaphenyl cyclotrisilazane in nitrogen at 1400° C, while Seyferth *et al* (1983) have shown that the polysilazane oil $(H_2SiNH)_x$ derived from reaction of dichloro-silane and ammonia in dichloromethane could be pyrolyzed in N_2 at 1150° C to get α-Si_3N_4 fragments.

It is of historical interest to note that Persoz as early as 1830 had obtained a white precipitate from the interaction of $SiCl_4$ and NH_3(g) in an inert solvent (benzene) at 0° C. This precipitate was then considered to be silicon tetramide $Si(NH_2)_4$ and subsequently confirmed by Lengfeld (1899). Nevertheless the precipitate was unstable

and decomposed at ambient temperatures to give silicon diamide $Si(NH_2)_2$ and ammonium chloride. Glemser & Newmann (1903) and Billy (1959) also obtained similar products on carrying out the reactions in liquid ammonia. Recently Segal (1985) has given a series of possible intermediates which are formed during the preparation of α-silicon nitride from silicon tetrachloride and ammonia.

$$SiCl_4\,(l)/NH_3\,(g) \xrightarrow{0^\circ C} \text{silicon diamide} + NH_4Cl$$

$$\downarrow \quad \text{Loss of } NH_4Cl \text{ and polymerisation up to } 360^\circ C$$

$$6\,[Si(NH_2)]_n$$

$$\downarrow \quad 400^\circ C$$

$$2\,[Si(NH)_3N_2]_n + 2nNH_3$$

$$\downarrow \quad 650^\circ C$$

$$3\,[Si_2(NH)N_2]_n + nNH_3$$

$$\alpha\text{-}Si_3N_4 \xleftarrow{1200\text{–}1400^\circ C}$$

Mazdiyasni & Cooke (1973) have shown that powder produced from pyrolysis is initially X-ray amorphous and that it is transformed into the β-phase on heating between 1200 and 1400° C for about 8 hours.

2.2 *Characterization*

The Si_3N_4 powders prepared by various methods have been characterized using high resolution electron microscopy, IR, Raman and X-ray photoelectron spectroscopies. These techniques also yield information about the quality of the preparation and the nature of impurities present in the powders.

Mehmet *et al* (1985) have discussed the usefulness of high resolution electron microscopy in analysing microstructural characteristics of light element ceramics in general. They have also presented evidence of the presence of amorphous phases of Si_3N_4 (also mullite and AlN ceramics) in the grain boundaries. The glassy phase was absent at some grain boundaries in Si_3N_4 and instead a second phase was noticed. The nature and composition of the surface of Si_3N_4 powder were investigated using high voltage – high resolution TEM, XPS and SIMS* by Rahaman *et al* (1986). Both XPS and SIMS studies indicate that oxygen is present as a major impurity. Minor impurities such as Cl, F, C, Fc and Na are also present in the sample. IR absorption and Raman spectroscopic studies (Takase & Tani 1986) have been carried out on sintered Si_3N_4 containing additions of Al_2O_3 and rare earth oxides (Y_2O_3, CeO_2, La_2O_3). It is noticed that there is an increase in the widths of the Raman bands in the spectral range of 400–1100 cm^{-1} as the Al_2O_3 content in Si_3N_4 is increased. It is attributed to the increasing degree of structural disorder in α-Si_3N_4 network caused by the replacement of Si and N by Al and O respectively. Toshio *et al* (1985) have employed inductively coupled plasma emission spectrometry to determine the impurities present in Si_3N_4. Nobuo *et al* (1985) have reviewed the possible use of

*Secondary ion mass spectroscopy.

thermal and analytical methods such as DTA, DSC and thermogravimetry in the characterization of ceramics. Use of TEM and electron diffraction for analysing fine ceramics in general has been reviewed by Yoshio (1985).

2.3 *Industrial production techniques, properties and uses*

Most high performance Si_3N_4 ceramic products rely on the quality of the starting elements, Si and N_2. However, it is necessary to sinter the products using sintering aids in order to ensure better performance of products. Negita (1985) has discussed the role of sintering aids on the basis of chemical bonding. His studies indicated that electronegativities and ionic radii of the cations in the additives are important parameters which affect the densification of Si_3N_4 ceramics. In general, the majority of Si_3N_4 products are produced either as hot-pressed silicon nitride (HPSN) or as reaction-bonded silicon nitride (RBSN). Hot-pressed Si_3N_4 can be produced by either uniaxial (Vasilos 1977, pp. 367–382) or hot isostatic pressing (Larker *et al* 1975). One generally starts with α-Si_3N_4 powder along with densification aids such as MgO or ZrO_2. Depending upon the purity of the starting Si_3N_4 powder, and the type of additives, milling procedures and hot pressing parameters used, one can obtain a very wide range of strength, creep, fracture toughness or oxidation behaviour. Hot-pressed silicon nitride (HPSN) obtained with Y_2O_3 additive possesses typically higher strengths at both room and elevated temperatures. It also possesses better oxidation resistance, fracture toughness and slower crack growth features as compared to MgO-containing HPSN (Gazza *et al* 1978). Si_3N_4 of very high strength has been obtained by Komeya *et al* (1977) with Y_2O_3 and Al_2O_3 as additives and by using the grain boundary crystallization approach.

The fabrication of RBSN components begins with a silicon metal powder preform which is made by slip casting, dry pressing, flame spraying, injection moulding or other techniques. The preform is then nitrided in an atmosphere of pure H_2 or N_2+H_2 with either a preselected temperature schedule (Messier & Wong 1974, p. 181) or by using a nitrogen demand cycle (Wong & Messier 1978). This process of nitriding of a Si preform is remarkable for its simplicity but is still imperfectly understood. While the reaction $3\,Si+2\,N_2\rightarrow Si_3N_4$ is associated with a 23% increase in the solid volume compared to Si when this reaction is carried out on a preform, there is essentially no change in dimensions (0·1%). The reason for this appears to be that Si_3N_4 is formed in the voids in Si-preforms via a vapour phase or surface diffusion reaction. This procedure is therefore of great importance and can be used in mass production of products to tight dimensional tolerances.

Reaction-bonded silicon nitride can exhibit creep rates significantly lower than those of HPSN (Larsen *et al* 1978). It has also been reported that as a consequence of the reaction bonding process, RBSN is of necessity at least 10% porous which makes it less oxidation resistant than HPSN at intermediate temperatures (McLean 1978) but limits its strength to less than 415 MPa. The quality of products obtained from reaction-bonded silicon nitride has been improved considerably over the past few years. However, when high strength and greater oxidation resistance is required, it would be desirable to have readily sinterable fully dense silicon nitride. This has been the impetus for the development of sintered silicon nitride (SSN).

Sintered Si_3N_4 of at least 95% density has been prepared successfully and it is reported that densities greater than even 99% have been achieved. Gazza *et al* (1978) have recently reviewed the status of SSN. SSN components which are formed by

injection moulding require little machining. It is also possible that sintered Si_3N_4 bodies of over 95% theoretical density may be used as preforms for cladless hot isostatic pressing. Materials like SSN and HPSN are only in the initial stages of development. Sinter densities of $\geqslant$ 95% could be obtained by adding only 2 wt% MgO. Products should be targeted to possess a low concentration of sintering aids at high temperatures. HPSN with Y_2O_3 as sintering aid is quite oxidation resistant. A HPSN product prepared from quartz sand and air has been found to be highly resistant to wear and thermal shock even at high temperatures. These are comparable to the Lulea hard metal oxide ceramics, cubic boron nitride and industrial diamonds.

Mechanical properties of both hot-pressed and reaction-bonded Si_3N_4 ceramics have been investigated in detail. Friction and wear properties of hot-pressed Si_3N_4 were studied by Ishigaki *et al* (1986). The friction coefficient was correlated with the fracture toughness of Si_3N_4. Frictional anisotropy was also observed in hot-pressed Si_3N_4. Kim *et al* (1986) have carried out wear tests on Si_3N_4 in dry rolling contact at room temperature. The wear rate of Si_3N_4 was found to be less than that of any other ceramic material. Observations of worn out surfaces and wear debris revealed that ceramic materials have two types of wear, one related to real contact area and the other related to Hertzian contact area. Brittle fracture dominates the wear process of ceramic materials in dry rolling contact. Nancy (1986) has recently reported that the microstructural changes associated with creep in Si_3N_4 are due to the operation of both cavitation and crack propagation mechanisms within the bonding phase below plastic deformation temperature of the matrix grains. Bandyopadhyay & French (1986) have reviewed the preparation of Si_3N_4 jet engine components by injection molding. Steinmann (1986) has reviewed crack-formation and propagation in hot-pressed Si_3N_4 during creep and on the durability of Si_3N_4 product as a function of temperature and load. These products have high corrosion resistance, good electrical insulation and are non-magnetic. Kaji & Mamoru (1986) have carried out systematic studies on microstructure and room temperature strength of Si_3N_4-Y_2O_3-Al_2O_3 pressureless sintered compacts. Thermal conductivity and microhardness of Si_3N_4 with and without additives have been studied by Tsukuma *et al* (1981). High pressure hot-pressing of Si_3N_4 without additives was performed by Shimada (1986) using a mixture of α-Si_3N_4, amorphous Si_3N_4 and β-Si_3N_4 in the ratio 4:1:2 as starting material. Figure 1 shows the variation of microhardness of Si_3N_4 with temperature in these studies.

3. Sialons

3.1 *Methods of preparation*

The term 'sialon' was chosen to particularize any composition containing elements Si, Al, O and N as major constituents (Oyama & Kamigaito 1971; Jack & Wilson 1972; Oyama 1972; Jack 1976). Sialons can be made by high temperature reaction between silicon nitride or oxynitride and alumina. During the reaction silicon and nitrogen are replaced partially and simultaneously by aluminium and oxygen atoms, respectively. The α'-structure results in M-Si-Al-O-N systems and is derived from the $Si_{12}N_{16}$ unit cell by partial replacement of Si^{4+} by Al^{3+} (M is Li, Mg, Ca or Y). All the sialons have the compositions represented by $M_x(Si, Al)_{12}$ (O, N)$_{16}$ where

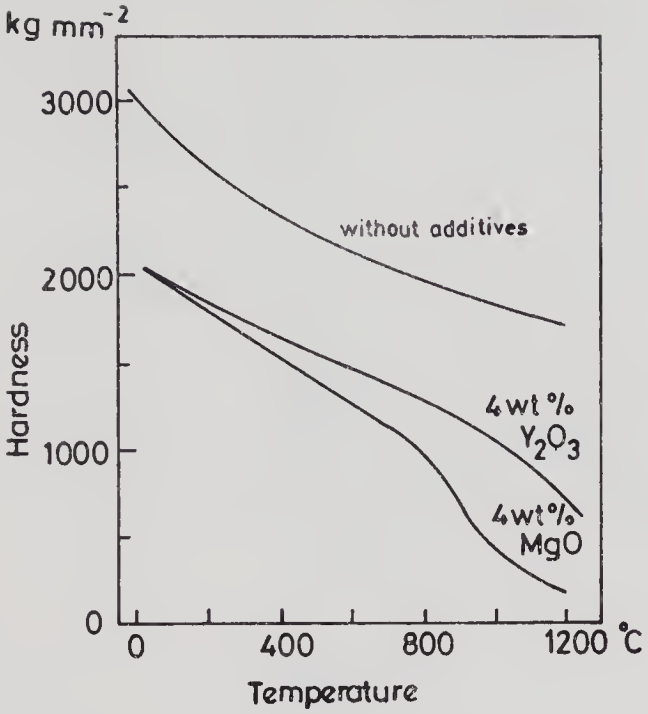

Figure 1. Variation of microhardness of silicon nitride with temperature (adapted from Shimada 1986).

$x \not> 2$ and are structurally related to α-and β-silicon nitrides (Hampshire *et al* 1978). Detailed compatibility and phase equilibria studies of sialons have been reported by a number of workers (Jack 1976; Hampshire *et al* 1978; Gauckler *et al* 1975). Jack has included the data obtained from specimens hot-pressed at temperatures ranging from 1550–2000°C in the phase diagram. According to Jack, the β'-sialon region extends from Si_3N_4 to $Si_{6-x}Al_xO_xN_{8-x}$ with $x = 4{\cdot}2$. β'-sialon forming regions are reported in other systems such as Si_3N_4-Al_2O_3-Be_2SiO_4, Si_3N_4-Al_2O_3-Li_2O and Si_3N_4-Al_2O_3-MgO etc by Jack (1973), Oyama (1973) & Husbey *et al* (1975). The possible reactions of Si_3N_4 and Al_2O_3 which produce β'-sialon with $x = 4$ are

$$4\,Si_3N_4 + 6\,Al_2O_3 \rightarrow 3\,Si_2Al_4O_4N_4 + 6\,SiO + 2\,N_2,$$
$$Si_3N_4 + 2\,Al_2O_3 + C \rightarrow Si_2Al_4O_4N_4 + SiO + CO,$$
$$Si_3N_4 + 2\,Al_2O_3 \rightarrow Si_2Al_4O_4N_4 + SiO_2.$$

Similar β'-sialon phases were obtained by reacting Si_3N_4 with lithium-aluminium spinel ($LiAl_5O_8$) and also with magnesium aluminium spinel ($MgAl_2O_4$). In addition to the sialon phases α', β', o′ and x which were originally reported by Jack (1973, 1976), six unidentified phases nearer to the AlN corner of the Si_3N_4-AlN-Al_2O_3-SiO_2 system have been prepared by Gauckler *et al* (1975). The complex phase diagram reported by Jack (1976) is shown in figure 2. Aluminosilicate minerals provide a convenient source of β'-sialon phases through the carbothermal reaction. β'-sialon powders prepared by this method have been characterized by Mostaghaci *et al* (1986). The effect of agglomeration in the sialon powder on densification and microstructure development during hot pressing has been examined. Baldo *et al* (1983, p. 437) have reported the preparation of sinterable sialon powders from hydrated silicates of aluminium with carbon and nitrogen. This route is considered to be more economical for preparing sialons. A variety of β'-sialon powders based on natural raw materials such as kaolin, clay, pyrophyllite, sillimanite and kyanite have been reported by Baldo *et al* (1983, p. 437). Table 1 indicates compositions of several natural silicates used as reacting materials.

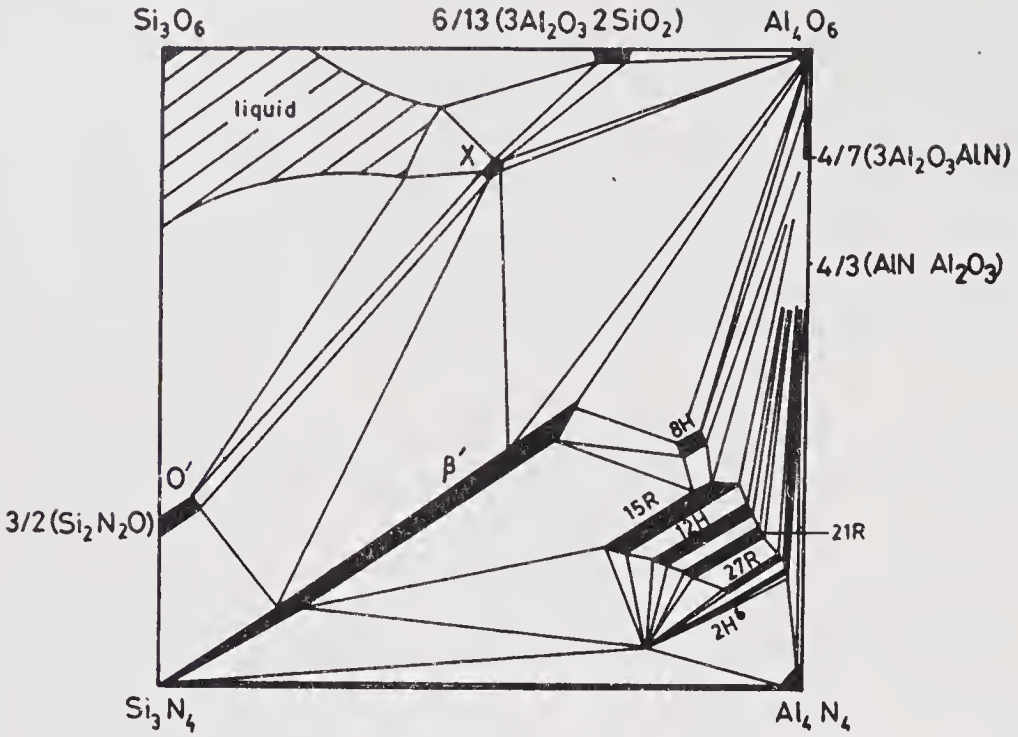

Figure 2. The complex pseudoquarternary phase diagram of Si-Al-O-N system at 1700°C (from Jack 1976).

Approximate compositions of β'-sialons ($Si_{6-x}Al_xO_xN_{8-x}$) obtained with the above materials are listed below.

Al/Si	*x*	*Sialon composition*
0	0	Si_3N_4
1/2	2	$Si_4Al_2O_3N_6$
1	3	$Si_3Al_3O_3N_5$
2	4	$Si_2Al_4O_4N_4$

A typical carbothermal reaction resulting in the formation of a sialon may be represented as follows.

$$3(Al_2O_3 . 4SiO_2 . H_2O) + 27C + N_2 \rightarrow 4[Si_3N_4 . 1/2(Al_2O_3N)] + 27CO + 6H_2O + N_2.$$

The preparation of β'-sialon from china clay and coal is described by Higgins & Hendry (1986). It is a chemical reaction in which the important stages are (i) dissociation of kaolinite to mullite and silica, (ii) formation of silicon carbide, and

Table 1. Natural silicate compositions and their ratios.

Silicate	Formula	Ratio (Al/Si)
Silica	SiO_2	0
Pyrophyllite	$Al_2O_3 . 4SiO_2 . H_2O$	1/2
Kaolinite	$Al_2O_3 . 2SiO_2 . 2H_2O$	1
Kyanite	$Al_2O_3 . SiO_2$	2

(iii) simultaneous reduction and nitridation of mullite by carbon and silicon carbide in the presence of nitrogen gas. The reaction rate is controlled by the nitrogen flow rate because of its effect on the removal of carbon monoxide formed by reduction of the oxides. The reaction corresponding to the formation of β' phase is reversible through the control of the carbon monoxide partial pressure. Hanna & Ghoneim (1986) have employed pure kaolin and coked rice hulls ($SiO_2:C=47:52$) for the preparation of sialon. The formation of β'-sialon powder was investigated by firing kaolin and coked rice hulls containing 20, 30, 40 and 50 wt% at 1300–1500°C under NH_3.

Translucent sialon ceramics have been prepared (Nobuyuki 1985) from Si_3N_4, Al_2O_3 and AlN. The resulting β'-sialon has the formula $Si_2Al_4O_4N_4$ and light transmissions of 43 and 70% at wavelength 0·4 and 4μm, respectively. These translucent materials are useful in making container tubes for high voltage sodium lamps, windows for high temperature vessels and integrated circuit substrates.

3.2 *Characterization*

Sialons have been characterized using X-ray diffraction analysis (Jack & Wilson 1972; Izumi 1983; Thommy & Bertil 1986; Thompson *et al* 1983, p. 61) and analytical electron microscopy (Thompson *et al* 1983; Izumi *et al* 1984; Bonnel *et al* 1986; Johnson & Hendry 1979). Investigations have been carried out on materials of different compositions prepared under different processing conditions. Greil & Weiss (1983, pp. 359–374) have used TEM to characterize a hot-pressed solid solution material with 11 wt% Al^{3+} and varying oxygen content. With increasing amounts of oxygen, it is found that prismatic grains containing increasing amounts of amorphous phase are formed. Raman studies have been used to determine the changes in force constants which occur when interatomic distances and bonding characteristics are altered (Jack 1976). Magic angle spinning high resolution solid state NMR (MASNMR) has been used to monitor the quantity and co-ordination of aluminium in sialon and other ceramic materials (Fyfe & Gobbi 1983). Aluminium and silicon are found to be present as AlO_4 and SiO_4 tetrahedra and as AlO_6 octahedra. It was noted that in addition to SiO_4 tetrahedra, SiO_3N, SiO_2N_2, $SiON_3$ and SiN_4 tetrahedra can also be present because each type of tetrahedra can be linked to neighbouring tetrahedra in five possible ways. Sanyal & Mukerji (1986) have used Mössbauer spectroscopic techniques to study the effect of iron on the conversion of clay into β'-sialon. These studies indicate that no Fe is present in the metallic state in sialon.

3.3 *Industrial production techniques, properties and uses*

Hot-pressing has been widely used in the fabrication of sialon products. Various material combinations listed in table 2 have been pressed at temperatures where simultaneous chemical reaction and densification were found to take place. MgO has been commonly used as an additive to promote densification. The most effective hot-pressing temperature and time appear to be 1650–1750°C and 30 minutes to 2 hours, respectively. The experimental studies indicated in table 2 illustrate the varied nature of investigations in hot-pressed β'-sialons.

Pressureless-sintering studies have been conducted with various material combinations with and without additives. Sintering was conducted at about one

Table 2. Fabrication of sialon by hot-pressing.

Starting materials	Addi-tives	Tempera-ture (°C)	Time (min)	Pressure (MN/m^2)	Nature of investigation (Reference)
Si_3N_4, Al_2O_3, Li_2CO_3	—[a]	1750	20	29	Solid solubility (Oyama & Kamigaito 1971)
Si_3N_4, Al_2O_3	—	1700	60	—	Formation, structure and thermal expansion (Jack & Wilson 1972)
Si_3N_4, AlN, Al_2O_3	—	1730	30	25	Solid solubility (Oyama 1972)
Si_3N_4, Ga_2O_3, Al_2O_3	—	1730–1800	20–180	25	Solid solubility and thermal expansion (Jack 1973)
Si_3N_4, Al_2O_3, AlN, SiO_2	—	1760	60–300	30	Phase equilibria and compatability relation (Arrol 1974, p. 729)
Si_3N_4, AlN, Al_2O_3, SiO_2, Si_2N_2O	—	1500–2000	—	—	Phase equilibria, compatibility and structure (Gauckler *et al* 1975)
Si_3N_4, Al_2O_3	—	1700	60	15	Microstructure & phase analysis (Drew & Lewis 1974)
Si_3N_4, Al_2O_3	—	1700	30	—	Phase analysis (Gugel *et al* 1975)
Si_3N_4, Be_3N_2, BeO, SiO_2	—	1765–1880	60–120	28	Phase equilibria (Husbey *et al* 1975)
Si_3N_4, Al_2O_3	—	1650–1850	6–60	25	Sintering, grain growth and phase equilibria (Oyama & Kamigaito 1971)
Si_3N_4, AlN, SiO_2	MgO	1750	60	20	Fabrication, chemistry and creep (Lumby *et al* 1975, p. 283)
Si_3N_4, Al_2O_3, AlN, SiO_2	MgO	1760	—	—	Physical, mechanical and thermal properties (Gauckler *et al* 1977)
Si_3N_4, AlN, SiO_2	MgO	1800	60	15	Formation, microstructure characterization (Lewis *et al* 1977)
Si_3N_4, Al_2O_3	—	1500–1700	120	5·5–27·5	Effects of pressure and temperature on sintering (Yeh & Watters 1977)

[a]dash indicates not reported.

atmosphere of nitrogen to produce bodies with as high as 98% theoretical densities. Various aspects of sintering of sialons have been discussed by Jack and others (Jack 1973; Gugel *et al* 1975; Gauckler *et al* 1978, p. 559; Drew & Lewis 1974). In a special sintering procedure known as 'transient liquid phase sintering' (TLP), sialon of composition $Si_{1·4}Al_{1·6}O_{1·6}N_{2·4}$ was obtained from two pre-reacted compositions, one of which was the X-phase which melts near 1700°C (Baldo *et al* 1983, p. 437). The microstructures of both hot-pressed and sintered-materials consist of β'-sialons as the predominant phase with some isolated porosity and metallic looking phase in a uniform β'-matrix. In some cases isolated grains of the X-phase and a 15R polytype phase were found with sizes varying between 0·2-2 μm (Greil & Weiss 1983, pp. 359–374; Takase & Tani 1984). The grain morphology in both sintered- and hot-pressed

materials was characteristic of the presence of a liquid phase during densification. This liquid phase was retained in intercrystalline spaces during cooling from hot-pressing (Evans & Moulson 1983, pp. 237–243) or sintering temperature (Takase & Tani 1984) and formed a glassy phase at the grain boundaries. Density values of hot pressed β'-sialons vary from 3·09 to 3·16 g/cm^3 while the densities of other phases (*X* and 15 *R*) have been found to be between 3·05 g/cm^3 and 3·08 g/cm^3 (Gauckler *et al* 1977).

Most of the mechanical properties reported in the literature refer to β'-sialon in (Si, Al, O, N) systems. Other systems such as (Si, Be, N, O), (Si, Al, Be, N, O) etc, have been examined primarily with respect to solid solubility, phase relationships and structure. The room temperature strength of sintered β'-sialon compares favourably with room temperature strength of sintered Si_3N_4. On the other hand, the room temperature strength of sintered β'-sialon is considerably lower than that of hot-pressed Si_3N_4. At high temperature (1370°C) the strength of sintered β'-sialon is equivalent to or higher than the strength of sintered Si_3N_4 but lower than that of hot-pressed Si_3N_4 (figure 3). Creep behaviour of several hot-pressed sialons have been measured and compared (Baldo *et al* 1983, p. 437) with available data on hot-pressed Si_3N_4, hot-pressed SiC and reaction-bonded Si_3N_4. The sintered sialon has a creep rate lower than that of hot-pressed or reaction-bonded Si_3N_4. Lumby *et al* (1975, p. 283) have noted a strong dependence of creep behaviour on AlN concentration.

Fracture toughness (K_{IC}) values have been reported in the literature for various compositions. Generally, the values are lower than those of hot-pressed Si_3N_4. Wills *et al* (1977) have suggested that the presence of *X*-phase should be kept at very low levels and preferably be eliminated completely to improve the fracture toughness of sialons. Lumby *et al* (1978, p. 893) have however observed a high fracture toughness

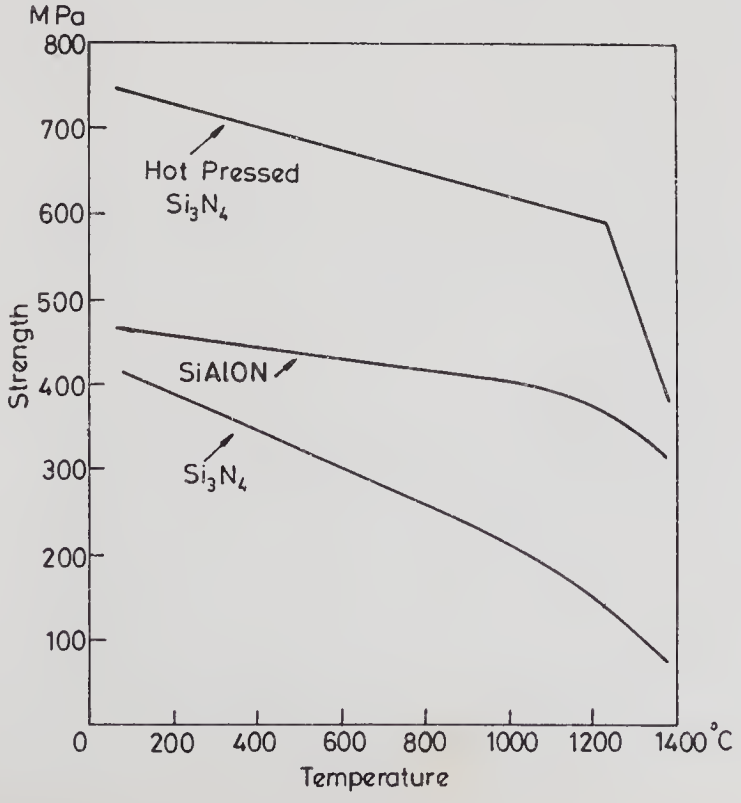

Figure 3. Comparison of strength of silicon nitride and sialon at various temperatures (adapted from Lumby *et al* 1978, p. 893).

value for a pressureless sintered sialon which is similar to that of hot-pressed Si_3N_4. It has also been suggested that the increase in K_{IC} values at high temperatures is associated with viscous deformation of the grain boundary phase. The variation in K_{IC} values could probably be attributed to variation in sialon composition as well as fabrication and measuring techniques. The oxidation resistance of β'-sialon is better than that of hot-pressed Si_3N_4 (Arrol 1974, p. 729). It has also been observed that the oxidation rate of TLP sintered $Si_{1\cdot4}Al_{1\cdot6}O_{1\cdot6}N_{2\cdot4}$ is an order of magnitude less than that of hot-pressed Si_3N_4 at 1400°C.

The coefficient of linear thermal expansion of β'-sialon is $2\cdot7 \times 10^{-6}K^{-1}$ and is less than that of β-Si_3N_4 ($3\cdot5 \times 10^{-6}K^{-1}$). Gauckler *et al* (1977) have reported an average value of $3\cdot4 \times 10^{-6}K^{-1}$ which compares with the value for pure β-Si_3N_4. It has been observed that essentially linear decrease (Gauckler *et al* 1977; Wills *et al* 1977) of the thermal expansion coefficient occurs with increasing Al concentration in sialons. Several investigators (Gauckler *et al* 1977; Lumby *et al* 1978, p. 893) have reported the value of water-quenched thermal shock resistance (ΔT_c) of several sialons. While ΔT_c values for β'-sialons are comparable to those of various silicon carbide ceramics and RBSN, they are considerably lower than that of hot-pressed Si_3N_4.

Aliprandi (1986) has reviewed sialon ceramics with regard to their suitability in extrusion and drawing of metals. Recently high temperature properties of ceramics in the (Si, Al, O, N) system were studied by Bonnel *et al* (1986). The fracture toughness generally decreases with temperature. Short time annealing raises the toughness at lower temperatures whereas further annealing brings it back to the value characteristic of hot-pressed material. The problems associated with mass transport processes in the oxidation of calcium doped β'-sialon were studied by Chukukere & Riley (1986). The effects of creep on anelastic strain recovery, bulk and surface morphologies of sialon ceramics were examined using 3-point bending creep tests in air at 1200°C and 240 MPa by Besson *et al* (1986). TEM examination showed a marked decrease in the amount of glassy phase in the bulk of the samples after creep. No cavitation was however detected.

4. Aluminium nitride

Aluminium nitride is another useful nitride ceramic which exhibits a number of interesting properties. These include excellent high temperature strength, oxidation and thermal shock resistance and resistance against the attack of liquid metals. It is a good thermal conductor while it is electrically insulating.

4.1 *Preparation and characterization*

AlN powder is usually synthesized by two methods. The first one which has been widely adopted is direct nitridation of aluminium powder (or Al_2O_3 with C-black or graphite) by heating in a nitrogen or NH_3 atmosphere (Pierre *et al* 1985; Liping *et al* 1986). In the second method a high purity free-flowing AlN powder with low oxygen content is prepared by treating Al_2S_3 with NH_3 or N_2 at > 1100°C (Ibrahim 1986).

Fumino *et al* (1986) have reported the deposition of amorphous AlN films by a plasma CVD method using a metal organic aluminium source and NH_3 as the starting materials. The powder samples of AlN were characterized using X-ray diffraction and ESCA (Ibrahim 1986). It is found that the particles are associated with high surface concentration of O and grain sizes are of the order of 2000 Å.

4.2 *Industrial production techniques, properties and uses*

Polycrystalline compacts of AlN have been prepared by several methods such as sintering of pressed powder (Matsue *et al* 1965), reaction sintering of Al-AlN mixture (Taylor & Lenie 1960) and hot-pressing (Komeya & Inoue 1969). Although AlN is difficult to sinter without any flux, Komeya & Inoue (1969) found that very fine powders can be easily sintered though the extent of oxygen impurity in such powders is not known. Sakai & Iwata (1977) used hot-pressing techniques and studied the sintering behaviour and strength of sintered samples with various oxygen contents. Densification has been carried out by hot-pressing (Weston & Carruthers 1973) in an inductively heated graphite die. To avoid reaction between AlN and graphite die at high temperatures, graphite was coated with high purity boron nitride suspended in an aqueous solution of methyl cellulose. Methods of preparing AlN multilayer ceramic substrates for hybrid integrated circuits have been described which are suitable for mass production (Nobuo *et al* 1984; Komeya & Inoue 1974; Billy & Mexmain 1985).

Fully densified AlN has a microhardness value of 150 on the Vicker's scale which is comparable to those of silicon oxynitride and Si_3N_4. The strength of AlN at room temperature is greater than that of RBSN but decreases when temperature increases and reaches a stable value between 800–1400°C. At 1400°C the strength is of the same order as that of other nitrides (Lecompte *et al* 1983, pp. 293–298). Trontelj & Kolar (1975, p. 39) have shown that with 99 AlN-1 Ni (wt%) powders, dense compounds could be sintered having a bend strength of 300 MN/m^2. Komeya & Inoue (1971) have studied the properties of AlN containing Y_2O_3 prepared by pressureless sintering. The highest value of the strength (328 MN/m^2) could be obtained with a composition of 75 AlN-25 Y_2O_3. AlN with single oxide additives such as Li_2O, CaO, MgO, SiO_2, B_2O_3, NiO, Cr_2O_3 (1 wt%) has been used to study the sintering effect. Complete densification has been achieved through sintering under nitrogen at comparatively low firing temperatures (Schwetz *et al* 1983, pp. 245–252). McCauley & Corbin (1979) have shown that it is possible to reactively sinter Al_2O_3 with 27–40 mol% AlN to form a single phase cubic oxynitride spinel. The resultant material has a unique combination of properties and possesses mechanical properties very similar to Al_2O_3 of similar grain size. The final product, AlON, is optically isotropic.

Kazuo *et al* (1986) have reported that AlN mixed with 3 wt% strontium oxalate hot-pressed at 1800°C under a pressure of 300 kg/cm^2 has a thermal conductivity of 58 W/mK. The effect of sintering parameters such as pressure, particle size and temperature of AlN powders (coated with a thin film of Al_2O_3) on the densification rate was investigated in order to determine the sintering mechanism of AlN (Gossain *et al* 1985). Effect of CaO additives on electrical conductivity of hot-pressed AlN ceramic was studied by Zulfequar & Kumar (1986). A review on heat conducting aluminium nitride boards have been presented by Nobuo & Kazuo (1986).

5. Boron nitride

Lately, boron nitride has been recognized as a potential material for use at high temperatures. There is a marked similarity between BN and carbon, as they are isoelectronic. Boron nitride is known to exhibit three polymorphic modifications;

hexagonal graphite type (*h*-BN), cubic zinc blende type (*c*-BN) and wurtzite type (*w*-BN).

5.1 *Methods of preparation*

Various methods of preparation of BN have been described in the literature (Giardini 1953). Sorrel & McCartney (1986) have reviewed the history of development, method of manufacture, properties and application of *c*-BN ceramics. Fujio & Kozo (1986) have reported the preparation of hexagonal BN. In this process borax and melamine are heated at 150° C in an N_2 atmosphere for about 1 h and cooled in the same atmosphere overnight. The powder is washed with HCl and water and dried at 100° C for 2 h when white BN powder with 90·6% yield is obtained. A summary of known methods of preparation of hexagonal boron nitride is given by Ingles & Popper (1960, pp. 144–167) and the preparation of powder by the reaction of a mixture of boric oxide and calcium orthophosphate with ammonia at 900° C is discussed in detail. A flow sheet for the preparation of boron nitride powder from boric oxide and ammonia (Ingles & Popper 1960, pp. 144–167) is given below.

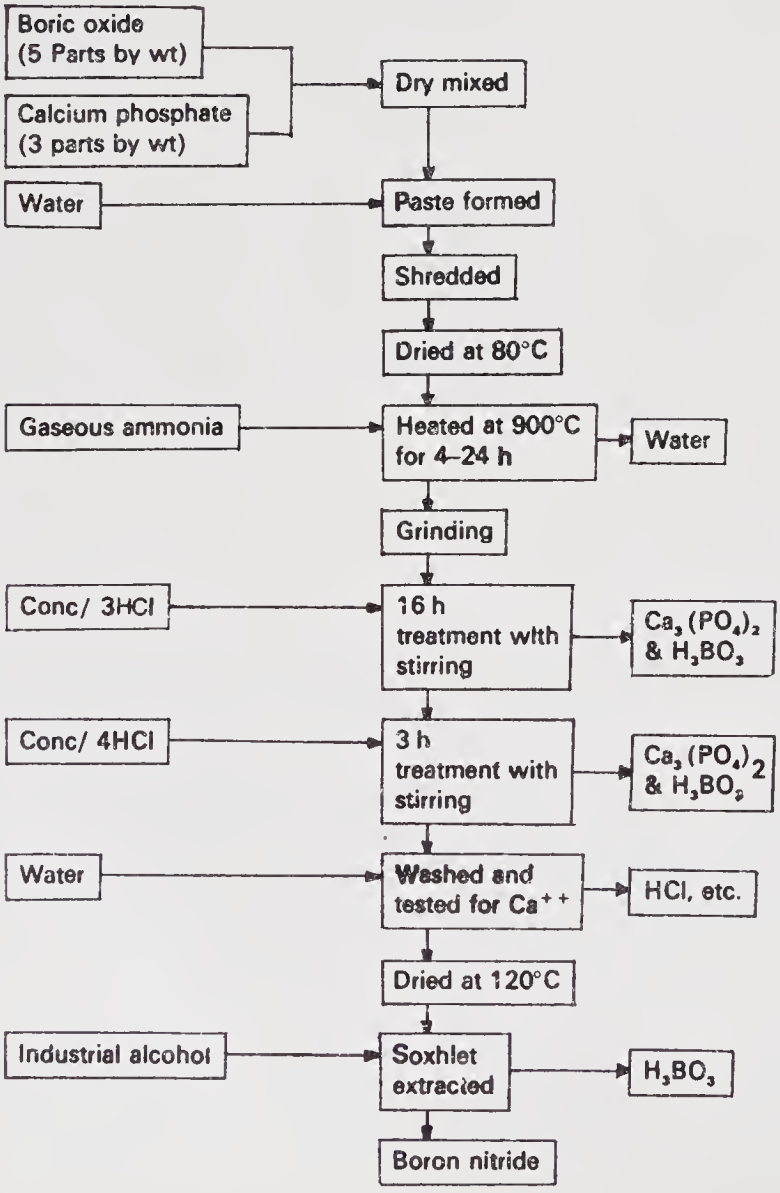

Cubic BN in general is synthesized from *h*-BN under high pressure–high temperature conditions, typically 65 kbar and 1700° C. The General Electric Company of America has succeeded in the preparation of *c*-BN from *h*-BN by applying very high pressure (60,000 atm) at a high temperature (1600°C) (Wentorf 1957). *w*-BN is also synthesized from *h*-BN employing even higher pressure, mostly by a shock process which involves a shear mechanism. The conversion of *h*-BN to *c*-BN is kinetically a difficult process, even in the thermodynamically stable regime of *c*-BN. This is due to the high activation barrier involved. Therefore the transformation is usually carried out in the presence of some catalyst material which lowers the activation barrier. *c*-BN compacts are synthesized at high temperature and pressure with suitable binders (Hibbs & Wentorf 1974; Fukunaga *et al* 1978, p. 328; Rapoport & Nadiv 1985).

5.2 *Industrial production techniques, properties and uses*

c-BN is an industrially important hard material, useful in abrasive and cutting tool applications. New methods for easier and more economical production are therefore constantly sought. Rapoport & Nadiv (1985) have examined mechano-chemical processing which can provide some extra activation to *h*-BN powder and assist in its conversion to *c*-BN. AlN was chosen as an additive to *h*-BN in view of its reported role as a catalyst in the conversion of *h*-BN to *c*-BN. Akashi & Sawaoka (1986) have prepared compacts of cubic boron nitride with 94% theoretical density and a Vickers microhardness value of 30·3 GPa from coarse *c*-BN powder by a shock compaction technique. According to them the mechanical and chemical properties of cubic boron nitride are very similar to those of diamond except for reduced reactivity with ferrous materials at high temperatures. Sintered *w*-BN compacts were characterized (Singh 1987) with regard to their different crystalline phases, which are formed at high temperatures and pressures, composition and particle size distribution. The cubic BN consists of particles with sharp blade edges and well-developed (111) faces and it is useful as a cutting and grinding material. Lavrenko & Alekseev (1986) have studied the oxidation resistance of BN samples obtained by various methods using thermogravimetric analysis, DTA and IR spectroscopy.

Composite materials were prepared using sialon and 5–20 vol % BN fibres by hot-pressing. The products had high thermal shock resistance and were used for the manufacture of special rings for horizontal continuous casting of steel (Peizhi *et al* 1986). The DC conductivities of hexagonal boron nitride and BN-containing composites were measured as a function of temperature up to 2400° C. The results confirm that at high temperatures BN is an intrinsic semiconductor with an energy gap of 6·2 ± 0·4 ev (Frederikse *et al* 1985).

The mechanical and chemical stability and the high electrical resistivity of hexagonal boron nitride at high temperatures (2500° C) makes this compound a principal candidate for use as microwave windows in re-entry vehicle communication systems. However hexagonal boron nitride sublimes at 2500° C (Ingles & Popper 1960, pp. 144–167).

6. Boron carbide

Boron carbide which has a high melting point is among the refractory carbides. The

commercial importance of refractory carbides is mainly due to their extreme hardness.

6.1 *Preparation*

Boron carbide was initially produced in an electric furnace by Joly (1883) and Moissan (1894). For the production of pure boron carbide on an industrial scale, boric acid, which is available in high purity and in adequate amounts, is generally used. The formation of boron carbide from B_2O_3 is represented by the equation

$$2B_2O_3 + 7C \longrightarrow B_4C + 6CO.$$

Recently boron carbide has been prepared by high temperature reaction involving boric oxide and carbon (Ramamurthy 1985; Seiji 1986).

6.2 *Characterization*

Boron carbide has already been known for 50 years, since its crystal structure was elucidated by Laves (1934–35). The elementary cell was described by Silver & Bray (1959) on the basis of NMR investigations. The B-C phase diagram has been described in detail by Samsonov (1958 a, b, c). X-ray data were used by Samsonov and coworkers for generating the phase diagrams. Metallographic investigations were also carried out along with measurements of density, hardness and electrical resistance.

6.3 *Properties, industrial production techniques and uses*

The most important property of boron carbide is its extraordinary hardness. After diamond and cubic boron nitride (the so-called Borazon), boron carbide is the hardest industrial material known. However, hardness values of boron carbide are reported in different ways in the literature (Knoop 1939). Figure 4 shows the

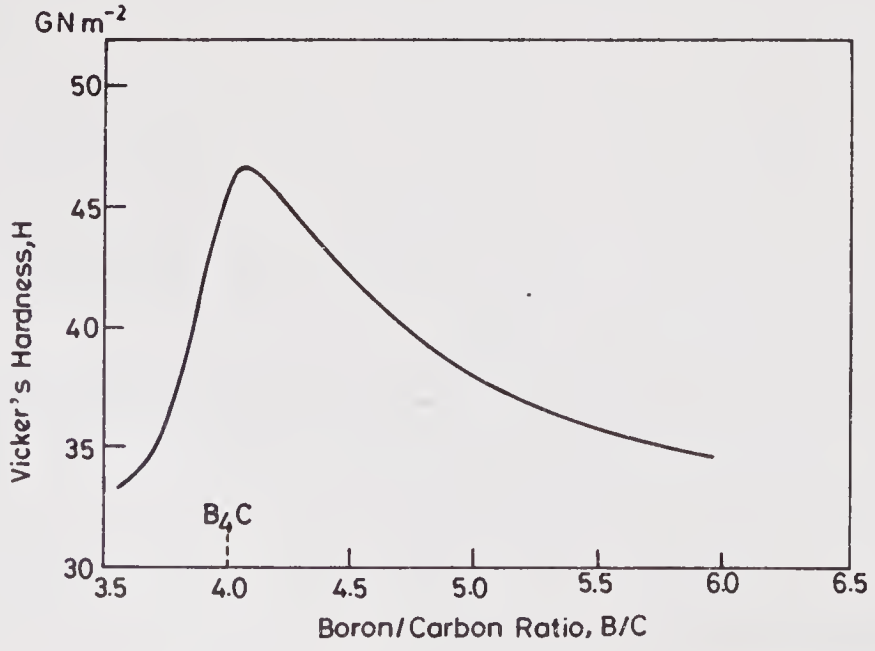

Figure 4. Vicker's hardness as a function of B/C ratio for boron carbide (adapted from Niihara *et al* 1984).

Vicker's hardness as a function of the B/C ratio for boron carbide. It appears that the hardness values range from 20–80 kN/mm^2 and lie between the hardness values of corundum and diamond. Lipp (1965) has presented an interesting review on the physico-chemical properties and reactivity of boron carbide.

7. Silicon carbide

Silicon carbide was first artificially produced and later discovered in the natural state. The mineralogical name of silicon carbide is moissanite. Moissan (1905) discovered hexagonal silicon carbide interlaced with diamond in the meteoric iron found in the Diablo Canyon (Arizona). Several authors (Kaypov & Baymuratov 1970) have reported the occurrence of Moissanite since 1950 in various volcanic rocks in the Soviet Union. About a decade ago, it was reported that silicon carbide along with some other compounds was detected in the gaseous phase of certain stars (Friedmann 1969; Gilman 1969; Lefevre 1970). SiC occurs most probably in the circumstellar space of cool stars that contain carbon and oxygen in almost equal proportions (Gilman 1969), the presence of silicon carbide was detected by absorption spectral analysis (Lefevre 1970). Acheson developed a process for the manufacture of silicon carbide on an industrial scale in 1891. The process is frequently mentioned in the literature as the Acheson process. Silicon carbide is produced batchwise in an electric furnace by high temperature solid phase reaction of coal and quartz sand. The production of silicon carbide even today is carried out exclusively by this process. Efforts (Lanyi 1955, p. 284) have been made over the past eight decades to produce silicon carbide on an industrial scale by improved methods. It is rather difficult to evaluate either the present situation or the current trends of development precisely because of the nonavailability of complete research literature on SiC production. However, a few standard methods of producing SiC are discussed below.

7.1 *Methods of preparation*

For the production of industrial SiC, silica and carbon are used as basic materials along with various additives: saw dust, sodium chloride and also other modifying components. The correct proportion of raw materials, their pretreatment, optimum grain size, applied additives and modifying components etc. are discussed in the literature (Acheson 1896, 1912; Dadape *et al* 1947; Tomonari 1956). The formation of silicon carbide can be summarized (Ruff 1935) in the following two steps,

$$SiO_2 + 2C \longrightarrow Si + 2CO \text{ (first step)}$$
$$Si + C \longrightarrow SiC \text{ (second step)}$$
$$\overline{SiO_2 + 3C \longrightarrow SiC + 2CO}$$

Production of silicon carbide starting from silicon and coal, silicon tetrachloride, trichloro silane, alkyl silanes and aluminium silicates etc. have been described in the early literature. Silicon carbide has been prepared from carbon tetrachloride and alkyl silanes in a hydrogen atmosphere on a glowing carbon rod at a temperature above 1700° C (Pring & Fielding 1909). It is also possible to obtain silicon carbide from a mixture of silicon tetrachloride and toluene using hydrogen as a carrier gas

on fibres of carbon using thallium carbide or zirconium carbide as crystal growth promoting agents (Agte & Moers 1931). Aluminium silicates have been used as starting materials instead of silica (Hayakawa 1949).

Hoch & Nair (1978, pp. 33–40) have reported the preparation of ultrafine powders of SiC from organometallic complexes. The process can be represented by the following equation,

$$Si(OH)_4 + CH_4 \longrightarrow SiC + 4H_2O$$

Fine powders of β-SiC were obtained by the vapour phase reaction of a SiH_4-CH_4 system at about 1400° C and by the thermal decomposition of $(CH_3)_4$ Si in hydrogen atmosphere above 1000° C (Okabe *et al* 1979). The formation processes of SiC particles in these reaction systems are summarized as follows

(a) $$SiH_4(g) + CH_4(g) \longrightarrow SiC(s) + 4H_2(g),$$

$$[SiH_4(g) \xrightarrow{500\text{–}700^\circ C} Si \text{ (particles)}$$

$$Si \text{ (particles)} + CH_4(g) \xrightarrow{1000^\circ C} SiC \text{ (particles)}];$$

(b) $$(CH_3)_4 Si(g) \longrightarrow SiC(s) + 3CH_4(g),$$

$$[(CH_3)_4 Si(g) \xrightarrow{700^\circ C} \text{polymer particles},$$

$$\text{polymer particles} \xrightarrow{900^\circ C} SiC \text{ (particles)}].$$

Silicon carbide whiskers can be made by a variety of methods. The most economical one is the carbothermic reaction of SiO_2 and carbon, which are constituents of ground rice hulls (Lee & Cutler 1975). Sharma *et al* (1984) have produced such whiskers and characterized them by transmission electron microscopy. Another method is the gas-phase reaction of $SiCl_4$, chlorosilane and/or silane in a carbonaceous atmosphere in the presence of Fe and Cr as catalysts (Mazdiyasni & Zangvil 1985). The effect of covalent bond additives, such as AlN, BN and BeO on the structural stability of SiC has been studied by Zangvil & Ruh (1985).

The detailed structure of silicon carbide has been given by Dietzel *et al* (1960) & Ueltz (1972, p. 1). The crystal structure and mechanical properties of green and black silicon carbides have been discussed by Gasilova & Saksonov (1966, p. 50).

Thermal and chemical properties of silicon carbide which include thermal expansion, thermal conduction and reaction of silicon carbide with various other chemicals have been summarized in the literature. Silicon carbide is attacked at high temperatures by gaseous fluorine, chlorine and hydrogen. It is resistant to mineral acids and is attacked only by a mixture of hydrogen fluoride and nitric acid and/or concentrated phosphoric acid at temperatures above 200° C.

7.2 *Industrial production techniques, properties and uses*

Silicon carbide based ceramic materials include hot-pressed SiC (HPSiC), reaction-bonded SiC (RBSiC), sintered SiC (SSiC), silicon carbide/silicon composites and chemical vapour deposited SiC (CVD-SiC).

Hot-pressed SiC can be formed with various densification aids, but only the HPSiC

prepared by utilizing Al_2O_3 additive has been considered for high performance engine applications (Prochazka 1975, p. 171). HPSiC is not as strong as HPSN at low temperatures, however, it retains useful strength upto ~1400° C.

Reaction-bonded silicon carbides cover a wide range of compositions and manufacturing processes (Alliegro 1974). Typical examples of these materials include UKAEA/BNF Rofel, KT, NI-430, NI-435 and Ford siliconized silicon carbide. Each material is formed by a unique proprietory process. In general, a plastic body is formed by SiC powder, graphite and a plasticizer. In some variants of this process, SiC powder and a char-forming plastic binder are used (Whalen *et al* 1978). A variety of experimental gas turbine components such as combustors or stators, have been made by this route. Since these materials and the processes are easily adopted to mass production techniques and since the products possess good shape retention, there is a strong incentive to use them for the production of automotive components.

Sintered silicon carbide is a recent development. The pressureless sintering of SiC to full density was thought untenable until Prochazka demonstrated that with boron and carbon additions, β-SiC could be sintered to a maximum denstiy at 2000° C (Prochazka 1974). He also demonstrated that sintered β-SiC could be formed into useful shapes by slip-casting, die-pressing and extrusion. Distribution of the carbon additive and exaggerated grain growth of α-SiC were found to interfere with densification. Coppola & McMurtry (1976) have developed sintered α-SiC partly in an effort to eliminate the problems associated with β-α transformation. The β-SiC structure appears stronger than α-SiC. Bending strengths of α and β forms are of the order of 300–450 MPa (Larsen *et al* 1983, pp. 695–710). The temperature variation of the bending strengths of α and β SiC is shown in figure 5.

Reaction-formed SiC/Si composites developed by Hillig (1974) are the first engineering composite ceramic/ceramic materials which offer the possibility of low cost structural components. In this process, the molten silicon reacts with graphite to form polycrystalline SiC fibres in a silicon matrix. This material has been used in a

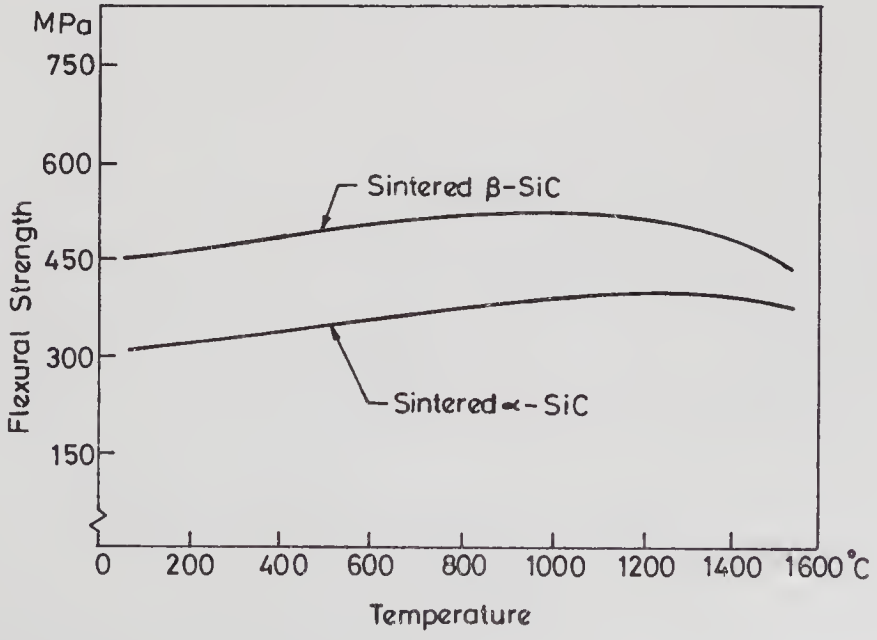

Figure 5. Flexural strength of silicon carbide materials as a function of temperature (adapted from Larsen *et al* 1983, pp. 695–710).

combustion chamber liner application at temperatures above 1400° C (Coppola & McMurtry 1976), although it is still in a very early stage of development.

CVD-silicon carbide in contrast to CVD-Si_3N_4 has been produced in bulk. Fabrication capability of gas turbine components including radial and axial rotors has also been demonstrated. CVD-SiC has proven to be an outstanding creep- and oxidation-resistant material. Its major drawback from an automative application point of view is likely to be the cost. This process may be useful in coating SiC ceramics formed by more conventional routes. A sintered body consisting of SiC and AlN has 90% theoretical density, specific resistance of $1–10^4$ ohm/cm (at room temperature), excellent bending strength and oxidation-resistance. It is useful for heaters, electrical resistors and temperature sensors.

8. Concluding remarks

The ceramics discussed in this article are the most important materials currently in demand for advanced and emerging technologies. Large volume ceramic applications appear to be round the corner in the automotive industry. Adiabatic engines made from advanced ceramics such as Si_3N_4 have the demonstrated ability to save power upto 20–30% which is too attractive to ignore by a world faced with an imminent energy crunch.

A variety of advanced technologies also make continuous demand on super hard materials for cutting tools and materials which are capable of standing extremes of temperature, pressure and chemical environment. Metals and alloys have been found to be incapable of answering these challenges, thus making ceramics the only candidates in the field; a ceramic age appears to have been ushered in. As pointed out earlier light element ceramics constitute choice materials for further development and exploration. Nature has distributed the light elements so evenly on our planet that they are there for all progressive countries to harvest for their own benefit.

References

Acheson E G 1896 BRD Patent 85197
Acheson E G 1912 US Patent 1014199
Agte C, Moers K 1931 *Z. Anorg. Allg. Chem.* 198: 233–243
Akashi T, Sawaoka A B 1986 *J. Am. Ceram. Soc.* 69: c78–80
Aliprandi G 1986 *Metall. Ital.* 78: 405–411
Alliegro R A 1974 *Ceramics for high performance applications* (eds) J J Burke, A E Gorum, R N Katz (Chestnut Hill, Mass: Brook Hill) chap. 13
Arrol W J 1974 *Ceramics for high performance applications* (eds) J J Burke, A E Gorum, R N Katz (Chestnut Hill, Mass: Brook Hill)
Baldo J B, Pandolfelli V C, Casarini J R 1983 *Ceramic powders* (ed.) P Vincenzini (Amsterdam: Elsevier Scientific Publ. Co.)
Bandyopadhyay G, French K W 1986 *J. Eng. Gas Turbine Power* 108: 536–539
Besson J L, Streicher E, Chartier T, Goursat P 1986 *J. Mater. Sci. Lett.* 5: 803–805
Billy M 1959 *Ann. Chim.* 4: 795–851
Billy M, Mexmain J 1985 *Sprechsaal* 118: 245–249
Bonnel D A, Ruehle M, Tien T Y 1986 *J. Am. Ceram. Soc.* 69: 623–627
Cannon W R, Danforth S C, Flint J H, Haggerty J S, Marra R A 1982a *J. Am. Ceram. Soc.* 65: 324–330
Cannon W R, Danforth S C, Haggerty J S, Marra R A 1982b *J. Am. Ceram. Soc.* 65: 330–335
Canteloup J, Mocellin A 1975 *Spec. Ceram.* 6: 209–222

Chukukere F N, Riley F L 1986 *Mater. Sci. Forum* 7: 307–316
Coppola J, McMurtry C H 1976 Substitution of ceramics for ductile materials in design, National Symposium on Ceramics in the Service of Man, Carnegie Institution, Washington DC
Dadape V V, Kane G P, Sathe P K 1947 *J. Sci. Ind. Res. (India)* B6: 123–127
Danforth S C, Haggerty J S 1983 *J. Am. Ceram. Soc.* 66: c58–59
Dietzel A, Jagodzinski H, Scholze H 1960 *Ber. Dtsch. Keram. Ges.* 37: 524
Drew P, Lewis M H 1974 *J. Mater. Sci.* 9: 261–269
Eaborn C 1960 *Organosilicon compounds* (London: Butterworths)
Evans J R G, Moulson A J 1983 *Progress in nitrogen ceramics* (ed.) F L Riley (Dordrecht: Martinus Nijhoff)
Fletcher F J, Ibrahim J, Kerry I M 1971 *Symposium on electrochemical engineering* (London: Inst. Chem. Eng.)
Frederikse H P R, Kahn A H, Dragoo A L, Hosler W R 1985 *J. Am. Ceram. Soc.* 68: 131–135
Friedmann C 1969 *Physica* 41: 139–143
Fujio M, Kozo K 1986 Jpn. Kokai Tokyo Koho JP 61, 111, 904
Fukunaga O, Endosh T, Akashi M, Osawa T, Yamaoka S 1978 Proc. Int. Symp. of Factors in Densification and Sintering of Oxide and Nonoxide Ceramics, Japan, p. 328
Fumino H, Tsuyosh T, Isaco O, Yasuo N 1986 *Ext. Abstr. Conf. Solid State Devices Mater.* 18: 663–666 (*Chem. Abstr.* 1987, 106: 42449r)
Fumiyoshi M, Hiroyuki K 1986 *Kinzoku Hyomen Gijutsu* 37: 401–405
Fyfe C A, Gobbi G C 1983 *Polyhedron* 3: 1267–1269
Gasilova E B, Saksonov Yu G 1966 *Karbid Kremniya* (ed.) I N Frantsevich (Kiev: Navkova Dumka)
Gauckler L J, Boskovic S, Naik I K, Tien T Y 1978 *Ceramics for high performance applications II* (eds) J J Burke, E N Lenoe, R N Katz (Chestnut Hill, Mass: Brook Hill)
Gauckler L J, Lukas H L, Petzow G 1975 *J. Am. Ceram. Soc.* 58: 346–347
Gauckler L J, Prietzel S, Bodemer G, Petzow G 1977 *Nitrogen ceramics* (ed.) F L Riley (Leiden: Noordhoff)
Gazza G E, Knoch H, Quinn G D 1978 *Am. Ceram. Soc. Bull.* 57: 1059–1060
Giardini A A 1953 *US Bur. Mines Inf. Circ.* No. 7664: 13
Gilman R C 1969 *Astrophys. J.* 155: L185
Glemser V O, Newmann P 1903 *Z. Anorg. Allg. Chem.* 298: 134
Goodwin C A 1982 *Ceram. Eng. Sci. Proc.* 3: 109–119
Gossain A, Didier B, Michel B, Sop H K, Pierre L 1985 *Rev. Chim. Miner.* 22: 473
Greil P, Weiss J 1983 *Progress in nitrogen ceramics* (ed.) F L Riley (Dordrecht: Martinus Nijhoff)
Gugel E, Petzenhauser I, Fickel A 1975 *Powder Metall. Int.* 7: 66–67
Hampshire S, Park H K, Thompson D P, Jack K H 1978 *Nature (London)* 274: 880–882
Hanna S B, Ghoneim N M 1986 *Interceram* 35: 42–45
Hanna S B, Mansour N A L, Taha A S, Abd-Allah H M A 1985 *Br. Ceram. Soc. Trans. J.* 84: 18–21
Hayakawa Y 1949 *J. Electrochem. Assoc. Jpn.* 17: 147
Hibbs L E Jr, Wentorf R H Jr 1974 *High Temp. High Pressures* 6: 409
Higgins I, Hendry A 1986 *Br. Ceram. Soc. Trans. J.* 85: 161–166
Hillig W B 1974 *Ceramics for high performance applications* (eds) J J Burke, A E Gorum, R N Katz (Chestnut Hill, Mass: Brook Hill) chap. 52
Hirao K, Miyamoto Y, Kozumi M 1986 *J. Am. Ceram. Soc.* 69: c60–61
Hoch M, Nair K M 1978 *Materials science research* (eds) Palmour Hayne III, R F Davis, T M Hare (New York: Plenum) Vol. 11
Hoch M, Nair K M 1979 *Am. Ceram. Soc. Bull.* 58: 187
Hoch M, Thompson A L, Houck J, Nair K M 1977 *J. Power Bulk Solids Technol.* 1: 34
Husbey I C, Lukas H L, Petzow G 1975 *J. Am. Ceram. Soc.* 58: 377
Ibrahim S 1986 PCT Int. Appl. No. 86, 06, 360
Ingles T A, Popper P 1960 *Special ceramics* (ed.) P Popper (London: Heywood)
Ishigaki H, Kawaguchi I, Iwasa M, Toibana Y 1986 *J. Tribol.* 108: 514–521
Izumi F 1983 *Adv. X-ray Chem. Anal., Jpn.* 14: 43
Izumi F, Mitomo M, Bando Y 1984 *J. Mater. Sci.* 19: 3115–3120
Jack K H 1973 *Br. Ceram. Soc. Trans. J.* 72: 376–384
Jack K H 1976 *J. Mater. Sci.* 11: 1135–1158
Jack K H, Wilson W I 1972 *Nature (London)* 238: 28–29
Johnson P M, Hendry A 1979 *J. Mater. Sci.* 14: 2439–2445

Joly F 1883 *Compt. Rend.* 97: 456
Kaji H, Mamoru K 1986 *Funtai Oyobi Funmatsuyakin* 33: 210–215 (*Chem. Abstr.* 1986, 105: 10186m)
Kaypov A D, Baymuratov M N 1970 *Izv. Akad. Nauk. Kaz. SSR, Ser. Geol.* 27: 68
Kazuo U, Makoto K, Toru K 1986 *Chem. Express* 1: 511–514
Kim S S, Kato K, Hokirigawa K, Abe H 1986 *J. Tribol.* 108: 522–526
Knoop F 1939 *J. Res. Natl. Bur. Stand.* 23: 39–61
Komeya K, Inoue H 1969 *J. Mater. Sci.* 4: 1045
Komeya K, Inoue H 1971 *Br. Ceram. Soc. Trans. J.* 70: 107–113
Komeya K, Inoue H 1974 *J. Am. Ceram. Soc.* 57: 411
Komeya K, Tsuge A, Hasimoto H, Kubo T, Ochia T 1977 Gas Turbine Soc. of Japan, Tokyo joint gas turbine conference, Paper No. 65
Lanyi B 1955 *Elektrotermikus Eljarasok* (*Electrochemical processes*) (Budapest: Akademiai Kiado)
Larker H T, Adlerborn J, Bohman H 1975 Fabrication of dense Si_3N_4 parts by hot isostatic pressing, SAE 770335
Larsen D C, Adams J W, Ruh R 1983 *Progress in nitrogen ceramics* (ed.) F L Riley (Dordrecht: Martinus Nijhoff)
Larsen D C, Bortz S A, Ruh R, Tallan N M 1978 *Ceramics for high performance applications II* (eds) J J Burke, E N Lenoe, R N Katz (Chestnut Hill, Mass: Brook Hill) chap. 36
Laves N 1934–35 *Gotting Ges.* 2, VI 1: 57–
Lavrenko V A, Alekseev A F 1986 *Ceram. Int.* 12: 25–
Lecompte J P, Jarrige J, Mexmain J 1983 *Progress in nitrogen ceramics* (ed.) F L Riley (Dordrecht: Martinus Nijhoff)
Lee J, Cutler I B 1975 *Am. Ceram. Soc. Bull.* 54: 195
Lefevre J 1970 *Astron. Astrophys.* 5: 37–44
Lengfeld F 1899 *Am. Chem. J.* 21: 531
Lewis M H, Powell B D, Drew P, Lumby R J, North B, Taylor A J 1977 *J. Mater. Sci.* 12: 61–74
Liping H, Xiongzhang H, Xiren F, Baozhen S 1986 *Guisnanyan Xuebao* 14: 332
Lipp A 1965 *Tech. Rundsch.* 14: 28–33
Lumby R J, North B, Taylor A J 1975 *Special ceramics–6* (ed.) P Popper (Manchester: Br. Ceram. Res. Assoc.)
Lumby R J, North B, Taylor A J 1978 *Ceramics for high performance applicaitons II* (eds) J J Burke, E M Lenoe, R N Katz (Chestnut Hill, Mass: Brook Hill)
Matsue S, Komeya K, Matsuki Y 1965 *Yogyo Kyokai Shi* 73: 82
Mazdiyasni K S, Cooke C M 1973 *J. Am. Ceram. Soc.* 56: 628–633
Mazdiyasni K S, West R, David L D 1978 *J. Am. Ceram. Soc.* 61: 504–508
Mazdiyasni K S, Zangvil A 1985 *J. Am. Ceram. Soc.* 68: c142–144
McCauley J W, Corbin N D J 1979 *Am. Ceram. Soc. Bull.* 62: 476–479
McLean A F 1978 *Ceramics for high performance applications II* (eds) J J Burke, E N Lenoe, R N Katz (Chestnut Hill, Mass: Brook Hill) chap. 1
Mehmet S, Ilhan A, Gareth T 1985 *Mater. Sci. Res.* 19: 167
Messier D R, Wong P 1974 *Ceramics for high performance applications* (eds) J J Burke, A E Gorum, R N Katz (Chestnut Hill, Mass: Brook Hill)
Moissan H 1894 *Compt. Rend.* 118: 556
Moissan H 1905 *Compt. Rend.* 140: 769
Morgan P E D 1984 *Mater. Res. Soc. Symp. Proc.* 32: 213
Morgan P E D 1986 *J. Mater. Sci. Lett.* 5: 372
Morgan P E D, Pugar E A 1985 *J. Am. Ceram. Soc.* 68: 699–702
Mostaghaci H, Fan Q, Riley F L, Bigay Y, Torre J P 1986 *Br. Ceram. Soc. Trans. J.* 85: 12–16
Nancy T 1986 *J. Mater. Res. Soc. Symp. Proc.* 62: 435
Negita K 1985 *J. Mater. Sci. Lett.* 4: 417–418
Niihara K, Nakahira A, Hirai T 1984 *J. Am. Ceram. Soc.* 67: C13–14
Nobuo I, Akihiko I, Yasuyuki S 1984 *Int. Hybrid Micro-electron* 7: 49–53
Nobuo I, Kazuo S 1986 *Densi Zairyo* 25: 40–46
Nobuo K, Aszmu S, Nobuyasu M 1985 *Seramikkusu* 20: 920
Nobuyuki K 1985 Jpn. Kokai Tokyo Koho JP60, 19, 064
Okabe Y, Hojo J, Kato A 1979 *J. Less Common Met.* 68: 29–41
Oyama Y 1972 *Jap. J. Appl. Phys.* 11: 15–72
Oyama Y 1973 *Jpn. J. Appl. Phys.* 12: 500–508

Oyama Y, Kamigaito O 1971 *Jpn. J. Appl. Phys.* 10: 1637
Peizhi G, Wanmer S, Hong C, Weiru Z 1986 *Gui Suanyan Xuebao* 14: 369
Pierre L, Florence M, Gossan A, Michel B 1985 *Rev. Chim. Miner.* 22: 534
Pring J N, Fielding W 1909 *J. Chem. Soc.* 95: 1497–1506
Prochazka S 1974 *Ceramics for high performance applications* (eds) J J Burke, A E Gorum, R N Katz (Chestnut Hill, Mass: Brook Hill) chap. 12
Prochazka S 1975 *Special ceramics-6* (ed.) P Popper (Manchester: Br. Ceram. Res. Assoc.)
Prochazka S, Greskovitch C 1978 *Am. Ceram. Soc. Bull.* 57: 579–581
Rahaman M N, Boiteux Y, DeJonghe L C 1986 *Am. Ceram. Soc. Bull.* 65: 1171–1176
Ramamurthy S 1985 *J. Mater. Sci. Lett.* 4: 603–605
Rapoport E, Nadiv S 1985 *J. Mater. Sci. Lett.* 4: 34–36
Ruff O 1935 *Trans. Electrochem. Soc.* 68: 87
Sakai T, Iwata M 1977 *J. Mater. Sci.* 12: 1659–1665
Samsonov G V 1958a *Ukr. Khim. Zh.* 24: 659
Samsonov G V 1958b *J. Phys. Chem.* 32: 2424
Samsonov G V 1958c *Technol. Buntmet.* 29: 367
Sanyal A S, Mukerji J 1986 *J. Mater. Sci. Lett.* 5: 787–788
Schwetz K A, Knoush R, Lipp A 1983 *Progress in nitrogen ceramics* (ed.) F L Riley (Dordrecht: Martinus Nijhoff)
Segal D L 1985 *Chem. Ind.* 544
Segal D L 1986 *Br. Ceram. Trans. J.* 85: 184–187
Seiji M 1986 *Kogyo Zairyo* 34: 21
Seiji M, Noriyuki I, Tatsuhiko H 1986 *J. Mater. Sci.* 21: 3836–3842
Seyferth D, Wiseman G H, Prudhomme C 1983 *J. Am. Ceram. Soc.* 66: c13–14
Sharma N K, Williams W S, Zangvil A 1984 *J. Am. Ceram. Soc.* 67: 715–720
Shimada M 1986 *Am. Ceram. Soc. Bull.* 65: 1153–1155
Silver A H, Bray P J 1959 *J. Chem. Phys.* 31: 247–253
Singh B P 1987 *J. Mater. Sci.* 22: 495
Sorrel C C, McCartney E R 1986 *Mater. Forum* 9: 148–161
Steinmann D 1986 *Sprechsaal* 119: 562
Sugawara F, Ajioka T, Ichikawa F, Ushio S 1986 *Mater. Res. Soc. Symp. Proc.* 54: 535–540
Szweda A, Hendry A, Jack K H 1981 *Proc. Br. Ceram. Soc.* 31: 107
Takase A, Tani E 1984 *J. Mat. Sci. Lett.* 3: 1058–1060
Takase A, Tani E 1986 *Am. Ceram. Soc. Bull.* 65: 1597–1600
Taylor K M, Lenie C 1960 *J. Electrochem. Soc.* 107: 308–314
Thommy E, Bertil A 1986 *Chem. Ser.* A26: 33–35
Thompson D P, Korgul P, Hendry A 1983 *Progress in nitrogen ceramics* (ed.) F L Riley (Dordrecht: Martinus Nijhoff)
Tomonari T 1956 *J. Electrochem. Soc. Jpn.* 24: 27
Toshio T, Yoshinori U, Akira T 1985 *Nagoya Kogya Gijutsu Shikensho Hokoku* 34: 235
Trontelj M, Kolar D 1975 *Special ceramics-6* (ed.) P Popper (Manchester: Br. Ceram. Res. Assoc.)
Tsukuma K, Shimada M, Koizumi M 1981 *Am. Ceram. Soc. Bull.* 60: 910–912
Ueltz H F G 1972 *Proc. Int. Grinding Conf.* (ed.) M C Shaw (Pittsburg: Carnegie Press)
Vasilos T 1977 *Nitrogen ceramics* (ed.) F L Riley (Leiden: Noordhoff)
Wentorf R H Jr 1957 *J. Chem. Phys.* 26: 956
Weston R J, Carruthers T G 1973 *Proc. Br. Ceram. Soc.* 22: 197
Whalen T, Koakes J E, Terner L L 1978 *Ceramics for high temperature applications II* (eds) J J Burke, E M Lenoe, R M Katz (Chestnut Hill, Mass: Brook Hill) chap. 9
Wills R R, Stewart R W, Wimmer J M 1977 *Am. Ceram. Soc. Bull.* 56: 194–196
Wong P, Messier D R 1978 *Am. Ceram. Soc. Bull.* 57: 525–526
Yeh H C, Watters W J 1977 Effects of pressure and temperature on hot pressing of sialon, NASA TM-78945
Yoshio B 1985 *Seramikkusu* 20: 1117–1126
Zangvil A, Ruh R 1985 *Mater. Sci. Eng.* 71: 159–164
Zulfequar M, Kumar A 1986 *J. Mater. Sci. Lett.* 5: 1230–1232

Science of zirconia-related engineering ceramics

S B BHADURI

Defence Metallurgical Research Laboratory, P O Kanchanbagh, Hyderabad 500 258, India

Abstract. In this paper, we comprehensively review the physical principles behind the improvement of mechanical properties of zirconia (ZrO_2) related ceramics. First, the transformation behaviour of different phases in zirconia is discussed. We next present an overview of two zirconia-related commercially important systems e.g. ZrO_2-MgO and ZrO_2-Y_2O_3. The commercial engineering ceramic materials, generated from these systems, are known as partially stabilized zirconia and tetragonal zirconia polycrystal respectively. The third important material is called zirconia toughened alumina. The evolution, characterization and importance of the microstructure in relation to the basic systems are also presented. Attention is then focussed on to three toughening mechanisms e.g. phase transformation toughening, microcrack toughening and crack deflection toughening. We carefully assess the roles they play in improving toughness. We discuss *R*-curve behaviour arising out of these toughening mechanisms and the implications of *R*-curve behaviour in engineering applications. Finally, the subcritical crack growth and tribological behaviour of these materials are discussed.

Keywords. Zirconia-related ceramics; partially stabilized zirconia; tetragonal zirconia polycrystal; zirconia toughened alumina; phase transformation toughening; microcrack toughening; crack deflection toughening; *R*-curve behaviour.

1. Introduction

Since the publication of the seminal paper on toughened zirconia by Garvie *et al* (1975), this material has become the most important ceramic material of the present. Along with high toughness and strength, zirconia also possesses good hardness, wear resistance, and thermal shock resistance. These superb properties have led to the usage of zirconia-based components in a number of engineering applications such as automobile engine parts, wire drawing dies, cutting tools, in chemical plants for handling corrosive slurries, and in the textile industry as thread guides. An understanding of the peculiar properties of zirconia have made all the applications and improved properties possible. The key to the improvement in properties lies in the controlled phase transformation of the metastable phase to the stabler phase during the crack propagation.

The present paper reviews the current understanding of the scientific aspects of toughened zirconia, emphasizing the role of the system and the microstructure for the development of the mechanical properties. The technological aspects are briefly touched upon.

Therefore, the different phases of zirconia, their stability and the transformation of the metastable phase are first discussed, followed by a review of commercially available systems and their microstructures. Finally, the various mechanical properties are elaborated. The emphasis throughout the paper is on commercially available/viable engineering materials. This is necessitated by the fact that zirconia-related materials have many other uses.

2. Phases and transformation

Polymorphism of zirconia is well-known; three crystallographic modifications exist – cubic (c), tetragonal (t) and monoclinic (m). They are stable at high, intermediate and low temperatures, respectively. Table 1 shows the relevant crystallographic data. Subbarao (1981) reviewed the evidence that clearly established the martensitic nature of the $t \rightarrow m$ transformation. The transformation strain ε^T can be expressed in terms of the matrix

$$\varepsilon^T = \begin{bmatrix} \dfrac{a_m \cos(90-\beta)/2 - a_t}{a_t} & 0 & \tan(90-\beta)/2 \\ 0 & \dfrac{b_m - b_t}{b_t} & 0 \\ \tan(90-\beta)/2 & 0 & \dfrac{a_m \cos(90-\beta)/2 - a_t}{a_t} \end{bmatrix}. \quad (1)$$

Substituting the lattice parameters in (1), it can be shown that there is 9% shear involved and that the change in volume $(\varepsilon_{11}^T + \varepsilon_{22}^T + \varepsilon_{33}^T)$ is equal to 4·7%. Therefore, in general, the $t \rightarrow m$ transformation is deleterious to the property of the material. But under controlled conditions, the transformation can lead to enhancement of properties. This is achieved by stabilizing the high temperature t-phase at room temperature. It has been experimentally shown by Hannink *et al* (1981) that there is

Table 1. Crystallographic data on various phases of zirconia.

Phase	Space group	Lattice parameters (Å)
Monoclinic	$P2_1/c$	$a_m = 5{\cdot}156$ $b_m = 5{\cdot}191$ $c_m = 5{\cdot}304$ $\beta = 98{\cdot}9°$
Tetragonal	$P4_2/nmc$	$a_t = 5{\cdot}094$ $c_t = 5{\cdot}177$
Cubic	F_{m3m}	$a_c = 5{\cdot}124$

a critical size of the tetragonal particle which is stable at room temperature. The reciprocal of the size of the particle is shown to be linearly proportional to M_s, the martensitic start temperature. There are several theoretical attempts to analyse this experimental fact. One of the approaches is to carry out a thermodynamic analysis without looking at the actual processes. Such end-point calculations were undertaken by Lange & Green (1981), Lange (1982), Garvie & Swain (1985). This simple approach provides us with a tangible explanation of the experimental facts. Following Garvie & Swain (1985), the change in free energy of a spherical particle of radius r can be given as

$$\Delta F_0 = \frac{4}{3}\pi r^3 (\Delta F_{\text{chem}} + \Delta F_{\text{dil}} + \Delta F_{\text{shr}}) + 4\pi r^2 (\Delta S_{\text{chem}} + \Delta S_{\text{tw}} + \Delta S_{\text{pm}}), \quad (2)$$

where F_0 is the total free energy and ΔF is the free energy change per unit volume. Subscripts chem, dil and shr denote chemical, dilatational and shear, respectively, ΔS denotes the change in free energy per unit area, and tw, pm refer to the contributions from twin boundaries and the second phase, respectively. Equation (2) can be written as:

$$\Delta F_0 / V = \Delta F_{\text{chem}} + \Sigma \Delta F_{\text{str}} + (3/r) \Sigma \Delta S, \quad (3)$$

where V is the volume of the particle, F_{str} is the sum of the strain energies and S is the sum of the interfacial energies. Equation (3) can be conveniently rewritten as

$$1/r_c = q\, T/3\, \Sigma \Delta S\, T_b - (9 + \Sigma \Delta S_{\text{str}})/3\, \Sigma \Delta S, \quad (4)$$

where c denotes a critical value, q is the enthalpy of transformation of an infinitely large crystal and T_b is the transformation start temperature (M_s) of a particle of radius r_c. It is evident that (4) describes the experimental behaviour perfectly. Garvie & Swain (1985) substituted all the relevant data in the above equation and showed that real systems obey (4). Further, these theories can also predict transformability under stress. They can approximately point out the causes of nucleation of martensite i.e. whether it is by a classical or by a non-classical mode (Burke & Garvie 1977).

Heuer *et al* (1982), Ruhle & Heuer (1984), Heuer & Ruhle (1985), on the other hand, emphasized the events taking place during transformation i.e. nucleation and the growth of plates. This kind of approach requires a substantial amount of electron microscopy and much more sophisticated modelling involving the nucleation aspect and proper constitutive relations. Modelling work has been initiated along these lines by Lambropoulus (1986, and unpublished work). These models are much more rigorous than the previous ones.

Thus, there is a critical particle size of the tetragonal phase that can remain stable at a given temperature. It undergoes controlled transformation only when the crack propagates in the vicinity of the particles. However, certain alloying elements can increase the stability of tetragonal particles by bringing down M_s temperature. Therefore, in binary systems of other oxides with zirconia, there must be a range of sizes of metastable tetragonal particles which are transformable in the stress field of the propagating crack. It is these particles which are responsible for increasing the toughness. If the tetragonal particle size is less than the critical value, they remain stable even in the stress field of the propagating crack. If they are above the upper bound, they transform spontaneously during cooling without contributing to the toughness.

3. Commercial materials and microstructures

It is known that the $t \rightarrow m$ transformation leads to severe cracking of the matrix. One solution of the problem known for about fifty years is to form solid solution alloys with CaO, MgO or Y_2O_3. All of these solutes are supposed to stabilize the cubic structure at room temperature and avoid $t \rightarrow m$ transformation. Actually, these solutes permit retention of cubic structure at lower temperatures than is possible in undoped material because most of the phase equilibrium diagrams now report eutectoid decomposition reactions at low temperatures. The so-called destabilization phenomenon is this eutectoid reaction. Because of this, cubic or fully stabilized zirconias (CSZ) fail.

Partially stabilized zirconias (PSZ) are two (or more) phase materials, with the matrix phase being cubic. Addition of a limited quantity of solute and proper heat treatment in the two-phase $(c+t)$ field gives rise to the above microstructure. Usually, the second phase is the metastably-retained tetragonal phase. There are several advantages of this material. During cooling, $t \rightarrow m$ transformation counteracts the contraction of the cubic phase. Therefore PSZ has better thermal shock resistance than CSZ. Further, the controlled $t \rightarrow m$ transformation at the crack tip imparts toughness to the material. That is why PSZ is the most important engineering material nowadays.

3.1 *The ZrO_2-MgO system*

We now describe the commercially available compositions. Figure 1 shows the phase diagram of the ZrO_2-MgO binary system. The group at CSIRO, Melbourne, has pioneered the development of commercial PSZ materials based on this system. Typical compositions are also shown in figure 1. A common procedure for producing partially stabilized zirconia is to solutionize and homogenize the desired composition in the cubic phase field, at a temperature of 1700°C or above, and then quench the

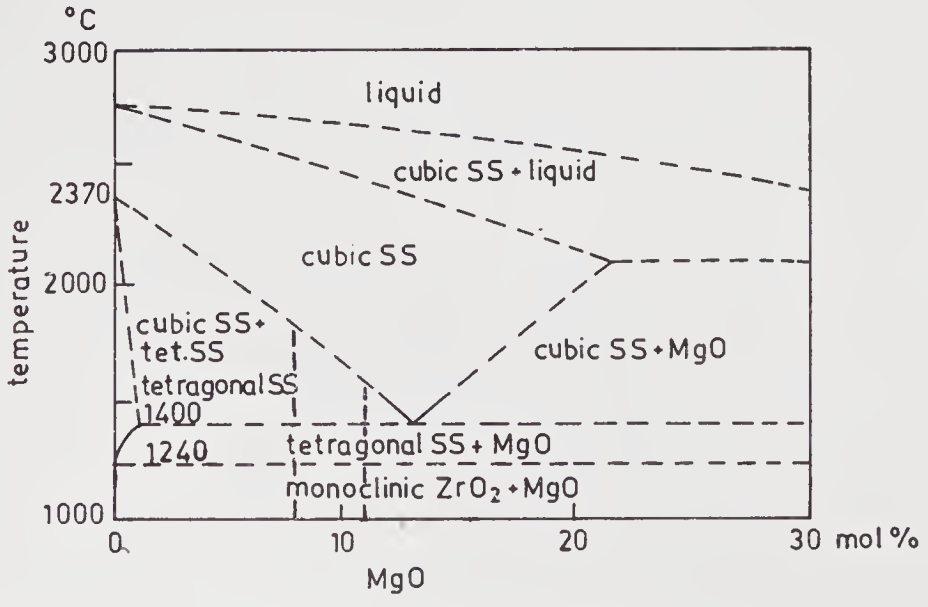

Figure 1. Phase diagram of the ZrO_2-MgO binary system.

material. The phase diagram suggests that the following reactions can take place during cooling/ageing in the $t+c$ phase field.

1) $c\text{-}ZrO_2 \rightarrow t\text{-}ZrO_2 + c\text{-}ZrO_2$,
   $Cool \rightarrow m\text{-}ZrO_2 + c\text{-}ZrO_2$;
2) $c\text{-}ZrO_2 \rightarrow t\text{-}ZrO_2 + c\text{-}ZrO_2$,
   $Cool \rightarrow t\text{-}ZrO_2$ (metastable) $+ c\text{-}ZrO_2$;
3) $c\text{-}ZrO_2 \rightarrow t\text{-}ZrO_2 + MgO$,
   $Cool \rightarrow m\text{-}ZrO_2 + MgO$;
4) $c\text{-}ZrO_2 \rightarrow m\text{-}ZrO_2 + c\text{-}ZrO_2 (< 1240°C)$,
5) $c\text{-}ZrO_2 \rightarrow m\text{-}ZrO_2 + MgO (< 1240°C)$.

Reaction (1) is the typically expected reaction. However, in the case of reaction (2), the size of the tetragonal particles that precipitate out of the cubic matrix is so small that they remain tetragonal when cooled below M_s temperature. Reaction (3) is the eutectoid reaction. Reactions (4) and (5) are the sub-eutectoid reactions. Of all the reactions mentioned above, it is expected that reaction (2) is the most important one, because it tends to retain the tetragonal phase metastably. However, they are optimally aged so that their size range is in between the lower and upper ranges of the transformability limit.

Figure 2a shows a typical microstructure of the optimally aged tetragonal precipitates in the cubic matrix. These precipitates can be easily detected by (111)-type diffraction patterns in the transmission electron microscope (TEM) as shown in figure 2b. The half reflection spots are the cubic forbidden spots and are ascribed to the tetragonal phase present in the cubic matrix. The dark field (DF) imaging technique using one of the tetragonal spots clearly reveals that they arise from the precipitates. These precipitates are lenticular in shape in the ZrO_2-MgO system. The tetragonal c axis is parallel to $\langle 100 \rangle$ of the matrix. This precipitate morphology can now be exactly predicted by the application of the Khachutoriyan (1983) theory as shown by Lanteri *et al* (1986). The critical particle size of $t\text{-}ZrO_2$ in Mg-PSZ is around 100 nm. Hannink (1978) explained the critical particle size by assuming that the coherency at the interface is lost if the particle exceeds a certain critical value. He used the one-dimensional Brooks' (1962, pp. 20–25) criterion to analyse the situation. However, the predictions are 2 or 3 times off the experimentally observed values. Clearly, better modelling is needed at the moment. These optimally aged zirconias have high strength and toughness. However, they still lack the high thermal shock resistance that is required in some engineering applications.

Further improvements of the properties were achieved by subeutectoid ageing of a suitably prefired material. This controlled heat treatment does not impart the highest strength but promotes higher toughness values and better thermal shock properties. Hannink & Garvie (1982), and Hannink (1983) have reported that a prefired material containing t-precipitates of 100 nm size can be aged at 1100°C to achieve improvement of the above properties.

During the ageing at this temperature, a very complicated reaction takes place. In fact both reactions (2) and (5) operate here simultaneously. Reaction (2) operates inside the grains whereas reaction (5) takes place at the grain boundaries. The reactions can be monitored easily by TEM. Initial ageing at subeutectoid temperature shows tetragonal spots in the diffraction pattern. But additional spots appear in the pattern showing some kind of ordered phase precipitating. This phase has been

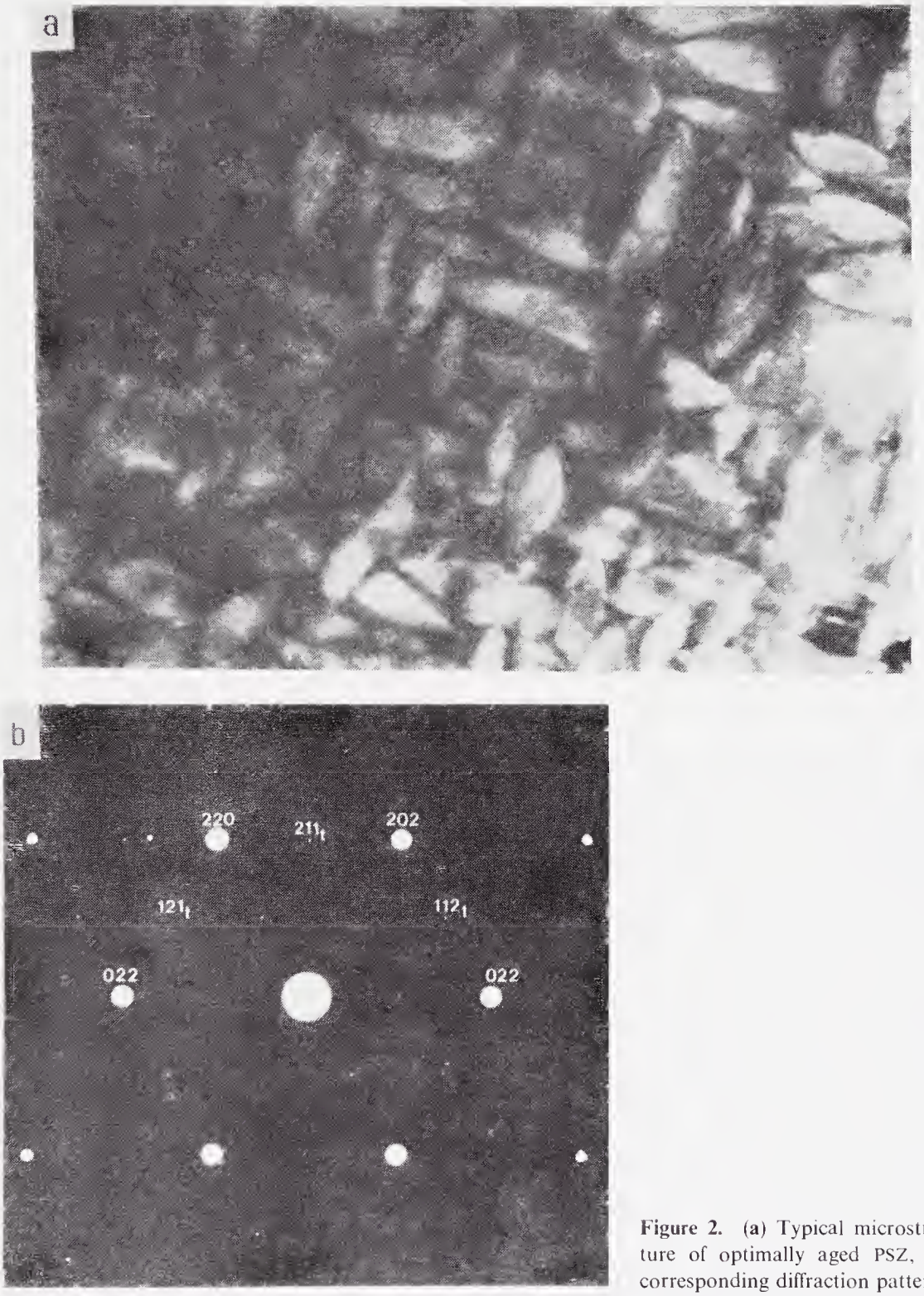

Figure 2. (**a**) Typical microstructure of optimally aged PSZ, (**b**) corresponding diffraction pattern.

identified by Hannink (1983), and Farmer *et al* (1983, 1984) as $Mg_2Zr_5O_{12}$. The detailed structure of this phase has been published by Delamarre (1976) who claims that it is a defect fluorite structure of trigonal symmetry. This phase is also called the δ phase. As opposed to the grain interior, the subeutectoid decomposition goes on along the grain boundary. Detailed microscopy shows that the diffraction pattern has both monoclinic ZrO_2 and MgO spots (Heuer *et al* 1983) DF imaging can be

performed using one of these spots. The procedure reveals that the grain boundary is full of alternate plates of MgO and *m*-ZrO_2. A schematic microstructure is shown in figure 3.

During the ageing treatment, the $Mg_2Zr_5O_{12}$ phase grows with diffusion of MgO and depletes MgO content in the stable tetragonal precipitates. So the formerly coherent tetragonal precipitates tend to lose coherency and become unstable. Therefore, the number of transformable tetragonal precipitates increases and hence the toughness goes up. Secondly, during the propagation of the crack, it interacts with the grain boundary substantially giving rise to *R*-curve behaviour. In other words, resistance to cracking increases as the crack grows. Both of the above processes improve toughness and thermal shock resistance, but with a slight decrease in strength.

3.2 *The ZrO_2-Y_2O_3 system*

The phase diagram of ZrO_2-Y_2O_3 is shown in figure 4. It is the single tetragonal phase field that is of commercial interest here. The idea was first proposed by Gupta *et al* (1977). The material is sintered in the tetragonal phase field with a final grain size of 0·3 μm and is completely (or mostly) tetragonal (figure 5) (Gupta 1978). Such materials are called tetragonal zirconia polycrystals (TZP). This is a very stringent condition indeed. One must choose suitable temperatures and soaking times to avoid grain growth. Second, the initial crystallite size of powders of ZrO_2-Y_2O_3 should not be very big. Third, the material has to be sintered in the single tetragonal phase field. Therefore, accurate knowledge of the phase diagram is also essential. Subbarao *et al* (1974) and Srivastava *et al* (1975) indicated that the two-phase field extends from 3·9 to 7·5 mol% Y_2O_3 with $t \rightarrow m + c$, the eutectoid composition value and temperature at 3·9 mol% Y_2O_3 and 565°C, respectively. Scott (1975) reported a eutectoid at 2·6 mol% Y_2O_3 and at 565°C. Pascual & Duran (1983) reported that eutectoid is at 4·5 mol% and at 490°C.

Such materials possess very high toughness and strength values. Masaki & Sayo

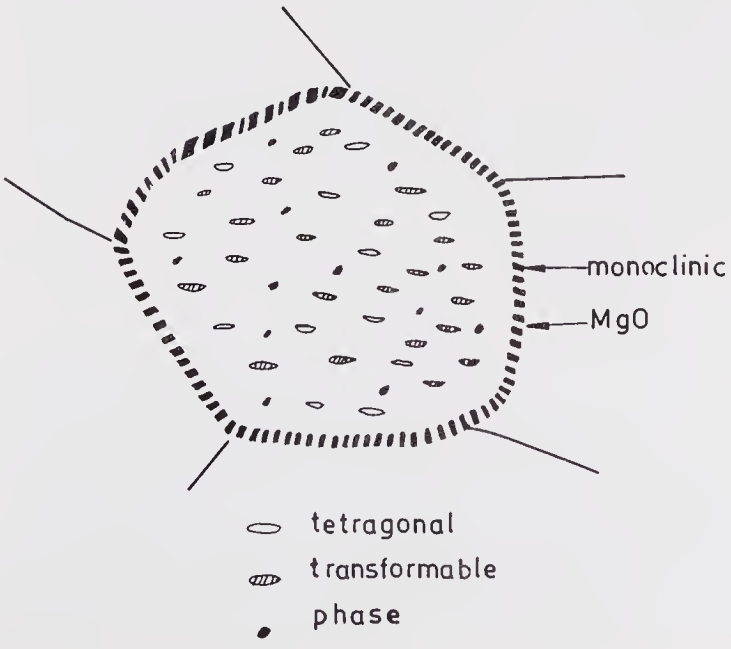

Figure 3. Schematic microstructure of subeutectoid aged ZrO_2(MgO).

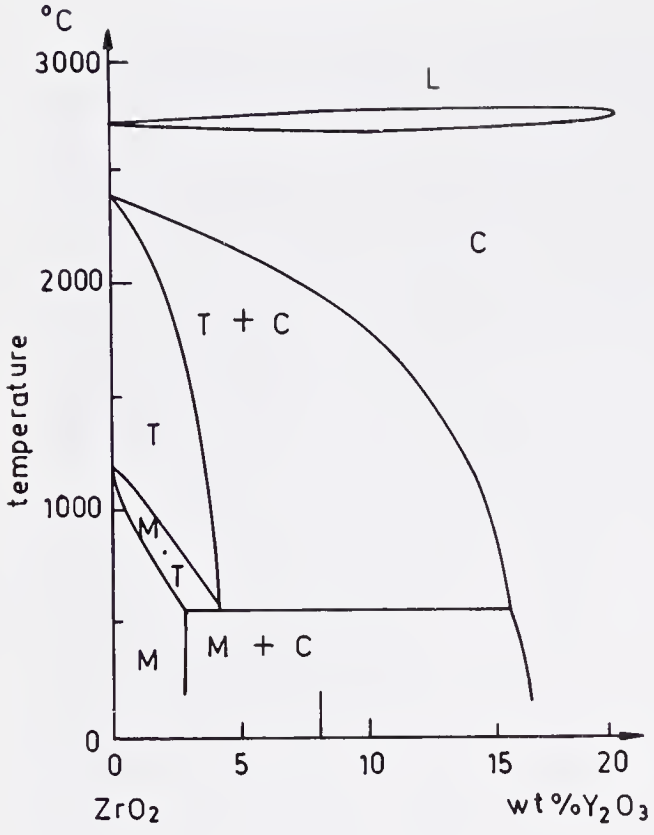

Figure 4. Phase diagram of the ZrO_2-Y_2O_3 binary system.

(1986) report strength values as high as 1700 MPa and fracture toughness values of $K_{Ic} = 20$ MPa $(m)^{\frac{1}{2}}$. Detailed TEM characterization results are reported by Ruhle *et al* (1984a). Most of the materials contain *t*-grains upto 0·8 μm. Y_2O_3 composition in each *t*-ZrO_2 grain varies between 1·8 and 4·6 wt%. The grain size and Y_2O_3 content do not correlate. Careful studies by Lange (1986) show that as Y_2O_3 content is increased from 0 to 4 mol% Y_2O_3, grain size decreases from 1·8 to 0·4 μm. Along with *t*-ZrO_2 – *c*-ZrO_2 grains are also present in the microstructure. Further studies show that *c*-ZrO_2 grains also contrain *t* precipitates. Also, most of the commercial materials contain a glassy grain boundary phase presumably picked up during mechanical milling of powder with SiO_2-containing balls. Transformation of *t*-ZrO_2 starts at the inhomogeneities at the grain boundaries or at defects present in the grains. Transformation strain frequently causes neighbouring grains to transform autocatalytically. Transformation also leads to some microcracking. A crack always leaves a continuous transformation zone in the wake of the propagating crack. This feature is discussed in § 4.1.

3.3 *Zirconia toughened alumina*

Zirconia toughened aluminas (ZTA) are classic examples of dispersion toughened ceramics. The second phase in these is unstabilized zirconia. Claussen (1976) and Claussen *et al* (1977) showed that a certain amount of very fine monoclinic zirconia can be well-dispersed in the Al_2O_3 matrix, and hot-pressed. Controlled microcracks are formed during cooling. This kind of controlled microcracking increases the toughness of the materials. Furthermore, some of the ZrO_2 particles may remain tetragonal in the compression stress field of the matrix. They may transform during

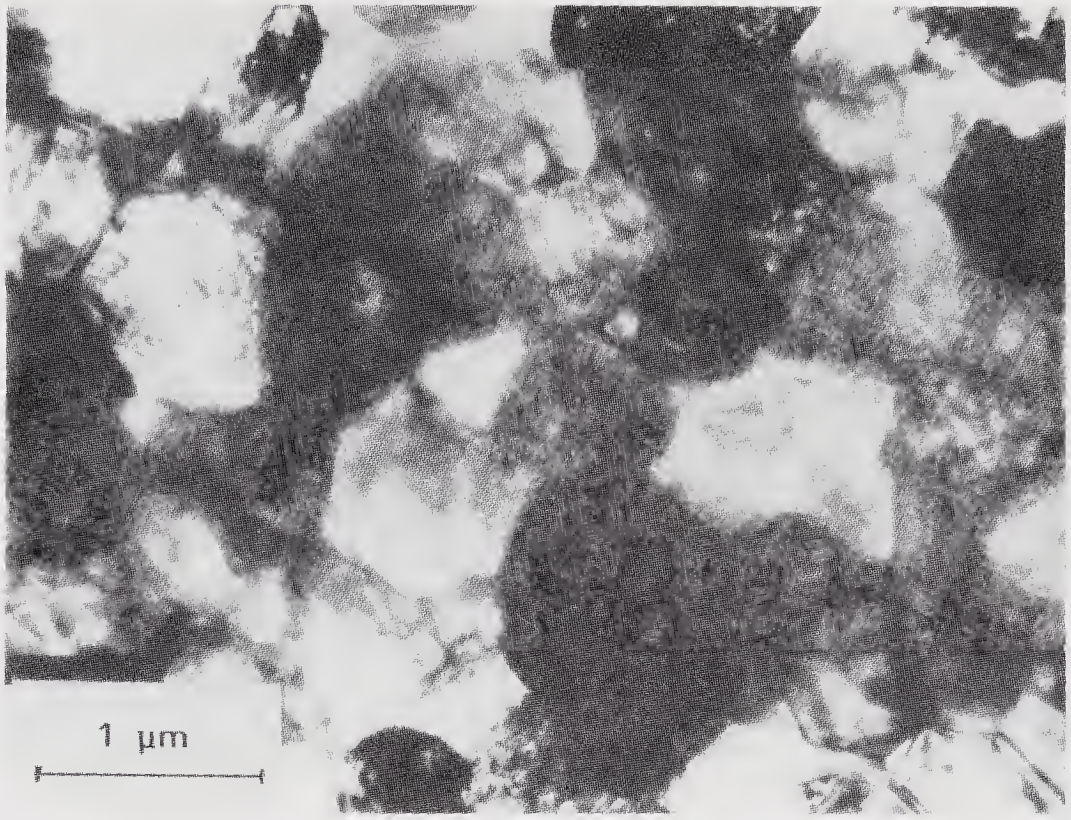

Figure 5. Microstructure of TZP.

the propagation of the crack. So in this case both phase transformation and microcracking improve toughness. Therefore, the key to the production of ZTA materials is the control of the microstructure during hot-pressing or sintering. Green (1982) studied the critical microstructures and experimentally obtained the lower and upper bounds of the particle sizes which are transformable.

The dilemma now is in deciding which of the two processes, e.g. phase transformation toughening or microcrack toughening, is important in ZTA. Ruhle *et al* (1984b) addressed the question by performing *in situ* straining experiments in the high voltage electron microscope (HVEM). Recent experimental results by Ruhle *et al* (1986) show that along with microcracking, phase transformation could also be an important toughening process.

Heuer *et al* (1982) examined the stability of ZrO_2 particles within Al_2O_3 grains and argued that the stability of ZrO_2 particles depends on the nucleation of martensite as well as the solute content. Nucleation can play a significant part in the faceted intergranular particles. The facets act as stress raisers during the cooling of the composites from the fabrication temperature. As opposed to the intergranular particles, the intragranular particles are round shaped and remain quite stable. This is again due to the difficulty of nucleation of the martensite. The typical microstructure of ZTA is shown in figure 6.

Finally we point out the fact that there are several major differences between t-ZrO_2 of ZTA and t-ZrO_2 of PSZ.

1) The interphase between the second phase and the matrix is coherent in PSZ and incoherent in ZTA (Kraus-Lanteri *et al* 1986).

2) In PSZ, t-ZrO_2 is under compressive stress. The strain field around the particle

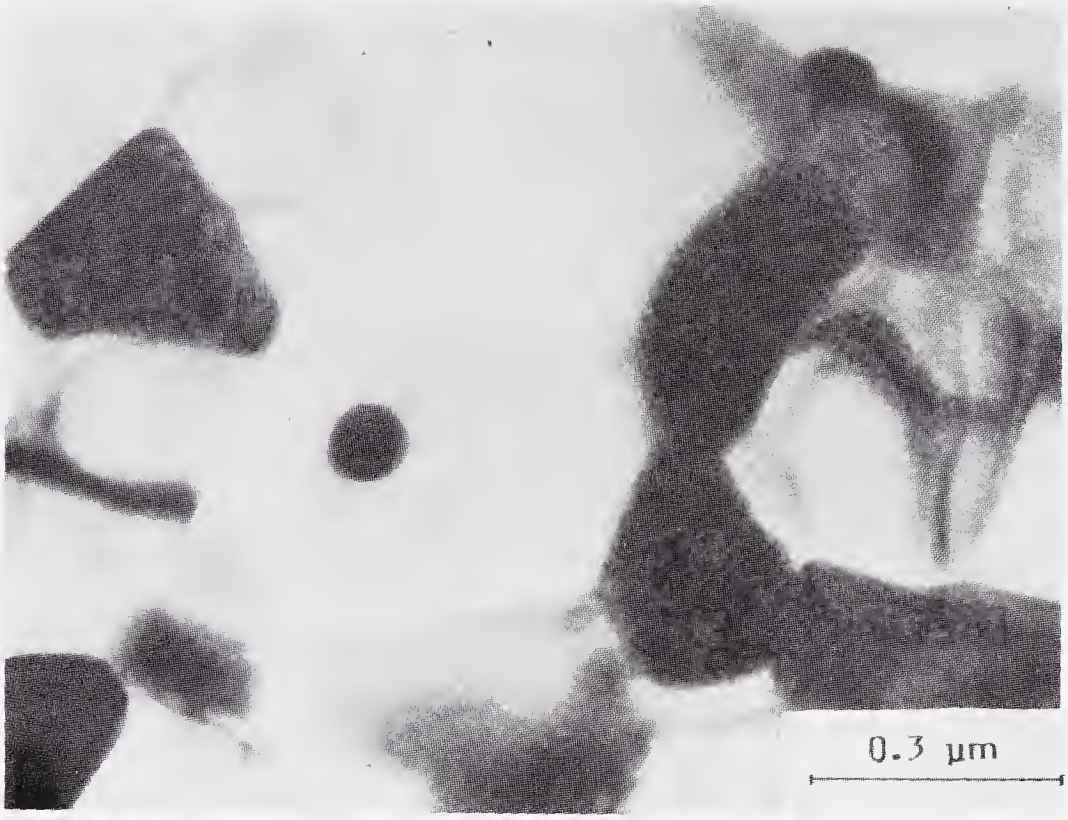

Figure 6. Typical microstructure of ZTA.

opposes transformation. In ZTA, the thermal mismatch causes tensile stresses in the particle which should encourage transformation.

Notwithstanding the above facts, there is a strong size dependence of t-ZrO_2 on M_s. The end-point thermodynamic calculations of Garvie & Swain (1985) predict experimentally observed results for PSZ and ZTA, without considering these facts. As noted in § 2 there is still need for better modelling.

4. Mechanical properties

Having described the commercially available materials and their microstructures, we will now concentrate on their important mechanical properties. Naturally, the most important and interesting mechanical property is their toughness. We discuss how the toughness of these materials can be increased by means of different toughening processes. Evans & Cannon (1986) have published a detailed review on this topic. In this paper we will follow their treatise.

Already we have noted that there are two different toughening processes e.g. phase transformation toughening and microcrack toughening. In addition, there is a third process known as crack-deflection. The crack interacts with the second phase and gets deflected. The effect leads to moderate increase in toughness. In the case of phase transformation as well as microcrack toughening, a nonlinear zone ahead of the crack tip is envisaged. One may compare this zone to the plastic zone in metals and crazed zones in polymers. The role of this zone is to reduce the effectiveness of the

propagating crack. This is known as crack tip shielding. In the following we elaborate these concepts.

4.1 *Phase transformation toughening*

We begin by quantifying the crack tip shielding concept. The materials that show crack tip shielding have a break in the linearity of their stress–strain curve at a critical stress. In the case of transformation toughening it is the critical stress of transformation (figures 7a & 7b). This break in stress is also reflected in the strain. The crack tip stress intensity is therefore lowered. That is, even if we apply K_∞ at the far end of the crack, stress at the tip is lowered by amount $K = K_\infty - K_{\text{local}}$. In other words, the zone in front of the crack shields the crack tip from the applied stress intensity. Hence the term 'crack tip shielding'. Since the crack tends to propagate when K_{local} attains the toughness of the fully transformed material ahead of the crack tip, we can write

$$K^c_\infty = K^c_T + \Delta K^c \tag{5}$$

where ΔK^c is the increase in toughness. Further analysis of the crack tip shielding can be made by taking either a mechanics, thermodynamics or dislocation approach. All the three approaches yield similar results.

Here, we will adopt the mechanics approach as developed by Budianisky *et al* (1983) and Evans (1984). The methodology is based on the path-independent J-integral concept of Rice (1968a), which is discussed in detail in another paper (Rice 1968b, pp. 191–230).

We now examine the development of the zone in front of the crack tip. We distinguish between two types of zones. The first one, called the frontal zone (figure 8a), becomes effective as the crack gets initiated. The frontal zone soon spreads to become the wake zone (figure 8b) as the crack propagates. Since the volume elements within the transformation zone do not experience unloading, the path independent J integral is applicable. We can choose any two paths – one within the frontal zone and

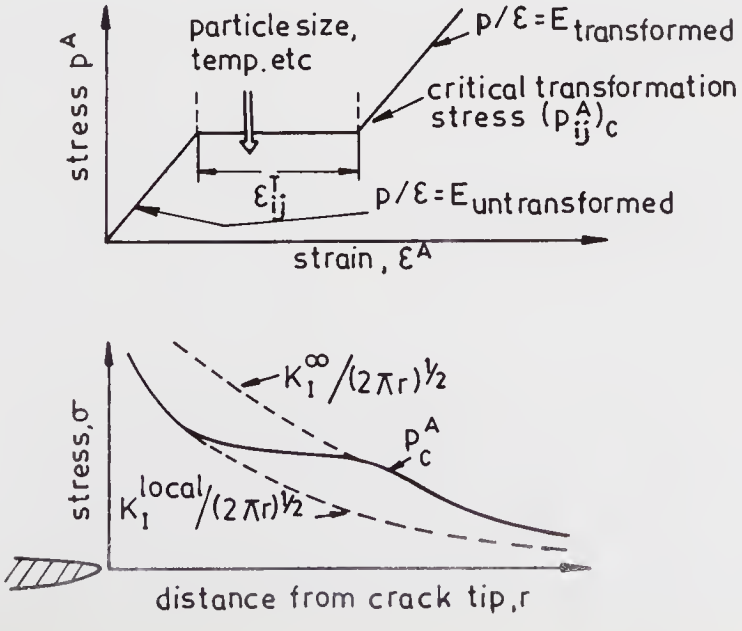

Figure 7. Explanation of crack tip shielding concept.

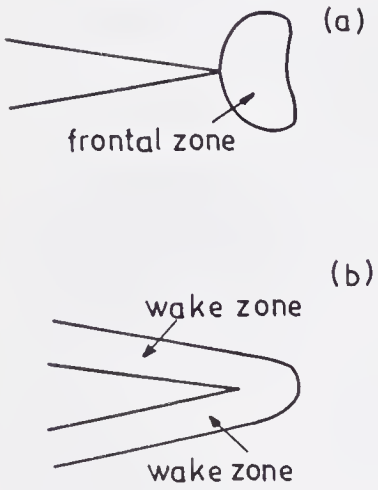

Figure 8. Sehematic drawing of (**a**) the frontal zone, (**b**) the wake zone.

the other outside it.

$$J=[(1-\nu^2)K_1^2]/E=[(1-\nu_1^2)(K_1^I)^2]/E_1=[(1-\nu_2^2)(K_1^\infty)^2]/E_2, \tag{6}$$

where ν_1, ν_2 and E_1, E_2 are Poisson's ratio and the Young's modulii of the frontal zone and the matrix, respectively. Since the ν's and E's are the same in the case of transformation-toughened material, we prove that $K_1^I=K_1^\infty$. This shows that the frontal zone does not provide any shielding to the crack tip.

Conversely, we consider a fully developed zone behind the tip that has experienced unloading and path independent J does not apply. In this case at the tip, the energy balance integral is $(1-\nu^2)(K_J^I)^2/E$. However, far from the tip it becomes

$$\left[(1-\nu^2)(K_1^I)^2/E\right]-\left[2\int_0^h u(y)\,dy\right], \tag{7}$$

where $u(y)$ is the residual energy in the wake. We are then left with the calculation of the energy density. This can be evaluated by considering the stress strain relationship as shown in the figure 9a, which takes place during the transformation of an elemental

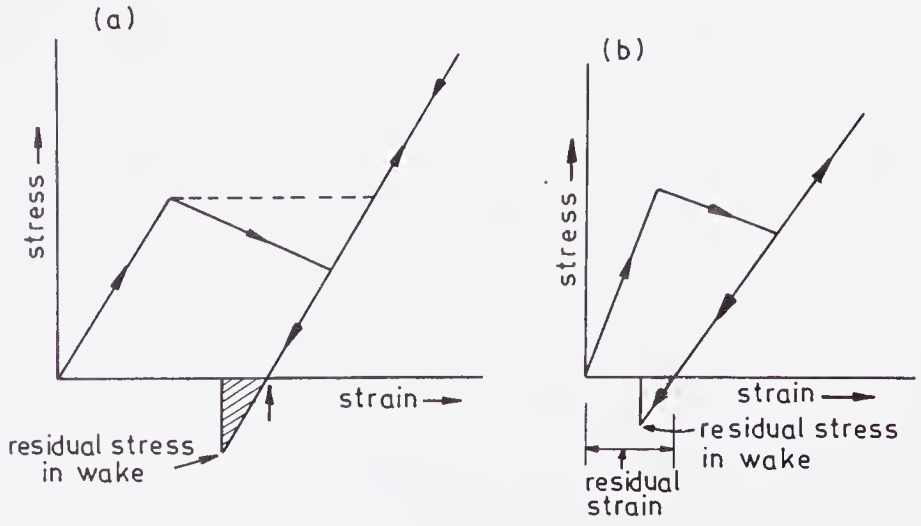

Figure 9. (**a**) Stress–strain behaviour of transformation toughened material; (**b**) stress strain curve of mierocraek toughened material.

volume as the crack runs through it. Note that each element in the wake is subjected to a residual compression during the transformation. The residual energy density can be evaluated as

$$u(y)=\sigma_c \varepsilon^T V_f+[\bar{B}(\varepsilon^T V_f)^2]/(1-\bar{B}/B)+[E(\varepsilon^T V_f)^2]/[9(1-\nu)]. \tag{8}$$

B is the bulk modulus and $\bar{B}$ is the slope of the transforming material. V_f is the fraction of transformable tetragonal particles. It is however inherent in the calculation that all the possible transformable particles have transformed during the propagation of the crack.

4.2 *Microcrack toughening*

The idcas of crack shielding can also be used in explaining microcrack toughening (Faber 1984). However, there are some differences as compared to the previous case. First, since the microcracks are present in the body, thc elastic modulus of the microcracked body is slightly smaller than that of the original material. The stress strain curve, therefore, has the configuration shown in figure 9b. It is assumed hcre that all the potential sites are cracked.

Under such conditions, we apply the principle of path independence around the frontal zone of the microcracked solid. The local stress intensity factor becomes

$$k_l^2=K_\infty^2(\bar{E}/E)\,[(1-\bar{\nu}^2)/(1-\nu^2)]. \tag{9}$$

However, since the material is damaged now, $K_l=k_c(1-f_s)$ where f_s is the saturation density of microcracks. O'Connell & Budianisky (1974) have shown

$$\bar{E}/E=1-[16(1-\bar{\nu}^2)(1-3\bar{\nu})f_s]/[45(2-\bar{\nu})]. \tag{10}$$

From the above equations,

$$k_\infty^c=k_l(1-f_s)\left\{1-[16(1-\bar{\nu}^2)(1-3\bar{\nu})f_s]/[45(2-\bar{\nu})]\right\}. \tag{11}$$

Similar analysis can also be carried out in thc wake zone. The energy balance gives an expression for increase in toughness. Proceeding the same way and after simplification, the increase in toughness can be written as

$$\cdot 4f_s+25f_s h^{\frac{1}{2}} E\varepsilon^{mc}/K_c. \tag{12}$$

This expression implies that for moderate microcrack density, crack shielding is not active and is independent of process zone size. However substantial toughening evolves from dilatation. Specifically, for a zone of 10 μm and a dilatation strain of 0·02 (for ZrO_2), we have $\varepsilon^{mc} h^{\frac{1}{2}} E/k_c=6$. Toughening levels of this magnitude have been measurcd in ZTA.

4.3 *Crack deflection toughening*

This is another toughening mechanism that may take place in zirconia-based materials (Faber & Evans 1983). This mechanism, though less important than the previous two, can be important in some cases. Cracks are usually deflected by the tough second phase or residual stress fields around the second phase particles.

Because of the deflection phenomenon, usually mixed mode propagation of the crack takes place, which in turn reduces the stress intensity.

The modelling of crack deflection is carried out assuming two basic configurations – tilt and twist – (figures 10a & b). These are very similar to tilting and twisting defects of grain boundaries. We will now choose a simple case to show how deflection toughening takes place.

To simplify the situation we choose only the tilt configuration. The angle of tilt θ is about 0. If mode I loading is applied at 0, the modified intensities can be obtained by transforming from Cartesian to polar coordinates as given by Lawn & Wilshaw (1975). Thus we have

$$\left.\begin{aligned}\sigma_{y'y'} &= \sigma_{\theta\theta}{}^{\mathrm{I}} = [K_{\mathrm{I}}/(2\pi r)^{\frac{1}{2}}]\cos^3(\theta/2)\\ \sigma_{x'y'} &= \sigma_{r\theta}{}^{\mathrm{I}} = [K_{\mathrm{I}}/(2\pi r)^{\frac{1}{2}}]\sin(\theta/2)\cos^2(\theta/2)\end{aligned}\right\},$$
$$\sigma_{x'z'} = 0. \tag{13}$$

The transformed stress intensity factors can be written as

$$K'_{\mathrm{I}}(\theta) = K_{\mathrm{I}}\cos^3(\theta/2) \text{ and } K'_{\mathrm{II}}(\theta) = K_{\mathrm{I}}\sin(\theta/2)\cos^2(\theta/2).$$

Therefore, the effective stress intensity becomes

$$K_{\mathrm{eff}} = K\cos\theta/2. \tag{14}$$

The angle θ is actually an averaged angle through many deflections. The simplified picture can be further expanded by considering the twist configuration and a mixture of tilt and twist configurations. Further, aspect ratios of the different particles can also be examined to check the influence of the aspect ratio on the toughening. We emphasize here that there is not much evidence of occurrence of deflection toughening in ZrO_2 bearing ceramics. Increase in toughness of ZnO, containing monoclinic ZrO_2, is attributed to deflection toughening. The increase in toughness with increase in volume fraction of second phase particles shows trends expected in deflection toughening (Ruf & Evans 1983).

Another example of deflection toughening is increase in toughness of PSZ at high temperature where tetragonal precipitates are stable and $t \rightarrow m$ transformation does not take place (Swain & Hannink 1984).

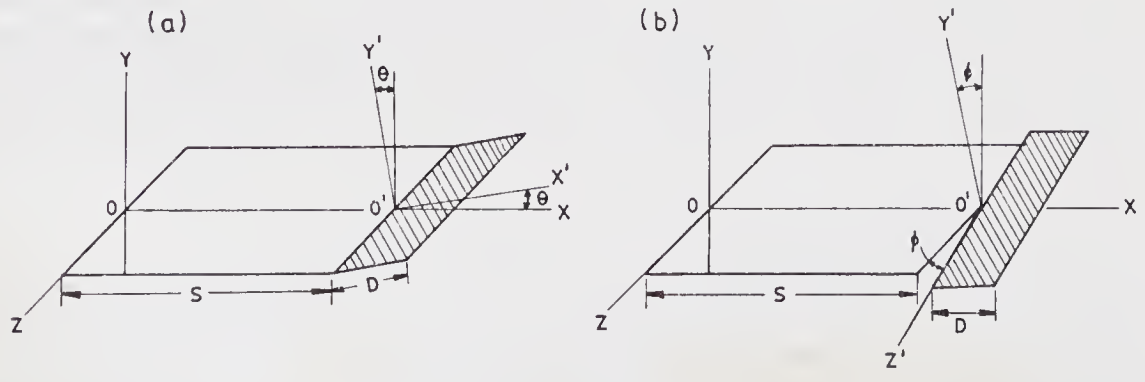

Figure 10. (a) Tilt, and (b) twist configurations.

4.4 *Discussion on mechanisms*

Having discussed the various mechanisms in detail it is worthwhile to compare them with one another. We consider phase transformation and microcraking first. We recall, in the case of transformation toughening, that increase in toughness is equal to $E\varepsilon^T V_f h^{\frac{1}{2}}$. In the case of microcrack toughening, the increment is given by $E\varepsilon^{mc} f_s h^{\frac{1}{2}}$. Recapitulating the results of phase transformation toughening and microcrack toughening, it is obvious that microcracking is the major toughening mechanism when the zone size is small. However, at larger zone sizes transformation toughening should prevail. The next question is whether these processes are additive. The answer to this question can be illustrated by figure 11. Curve 1 shows the behaviour of the transformation toughened material. Curve 2 shows the behaviour when phase transformation and microcracking take place together. This means that the residual stress is lessened and there is decrease in toughness. Hence these two processes reduce toughness by operating simultaneously. However, crack deflection can still occur along with them thereby giving rise to moderate increase in toughness. Also note here that transformation toughening and microcrack toughening processes are temperature-dependent whereas the deflection process is not. Hence it is always better to utilize the deflection toughening process wherever possible.

The other point is that the above models show toughness determinations depending on the choice of geometry. This is due to the nonlinear behaviour of the material at the crack tip. The notched beam (NB) technique gives lower values than those obtained from the double cantilever beam (DCB) technique. This can be explained in terms of the toughening in frontal zone and wake zone, respectively. In notched beams, cracks propagate from a blunt notch. That is why a frontal zone develops in front of the crack. Hence, the measured increase in toughness is negligible. On the other hand, in the DCB technique, the crack propagates further leaving a wake zone behind. Hence considerable toughness increase can be measured here.

4.5 *R-curve behaviour*

We have already shown that nonlinearity in the stress–strain relationship of toughened material causes a crack-shielding effect at the crack tip. Also, it is known that the shielding effect is not constant during the growth of the crack. Initially, the increase in shielding (or increase in toughness) starts from a small value. As the crack grows, shielding increases as the frontal zone becomes a fully developed wake zone.

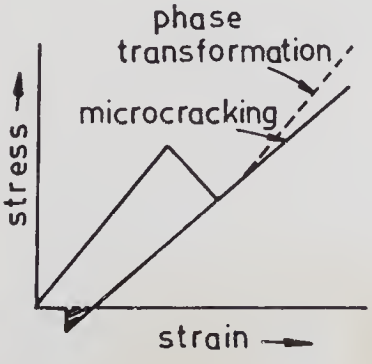

Figure 11. Stress–strain behaviour (hypothetical) of phase transformation toughened and phase transformation + microcrack toughened material.

In other words, the fracture toughness goes on increasing as the crack grows. In fracture mechanics terminology, this is called *R*-curve behaviour. Swain and coworkers (Swain 1983; Swain & Rose 1984, pp. 473–494; Rose & Swain (1986); Burns & Swain 1986) have experimentally obtained *R*-curve behaviour in many of the commercially available ceramic materials. However, we have now begun to realize the far-reaching implications of this property in engineering applications.

Figure 12 schematically represents a system showing *R*-curve behaviour. The stress intensity factor is plotted against the crack length. For the initial crack length C, the stress intensity factor is low. As the crack grows, its resistance to growth increases. The condition of failure requires the comparison of K_R to the applied stress intensity. Failure conditions are reached where $K_R(C)$ and $K_a(C)$ curves become tangential to each other. C^* is the critical flaw size and K_R^* is the critical stress intensity factor. Therefore, if a pre-existing flaw is less than C^*, it can grow stably, and the material will not fail. The strength in this region is controlled by the *R*-curve. However, if the flaw is greater than C^*, the material will fail in the usual brittle manner. The other important feature of these materials is that K_R^* is not a material property but depends on the geometry used for the experimentation. This point was noted earlier by saying that notched beam and double cantilever beam specimens will lead to different fracture toughness values.

Because of the *R*-curve behaviour in ZrO_2-based ceramics, we cannot get a material with both high toughness and strength. In other words, the peak in strength and that of toughness do not match. Swain (1985) demonstrated this aspect in a number of toughened materials. He plotted strength along the Y axis and toughness along the X axis. In all the cases that he examined, the strength increased with the increase in toughness values and then decreased. If the flaw sizes are calculated on both sides of the peak there is a wide difference in their sizes which leads to the fact that the Griffith theory is not valid in at least part of the data considered. Swain argued that the left hand side of the optimum point is still controlled by the Griffith theory whereas the right hand is controlled by *R*-curve behaviour. The optimum point has been interpreted by Swain as the stress required for $t \rightarrow m$ transformation.

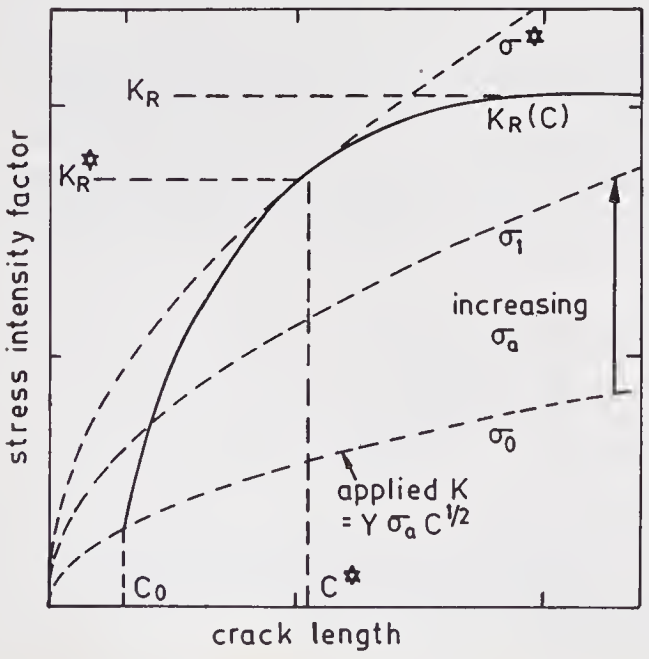

Figure 12. Toughness vs. strength plot of ZrO_2 material showing *R*-curve behaviour.

Further experiments by Swain & Rose (1986) divided the materials into two categories, (1) high strength and low toughness ones, and (2) low strength and high toughness ones. While both of them show *R*-curve behaviour it is the $t \rightarrow m$ transformation that is more important in the first case and the *R*-curve behaviour in the second case. S Bhaduri & N E Prasad (unpublished) have expanded this concept further by showing that similar behaviour is also observed in microcracked materials such as ZTA. They have interpreted the optimum point as the criticality point of the *R*-curve. This discussion shows that this kind of strength toughness relationship is fairly common to any ceramic material showing *R*-curve behaviour.

We now discuss the implications of *R*-curve behaviour. It is known that in these materials a flaw can grow stably to the critical flaw size provided it is less than the critical flaw size. Under such circumstances, the statistics of flaw population has no effect on the strength of the material. The strength of the material is not probabilistic but deterministic. Indeed, the Weibull modulus is ≈ 20 for PSZ as reported by Hannink *et al* (1984) and Lamon *et al* (1986). However in the light of the above discussion, application of the Weibull statistics is invalid in the present case. This has a far-reaching effect on the designing aspects with these materials. This concept should revolutionize the manufacturing technology. Currently it is thought that, for reliable components, one has to start with very fine powder, sinter it well and subject it to hot isostatic pressing (HIP) treatment for removing small pores. But in the materials being considered here all such specialized processing is really not necessary. However, what is important is proper heat treatment which leads to *R*-curve behaviour.

Materials showing *R*-curve behaviour have a great deal of resistance to thermal shock. This has been experimentally shown by Hannink & Garvie (1982), Swain (1983) in PSZ. During the thermal shock condition, the thermal stresses generated tend to propagate the flaws, thereby reducing the strength. However, in the present materials, propagation of flaws do not alter the strength. Hence, these materials are more resistant to thermal shock. Therefore, materials on the right hand side of the optimum point in the strength–toughness curve have fantastic engineering applications. We emphasize here that this behaviour is due to the non-linearity of the stress-strain relationship. One can really say that toughened zirconia materials are no longer brittle.

4.6 *Subcritical crack growth*

Subcritical (slow) crack growth behaviour in ceramics is a phenomenon which leads to failure of the bodies at stress levels much lower than the critical stress of fracture. Study of subcritical crack growth is, therefore, important in predicting the life time of a structure. The crack velocity and the applied stress intensity factor are given by a power law relationship

$$V = A(K_I)^N, \tag{15}$$

where V is the slow crack growth velocity and K_I is the applied stress intensity factor, N is the subcritical crack growth susceptibility coefficient.

Since phase transformation increases K_{IC} it is pertinent to ask whether it affects K_I values that are in the subcritical range. Li & Pabst (1980) carried out experiments to seek an answer to this question. Subcritical crack growth experiments were performed with two different materials e.g. the as-received materials and in annealed

condition where no tetragonal phase was present. The data showed considerable scatter in the experimental curves. Similar experiments with ZTA materials were conducted by Becher (1983). Further, Becher (1986) obtained subcritical crack growth data with high strength PSZ materials recently. All of the data as mentioned above showed that phase transformation affects the mechanical properties in the subcritical region as well. Recently, Bhaduri (1986) has modelled the subcritical crack growth behaviour in PSZ and ZTA in terms of crack deflection mechanisms. This postulate, that crack deflection can explain the experimentally observed data, was motivated by the microstructures of the crack path presented by Becher. The formulation of the model is basically a continuation of the crack deflection model of Faber & Evans (1983) and predicts how lifetimes of the structures could change due to these effects.

4.7 *Tribological properties*

There are relatively few studies on tribological properties of zirconia and related materials. Scott (1985) performed some experiments with commercial grades of PSZ at very low speeds using a reciprocating slider on a flat sample. At room temperature clean unlubricated zirconia on zirconia has coefficients of friction between 0·2 and 0·3. This value is slightly less than the zirconia on metal case. The presence of water increased the coefficient of friction and long chain fatty acids reduced it. With increase in temperature, the coefficient of friction goes up till 500°C and then drops. The rate of wear with PSZ on PSZ is in the range $10^{7} - 10^{8}$ mm^3/mN and is similar to alumina and better than sialon. Presence of water increases the wear rate of zirconia. The effect of temperature on wear rate is complicated. At room temperature and above 300°C the wear rate is less. However, in the vicinity of 200°C anomalously high wear rates occur. This has been ascribed to tetragonal to monoclinic transformation around that temperature. Monoclinic phase has much lower hardness and hence the above hypothesis seems to explain the experimental data.

5. Concluding remarks

The discussions, presented above, bring out a clear picture of the interrelationship between the microstructures and the toughening processes. Based on this unified picture one can specify that a particular microstructure is required in order to achieve certain properties. Once the microstructure is agreed upon, one can finalize the raw material and the approximate sintering process, for example, whether to start off with a coarse powder and heat-treat it carefully or to begin with fine powders and sinter them. In between there is a step involving green-shaping. These are uniaxial die pressing, cold isostatic pressing, injection moulding, slip casting etc. Plenty of literature is available on these processes excepting perhaps injection moulding. Hence we have excluded these topics from the review.

We have discussed the different properties that commercial materials have. For example, subeutectoid aged PSZ does not have as high strength as that of optimally aged PSZ. However, the subeutectoid aged material shows more R-curve behaviour as compared to the other materials and therefore is resistant to thermal shock. These materials are used where improved thermal shock resistance is the most important criterion for the choice of the material. Wire drawing is such an application.

Finally, development of these materials is taking place very fast as the science of these materials is advancing at a rapid pace. So every now and then better materials are replacing older ones for a given application. At the same time, many newer applications can be envisaged for such improved materials.

The author thanks Dr P Rama Rao, for his keen interest and encouragement in the development of zirconia-related materials. Thanks are also due to his colleagues – D Banerjee, J Subrahmanyam, Y Mahajan, J A Sekhar, R Mohan Rao, N Eswara Prasad, K Muraleedharan and A Chakraborti for their respective inputs – both intellectual and physical.

List of symbols

a_m, b_m	lattice parameters of monoclinic lattice;
a_t, b_t	lattice parameters of tetragonal lattice;
c	critical flow size;
$E_1, E_2, \bar{E}$	elastic modulii of the frontal zone, matrix and microcracked material, respectively;
ΔF_0	change in total free energy;
$\Delta F_{\text{chem}}, \Delta F_{\text{dil}}, \Delta F_{\text{shr}}$	change in free energy/volume due to chemical, dilatational and shear energies, respectively;
f	saturation density of microcrack;
h	process zone dimension;
J	'J' integral of Rice (1968);
$K, K_\infty, K_{\text{local}}$	stress intensity factors at a given point, at infinity and near the crack tip, respectively;
ΔK	change in stress intensity factor;
$K_{\text{I}}^l, K_{\text{I}}^\infty$	mode I stress intensity factors in the vicinity of the crack tip and away from it;
$K_\infty^c, K_T^c, \Delta K^c$	critical fracture toughness at the tip, near crack tip, and difference between the two, respectively;
$K_R(c), K_a(c)$	stress intensity factors due to R curve and applied stress intensity factor, respectively;
M_s	martensite start temperature;
r, r_c	radius and critical radius of martensite particles, respectively;
$\Delta S_{\text{chem}}, \Delta S_{\text{tw}}, \Delta S_{\text{pm}}$	change in free energy/area due to chemical, twinning and second phases, respectively;
T, T_b	given temperature and critical temperature, respectively;
V	volume of the martensite;
V_f	volume fraction of second phase;
ε^T	transformation strain;
$\varepsilon_{11}^T, \varepsilon_{22}^T, \varepsilon_{33}^T$	transformation strains along three principal directions;
ε^{mc}	strain for microcracking;
σ_c	critical stress of transformation;
$\nu, \bar{\nu}$	Poisson's ratio of original material and microcracked material, respectively;
θ	angle of tilt.

References

Becher P F 1983 *J. Am. Ceram. Soc.* 66: 485–488
Becher P F 1986 *J. Mater. Sci.* 21: 297–300
Bhaduri S B 1986 *Trans. Indian Ceram. Soc.* 45: 109–113
Brooks H 1962 *Metal interfaces* (Cleveland: The American Society of Metals).
Budianisky B, Hutchinson J W, Lambropoulos J C 1983 *Int. J. Solids Struct.* 19: 337–355
Burke S, Garvie R C 1977 *J. Mater. Sci.* 12: 1487–1490
Burns S J, Swain M V 1986 *J. Am. Ceram. Soc.* 69: 226–230
Claussen N 1976 *J. Am. Ceram. Soc.* 59: 49–51
Claussen N, Steeb J, Pabst R F 1977 *Bull. Am. Ceram. Soc.* 56: 559–562
Delamarre C 1976 *Rev. Hautes Temp. Refract* 9: 209–230
Evans A G 1984 *Advances in ceramics* (eds) N Claussen, M Ruhle, A H Heuer (Columbus, Ohio: Am. Ceram. Soc.) 12: 193–212
Evans A G, Cannon R M 1986 *Acta Met.* 34: 761–800
Faber K T 1984 *Advances in ceramics* (eds) N Claussen, M Ruhle, A H Heuer (Columbus, Ohio: Am. Ceram. Soc.) 12: 293–305
Faber K T, Evans A G 1983 *Acta Met.* 31: 565–576
Farmer S C, Schoenline L H, Heuer A H 1983 *J. Am. Ceram. Soc.* 66: C107–109
Farmer S C, Schoenline L H, Heuer A H 1984 *Advances in ceramics* (eds) N Claussen, M Ruhle, A H Heuer (Columbus, Ohio: Am. Ceram. Soc.) 12: 152–163
Garvie R C, Hannink R H J, Pascoe R T 1975 *Nature (London)* 258: 703–704
Garvie R C, Swain M V 1985 *J. Mater. Sci.* 20: 1193–1200
Green D J 1982 *J. Am. Ceram. Soc.* 65: 610–614
Gupta T K, Bechtold J H, Kuznicki R C, Cadoff L H, Rossing B R 1977 *J. Mater. Sci.* 2421–2426
Gupta T K 1978 *Fracture mechanics of ceramics* (eds) R C Bradt, D P H Hasselman, F F Lange (New York: Plenum) 4: 877–890
Hannink R H J 1978 *J. Mater. Sci.* 13: 2487–2496
Hannink R H J 1983 *J. Mater. Sci.* 18: 33–62
Hannink R H J, Garvie R C 1982 *J. Mater. Sci.* 17: 2637–2643
Hannink R H J, Johnston K A, Pascoe R J, Garvie R C 1981 *Advances in ceramics* (eds) A H Heuer, L W Hobbs (Columbus, Ohio: Am. Ceram. Soc.) 3: 116–136
Hannink R H J, Marmach M, Murray M J, Swain M V 1984 *Proc. Austceram.* (Kensington: Aust. Ceram. Soc.)
Heuer A H, Claussen N, Kriven W M, Ruhle M 1982 *J. Am. Ceram. Soc.* 65: 642–649
Heuer A H, Ruhle M 1985 *Acta Met* 33: 2101–2112
Heuer A H, Schoenline L H, Farmer S C 1983 *Science of ceramics* (ed.) P Vincenzini (St Vincent: Assoc. Eur. Ceram.) 12: 259–266
Khachutoriyan A G 1983 *Theory of structural transformation in solids* (New York: Wiley) chap. 7, 8, 11
Kraus-Lanteri S P, Mitchell T E, Heuer A H 1986 *J. Am. Ceram. Soc.* 69: 256–258
Lambropoulos J C 1986 *J. Am. Ceram. Soc.* 69: 218–222
Lamon J, Thorel A, Broussaud 1986 *J. Mater. Soc.* 21: 2277–2282
Lange F F 1982 *J. Mater. Sci.* 17: 225–235
Lange F F 1986 *J. Am. Ceram. Soc.* 69: 240–242
Lange F F, Green D J 1981 *Advances in ceramics* (eds) A H Heuer, L W Hobbs (Columbus, Ohio: Am. Ceram. Soc.) 3: 217–222
Lanteri V, Mitchell T E, Heuer A H 1986 *J. Am. Ceram. Soc.* 69: 564–569
Lawn B R, Wilshaw T R 1975 *Fracture mechanics of brittle* solids (Cambridge: University Press)
Li L S, Pabst R F 1980 *J. Mater. Sci.* 15: 2861–2866
Masaki T, Sayo K 1986 in *Zirconia 3* (Tokyo: Jpn. Ceram. Soc.) paper no. 3 P17
O'Connell R J, Budianisky B 1974 *J. Geophys. Res.* 79: 5412–5426
Pascual C, Duran P 1983 *J. Am. Ceram. Soc.* 66: 23–27
Rice J R 1968a *J. Appl. Mech.* 35: 379–386
Rice J R 1968b *Treatise on fracture* (ed.) H Liebowitz (New York: Academic Press)
Rose L R F, Swain M V 1986 *J. Am. Ceram. Soc.* 69: 203–207
Ruf H, Evans A G 1983 *J. Am. Ceram. Soc.* 66: 328–332
Ruhle M, Claussen N, Heuer A H 1984a *Advances in ceramics* (eds) N Claussen, M Ruhle, A H Heuer (Columbus, Ohio: Am. Ceram. Soc.) 12: 352–370

Ruhle M, Claussen M, Heuer A H 1986 *J. Am. Ceram. Soc.* 69: 195–197

Ruhle M, Heuer A H 1984 *Advances in ceramics* (eds) N Claussen, M Ruhle, A H Heuer (Columbus, Ohio: Am. Ceram. Soc.) 12: 14–32

Ruhle M, Kraus B, Streeker A, Waidelich D 1984b *Advances in ceramics* (eds) N Claussen, M Ruhle, A H Heuer (Columbus, Ohio: Am. Ceram. Soc.) 12: 256–274

Scott H G 1975 *J. Mater. Sci.* 10: 1527–1535

Scott H G 1985 paper presented at Int. Conf. on Wear of Materials, Vancouver, Canada

Srivastava K K, Patil R N, Chaudhury C B, Gokhale K V G K, Subbarao E C 1975 *Trans. J. Br. Ceram. Soc.* 73: 85–91

Subbarao E C 1981 *Advances in ceramics* (eds) A H Heuer, L W Hobbs (Columbus, Ohio: Am. Ceram. Soc.) 3: 1–24

Subbarao E C, Maiti H S, Srivastava K K 1974 *Phys. Status Solidi* A21: 9–40

Swain M V 1983 *Fracture mechanics of ceramics* (eds) R C Bradt, A G Evans, D P H Hasselman, F F Lange (New York: Plenum) 6: 355–370

Swain M V 1985 *Acta Met.* 33: 2083–2088

Swain M V, Hannink R H J 1984 *Advances in ceramics* (eds) N Claussen, M Ruhle, A H Heuer (Columbus, Ohio: Am. Ceram. Soc.) 12: 225–239

Swain M V, Rose L R F 1984 *Advances in fracture research* (eds) S R Valluri, D M R Taplin, P Rama Rao, J F Knott, R Dubey (London: Pergamon)

Swain M V, Rose L R F 1986 *J. Am. Ceram. Soc.* 69: 511–518

Advanced ceramic tool materials for machining

RANGA KOMANDURI*

Division of Design, Manufacturing, and Computer-Integrated Engineering, National Science Foundation, Washington, DC 20550, USA

*On research sabbatical from General Electric Co. Corporate Research and Development, Schenectady, NY 12309, USA

Abstract. Cutting tools made of advanced ceramics have the potential for high-speed finish machining as well as for high-removal-rate machining of difficult-to-machine materials. The raw materials used in these ceramics are abundant, inexpensive, and free from strategic materials. In spite of this, solid or monolithic ceramic tools are currently used only to a limited extent partly due to certain limitations of these materials and partly due to the inadequacy of the machine tools used. The advances in ceramic materials and processing technology, the need to use materials that are increasingly more difficult to machine, increasing competition, and the rapidly rising manufacturing costs, have opened new vistas for ceramics in machining applications. The development of ceramic tool materials can be broadly categorized into three types: monolithic forms, thin coatings, and whisker-reinforced composites. Such a classification provides a totally new perspective on ceramic tool materials and broadens their scope considerably, and is justified on the basis that it is the ceramic addition that makes the tool material more effective. A brief overview of these materials is presented in this paper.

Keywords. Ceramic tools; coatings; high-speed machining; SiAlON; SiC whisker-reinforced alumina; cubic boron nitride; SiC whisker-reinforced silicon nitride.

1. Introduction

Ceramics are the newest upcoming class of tool materials with potential for a wide range of high-speed finishing operations as well as for high-removal-rate machining of difficult-to-machine materials. Advances in the ceramic tool materials are partially a spin-off of the high temperature structural ceramics technology developed in the 1970's for automotive gas turbine and other high temperature structural applications. Of the advanced ceramics, namely, alumina, partially stabilized zirconia (PSZ), silicon carbide, and silicon nitride, PSZ in bulk form is not used as a cutting tool in machining because of its limited hardness (Knoop hardness ~ 1500 kg/mm^2) and neither is silicon carbide for its brittleness as well as its reactivity with ferrous work materials. However, all these materials as well as others are used in various forms for cutting tool applications as will be elaborated in this paper. Other ceramic

tool materials include the super-abrasives, namely, the single crystal and polycrystalline diamond and the polycrystalline cubic boron nitride (CBN).

The development of ceramic tool materials for machining applications can be classified into the following three broad categories:

- monolithic forms;
- thin coatings;
- whisker-reinforced composites.

Hot pressed alumina and alumina-TiC, SiAlON, Si_3N_4, polycrystalline diamond or cubic boron nitride (CBN), and CBN-TiC come under the first category. Thin coatings (2–10 μm) of Al_2O_3, TiC, and TiN, singly or in combination, on substrates of cemented carbide, high-speed steel or ceramic fall under the second category. Silicon carbide whisker-reinforced-alumina and -silicon nitride belong to the third category.

2. Factors to be considered in the choice of ceramic tool materials

The following factors have to be considered for the appropriateness of a ceramic tool material for machining (Komanduri 1986a):

(i) Which cutting processes can employ ceramic tools to advantage or, alternatively, which processes are unsuitable for ceramic tools?
(ii) Which work materials can or cannot be machined by ceramics?
(iii) What are the machine tool limitations with regard to the use of ceramic tools?
(iv) What are the strengths and weaknesses of ceramic tools? How can some of the drawbacks be overcome?

These questions will be addressed in the following sections. Successful implementation of the solutions can lead to wider use of ceramic cutting tools.

2.1 *Machining process limitations*

Figure 1 is a pie chart showing the percentage cost distribution in the United States of various machining operations (*Machinability data handbook* 1980, pp. 21–23). In grinding, polishing, and cut-off operations, ceramics (alumina, silicon carbide, diamond, and CBN abrasives) are invariably used. Of the other operations, drilling is generally not amenable to the use of ceramic tools because of small-diameter holes and consequent lower cutting speeds at which ceramics are not efficient. Of the other operations, turning ($\sim$22%) and milling ($\sim$13%), together account for a substantial portion ($\sim$1/3) of the cutting processes. The strength and fracture toughness limitations of current ceramics somewhat restrict their application to milling, although some recently introduced ceramics are being applied successfully in milling of selected work materials. Rapid advances in ceramic tool technology by way of toughened ceramics should, however, enable wider application of ceramics to turning operations.

2.2 *Work material limitations*

Not all materials can be machined presently with ceramics. Ceramic tools can be

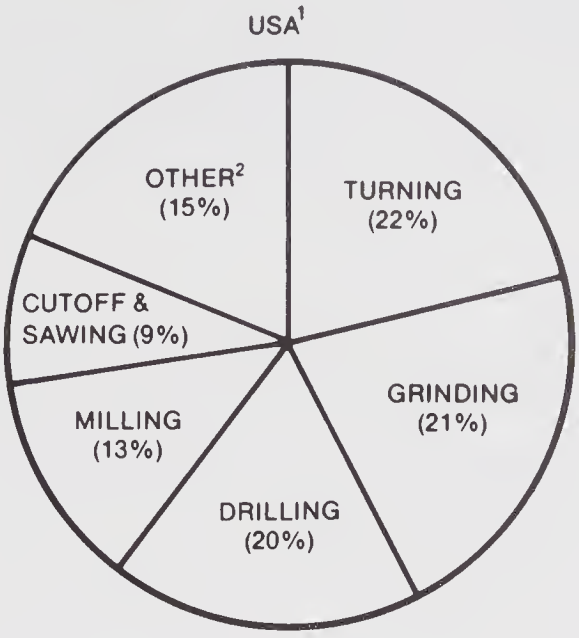

Figure 1. Pie chart showing approximate percentage cost distribution of various machining processes used in the United States.

used successfully to machine most steels, cast iron, and nickel-base superalloys, even in their hardened condition, as well as many nonferrous alloys and composites. Titanium alloys, aluminum alloys, and some stainless steels cannot be machined with most ceramic tools available today due to chemical interactions between the ceramic tools and these work materials.

In contrast, both high speed steels (HSS) and cemented carbides (e.g., WC base and TiC base) are capable of machining a wide range of work materials. This is because both classes of materials were developed to exhibit a range of hardness and toughness for a variety of applications. They are, therefore, very versatile.

Unless ceramic tools can also be developed to broaden the field of applications, their use will be limited to niche areas. The challenge lies in the ability to develop ceramic tool materials for machining a wide range of work materials, at cutting speeds significantly higher than those currently used. It should, however, be realized that both economics and machinability needs dictate the final choice of tool materials for a given application.

2.3 *Machine tool limitations*

Ceramic tools, being brittle (low strength and fracture toughness), require rigid, high precision machine tools for best performance. This is because even the smallest amplitude of vibration of the machine tool system can lead to chipping and failure of

the tool, thus abruptly terminating its useful life. Further, many of the older machine tools were not designed for ceramic tool applications. As a result, they are inadequate in terms of cutting speed capability, power, precision, and rigidity requirements for this application. A new generation of machine tools with the above requirements are required to take full advantage of ceramic tools.

2.4 *Potential strengths and limitations of ceramic tools*

Ceramic tools have great potential for the following applications:

- High-speed (> 15 m/s or 1000 ft/min) finish-machining of many hard and difficult-to-machine materials;
- High-removal-rate (up to several thousand cm^3/min or several hundred $in.^3$/min) machining of some of the above materials with high-horsepower, high-rigidity machine tools using low to conventional cutting speeds;
- Machining of extremely difficult-to-machine materials such as hardened steels, alloy and white cast irons, and nickel-base superalloys;
- Producing superior finish and accuracy of parts. This potential exists because ceramics have the following characteristics:
  - high room temperature and elevated temperature hardness;
  - high strength in compression;
  - good chemical stability up to high temperatures.

An additional advantage of ceramics is that the raw materials used in their synthesis include the elements Si, Al, O, N, and C, which are abundant in nature, inexpensive, and free from dependence on strategic materials. In spite of these advantages, monolithic or solid ceramic tools are currently used in industry only to a limited extent. This is due partly to certain limitations of current ceramic tools (e.g., fracture toughness, strength, and hardness, chemical stability and reactivity with work materials), and partly to the lack of adequate machine tools (e.g., rigidity, precision and power). Also, there is a lack of training on the use and application of ceramic tools and on their proper industrial implementation. The inadequate strength and inconsistency in performance of some of the earlier ceramics did not help in promoting their use, especially when they were used in conjunction with low-power, low-speed, and less rigid machine tools.

The main limitations of the ceramics as compared to cemented carbides are listed below:

- lower transverse rupture strength (TRS);
- lower edge strength;
- lower fracture toughness;
- greater proneness to chipping, both micro- and macro-, and even gross chipping;
- high processing and finishing costs of the ceramic cutting tools, even though raw materials are relatively inexpensive. If these costs can be reduced by technological advances, then it would result in less expensive ceramic tools;
- lack of amenability to forming complex shapes in some cases;
- lack of consistency of the product and of predictability in performance;
- proneness to notching at the depth-of-cut line and at the point at which the tool edge leaves the finish surface;

- abrupt ending of tool life without prior warning, compared to gradual tool wear at the end of tool life in the case of carbide tools;
- more limited scope for machining of a variety of work materials, or for use in different machining operations;
- competition among ceramic tools and consequent replacement of one for another;
- need for high-power, high-speed, rigid machine tools.

While the cutting tool is a vital element of the machining system, there are other elements that affect the overall performance (Komanduri 1986b, pp. 1003–1112). These elements include:

- work material characteristics (chemical and metallurgical state);
- part characteristics (geometry, accuracy, finish, and surface-integrity requirements);
- machine tool characteristics (adequate rigidity with high horsepower and high-speed capabilities);
- support systems (operator's ability, sensors, controls, method of lubrication, and chip control);
- cutting conditions and tool geometry.

In the case of ceramics, improved (high-speed, high-power, rigid) machine tools and the development of tougher ceramics (together with sensors to monitor the tool condition and give warning of tool failure) are two significant areas of concern for increasing the efficient use of ceramics. Implementation of the former and research on the latter are crucial for extensive application of ceramic tools.

3. Historical background

The use of ceramic tools dates back to the dawn of civilization when man used stone as a tool to aid in achieving his basic needs of food, shelter and protection (Suh 1980). Although ceramic tools were considered for certain machining applications as early as 1905, strength under the conditions of cutting was inadequate and the performance inconsistent (King & Wheildon 1966). In the mid-1950's, ceramic tools were reintroduced for high-speed machining of gray cast iron for the automobile industry, and for slow-speed, high-removal-rate machining of extremely hard (and difficult-to-machine) cast or forged steel rolls in the steel industry. These materials were typically fine grain ($< 5\ \mu$m) alumina-based materials, either almost pure or alloyed with suboxides of titanium or chromium to form solid solutions, and containing small amounts of magnesia as a sintering aid and as a grain growth inhibitor. For example, Goliber (1960) developed an alumina-TiO ceramic made by cold pressing and liquid phase sintering. It is characterized by fine grain size (> 3–$5\ \mu$m) and uniform microstructure. TiO constitutes about 10% of the material. A hardness of 93–94 R_A and a transverse rupture strength (TRS) > 550 MPa (~ 80 ksi) were achieved. However, due to limited strength and inconsistency, the applications of these materials were extremely limited. The main success stories include the high removal-rate machining of chill cast iron rolls on an extremely rigid, high powered (up to 450 kW or 600 hp), high precision Binns Superlathe (figure 2) (Binns 1963) and the selective high-speed, finishing application on carbon steels and cast iron for automotive applications.

Several factors have recently rejuvenated interest in the development and

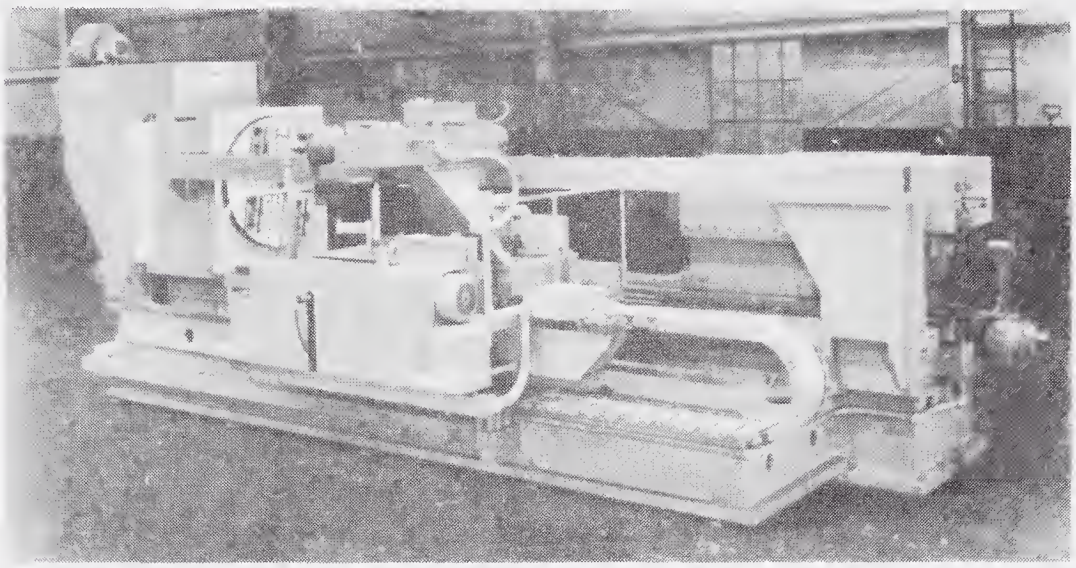

Figure 2. Photograph of an extremely rigid, high precision, high horsepower Binns Superlathe (courtesy, J Binns Sr).

application of ceramic cutting tools. These include the introduction of new ceramic materials, advances in the ceramic-processing technology, new opportunities (higher cutting speeds and removal rates) for reducing manufacturing costs, the need to use materials that are increasingly difficult to machine, advances in machining science and technology, rapidly rising manufacturing costs, and global competition.

4. Advanced ceramic tool materials

Advanced ceramic tool materials can be broadly classified into the following three categories, which will be discussed in the next section: monolithic forms, thin film coatings, and fibre-reinforced composites.

4.1 *Monolithic forms*

Over the past two decades, several monolithic ceramic tool materials were developed. These include:

- hot pressed alumina and alumina-TiC;
- polycrystalline diamond or CBN and CBN-TiC;
- SiAlON;
- silicon nitride.

These materials will be discussed briefly below.

4.1a *Alumina and alumina-TiC ceramics*: Advances in ceramic processing technology, such as hot pressing and hot isostatic pressing (HIP) and the development of pure, fine grain (micron size) ceramic powders led to the introduction of tougher (TRS ~750 MPa or 110 ksi) ceramic tools in the early 1970's. The first tool material introduced was the hot-pressed, fully dense (>99·5%) fine grain

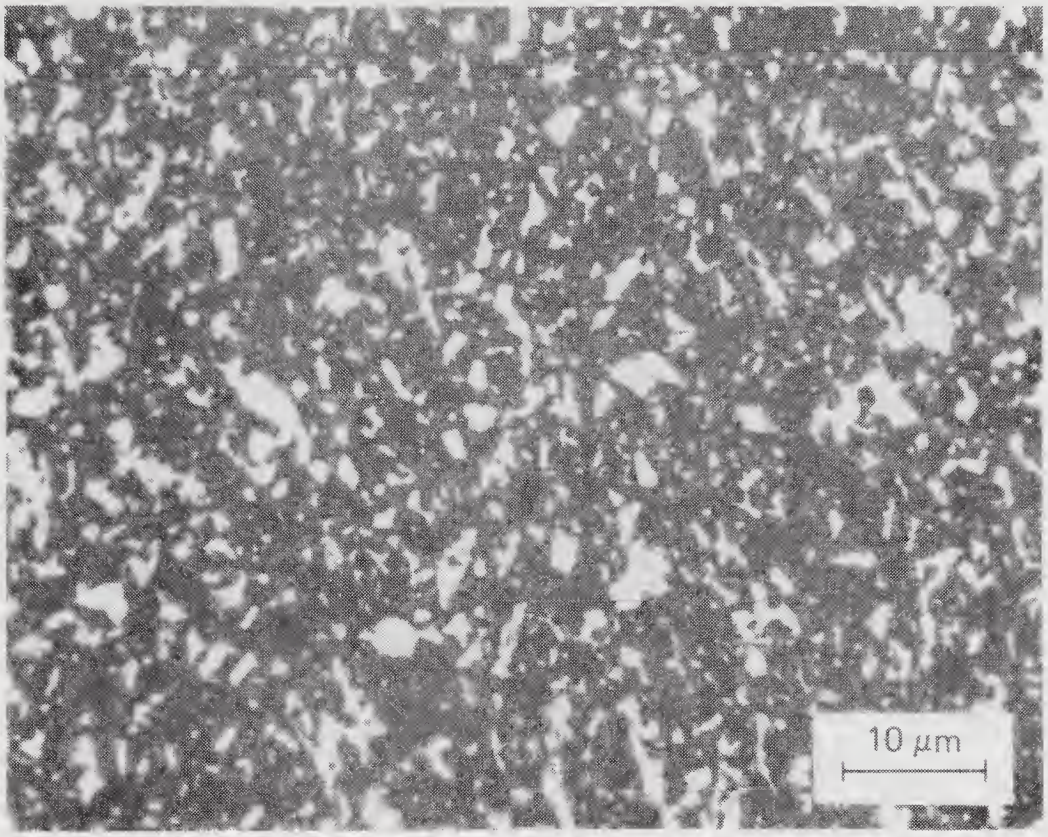

Figure 3. Optical micrograph of a hot-pressed alumina TiC ceramic tool material.

alumina which is significantly tougher (TRS > 685 MPa or 100 ksi) than the alumina-TiO tools (TRS ~ 550 MPa or 80 ksi) (Hatschek 1981). This was soon followed by another hot-pressed ceramic tool material, alumina-TiC (alumina with 30% by volume of TiC and small amounts of yttria as a sintering aid) with enhanced mechanical and thermal shock resistance (figure 3). These two materials are used for high-speed, finish machining of steel and high temperature superalloys.

4.1b *Ultrahard ceramic tools*: The synthesis of diamond, the hardest material (8000 kg/mm^2) known, and the discovery of the cubic form of boron nitride (CBN), the second hardest (~4700 kg/mm^2) material, by a high temperature-high pressure process and in the presence of catalyst-solvents led to the development of ultrahard ceramic tools, namely, polycrystalline diamond and polycrystalline CBN (Wentorf *et al* 1980).

The polycrystalline diamond/CBN tools consist of a thin layer (0·5 to 1·5 mm) of fine grain (1–30 μm) diamond/CBN powder sintered together and metallurgically bonded to a cemented carbide substrate (figure 4). The cemented carbide substrate provides the necessary elastic support for the hard and brittle diamond/CBN layer above it. At the appropriate conditions of pressure (~5 MPa or 50 kbar) and temperature (~1500°C), full densification, extensive diamond-to-diamond bonding, and bonding between diamond/CBN and the tungsten carbide substrate takes place (figure 5). In addition, small amounts of binder phase, predominantly cobalt, present at the grain boundaries, infiltrate throughout the body. Because of this, both diamond and CBN tools can be thermally affected at temperatures above 700°C. The

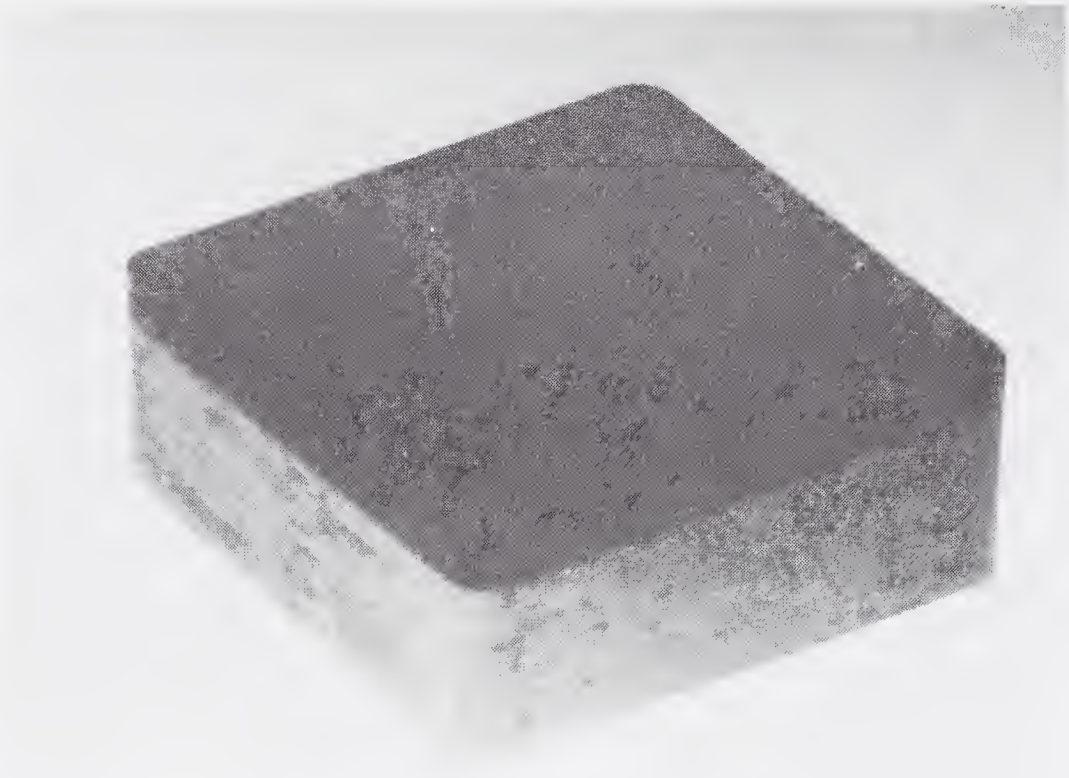

Figure 4. Photo macrograph of a sintered polycrystalline diamond tool showing a dark, thin diamond layer (~0·5 mm) on top metallurgically bonded to a lighter coloured cemented tungsten carbide substrate. Sintered polycrystalline CBN tools also look similar to this tool.

resistance to thermal degradation can, however, be improved significantly by leaching the infiltrant using aqua regia (Bovenkerk & Gigl 1980). The issue of thermal degradation assumes importance when the cutting temperatures are high as in the machining of hardened steels, alloyed cast iron, and nickel-iron base superalloys at higher speeds.

Polycrystalline diamond tools are used for machining of polymer and glass epoxy composites, aluminum-silicon alloys, cast iron, and other nonferrous and nonmetallic materials. Due to high reactivity with ferrous alloys, diamond tools are not recommended for machining carbon steel. Polycrystalline CBN tools, on the other hand, are less reactive with ferrous alloys. They are recommended for machining of hardened (> 55 R_c) steels, alloyed cast iron, and nickel-iron base superalloys.

To increase the toughness and to extend the fields of application of polycrystalline diamond/CBN tools, diamond or CBN is alloyed with TiB_2, TiC, TiN, etc. although this addition is at the expense of hardness (Hara & Yazu 1980, 1982). Polycrystalline CBN tools alloyed with TiC can be used for machining medium hard (~40–50 R_c) steels (Tabuchi *et al* 1978).

Sintered polycrystalline diamond or CBN tools can be fabricated in an assortment of shapes (squares, rounds, triangles, and sectors of a circle of different included angles) and sizes from round blanks. These tools are more expensive (an order of magnitude or more) than the conventional cemented carbides or ceramic tools because of the high cost of both the processing techniques, which involve high-temperature and high-pressure sintering, final shaping etc., and the finishing

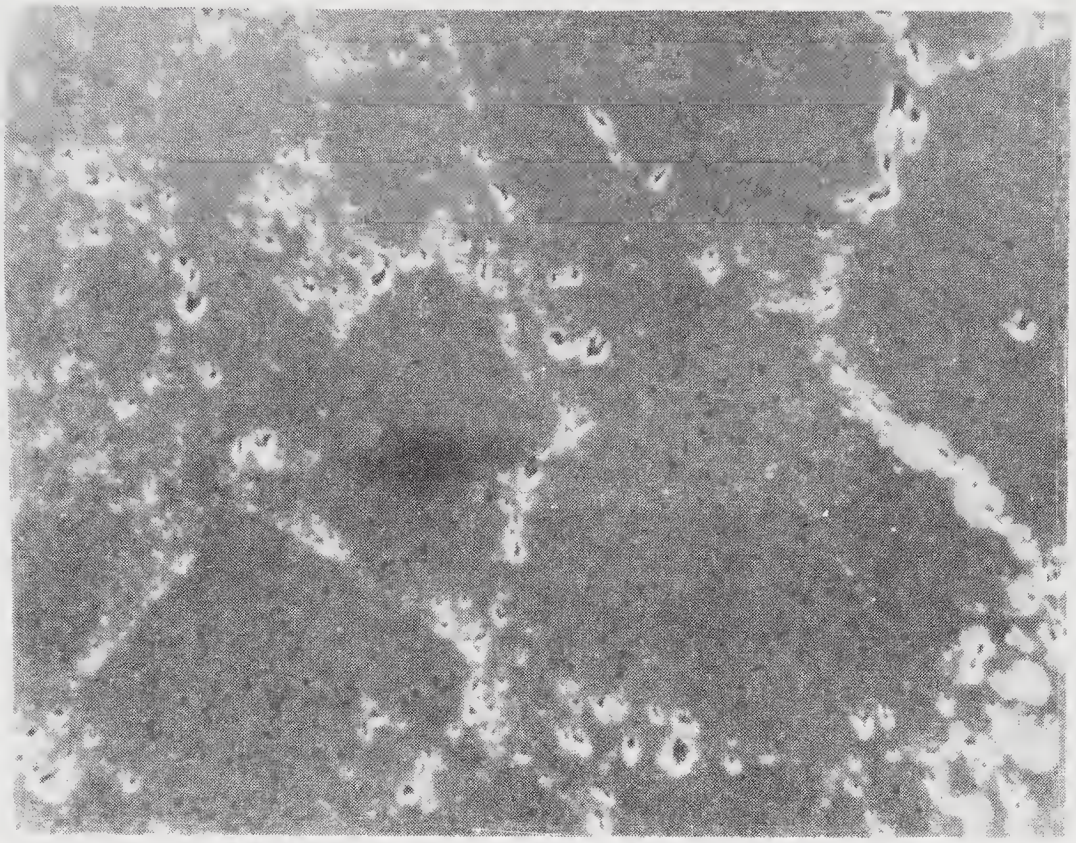

Figure 5. Micrograph of a polished polycrystalline sintered diamond tool showing diamond-to-diamond bonding, and presence of binder phase, impurities and voids at the grain boundaries.

methods. In spite of the higher cost, these tools are used for specific applications because they increase productivity, provide long tool life, and are economical on the basis of overall cost per part.

4.1c *Silicon nitride and SiAlON ceramics*: Yttria (or magnesia) stabilized, dense silicon nitride is one of the more attractive ceramic tool materials recently introduced for the high-speed machining (> 25 m/s or 5000 ft/min) and/or high-removal-rate machining (several thousand cm^3/s or several hundred to a thousand $in.^3/min$) of gray cast iron for automotive and other applications, thus opening new opportunities for ceramic tool materials (Ezia *et al* 1983, 1984; Samanta & Subramanian 1985). New machine tools with high power (up to 375 kW or 500 hp), high r.p.m. (to provide cutting speeds of up to 50 m/s or 10,000 ft/min), high rigidity, and high precision are being built specifically for this purpose. Silicon nitride is, unfortunately, not suitable for machining other ferrous materials or high temperature superalloys, thus limiting its application to the machining of cast iron.

Fully dense silicon nitride has an unique combination of properties, namely, high strength and toughness, moderate hardness, good wear resistance, and low thermal expansion coefficient and consequent excellent thermal shock resistance. It is a covalently bonded material with a small self-diffusivity and hence cannot be easily densified by sintering without a sintering aid. Dense material of β-Si_3N_4 is fabricated by hot pressing α-Si_3N_4 powder with a suitable densification additive (e.g., yttria or MgO) at 30 MPa in a graphite die at 1700–1800°C. The Si_3N_4 powder is generally

covered with a thin layer of silica. The purpose of the additive is to react with this silica and a small amount of Si_3N_4 at the high hot-pressing temperature to form an oxynitride liquid in which α-Si_3N_4 dissolves and from which β-Si_3N_4 is precipitated.

Densification occurs by liquid-phase mechanisms; but, unfortunately, the liquid that is necessary for densification cools to give secondary crystalline or vitreous phases which affect the properties of the hot pressed material at the glass softening temperature (900°C). For example, with the yttria stabilized β-Si_3N_4, yttrium-silicon oxynitride is formed at elevated temperature (> 900°C) with a pronounced change in specific volume that causes microcracking. It is somewhat difficult, if not impossible, to produce dense, pure β-Si_3N_4 without any additive. Yttria- or MgO-stabilized silicon nitride material, produced by hot pressing and subsequently fabricated into cutting tools by dicing and shaping with diamond grinding, is rather expensive. Need, therefore, exists for a less expensive near net-shape processing technique for this material.

Since additives degrade the properties of Si_3N_4 at elevated temperatures, the alternative is to alloy Si_3N_4 with other inorganic compounds. This led to the development of another exciting, tough ceramic tool material, SiAlON, for machining of nickel-iron base superalloys (Oyama & Kamigaito 1971; Jack & Wilson 1972; Bhattacharyya & Jawaid 1981; Jack 1982). This material is yttria-stabilized silicon aluminum oxynitride (SiAlON) which is isostructural with β-Si_3N_4. Because of the similarity of crystal structure, β'-SiAlON has physical and mechanical properties similar to those of silicon nitride; because of its composition, its chemical properties approach those of alumina (Jack 1982).

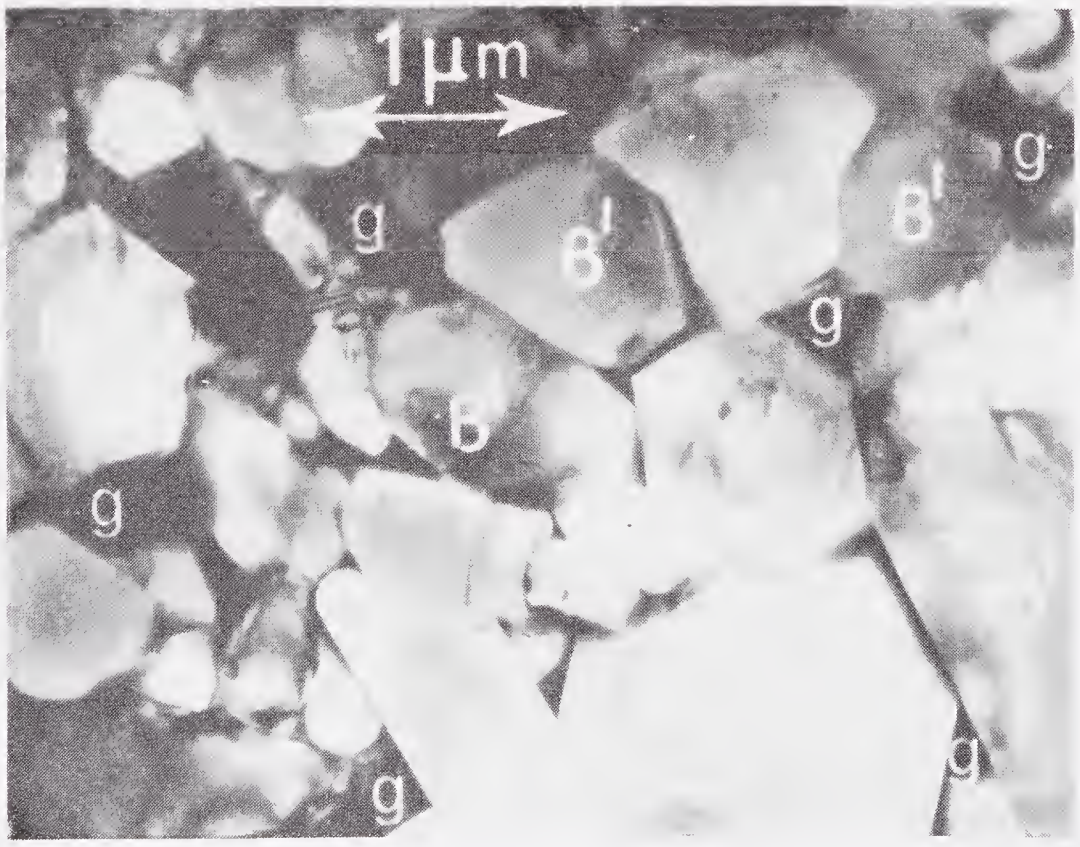

Figure 6. Micrograph of a SiAlON tool showing β'-SiAlON grains and presence of glassy phase at the grain boundaries (courtesy, S K Bhattacharyya).

To produce β'-SiAlON, a mixture of alumina ($\sim$13%), silicon nitride ($\sim$77%), yttria ($\sim$10%), and aluminum nitride is used as the starting material. Since this mixture produces, during sintering, a larger volume of lower viscosity liquid than in the synthesis of yttria-stabilized silicon nitride and its surface silica under similar conditions, β'-SiAlON can be fully densified by pressureless sintering. The powder mix for β'-SiAlON is first ball-milled, then preformed by cold isostatic pressing, and subsequently sintered at a maximum temperature of $\sim$1800°C under isothermal conditions for $\sim$1 h before it is allowed to cool slowly. The microstructure of β'-SiAlON consists of β' grains cemented by a glassy phase (figure 6) (Bhattacharyya *et al* 1984, pp. 245–262).

SiAlON tools were originally developed by Joseph Lucas Industries Ltd. of the UK. It is marketed under licence by Kennametal, Inc. in the US and by Sandvik in Sweden. It is much tougher than alumina-TiC and is used for rough machining of nickel-iron base superalloys. Further developments in microstructure and composition of SiAlON are likely to yield an even tougher material consisting of β' SiAlON and an intergranular phase of yttrium aluminum garnet (YAG) without any intergranular glassy phase. Similarly, addition of TiC is likely to yield a much harder and tougher SiAlON with enhanced mechanical and thermal shock resistance. The introduction of SiAlON tool material was for a time very exciting since it led major tool manufacturers to concentrate on developing a similar material till another tool material, SiC whisker-reinforced alumina, a far tougher material, was introduced.

4.2 *Thin ceramic coatings*

An analysis of the cutting process indicates that the characteristics of the tool at or near the surface should be different from those of the bulk. To be abrasive-resistant, the surface has to be hard; to be chemically wear-resistant, it has to shield the constituents of the tool and the work material from each other under the conditions of cutting, especially at high cutting speeds. The bulk of the material, by contrast, should be tough enough to withstand high-temperature plastic deformation and resist breakage under the conditions of cutting. Since the surface and bulk requirements are markedly different, it is logical to consider engineered tool materials. This was the basis for the development of thin (2–10 μm) ceramic coatings on cemented carbide tools in the late 1960's and on HSS in the late 1970's which are now used very extensively.

In cemented tungsten carbide cutting tools, cobalt metal is used as the binder. The cutting speed capability of these tools is limited primarily by the binder phase. Reducing the volume fraction of the binder phase increases the refractoriness of the tool material, at the expense of strength. It is somewhat difficult to develop a bulk material with the above diverse characteristics. If, however, a binderless ceramic coating were deposited on a tough cemented carbide tool such that the coating is thin enough and strongly bonded metallurgically to the substrate, then such a coating may not affect the strength significantly, resulting in longer tool life and/or higher cutting speed capability. This idea has led to the development of single and multiple, hard, refractory ceramic coatings on cemented carbide tools by the chemical vapour deposition (CVD) technique (Whalen 1971).

To be effective, the coatings should be

- hard;

- refractory;
- chemically stable;
- chemically inert, to shield the constituents of the tool and the work material from interacting chemically under cutting conditions;
- binder-free;
- of fine grain size with no porosity;
- metallurgically bonded to the substrate with a graded interface to match the properties of the coating and the substrate;
- thick enough to prolong tool life, but thin enough to prevent brittleness;
- free from the tendency of the chip to adhere (or seize) to the tool face;
- easy to deposit in bulk quantities;
- inexpensive.

Several hard, refractory, ceramic coatings, including single coatings of TiC, Al_2O_3, TiN etc.; double coatings of Al_2O_3 on TiC, TiN on Al_2O_3 or TiC; and triple coatings of TiN on Al_2O_3 on TiC were developed by the CVD process. To deposit a coating of TiC, the tools are heated to 1000°C, and $TiCl_4$ and methane (CH_4) are reacted in hydrogen at a pressure of $\leqslant$ one atmosphere. The hard reaction product, TiC, deposits on the tool and forms a metallurgical bond with the substrate at high temperature. A coating thickness of 5 μm is found to be optimum from the standpoint of best performance and requires about 8 h of processing time.

Multiple coatings are developed with the following objectives:

- prolong the life of the tool by building up the thickness without encountering the deleterious effects of thick, hard coatings, such as delamination and chipping;
- form a stronger metallurgical bond with a graded interface;
- take advantage of the desirable features of each coating material without causing delamination.

Figure 7 is a micrograph of a representative multiple coating of Al_2O_3 on TiC on a cemented carbide tool. The microprobe traces of Al and Ti show clearly the graded interface between the substrate and TiC as well as between TiC and Al_2O_3. Currently, titanium nitride coating is deposited as the upper layer on most coated tools because it minimizes metal build-up and reduces friction.

At the cutting speeds at which HSS tools (e.g., drills, end mills) operate, metal build-up or periodic seizure between the chip and the tool is the main problem limiting tool life and productivity. To overcome this problem and to reduce friction, a titanium nitride (TiN) ceramic coating has been developed successfully for HSS tools. However, the CVD technique (used for coating cemented carbide tools) cannot be used for this application as the substrate temperature used ($\sim$1000°C) is too high, resulting in alterations of the metallurgical structure of HSS. Hence, only those coatings and processes that require heating below the HSS transformation temperature can be applied to HSS. A coating of titanium nitride by the physical vapour deposition (PVD) technique at low substrate temperature ($\sim$400°C) is increasingly used for HSS tools. The attractive golden colour of the coating is an added aesthetic feature.

To take full advantage of the coating potential, substrate materials are being carefully matched with the coatings or appropriately altered to optimize properties, resulting in significant gains in productivity. Also, for strong bonding between the

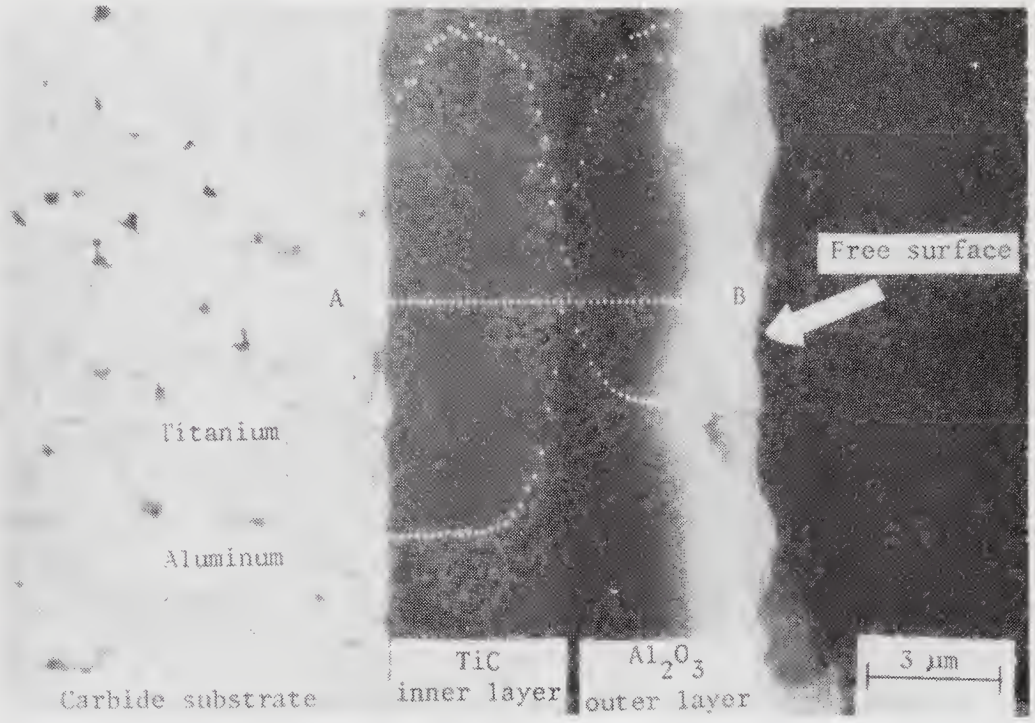

Figure 7. Micrograph of the cross-section of Al_2O_3-TiC coating on a cemented tungsten carbide substrate.

coating and the substrate, there should be good chemical and metallurgical compatibility between them. Since the mode of wear is different on the rake face and on the clearance face, coated-tool technology is advancing in the direction of selective compositions and/or modifications of the substrate in these areas to further prolong tool life and to make the coated tool more versatile for special or general purpose applications. An example in this direction is the recent development of a multilayer-coated (TiC-TiCN-TiN or TiC-Al_2O_3-TiN), cemented carbide tool that has a cobalt-enriched layer (25 μm deep) on the rake face to provide superior edge strength and a cobalt depleted layer in the clearance face for high abrasion resistance and high temperature deformation resistance (figure 8) (Nemeth *et al* 1981, pp. 613–627).

Ceramic coatings are also being developed on ceramic substrates mainly to limit chemical interactions between the tool and the work material. For example, silicon nitride tools are used successfully for high-speed machining of cast iron. However, they react significantly with steels and hence cannot be used for this application as such. To take advantage of the high-temperature deformation resistance of this material and to minimize chemical interactions when machining steels at high-speeds, multiple coatings of TiC-TiN, or Al_2O_3-TiC on silicon nitride, and SiAlON substrates were developed similar to those for cemented carbides (Sarin & Buljan 1983, 1984). Figure 9 is a cross-section of multiple coatings of TiN on TiC on silicon nitride tool material. However, the extent to which such coated ceramic tools will be used as compared to other competing materials for high-speed machining of steels depends upon the need and the economics of machining.

4.3 *Fibre-reinforced composites*

Recently, a fibre-reinforced ceramic composite material possessing improved fracture

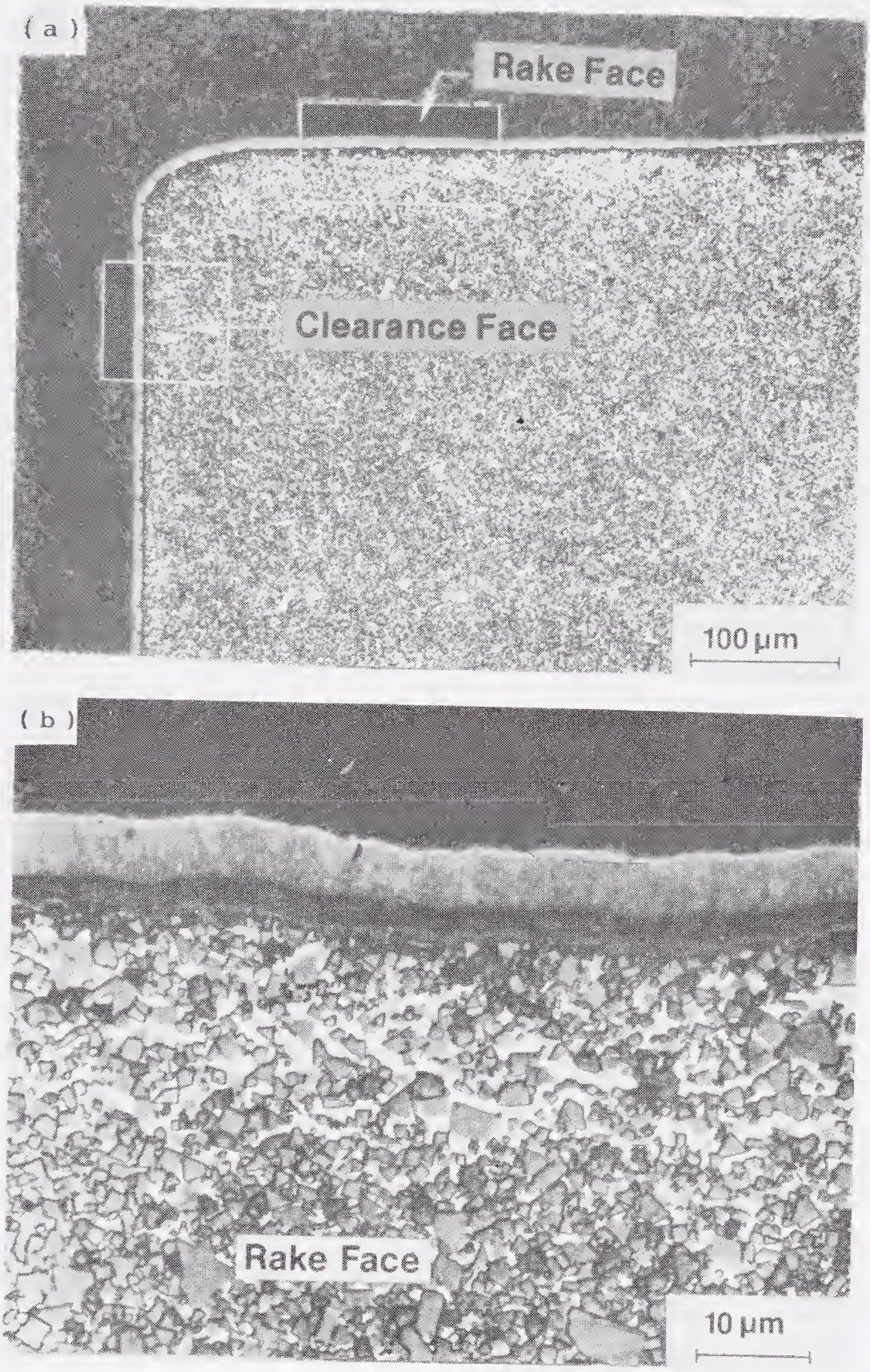

Figure 8. (**a**) and (**b**). (Caption on facing page.)

toughness ($K_{IC} \approx 9$ MN m$^{-3/2}$) has been introduced as a cutting tool for machining of nickel-iron base superalloys used in aircraft engines (Wei 1985; Smith 1986). This

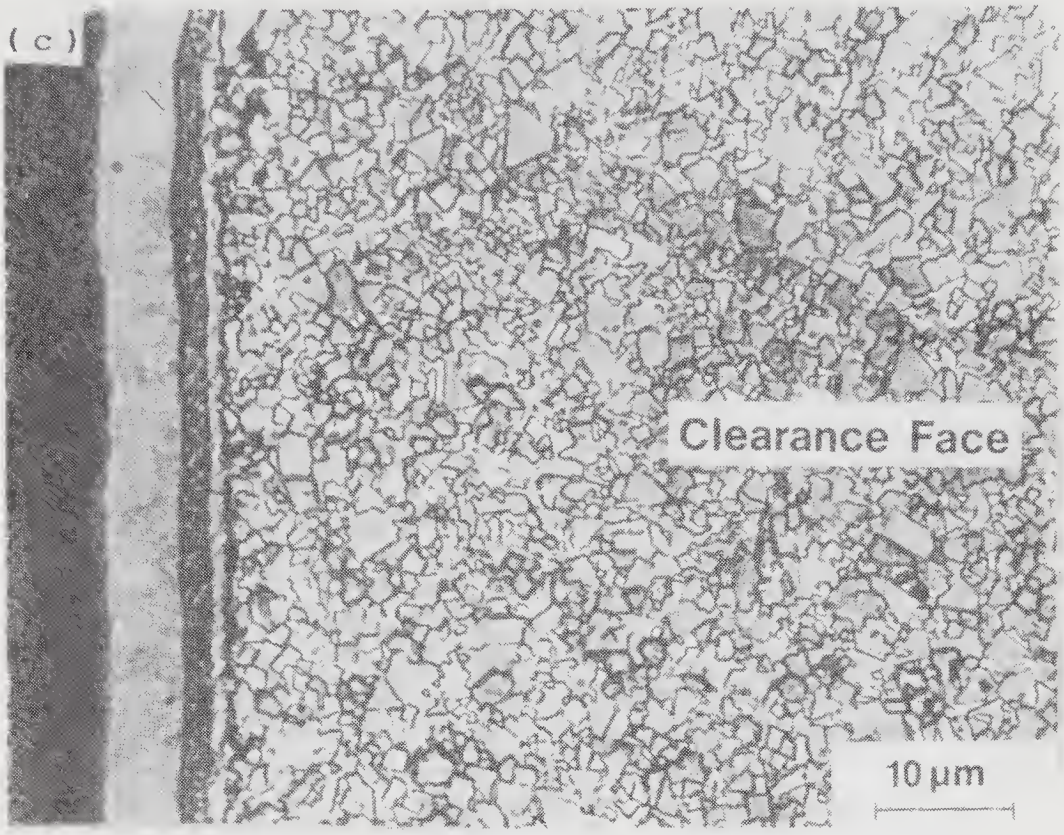

Figure 8. Micrograph of a multicoating of TiN-Ti (C, N)-TiC on an engineered cemented carbide substrate (note the top layer is TiN). (**a**) A low magnification micrograph showing the areas around the rake face and the clearance face of the tool. (**b**) Micrograph at higher magnification of an area around the rake face showing a thin cobalt-enriched straight WC layer near the rake face for increased toughness and edge strength, and (**c**) micrograph at higher magnification of an area around the clearance face showing a thin layer of cobalt-depleted multicarbide near the clearance face for increased wear resistance and high temperature deformation-resistance (courtesy, A T Santanam).

material is silicon carbide (SiC) whisker-reinforced alumina (figure 10). Single-crystal whiskers of SiC possess very high tensile strength (7 GPa). SiC also has higher thermal conductivity and coefficient of thermal expansion than alumina. Consequently, the composite exhibits higher strength and thermal shock resistance.

In the preparation of this composite material, SiC whiskers (0·5 to 1 μm in diameter and 10 to 80 μm long) about 20% volume fraction are mixed homogeneously with micron-sized fine powder of alumina. The mixture is then hot-pressed to over 99% of the theoretical density at a pressure in the range of 28–70 MPa and temperature in the range of 1600–1950°C for pressing times varying from about 0·75 to 2·5 h. The fracture toughness of this material is by far the highest among ceramic cutting tools, nearly twice that of its closest ceramic, namely, Si_3N_4 and SiAlON. Although details of the micromechanisms for improved fracture toughness of this ceramic composite tool material are not clearly established at this time, a plausible mechanism for the toughness is given in the following paragraph based on current knowledge of the behaviour of composite materials in general (Lewis 1986).

As a crack propagates through the ceramic matrix, bonds between the matrix and the whiskers are broken. However, the SiC whiskers, because of their inherently high

Figure 9. Micrograph of the cross-section of Al_2O_3-TiC coating on a silicon nitride-based ceramic tool (courtesy, V Sarin).

strength (7 GPa) remain essentially intact. Consequently, whisker pullout occurs due to the separation of the matrix from the whiskers. Interfacial shear stress resisting the whisker pullout absorbs a substantial amount of this fracture energy and inhibits crack propagation. For improved fracture toughness, a strong metallurgical bond between the fibres and the matrix is not desirable for it causes the whiskers to fail along with the matrix. This is the case with SiC whisker-reinforced alumina composites because the bond between the matrix and the fibres is not particularly strong. The bonding is weak because alumina and SiC are not metallurgically compatible. For best results, the fracture energy of the interface (J_i) is recommended not to exceed a fraction (0·1) of the fracture energy of the matrix (J_O). Although Si_3N_4 is a tough ceramic, its fracture toughness is not sufficiently high for interrupted cutting such as milling of cast iron. So, using the above approach a tougher SiC whisker-reinforced silicon nitride was developed for high-speed milling applications. When whiskers of other refractory materials become available, new tool materials incorporating them may be developed. The SiC whisker-reinforced alumina composite has opened new vistas for tool material development. One can consider this material as a model engineered material and develop other composites for machining different work materials and for different applications. However, to accomplish this it is necessary to thoroughly analyse this material and its performance. For example, why is this tool not suitable for machining ferrous materials, such as steel or cast iron? What is the role of SiC whiskers? Can they be replaced with whiskers of other materials such as TiC, Al_2O_3, ZrO_2, Si_3N_4, and SiAlON? What is the optimum size (diameter and aspect ratio), volume fraction, and geometric distribution of the fibres? Can ceramic coatings be applied to shield the

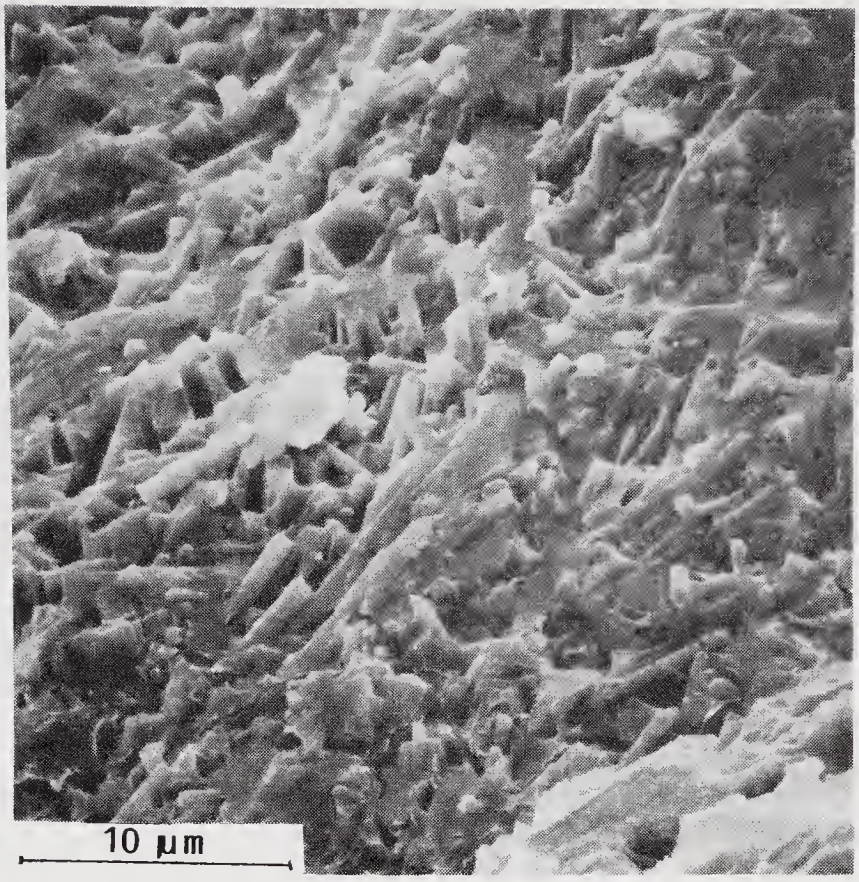

Figure 10. Fractograph of a SiC whisker-reinforced alumina tool.

ingredients of the tool and work material from each other? Can one design a composite ceramic tool material based on the knowledge of the properties of the various ingredients of the tool and work materials as well as the cutting conditions for a given application?

5. Concluding remarks

Significant innovations and technological advances were made in the last three decades in the adaptation of ceramic materials for many cutting tool applications. Thin ceramic coatings, synthesis of diamond and CBN, whisker-reinforced ceramic composites, processing techniques that produce ceramics close to the theoretical density, and toughened ceramics presented in this paper are examples in that direction. Basically many advanced ceramics are hard enough to machine a range of work materials with the possible exception of hard ceramics themselves. To extend the field of applications and to open up new opportunities, ceramic cutting tools have to be developed even further, as future applications are bound to be more challenging than at present. Some of the future directions in the development of ceramic tools include the following:

(1) Ceramics with considerable increase in transverse rupture strength (TRS) and fracture toughness than currently available.
(2) A class of ceramics with a range of hardness, and improved strength and fracture toughness characteristics, similar to HSS and cemented carbide tools.

(3) Ceramics that are relatively inert chemically for machining a range of work materials at higher cutting speeds. For example, the development of a cutting tool material for high-speed machining of titanium alloys. This is not an esoteric problem since titanium is very reactive chemically with most tool materials at elevated temperatures. However, in the event that such a material is developed, it may revolutionize the way we make cutting tools in general.
(4) New ceramic tool materials developed on the basis of fundamental understanding on the nature and performance of current toughened ceramics, whisker-reinforced ceramics etc.
(5) New engineered ceramics with hierarchical structures, nano grain size, amorphous structures and artificially layered structures.

The author wishes to thank the National Science Foundation for the opportunity to prepare this paper. Thanks are also due to Sri Komanduri and Prof. Ephraim M Sparrow for patience, inspiration and advice, and to the General Electric Corporate Research and Development, Schenectady, New York, for permission to publish this work. The author would like to thank Drs A T Santanam, V Sarin and S K Bhattacharyya for providing some of the micrographs presented in this paper.

References

Bhattacharyya S K, Jawaid A 1981 *Int. J. Prod. Res.* 19: 589–594

Bhattacharyya S K, Jawaid A, Wallbank J 1984 *Proc. AMSE High-speed Machining Symposium PED* (eds) R Komanduri, K Subramanian, B F von Turkovich (New York: Am. Soc. Mech. Eng.) vol. 12

Binns J 1963 Cutting performance on rough turning and hogging cuts, ASTME (now SME) paper No. 633, pp. 1–15

Bovenkerk H P, Gigl P D 1980 The temperature resistant abrasive compact and method for making same, US Patent 4, 224, 380

Ezia A, Samanta S K, Subramanian K 1983 Ceramic cutting tool formed from Si_3N_4-Y_2O_3-SiO_2 and method of making, US Patent 4, 401, 617

Ezia A, Samanta S K, Subramanian K 1984 Ceramic cutting tool formed from Si_3N_4-Y_2O_3-SiO_2 and method of making, US Patent 4, 401, 238

Goliber E W 1960 Ceramic and cermet compositions containing TiO, *Proc. 66th Annual Meeting of the American ceramic Society* (Westerville, Ohio: Am. Ceram. Soc.)

Hara A, Yazu S 1980 Method of producing a sintered diamond compact, US Patent 4, 231, 762

Hara A, Yazu S 1982 Sintered compact for a machining tool and a method of producing the compact, US Patent 4, 334, 928

Hatschek R L 1981 *Am. Mach.* 165–176

Jack K H 1982 *Met. Technol. (London)* 9: 297–301

Jack K H, Wilson W I 1972 *Nature. Phys. Sci. (London)* 238: 28–29

King A G, Wheildon W M 1966 *Ceramics in machining processes* (New York: Academic Press)

Komanduri R 1986a *Carbide Tool J.* 18(4): 33–38

Komanduri R 1986b *Encyclopedia of materials science and engineering* (ed.) Michel B Bever (New York: Pergamon Press)

Lewis C F 1986 *Mater. Eng.* July: 31–35

Machinability data handbook 1980 3rd edn (Cincinnati: Metcut Research Association) vol. 2

Nemeth B J, Santhanam A T, Grab G P 1981 *Proc. 10th Plansee Seminar on Trends in Refractory Metals and Special Materials and their Technology* (ed.) H Mortner (Ruettle, Austria: Metallwork Plansee)

Oyama Y, Kamigaito O 1971 *Jpn. J. Appl. Phys.* 10: 1637

Samanta S K, Subramanian K 1985 Hot-pressed SiN as a high performance cutting tool material, Proc. North American Manufacturing Research Conference, University of California, Berkeley, CA

Smith K H 1986 *Carbide Tool J.* 18(5): 8–10

Sarin V K, Buljan S J 1983a Nitride coated silicon nitride cutting tools, US Patent 4, 406, 668

Sarin V K, Buljan S J 1983b Carbo-nitride coated composite modified silicon aluminium oxynitride cutting tools, US Patent 4, 406, 669

Sarin V K, Buljan S J 1983c Nitride coated composite modified silicon aluminium oxynitride cutting tools, US Patent 4, 406, 670

Sarin V K, Buljan S J 1984 Alumina coated silicon nitride cutting tools, US Patent 4, 440, 547

Suh N P 1980 *Wear* 62: 1–20

Tabuchi N, Hara A, Yazu S, Kono Y, Asai K, Tsuji K, Nakaltani S, Uchida T, Mori Y 1978 *Sumitomo Electr. Tech. Rev.* 18: 57

Wei G C 1985 Silicon carbide whisker-reinforced ceramic composites and method for making same, US Patent 4, 543, 345

Wentorf R H Jr, DeVries R C, Bundy F P 1980 *Science* 208: 873–880

Whalen S J 1971 Vapor deposition of titanium carbide, ASTME (now SME) Tech. paper No. 690

Ceramic coating technology

J KARTHIKEYAN[1] and M M MAYURAM[2]

[1]Plasma Physics Division, Bhabha Atomic Research Centre, Bombay 400 085, India

[2]Machine Elements Laboratory, Mechanical Engineering Department, Indian Institute of Technology, Madras 600 036, India

Abstract. Modern technology calls for systems performing satisfactorily under extreme and often adverse operating conditions; hence it has become a technical and economic necessity to protect structural materials from the hostile environment. Thus ceramic coating technology (CCT) has found widespread applications in many diverse industries for the protection of structural materials. Ceramic coatings are used to minimise effects such as high temperature degradation, corrosion, erosion and wear.

Two techniques, viz. thermal spray and chemical vapour deposition, are well-developed and commercially established for preparing coatings of almost all ceramic materials. Each process has its own advantages and disadvantages and the choice of any particular method depends on the application, economics etc.

CCT is both technically and commercially well-established abroad. Commercial equipment suitable for general application in coating shops as well as custom-engineered ones to suit specific requirements are readily available. Raw materials such as powders, wires, rods, gases, chemicals etc. are readily available and are moderately priced. R & D is continuously in progress adding new materials, techniques and applications every year.

In India, the full potential of the technology has not been tapped as yet. A few governmental organisations such as BARC, BHEL, DMRL, HAL, Air India etc., have exploited the application potential of the technology, while the private industry has begun to adopt the technology only recently. Such a situation is due to a variety of reasons including limited awareness of these new techniques amongst our user industries, non-availability of raw materials and equipment indigenously etc.

Keywords. Ceramic; coating; thermal spray; protection; chemical vapour deposition.

1. Introduction

The development of the nation through science and technology is essentially determined by the possibility of creating and of producing, in sufficient quantities, structural materials meeting the requirements of technology. As the frontiers of

science and technology expand into complex and more sophisticated areas, operating systems face more and more severe environments, which they have to withstand.

1.1 *Importance of ceramic coatings*

Any high technology system – nuclear, space, power, missile, aeronautics etc. operates under extreme conditions – like very high and very low temperatures, very high and very low pressures, high rates of gas flow, highly corrosive–erosive fluids and concentrated energy fluxes – which take a severe toll of the materials of construction. Considerable amount of work is being carried out to find new materials which can withstand severe environments. Ceramics, with their excellent properties such as high temperature stability, resistance to corrosion, erosion and wear, chemical inertness etc., have found increasing use in high technology systems. However, it is not always possible to replace structural parts made of metals and alloys with ceramic ones, since ceramics have poor mechanical properties. Moreover in many applications, properties desired at the surface are different from those required at the core of many engineering components. For instance, a shaft requires good toughness at the core, wear resistance at the seal and fatigue resistance on the outer surface.

Ceramic coating technology, the process of preparing or depositing a ceramic layer on a surface, offers the best solution in such situations. Ceramic coatings have found use, not as a substitute for metals and alloys, but in complementing metal characteristics by imparting additional refractoriness, insulation, erosion resistance, oxidation and corrosion resistance, electrical resistance or different optical characteristics. Moreover, coating technology allows the design engineer to select the base material on mechanical and other design considerations and then prepare the surface for meeting requirements simply by making a ceramic coat on it.

1.2 *Applications of ceramic coatings*

Ceramic coating technology is used to prepare coatings for various applications. They can be broadly classified as follows:

a) *Protective coatings* – corrosion, erosion and wear resistant surfaces and high temperature and electrical insulation coatings etc.
b) *Process improvement and control coatings* – thermal barrier coatings on internal combustion engine components, coatings with specific optical characteristics on space vehicles, neutron absorbing coatings on nuclear components etc.
c) *Free standing structures* – fabrication of complex thin-wall components for various applications by the coating process.
d) *Reclamation coatings* – preparation of coatings on worn-out components for reclamation.

2. Ceramic coating processes

Ceramic coatings are required in various industries for different applications and hence the requirements and specifications of the coatings vary with a particular

application. It can be summarised that an ideal ceramic coating should have the following properties:

(i) good mechanical properties over a wide temperature range;
(ii) resistance to thermal and mechanical cycling;
(iii) good dense layers;
(iv) hardness and resistance to wear;
(v) chemical inertness and thus resistance to corrosion and high temperature oxidation;
(vi) resistance to erosion;
(vii) resistance to atomic diffusion and inter-diffusion at high temperatures.

Such an ideal coating material does not exist, and it is often necessary to find a suitable coating such that the combined coating/substrate system can satisfy the operating conditions. The choice of any coating for a given application depends on operating environment, the substrate material, the coating availability and economics.

Fortunately, a large number of ceramic materials are available that can be prepared in the form of coatings by the thermal spray (TS) or the chemical vapour deposition (CVD) process which show satisfactory performance in many applications.

2.1 *Thermal spray process*

The thermal spray process is the most versatile one for preparing ceramic coatings. In this process (Hecht & Gerdeman 1972) any material which melts without decomposing or vapourising can be spray-coated. Moreover there is no limitation on the size and shape of the substrate and, as required in some special applications, the coatings can be prepared *in situ*. Hence this process has found widespread applications in many diverse industries. Though some exotic techniques like pulse arc spray (Rykalin & Kudinov 1976), liquid fuel gun spray (Hecht & Gerdeman 1972) etc. have been tried for spray coating, only two processes, viz. combustion flame spray and plasma spray are commercially used as routine techniques (Chagnon & Fauchais 1984).

2.1a *Principles and techniques*: In the thermal spray process (Zaat 1983) a ceramic coating is created by a solid or powdered ceramic material, which is heated in a flame, atomized and projected, while still in the form of molten particles, by a stream of gas moving at a high velocity onto the relatively cold surface of the article to be coated.

These impacting particles flatten, interlock and overlap one another, so that they are securely bonded together to form a dense coherent coating which is built up to the desired thickness. The adherence of the coating to the surface results primarily from the mechanical fastening of spray particles as they deform to take the shape of the suitably prepared surface being coated.

The basic systems for thermal spray application of ceramic coatings may be classified as follows:

(i) combustion flame-spray using a (a) powder torch, (b) rod or wire torch, or (c) detonation gun;
(ii) plasma spray using a (a) powder torch, (b) rod or wire torch, or (c) plasma transferred arc torch.

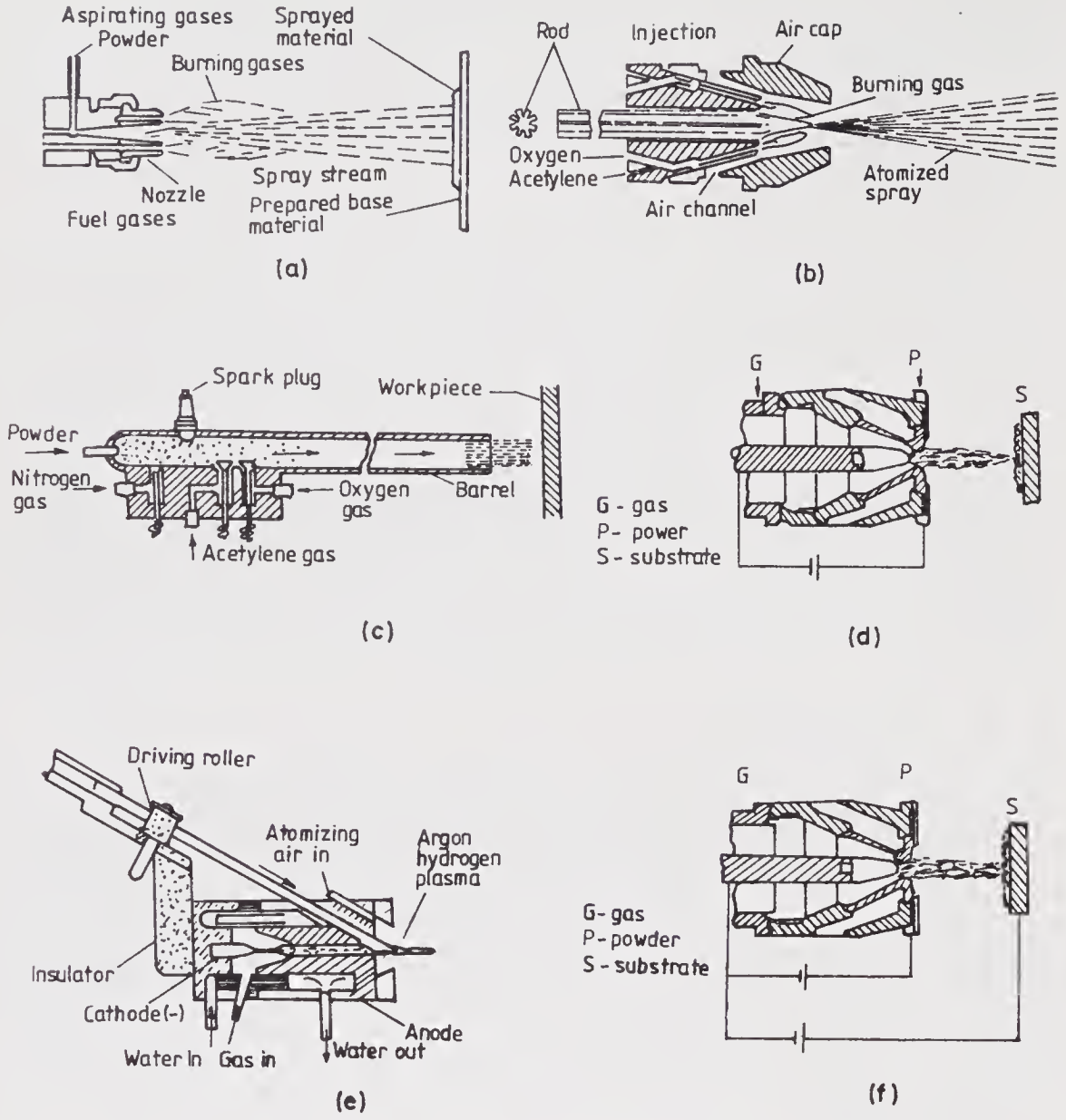

Figure 1. Spray torches used in thermal spray processes; (**a**) combustion-powder, (**b**) combustion-rod or wire, (**c**) detonation-gun, (**d**) plasma-powder, (**e**) plasma-rod or wire, (**f**) plasma-transferred arc.

Figure 1 gives the schematic of different torches used for spraying ceramic materials and these are discussed below.

Combustion flame spray process – In the combustion flame spray process, oxygen and a fuel gas are ignited and the exhaust gas is used as the heat source for melting and for projecting the spray material (figure 2). The fuel gases used in this process are acetylene, hydrogen and propane. The flame temperature achieved by this process is approximately 3000 K. Material to be sprayed is introduced into the hot flame in powder, rod or wire form.

In the flame powder (FP) spray system, ceramic powder is introduced directly into a portion of the oxygen flow, which aspirates it through the centre of the burner

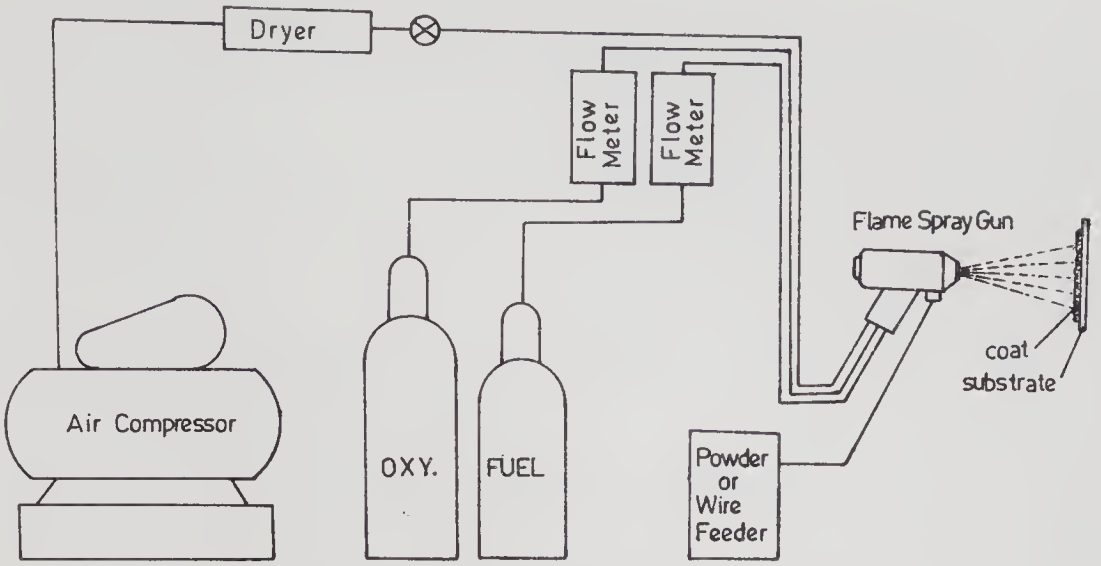

Figure 2. Schematic of combustion flame spray system.

nozzle where it is heated and carried to the substrate with an average velocity between 50 and 150 m/s. Ceramics with melting points less than 3000 K can be sprayed (Hecht & Gerdeman 1972).

In the combustion flame-rod or wire (FR) spray system the rod or wire is fed into the high temperature flame where the end of the rod is melted, the molten material is disintegrated by a rapid flow of compressed gas and the resulting spray is delivered by the high velocity flow of gases to the substrates (Chagnon & Fauchais 1984). Such a system has the advantage that the spray material cannot be propelled with the effluent until it is completely molten as opposed to powder particles which may remain incompletely melted on impact. The spray rate is controlled by the melting rate of the rod, which in turn is a function of the gas enthalpy and melting characteristics of the rod. The viscosity of the liquid phase is also an important factor. The average particle velocity in the rod spray system is 150–200 m/s, which is higher than the velocity of the powder-sprayed particles. The biggest disadvantage of the rod spray process is that not all materials can be fabricated in wire or rod form, and only a few ceramics like Al_2O_3, ZrO_2, CrO_2, $ZrSiO_4$ and $MgAl_2O_4$ can be coated by this process.

In the detonation gun (D-gun) process (Hecht & Gerdeman 1972) a mixture of acetylene, oxygen and powdered coating material is pressure-fed into a chamber and detonated by a spark plug. The detonation wave heats and accelerates the particles onto the substrate. The barrel is detonated approximately four times per second. The detonated gas accelerates the powder to a velocity of about 750 m/s. The detonation-gun process has been used to spray a number of ceramics including Al_2O_3, Cr_2O_3, WC, CrC, NiC etc. Of all thermally sprayed coatings the detonation-gun sprayed ones have the highest density (99%, which is not normally possible by other conventional powder metallurgy techniques) and very high bond strength (40–65 MPa). However, the detonation equipment should be operated in a sound-proof, explosion-proof room because of the high sound levels of about 150 dB and the danger of explosion. Hence the detonation process has not found wide use in industrial applications in spite of the superiority of the properties of the coatings.

Plasma spray process–In the plasma spray process (Fauchais *et al* 1983), a high current arc (300–600 A) is formed between a tungsten-tipped conical cathode and a copper nozzle anode (figure 1d). The plasma gas (usually inert gases like argon, helium, nitrogen and hydrogen) flowing through the arc is heated to an average temperature of approximately 10,000 K and jets out of the nozzle at a high velocity. The coating material, introduced either in the powder form or in wire or rod form into this flame, melts and sprays the coating material onto the substrate with velocities around 200 m/s. Figure 3 gives a schematic of the plasma spray system.

Since the temperature in the plasma flame is an order of magnitude greater than in the combustion flame, all materials with well-defined melting points can be sprayed. In the plasma spray process, the spray efficiency and the coating quality are affected by a large number of variables and table 1 gives a list of important variables. Many of these variables are inter-related, and hence, careful optimization of the spray parameters is of paramount importance for obtaining coatings with the desired properties (Fisher 1972).

Almost all oxides, nitrides, carbides and borides can be coated by use of the plasma spray powder gun, since the plasma temperature is higher than the melting point of any known material (Fauchais *et al* 1983). However, since the dwell time of the powders in the plasma is only a few milliseconds, coatings with inadequate qualities will be obtained if extreme care is not taken while preparing coatings (Hecht & Gerdeman 1972).

Though some systems with rod feed have been introduced, because of the difficulties in preparing ceramic rods, the rod-fed plasma spray system has not been commercially successful.

The plasma transferred arc (PTA) process is more of a weld surfacing technique than a spray process. This process effectively combines the plasma spraying and plasma welding techniques in a semitransferred arc mode (Shull *et al* 1984, pp. 297–301). In this system a pilot arc, the same as in a normal plasma spray process, is used to melt and spray the coating material while a transferred arc is used to form a puddle at the surface where the coating material is welded resulting in a metallurgi-

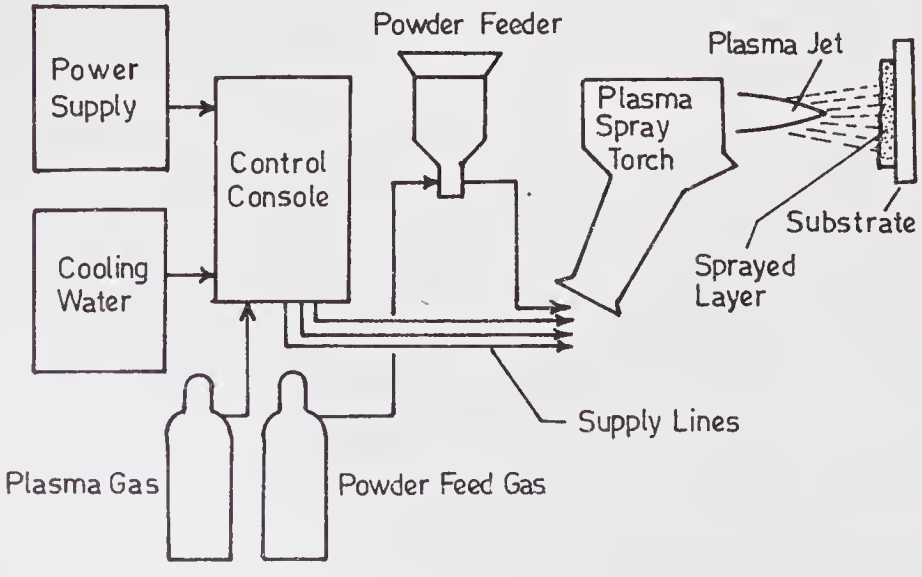

Figure 3. Schematic of the plasma spray system.

Table 1. Plasma spray variables.

Plasma	*Spraying procedure*
Power input	Torch to work distance
Type of arc gas	Traverse rate
Flow of arc gas	Angle of torch to work
Plasma torch geometry	Cover gas
Type of arc	Spray atmosphere
Powder	*Substrate*
Composition	Composition
Physical properties	Surface preparation
Method of manufacture	Surface roughness
Powder size	Temperature
Size distribution	
Powder feed	
Type of feed system	
Rate of powder addition to carrier gas	
Type of carrier gas	
Angle and position of powder entry port	

cally bonded (or welded) coating. This process is used in general for preparing hard surfaces with refractory carbides like TiC, WC, CrC etc. with or without binder materials.

2.1b *Thermal spray coated ceramics*: Though a general statement that materials which do not vaporize or sublime can be sprayed is often made, because of the short dwell time of the particles, some materials which have high specific heat and low thermal conductivity yield poor quality coatings. Moreover, other materials, such as pure carbides of tungsten and boron produce coatings with weak particle-bonding due to the inability of the material to wet itself or because of loss of stoichiometry. Still the widest range of ceramics have been thermal spray coated.

2.1c *Properties of* TS *coatings*: *Microscopic properties*

(i) Structure–In the thermal spray process the powder particles melt in the flame and then solidify as they impinge on the substrate. Hence, the properties of the coatings depend on both the melting and the solidification process. It has been found that unless the melting point of the powder is well-separated, by at least 200 to 300 K, from the decomposition or evaporation temperature the material can not be coated onto a surface.

Heat transfer calculations (Zaat 1980) have shown that:
(a) the heating and melting of the powder particles take place in about 1–10 ms, (b) the entire cooling cycle takes less than 100 μs, (c) the particles are always deposited on already solidified layers, (d) the temperature gradients during cooling reach around 10^5 K/cm. Since the coating is formed by the flattening of the particles on impact (which occurs only when the particle is still in the molten or plastic state), the liquid density (ρ), viscosity (μ) and surface tension (J) of the particles play an important role in determining the properties of the coating (e.g. density, adhesion etc.). The degree of flattening (the ratio of diameter on the flattened disc, D, to the

diameter of the particle, d) is given by

$$D/d = 1{\cdot}29\,(\rho v d/\mu)^{0{\cdot}2}. \tag{1}$$

As can be seen, lower values of viscosity and higher values of ρ and particle impact velocity (v) give higher degrees of flattening, resulting in dense and strong coatings.

(ii) Composition–Compositional changes in the particle may occur during melting in the flame. However, this requires diffusion of hot gas towards the condensed phase and reverse diffusion of gaseous products. This diffusion occurs at a lower rate (10^{-2}–10^{-1} s) compared to the melting time (10^{-4}–10^{-2} s). Hence, stable compounds like oxides are sprayable even in reducing atmospheres while surface reactions may occur during spraying of carbides, nitrides and borides.

Rapid quenching of molten particles result in the formation of metastable high temperature phases in the coatings, like η, γ, δ and θ Al_2O_3 while spraying α Al_2O_3. The formation of various metastable phases depends on the rate of transformation from one metastable phase to another and to the stable phase, which in turn strongly depends on spraying conditions, size and shape of the particles, temperature of the substrate etc.

(iii) Residual stresses–There are two types of residual stresses in coating, viz. the microstresses within the individual particles and the macrostresses in the coating as a whole. The microstresses arise because of the restraint on the thermal contraction of the individual particles when they cool in the solid state as they are bound to the relatively cold underlying layer which is at constant temperature. These stresses depend on the thermal expansion coefficient and the elastic constants of the coating material (as well as the substrate for the first layer of the coating).

The macrostresses arise due to the difference in the thermal expansion coefficients between the coating and the substrate material and the temperature gradient during the formation of the coating. Interfacial stresses increase with increasing coating thickness resulting in the peeling off of the coating when the coating thickness reaches about 0·3 to 0·4 mm. High tensile stresses in the coating result in cracking of the coatings.

(iv) Adhesion–The most important phenomenon responsible for adhesion of the coatings is believed to be mechanical i.e. interlocking of the particles as they deform to take the shape of the underlying surface.

Two factors which result in high physical adhesion of two surfaces on contact are: (a) an intensive and permanent contact, and (b) a decreasing Gibb's free energy of the substrate–particle system. Zaat (1981) has shown that when contact occurs between two surfaces the total decrease in Gibb's free energy is given by

$$\Delta G = \Delta H_s - (T_{\text{cont}}\,\Delta S_s) + \Delta G_{\text{surf}}, \tag{2}$$

where ΔH_s is the change of the enthalpy because of different potential curves for the atom combinations *SS*, *CC* and *SC* (*SS*, *CC* and *SC* are the atom configurations in the substrate, coating and interface, respectively); T_{cont} is the contact temperature; ΔS_s is the increase in the entropy due to surface diffusion and ΔG_{surf} is the decrease in Gibb's free energy due to surface energy.

The first two terms represent the change in Gibb's free energy due to the enthalpy and the entropy of formation of the solid solution of the substrate-coating material system. The formation of solid solution requires the interdiffusion of the two

materials and ordering which take place at the slow rate of 10^{-2}–10^{-1} s whereas the quenching of the solid particles takes place at about 10^{-4} s. Hence the resultant fall in Gibb's free energy due to these two terms is negligible in the case of ceramic coatings.

The last term ΔG_{surf} represents the decrease in Gibb's free energy when two surfaces are brought in intimate contact and can be written as

$$\Delta G_{surf} = \gamma_{SC} - (\gamma_s + \gamma_c), \tag{3}$$

where γ_s is the substrate surface energy; γ_c is the surface energy of the coating particle and γ_{SC} is the interface energy when contact occurs between substrate and coating particle. This term will have a large negative value if (a) the substrate surface is clean and plastically deformed (γ_s is large); (b) the particle is impinged with high velocity and its surface is clean (γ_c is large); (c) the contact is intimate (γ_{sc} is small).

As can be seen, cleaning, degreasing and sand blasting of the substrate prior to spraying not only increase the surface area (for contact to be increased) but also increase the surface energy by cleaning and plastic deformation.

Bulk properties–The bulk properties of thermal-sprayed coatings vary with coating and substrate materials, spray process variables, pre- and post-spray treatments as well as the applications. For instance, the density of the coatings can be changed by changing the spray parameters as can be seen in figure 4. Again the spray process variables are selected to obtain a highly dense tungsten carbide coating if it is to be used as a wear-resistant surface or a highly porous coating if required for an abrasive surface.

An exhaustive list of physical, mechanical, optical, electrical and chemical properties of various thermally sprayed coatings has been given in Hecht &

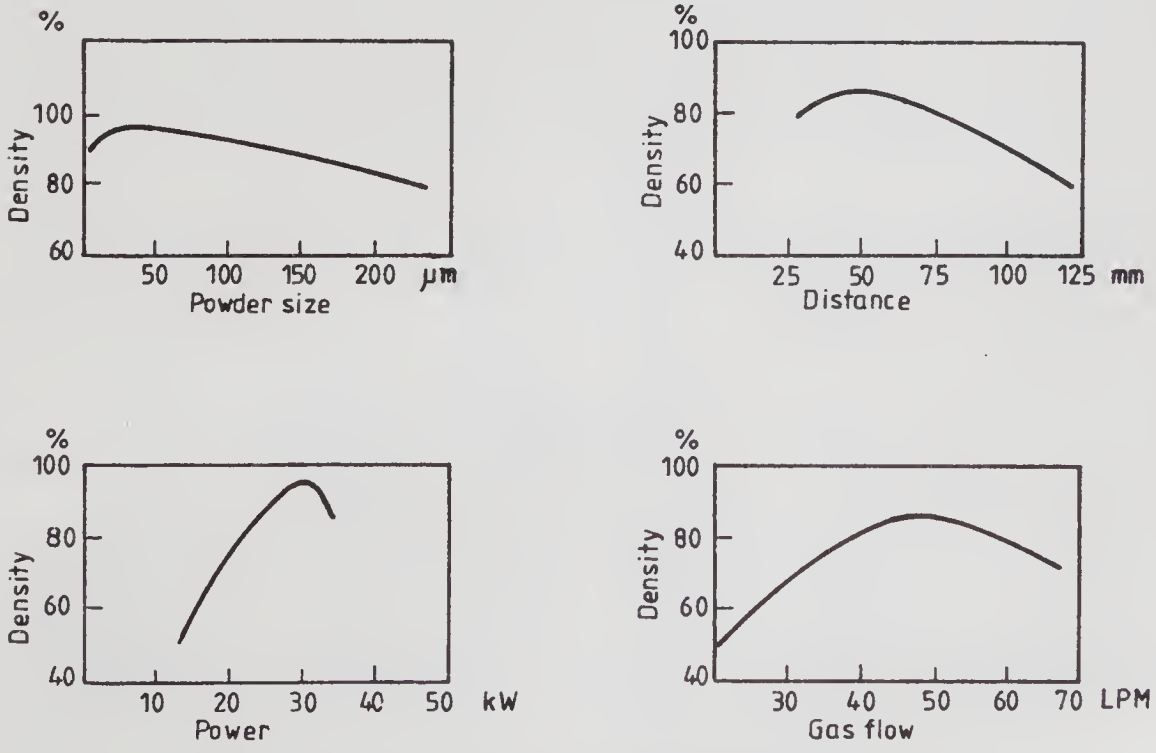

Figure 4. Variation of density of the coating with spray parameters.

Gerdeman (1972), Fisher (1972), and Fauchais *et al* (1983). The following general comments can be made on data published by various authors.

(i) Though it is possible to obtain coatings with less than 1% porosity using the D-gun process, typical thermal-sprayed coatings have about 5–20% porosity.
(ii) The adhesion of the coatings to the substrate is only mechanical though some degree of metallurgical bonding has been reported in some cases. However, in case of PTA coatings, definite metallurgical bonding is obtained. The majority of the literature quotes adhesion values of about 35 MPa. The adhesion of the coating to the substrate strongly depends on (a) the substrate surface preparation before spray, (b) thermal and physical properties of the coating and substrate, (c) thickness of the coating, and (d) post-spray heat-treatment. Usually, under-coat and/or graded coatings have been used successfully to increase adhesion.
(iii) Since the coatings are developed by quenching the molten particles, they can have hardness values even higher than the bulk properties of the material. For the same reason, the as-sprayed coatings have high internal stresses.
(iv) Since the general physical and mechanical properties of the coatings strongly depend on the strength of the bonding between the quenched particles (cohesive strength), it has been found that, in general, the physical and mechanical properties of the coatings are slightly inferior to those of bulk materials.

2.1d *Comparison of thermal spray processes*: Table 2 presents a compilation of selected characteristics of different spray processes (Hecht & Gerdeman 1972). As compared to the combustion flame process, the plasma process is more expensive and requires more complex equipment. However, the combustion process is limited to materials which melt below 3000 K and which are not severely deteriorated by an oxidising atmosphere. Combustion flame-produced coatings tend to have lower densities and bond strengths, and looser tolerances than plasma-sprayed ones.

Coatings prepared by the detonation process have higher density and greater bond strength than those normally found for plasma-sprayed coatings. In addition the tolerances are closer and the surface finish and physical properties are somewhat better. However, the cost of the detonation process is greater and is not effective for

Table 2. Comparison of thermal spray processes.

Process	Plasma	Combustion powder	Combustion rod	D-gun	PTA
Coating material	All	Ceramics with m.p. < 3000 K	Selected oxides	Selected oxides + carbides	Selected carbides
Coating thickness and tolerances (mm)	0·05–2·5 0·025	0·1–5·0 0·075	0·03–0·5 —	0·03–0·04 0·025	2·5–12·5 Variable
Porosity of coating (%)	5–15	10–20	5–10	1–5	—
Base material	All	All	All	All	Weldable material
Base temperature (°C)	50–200	250–320	200–350	200	Locally 1000 to m.p.
Type of bond	Mechanical	Mechanical	Mechanical	Intimate mechanical	Metallurgical
Particle velocity (m/s)	200	50–150	150–200	750	—

large surface area coverage or coverage of complex shapes. Moreover D-gun coatings require post-spray finishing as well.

Rod-sprayed coatings have better properties as compared to powder-sprayed ones. However, the primary limitation is the necessity of obtaining the ceramic materials in the rod form. All rod-sprayed coatings have been obtained only with combustion flames and plasma-based units have not been commercialised though some lab-based units are in operation.

PTA processed coatings have excellent adhesive strength and can take the higher wear load. The disadvantage is that the high local heating may cause distortions and thus nonconductors and low melting point materials are not suitable as substrates. Deposits are usually applied in thick sections to heavy machinery rather than to precision pieces, since welded parts are generally not subsequently ground to close tolerances. The deposits usually contain some blow holes or pores.

2.2 *Chemical vapour deposition process*

This is perhaps the oldest technique for preparing coatings. Well-known case-hardening processes like carburizing, nitriding and carbonitriding are the most popular CVD coating processes. Recently many techniques to produce overlay coatings have been developed and a few have found immediate industrial applications as well.

2.2a *Principles and techniques*: The CVD process is defined as the deposition of a solid material onto a (usually) heated substrate surface as a result of chemical reactions in the gas phase (Yee 1978). These reactions may occur on, at or near the substrate surface. A unified classification of the various CVD processes is given in table 3. These processes are differentiated by the principal mode of supply of chemicals and activation of the chemical reactants. Figure 5 gives schematic diagrams of various CVD processes.

In the *conventional CVD (CCVD)* process stable gaseous chemical reactants are transported to the reaction chamber, activated thermally in the vicinity of the heated substrate and made to react under controlled conditions to form a solid deposit on the substrate surface. A schematic diagram of the system for the deposition of tungsten carbide coatings is shown in figure 6. The most widely used case-hardening

Table 3. Classification of CVD processes.

Principal mode of reactants		Processes
Supply	Activation	
Gaseous	T	Conventional CVD (CCVD)
	P (with or without T)	Plasma activated CVD (PACVD)
	P (with or without T)	Chemical ion plating (CIP)
Liquid	T	Chemical spray deposition (CSD)
Evaporation	T (or EB)	Reactive evaporation (RE)
	P, T (or EB)	Activated reactive evaporation (ARE)
	P, T (or EB)	Reactive ion plating (RIP)
Sputtering	P	Reactive sputtering (RS)

Abbreviations: T-thermal; P-plasma; EB-electron beam

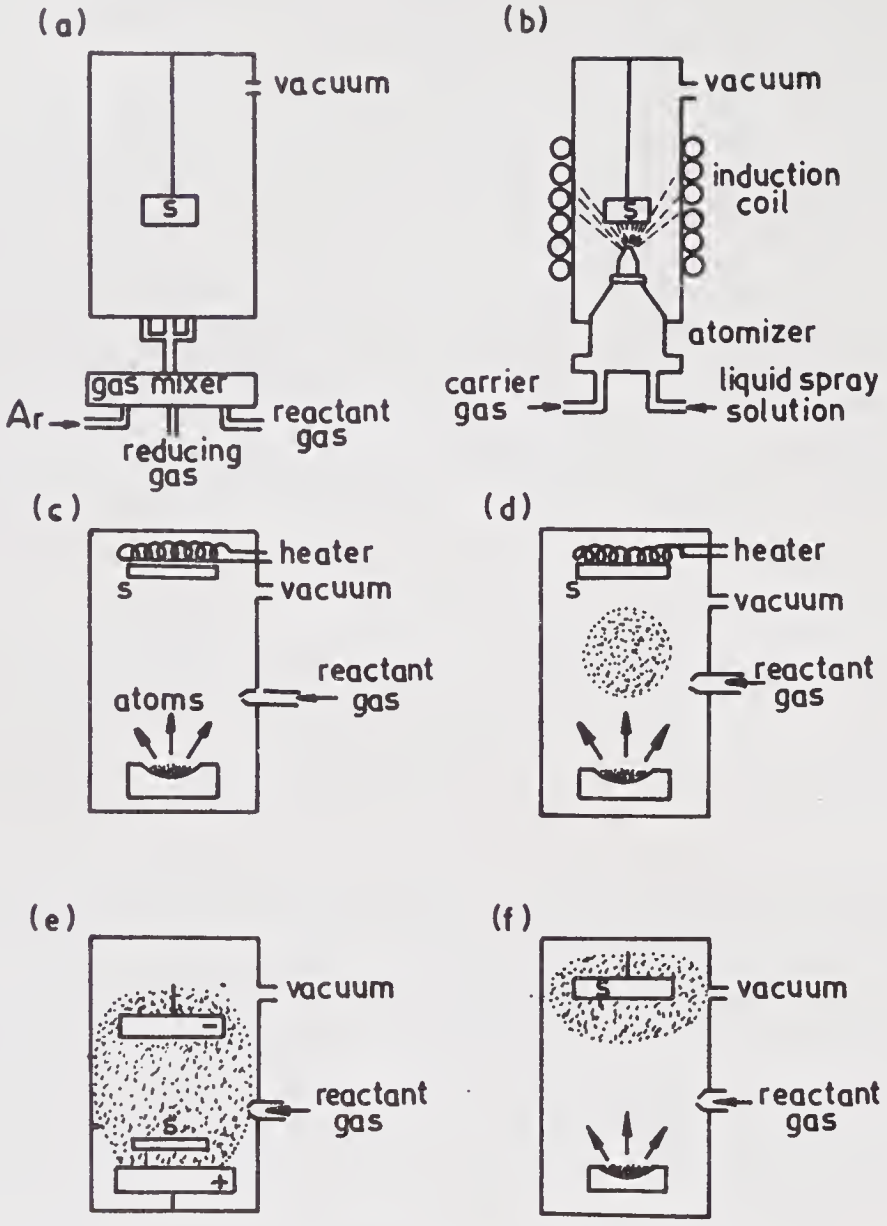

Figure 5. Schematic diagram of various CVD processes; (**a**) CCVD, (**b**) CSD, (**c**) RE, (**d**) ARE, (**e**) RS, (**f**) RIP. (S – substrate; dotted space – plasma zone.)

processes such as carburizing, nitriding, and carbo-nitriding are well-known CCVD processes.

Most chemical reactions in CCVD are endothermic, so that thermal energy must be supplied by the heated substrate and/or by the environment in the neighbourhood of the substrate. There are several established methods of heating the substrate like direct-resistance heating, RF induction heating, thermal radiation heating, photo-radiation heating etc.

The high temperature ($>600^{\circ}C$) of the substrate material places an undesirable limitation on the types of substrate material which may be coated. Though recently many techniques like selection of suitable chemical systems, plasma activation etc. have been incorporated in order to reduce coating temperatures, many of the established CCVD coatings still use high substrate temperature.

In the *chemical spray deposition* (*CSD*) process, instead of gases, reactants enter the

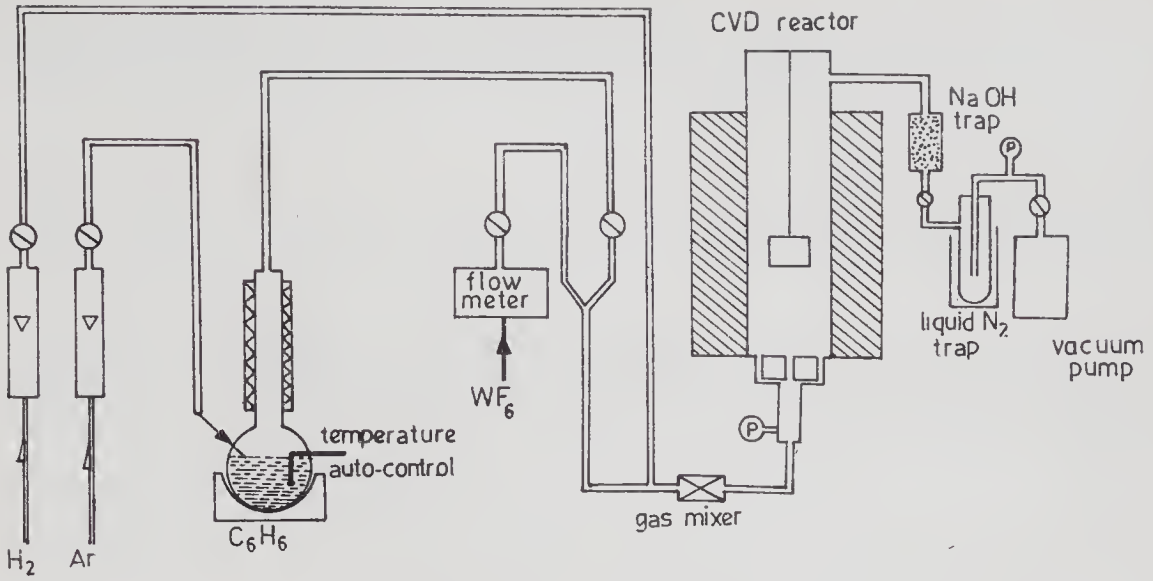

Figure 6. Schematic diagram of CVD system for preparing tungsten carbide coating.

reaction chamber in the form of atomized liquid spray. CSD is very similar to CCVD, the main difference being the mode of transport of the chemicals. Deposition can be carried out in vacuum, at atmospheric pressure and in some cases even in air. CSD is capable of depositing coatings at relatively low temperatures. Its utility depends, however, on the price and availability of suitable liquid reactants.

In the *reactive evaporation* (*RE*) method, the reactive metal atoms are evaporated either by resistance-heating or by an electron-beam gun. These metal atoms react with the reactant gas at the heated substrate surface to form a chemical compound coating. TiO_2, Al_2O_3, Y_2O_3, AlN and TiN are some of the materials that have been coated by the RE process. In principle, this technique is suitable for low temperature depositions.

Activated reactive evaporation (*ARE*) is essentially an RE process with plasma activation. The plasma in the activation zone can be generated by a microwave, RF or electrical discharge. Various metal carbides, nitrides, and oxides have been deposited using the ARE technique at relatively low temperatures.

A more generalised ARE is called the *plasma activated CVD* (*PACVD*) process. Here the starting chemical includes non-reactive as well as reactive species. SiO_2, SiN and BN have been deposited by the PACVD process using stable starting chemicals.

In the *reactive sputtering* (*RS*), the negatively biased coating material (the target) is bombarded by positively charged inert gas ions, usually Ar^+. The chemical species ejected from the target surface react with the reactant gas, which is activated in the plasma zone, to form a coating on the substrate surface. RS, like ARE, is thus very suitable for deposition at low temperatures. Both d.c. and RF sputtering systems have been used to deposit SiN, TiO_2, TiN, SiC etc.

The *reactive ion plating* (*RIP*) is a hybrid CVD process, combining ion plating and ARE. As in the ARE process both vaporized reactive atoms and the reactant gas are activated in a plasma flame. However, in RIP, the reactive atoms are ionised as well in the plasma flame and accelerated towards the surface of the negatively biased substrate, resulting in strongly adherent deposits. Various compound coatings have been made using the RIP process. Typical examples are TiC, ZrC, TiN, ZrN, Cr_3C_2 and SiN.

A variation of RIP is the use of stable, gaseous reactants instead of a combination of evaporated atoms and a reactant gas. This variation, which, in principle, may be considered as a generalisation of RIP, is called *chemical ion plating* (*CIP*).

2.2b *CVD coated ceramics*

Many CVD processes for depositing metals, non-metals and metal carbides, nitrides, oxides, borides and silicides have been reported in the literature (Yee 1978).

2.2c *Properties of CVD coatings*: In any CVD process, there are several inter-related deposition parameters which collectively decide the properties of the deposited coatings. These parameters include not only the temperature, pressure, chemical concentration and velocity of gas flow, but also the geometry of the gas inlet and the substrate, and the configuration of the reactor. Therefore, the desired properties of the coatings can be obtained by careful optimization of the deposition parameters. For instance, the chemical composition of the coatings can even be tailored to meet requirements by suitably varying the concentration of the reactants in the chamber.

In general, CVD coatings have been reported to have very high density and very low porosity, and thus are highly resistant to corrosion, erosion and wear. The microhardness values of various CVD coatings have been presented in figure 7 (Yee 1978).

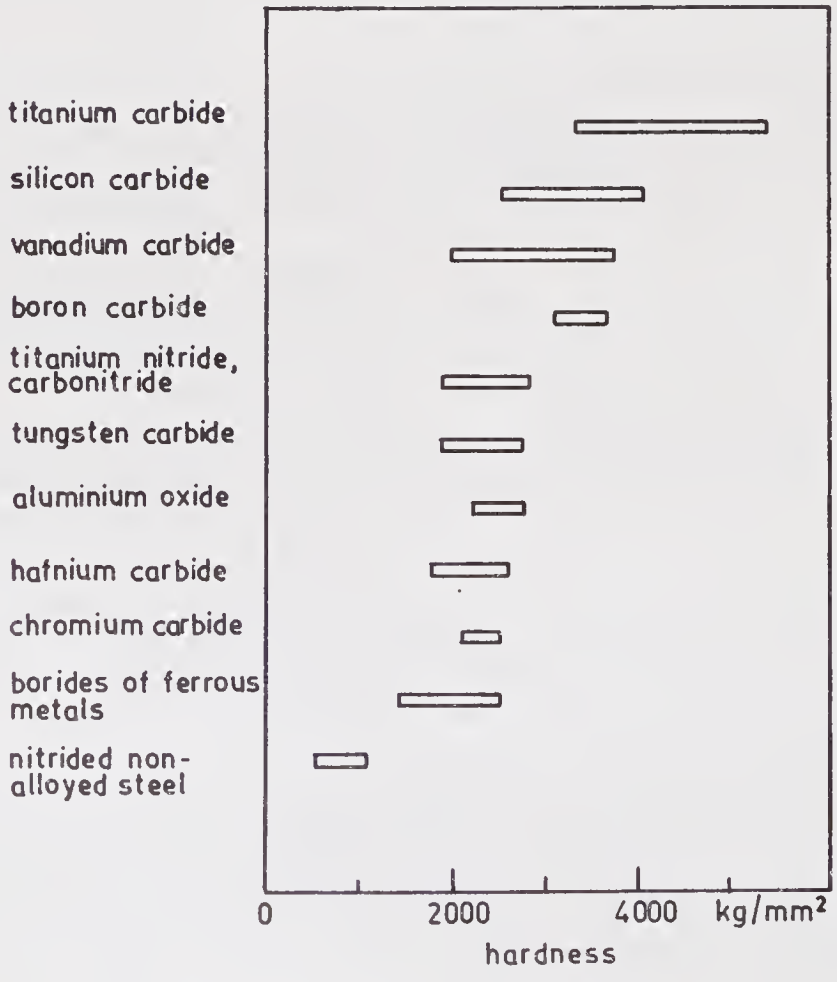

Figure 7. Microhardness of CVD coatings.

Adhesion or bonding of the coatings to the substrate, which is one of the most important properties on which the successful application of coatings depends, has been the subject of investigation in many reports. However, the reported adhesion values vary from one another, showing the strong dependence of adhesion on various coating process parameters. However, the following general comments can be made:

(i) stresses are invariably produced at the coating/substrate interface during the cooling period after deposition and during service, because of the differences in the thermal properties of coatings and substrate;
(ii) higher internal stresses tend to build up in thick coatings, which result in weaker bonding;
(iii) these stresses can be reduced by using intermediate layer (under-coat) and/or graded coating procedures;
(iv) coatings deposited at high temperatures generally havc better adhesion than those produced at low temperatures because of diffusion bonding.

2.2d *Comparison of CVD processes:* As can be seen from table 4, each process has its own advantages and disadvantages. For instance, the CCVD process is well-established and coatings of almost all ceramic materials have been obtained with very good density and excellent adhesion. Moreover, CCVD gives good uniform coating over the entire substrate surface unlike other processes which are mostly line-of-sight techniques only. But CCVD coatings are deposited at high temperature and hence the selection of substrate materials is limited.

2.3 *Comparison of ceramic coating processes*

Both thermal spray and CVD are well-established and coatings prepared by these techniques are already in standard usage in almost all branches of science and engineering.

Each process has its own advantages and disadvantages. The selection of a particular process is entirely decided by the particular application. For instance, if the application demands a near-theoretical-density coating with as high an adhesion value as possible, then CVD is the best process. However, the CVD process sets

Table 4. Comparison of CVD coating processes.

Process		CCVD	CSD	PACVD	RE	ARE	RS	RIP	CIP
Coating materials		Almost all	Proper solution	Almost all	Good VP materials		Target EC	Same as RE	Almost all
Substrate	Material	High temperature material		All materials			Mostly EC	EC	EC
	Temperature (°C)	400–1600		25–1000	25–300	20–1200 ~500	25–1100 ~100	100–900 ~900	500
	Size limitation	Reactor size			Vacuum chamber size				
Throwing power		Very good			Mostly line-of-sight			Good	

Abbreviations: VP: vapour pressure; EC: electrical conductor.

limitations on the size of the substrate and the normal coating process takes place at fairly high temperature. These factors should also be taken into account while selecting the CVD process.

Salient aspects of various ceramic coating processes have been compared in table 5, which in a way summarizes the advantages and disadvantages of each technique.

3. Applications of ceramic coating technology

The general range of applications of ceramic coatings is as follows:

(a) thermal barrier coatings;
(b) heat and oxidation resistance surfaces;
(c) high temperature wear and abrasion resistance surfaces;
(d) corrosion and erosion resistance layers;
(e) electrical insulation coatings;
(f) diffusion barrier coatings.

Though thermal barrier coatings are usually prepared by thermal spray, and wear-resistant coating on tools and tool inserts is a speciality of the CVD process, in most cases both processes have been used to prepare ceramic coatings on various industrial components. A sampling of industry-wise applications is given in table 6.

4. Present status of the technology abroad and in India

4.1 *Thermal spray process*

4.1a *Status abroad:* Commercial equipment suitable for general application in coating shops as well as custom-built ones to suit specific needs are readily available. Special systems (Muehlberger 1975) like high power systems, supersonic flame facilities, controlled environment and vacuum deposition systems etc., have also been commercialised.

Table 5. Comparison of ceramic coating processes.

	Process	
	Thermal spray	CVD
Coating		
Material	All	Almost all
Thickness (μm)	25–3000	10–500
Porosity	Slightly porous	Almost non-porous
Substrate		
Material	All	Mostly high temperature
Size limited by	Nil	Reactor size
Process temperature (°C)	50–200	400–1600
Type of bond	Mechanical	Metallurgical
Throwing power	Line-of-sight	Very good
Coating speed	Fast	Slow
Main application area	Thermal barrier; corrosion, erosion and wear resistance; electrical and thermal insulation	Wear, erosion and corrosion resistance; diffusion barrier

Table 6. Industrial applications of coatings.

Industry	Environment	Typical coated parts
Aircraft and space	Vibration, fretting, impact, hammerwear	Compressor and turbine blades, mechanical seals, compressor and fan casings, combustion chamber lining
Automotive	Vibration, fretting, impact, hammerwear	Cylinder heads and walls, piston walls, crowns and rings, valves and valve stems
Chemical	Corrosion, wet and dry particle abrasion, high pressure and temperature, friction	Pumps, pistons, turbine rotors, valves
Textile	Abrasion, corrosion	Rollers, guides, tensioners
Paper	Precision, corrosion	Surfaces
Iron & steel	Wear, abrasion, oxidation, heat, corrosion	Furnace rolls, shrouds, pumps, shafts
Nuclear		Fuel handling, machine parts, boiler and circulation seals, core rod drives
Machine tools	Wear, high temperature	HSS drills, end mills, reamers, broaches, form tools, hobs, shapers, slitting saws, milling cutters, routers, punches, dies
Electronics		Oxide coatings on LSI and VLSI

Robot-controlled job-handling systems, microprocessor based powder feeders and similar novel ancillary equipment are also being marketed (Kaczmerek *et al* 1984, pp. 205–215). Raw materials such as spray quality powders, rods, wires etc., are readily available and are moderately priced. User industries are very well aware of the potentialities and a large number of industries have incorporated coating systems for routine in-house applications and in research and development.

4.1b *Status in India*: *Equipment*–Bhabha Atomic Research Centre (BARC) has developed a plasma spray system consisting of 40 kW plasma torch with necessary power, gas and water cables, constant current power supply, screw feed powder feeder and a control console for safe and easy operation of the system. This technology has been transferred to the Vikram Sarabhai Space Centre (VSSC), Trivandrum, Gas Turbine Research Establishment (GTRE), Bangalore, and M/s Kirloskar Electric Co., Bangalore.

M/s Metallizing Equipment Co. (P) Ltd., Jodhpur, has commercialised rod or cord-fed combustion flame systems. It has also recently introduced powder flame type units to the market. M/s Ewac Alloys Ltd. has marketed a rod-fed flame-spray system to spray tungsten carbide coatings.

Coatings–A few organisations like BARC (Karthikeyan 1983; Karthikeyan *et al* 1985), VSSC, Defence Metallurgical Research Laboratory (DMRL), Hyderabad, Bharat Heavy Electricals Ltd. (BHEL), Trichy, Air India, Bombay etc., are using the plasma spray process for a variety of their own in-house applications. A private company, Plasma Spray Processors, has come to the market recently to undertake jobs on commercial basis.

In the Metallizing Equipment Co. wear-resistant coatings have been prepared over piston rods, plungers, pump shafts, compressor blades and extrusion dies. They have observed a 4–10 fold increase in life of the items because of the coatings.

4.2 *Chemical Vapour Deposition Process*

4.2a *Status abroad*: Various equipments and systems of thermal and plasma activated CVD processes are commercially available. Diffusion bonded case hardening processes like carburizing, nitriding etc., have been incorporated in most of the engineering industries.

4.2b *Status in India*: A few commercial organisations like M/s Sandvik Asia, Pune, M/s Indicarb Ltd., Hosur, have CVD systems for in-house coating of tools and tool inserts. M/s Dura Coaters of Bombay prepare coatings on a commercial basis. Coated machine tools such as drills, broachers, end mills, punches etc. are available in the market.

5. Conclusions

The tremendous potential of the ceramic coating technology has been well-proved, and many industries abroad have used ceramic coatings for both life elongation and process improvement. However, in India, the full potential of the technology has not been tapped as yet.

This article is based on a report co-authored with three other scientists and submitted to the Department of Science and Technology, New Delhi. We are thankful to the DST as well as the Bhabha Atomic Research Centre, Bombay, for assistance. We appreciate the help of scientists from different organisations, working on coating technology, who responded to our queries and sent us technical details about their work. We are grateful to Prof. E C Subbarao for continued guidance and encouragement.

References

Chagnon P, Fauchais P 1984 *Ceram. Int.* 10: 119 131

Fauchais P, Bourdin E, Coudert J F, McPherson R 1983 in *Plasma chemistry IV, Topics in current chemistry* (eds) S Veprek, M Venugopalan (New York: Springer-Verlag)

Fisher I A 1972 *Int. Metall. Rev.* 17: 117–129

Hecht N L, Gerdeman D A 1972 *Arc plasma technology in material science* (New York: Springer-Verlag)

Kaczmerek R, Robert W, Jurewicz J, Boulds M I, Dallaire S 1984 in *Plasma processing and synthesis of materials* (eds) J Szekely, D Apelian (New York: North-Holland)

Karthikeyan J 1983 *Study of reaction kinetics in alumina-slag and CSZ-slag systems*, Ph.D. thesis, Bombay University

Karthikeyan J, Sreekumar K P, Rohatgi V K 1985 Proc. Seventh International Symposium on Plasma Chemistry, Eindhoven

Muehlberger E 1975 Proc. Seventh International Metal Spraying Conference, London

Rykalin N N, Kudinov V V 1976 in *Plasma chemistry-2, Plasma chemistry and transport phenomena in thermal plasmas* (eds) A T Bell, C Bonet (Oxford: Pergamon)

Shull R D, Boyer P A, Ives L K, Bhansali K J 1984 in *Plasma processing and synthesis of materials* (eds) J Szekely, D Apelian (New York: North-Holland)

Yee K K 1978 *Int. Metall. Rev.* 23: 19–42

Zaat J H 1980 Proc. Ninth International Thermal Spraying conference, La Hasye

Zaat J H 1981 Fysiche Metal. Kunde, THE-diktaat No. 4498, Eindhoven University of Technology

Zaat J H 1983 in *Annu. Rev. Mater. Sci.* 13: 9–42

Author Index

Subject Index

ACADEMY PUBLICATIONS IN ENGINEERING SCIENCES

General Editor: R Narasimha

Volume 1. The Aryabhata Project (eds U R Rao, K Kasturirangan)

Volume 2. Computer Simulation (eds N Seshagiri, R Narasimha)

Volume 3. Rural Technology (ed. A K N Reddy)

Volume 4. Alloy Design (eds S Ranganathan, V S Arunachalam, R W Cahn)

...written by eminent scientists of India and abroad...Academy deserves all praise in bringing out these [papers]

Powder Metall. Assoc. India, Newslett.

Volume 5. Surveys in Fluid Mechanics (eds R Narasimha, S M Deshpande)

An informal and stimulating publication...(provides) a survey of many important topics in Fluid Mechanics...All the papers are of excellent technical content and most are very well written. Many include lengthy reference lists, which are as useful as the body of the paper...The publishing quality is very good...

IEEE J. Ocean Eng.

...The general level (of papers) is high... Several are likely to have wide appeal...

J. Fluid Mech.

Volume 6. Wood Heat for Cooking (eds K Krishna Prasad, P Verhaart)

...interesting and stimulating account of technical thinking on the wood stove problem up to date...excellent collection of valuable and thought-provoking investigations.

Rev. Projector (India)

Volume 7. Remote Sensing (eds B L Deekshatulu, Y S Rajan)

...Several contributions are specifically addressing topics of national interest, however, the majority of the papers is of general interest for a wide community. The book can serve not only as an inventory of the Indian activities, but also as a textbook on techniques and applications of remote sensing.

Photogrammetria

...particularly refreshing...

Int. J. Remote Sensing

Volume 8. Water Resources Systems Planning (eds M C Chaturvedi, P Rogers)

...well got up and very well printed...forms a valuable addition to our limited literature on Water Resources of India.

Curr. Sci.

Volume 9. Reactions and Reaction Engineering (eds R A Mashelkar, R Kumar)

...eighteen portraits of some major frontiers of research in CRE by a Micro-Who's Who of contemporary CRE researchers....good mix of theory and experiment that will provide many a good read for the specialist as well as the generalist researcher.... "must-buy" for all research libraries, corporate or personal that contain CRE titles.

Can. J. Chem. Eng.

Volume 10. Reliability and Fault-Tolerance Issues in Real-Time Systems (ed. N Viswanadham)

Volume 11. Composite Materials and Structures (ed. K A V Pandalai)

Volume 12. Developments in Fluid Mechanics and Space Technology (eds R Narasimha, A P J Abdul Kalam)